

Aus dem Institut für Schlaganfall- und Demenzforschung (LMU Klinikum)

Klinikum / Institut der Ludwig-Maximilians-Universität München



Dissertation  
zum Erwerb des Doctor of Philosophy (Ph.D.)  
an der Medizinischen Fakultät der  
Ludwig-Maximilians-Universität zu München

***Role of the COP9 Signalingosome in Atherogenic Inflammation***

vorgelegt von:  
Jelena Milic

aus:  
Petrovac na Mlavi, Serbia

Jahr:  
2022

Mit Genehmigung der Medizinischen Fakultät der  
Ludwig-Maximilians-Universität zu München

**First evaluator (1. TAC member):** Prof. Dr. Jürgen Bernhagen

**Second evaluator (2. TAC member):** Univ.-Prof. Dr. Dr. med. Oliver Söhnlein

**Third evaluator:** Univ.-Prof. Dr. rer. nat. Sabine Steffens

**Fourth evaluator:** Prof. Dr. Andreas Dendorfer

**Dean:** **Prof. Dr. med. Thomas Gudermann**

Date of the defense:

19/10/2022

## Table of Content

<b>Table of Content.....</b>	<b>4</b>
<b>List of Figures.....</b>	<b>8</b>
<b>List of Tables .....</b>	<b>9</b>
<b>List of abbreviations .....</b>	<b>10</b>
<b>Abstract (English):.....</b>	<b>13</b>
<b>1. Introduction .....</b>	<b>14</b>
1.1 Atherosclerosis .....	14
1.2 Cellular Mechanism of Atherosclerosis .....	15
1.2.1 Role of endothelial cells in Atherosclerosis .....	15
1.2.2 Role of mononuclear cells in Atherosclerosis .....	19
1.2.2.1 Monocytes .....	19
1.2.2.2 Macrophages.....	20
1.2.2.3 Foam Cells.....	23
1.3 Atherogenic Inflammation.....	24
1.3.1 NF- $\kappa$ B signalling .....	24
1.3.2 MAP kinases(MAPK) .....	27
1.3.3 AP-1(activator-protein-1) signaling .....	29
1.4 Atherosclerotic Pathology.....	31
1.4.1 Plaque Pathology .....	32
1.4.2 Plaque Remodeling and atherosclerotic classification .....	35
1.4.2.1 The ECM.....	35
1.4.2.2 The matrix metalloproteinases .....	36
1.4.2.3 Tissue Inhibitors of Metalloproteinases.....	39
1.4.3 Current Therapy Approaches in Atherosclerosis .....	41
1.5 COP9 signalosome .....	43
1.5.1 Structure and Function .....	43
1.5.2.1 Csn5 in atherogenic Inflammation .....	47
1.5.2.2 Csn8 in atherogenic Inflammation .....	50
1.5.2.3 Potential therapies based on the CSN.....	50
<b>2. Material and Methods.....</b>	<b>55</b>
2.1 Materials .....	55
2.1.1 Chemical and Reagents .....	55
2.1.3 Enzymes and Buffers for the Enzymes .....	56
2.1.2 Primer pairs for qPCR .....	56
2.1.2.1 Mouse primers .....	56
2.1.2.1 Human Primers.....	55
2.1.3 Antibodies.....	57
2.1.3.1 Primary Antibodies.....	58
2.1.3.1 Secondary Antibodies.....	58
2.1.4 Media, buffers and Solutions.....	60
2.1.4.1 Cell culture media.....	60
2.1.4.2 Buffers and Solutions .....	60
2.1.5 Inhibitors.....	61
2.1.6 Multi-component Systems.....	62
2.1.7 Equipment and Consumables .....	62
2.1.8 Consumables.....	63

2.1.9 Software.....	63
2.1.10 Cell lines.....	64
2.1.11 Mice.....	64
2.2 Methods .....	64
2.2.1 Primary cell culture and Csn5/Csn8 siPOOL depletion in vitro.....	64
2.2.1.1 Freezing and Thawing .....	66
2.2.2 Cell Lysis and Western Blot.....	66
2.2.3 Real-time qPCR .....	66
2.2.4 The mouse cytokine array.....	68
2.2.5 Zymographie .....	69
2.2.6 MMP activity assay .....	70
2.2.7 ELISA .....	70
2.2.8 Mouse work .....	70
2.2.8.1 Generation of tamoxifen-inducible arterial endothelial-cell specific deletion of CSN5 .....	71
2.2.9 Generation of myeloid-specific deletion of Csn8 .....	71
2.2.9.1 MLN4924 tretament of mice .....	71
2.2.9.2 Genotyping of mice .....	72
2.2.9.2.1 DNA isolation protocol.....	72
2.2.9.2.2 Genotyping Protocol .....	72
2.2.9.2.2 Genotyping Primers .....	72
2.2.9.2.3 Genotyping Protocols .....	72
2.2.9.2.4 Genotyping PCR programme.....	74
2.2.9.2.5 Agarose gel .....	76
2.2.10 Mouse Model of atherosclerosis disease progression .....	76
2.2.11 Phenotyping mouse atherosclerosis.....	76
2.2.11.1 En-face aorta preparation.....	76
2.2.11.2 ORO staining of aortic root .....	76
2.2.11.3 Pico-Sirius red staining.....	77
2.2.11.3 Hematoxylin and Eosine Staining.....	77
2.2.12 Immunohistochemistry and Immunofluorescence .....	77
2.2.13 Analysis of Vulnerability .....	78
2.2.14 FACS .....	79
2.3 Blood Analysis.....	79
2.4 Isolation of bone-marrow cells and generation of bone marrow-derived macrophages .....	79
2.5 Immunohistochemistry and immunofluorescence of human lesions .....	80
2.5.1 Isolation of human PBMCs .....	80
2.6 Statistical Analysis .....	81
<b>3. Aims .....</b>	<b>82</b>
<b>4. Results.....</b>	<b>83</b>
4.1 Arterial-endothelial Csn5 deletion .....	83
4.2 Arterial-specific deletion of Csn5 enhances early atherosclerosis .....	86
4.3 MLN4924 mimics athero-protection by CSN5 in vivo after 4 weeks of the Western diet .....	88
4.4 Csn5 depletion in arterial endothelial cells promotes advanced atherosclerosis.....	91
4.5 Csn5 loss in arterial endothelial lining enhances atherosclerotic plaque vulnerability ...	94

4.6	Arterial-endothelial specific depletion of Csn5 downregulates TIMP1 levels in vivo ...	96
4.7	Timp1 is downregulated in mouse aortic endothelial cells upon arterial-endothelial specific depletion of Csn5 in vitro.....	101
4.8	MLN4924 treatment up-regulates TIMP1 levels in vivo and in vitro.....	104
4.9	Csn5 overexpression reveals the involvement of MAPKs and the AP-1 signalling axis in determining the Timp-1 levels.....	106
4.10	The CSN holo-complex plays a role in atherosclerosis progression in vivo.....	108
4.11	The CSN holo-complex plays a role in regulating the levels of the TIMP1 via the AP-1 signalling axis in BMDMs .....	115
4.12	TIMP-1 levels are changed in human atherosclerotic lesions depending on the plaque stability.....	117
4.13	Human aortic endothelial cells Csn5 depletion determines Timp1 levels and matrix-metalloproteinase activity.....	119
4.14	MLN4924 treatment of human aortic endothelial elevates Timp1 levels .....	120
<b>5.</b>	<b>Discussion .....</b>	<b>122</b>
5.1	Arterial-specific Deletion of Csn5 enhances early atherosclerosis while MLN4924 mimics atheroprotection by CSN5 in vivo after 4 weeks of a Western diet .....	123
5.2	Csn5 loss in arterial endothelial lining promotes advanced atherosclerosis and enhances atherosclerotic plaque vulnerability in vivo via eliciting matrix-remodelling players .....	124
5.3	Endothelial Csn5 depletion downregulates the TIMP1 levels, while MLN4924 treatment up-regulates TIMP1 levels in vitro.....	127
5.4	Csn5 overexpression in mouse fibroblasts reveals involvement of the MAPK and AP-1 signalling axis to control the levels of TIMP-1.....	130
5.5	The CSN holo-complex plays a role in regulating the levels of the TIMP1 via the AP-1 signalling axis and impacts atherosclerosis progression.....	131
5.6	Human atherosclerosis and atherogenic inflammation in endothelial cells show that Timp1 levels determine plaque stability.....	133
<b>6.</b>	<b>Conclusion .....</b>	<b>136</b>
	<b>References.....</b>	<b>137</b>
	<b>Acknowledgements .....</b>	<b>172</b>
	<b>Affidavit .....</b>	<b>173</b>
	<b>Confirmation of congruency.....</b>	<b>174</b>
	<b>List of publications.....</b>	<b>175</b>



## List of Figures

**Figure 1.** Schematic representation of the arterial vessel wall

**Figure 2.** Leukocyte transmigration into the subendothelial space

**Figure 3.** The major NF- $\kappa$ B signalling pathways

**Figure 4.** MAPK signalling pathways

**Figure 5.** Atherosclerotic pathology

**Figure 6.** Lesion types in human atherogenesis

**Figure 7.** Schematic representation of plaque vulnerability

**Figure 8.** Arterial remodelling of the ECM under atherogenic inflammation

**Figure 9.** MMPs in atherosclerotic plaque

**Figure 10.** The structure of the TIMP-1

**Figure 11.** COP9 signalosome structure.

**Figure 12.** The modular structure of the CRL E3 ligases

**Figure 13.** Comparable ubiquitination and neddylation cascades

**Figure 14.** COP9 regulates NF- $\kappa$ B signalling

**Figure 15.** Neddylation inhibitors activity

**Figure 16.** List of analysed cytokines and chemokines in this assay.

**Figure 17.** Images of a single lesion

**Figure 18.** PCR products of genomic DNA of *Csn5*<sup>Δarterial</sup> *Apoe*<sup>-/-</sup> mice run on an agarose gel

**Figure 19.** *Csn5* depletion in the endothelial lining of the *Csn5*<sup>Δarterial</sup> *Apoe*<sup>-/-</sup> mice.

**Figure 20.** Arterial-endothelial specific depletion of *Csn5* enhances early atherosclerosis.

**Figure 21.** MLN4924 mimics atheroprotection by *Csn5* after 4 weeks of HFD and impacts small lesions

**Figure 22.** MLN4924 does not confer atheroprotection in female *Apoe*<sup>-/-</sup> mice.

**Figure 23.** Arterial-endothelial specific depletion of *Csn5* promotes advanced atherosclerosis in the aorta but doesn't impact mouse well-being and lipid mouse metabolism

**Figure 24.** Arterial-endothelial specific depletion of *Csn5* isn't affecting atherosclerosis progression in female mice after 12 weeks of HFD.

**Figure 25.** Arterial-endothelial specific depletion of *Csn5* promotes advanced atherosclerosis and enhances factors of atherosclerotic plaque vulnerability after 12 weeks of HFD

**Figure 26.** *Csn5* depletion in arterial endothelial lining enhances atherosclerotic plaque vulnerability after 12 weeks of HFD

**Figure 27.** Arterial-endothelial *Csn5* depletion downregulates the systemic TIMP1 levels in vivo

**Figure 28.** Arterial-endothelial *Csn5* depletion downregulates the TIMP1 levels in vitro

**Figure 29.** MLN4924 treatment up-regulates TIMP1 levels and impacts the activity of the matrix-metalloproteinase in vivo and in vitro.

**Figure 30.** *Csn5* regulates TIMP-1 via stabilising the AP-1 signalling axis independently of the JNK signalling in a mouse fibroblast in vitro.

**Figure 31.** *Csn5* regulates the AP-1 signalling axis independently of the JNK signalling in a mouse fibroblast in vitro

**Figure 32.** Targeted deletion of the *Csn8* gene in mouse macrophages

**Figure 33.** Macrophage-specific deletion of *Csn8* accelerates atherosclerosis.

**Figure 34.** Macrophage-specific deletion of *Csn8* doesn't promote atherosclerotic plaque vulnerability

**Figure 35.** FACS analysis of the male *Csn8*<sup>Δmyeloid</sup> *Apoe*<sup>-/-</sup> and their littermate controls *Csn8*<sup>wt</sup> *Apoe*<sup>-/-</sup> whole blood after the 12 weeks of HFD

**Figure 36.** Myeloid-specific deletion of *Csn8* has no adverse effects on female mouse atherosclerosis

**Figure 37.** Targeted deletion of the *Csn8* gene in murine macrophages lowers TIMP1 expression via the AP-1 signalling axis

**Figure 38.** TIMP-1 expression is changed in human carotid artery atherosclerotic lesions depending on the plaque stability

**Figure 39.** CSN5 regulates matrix remodelling players in human aortic endothelial cells (HAoECs).

**Figure 40.** Neddylation ablation by employing MLN4924 upregulates TIMP1 levels and ablates pro-MMP9 activity in human aortic endothelial cells, while it has no impact on the overall MMP activity

**Figure. 41** Graphical Abstract

## List of tables

**Table 1.** *Male Apoe<sup>-/-</sup>* blood cell count after receiving the MLN4924 or Vehicle treatment

**Table 2.** Blood cell count of male *Csn5<sup>Arterial</sup>/Apoe<sup>-/-</sup>* compared to the *Csn5<sup>wt</sup>/Apoe<sup>-/-</sup>* controls

**Table 3.** Blood cell count of female *Csn5<sup>Arterial</sup>/Apoe<sup>-/-</sup>* compared to the *Csn5<sup>wt</sup>/Apoe<sup>-/-</sup>* controls

**Table 4.** Blood cell count of male *Csn8<sup>Ameloid</sup>/Apoe<sup>-/-</sup>* compared to the *Csn8<sup>wt</sup>/Apoe<sup>-/-</sup>* controls

**Table 5.** Blood cell count of female *Csn8<sup>Ameloid</sup>/Apoe<sup>-/-</sup>* compared to the *Csn8<sup>wt</sup>/Apoe<sup>-/-</sup>* controls

## List of abbreviations

Abbreviation	Description
ABCA1	ATP-binding cassette protein A1
ACAT1	Acetyl-coenzyme A:cholesterol acetyltransferase 1
ADAM	A disintegrin and metalloproteinase
ADAMTS	A disintegrin and metalloproteinase with thrombospondin domains
AIT	Adaptive intimal thickening
AMI	Acute myocardial infarction
Ang	Angiotensin
AP-1	Activator protein-1
ApoB	Apolipoprotein B
apoE	Apolipoprotein E
Arg1	Arginase 1
CAND1	Cullin-associated and neddylation-dissociated 1
CBP	CREB-binding protein
CCL	Chemokine (C-C motif) ligand
CCR2	C-C motif receptors 2
cDNA	Copy DNA
COP9	Constitutive photomorphogenesis 9
CREB	CAMP response element binding protein
CRL	Cullin ring ubiquitin ligase
CSN	COP9 signalosome
CVD	Cardiovascular disease
CX <sub>3</sub> CL	Chemokine (C-X3-C motif) ligand
CX3CR	Chemokine (C-X3-C motif) receptor
CX3CR1	C-X3-C motif receptor 1
CXCL1	Chemokine (C-X-C motif) ligand
DAMPs	Damage associated molecular patterns
DCN1	Defective in cullin neddylation 1
DCs	Dendritic cells
DEN1	Deneddylose 1
DMSO	Dimethyl sulfoxide
DNA	Deoxyribonucleic acid
DTT	Dithiothreitol BSA bovine serum albumin
DUB	Deubiquitinase
ECD	Endothelial cell dysfunction
ECM	Extracellular matrix
ECs	Endothelial cells
EDTA	Ethylenediaminetetraacetic acid
ELISA	Enzyme-linked immunosorbent assay HRP horseradish peroxidase
ERK	Extracellular signal regulated kinase
ESS	Endothelial shear stress
ET	Endothelin
FACS	Fluorescent activated cell sorting

FCS	Fetal calf serum
GAPDH	Glyceraldehyde 3-phosphate dehydrogenase
GM-CSF	Granulocyte-macrophage colony-stimulating factor
GPCR	G protein-coupled receptor
HBSS	Hank's balanced salt solution
HIF	Hypoxia-inducible factor
HUVECs	Human umbilical vein endothelial cells
ICAM-1	Intercellular adhesion molecule-1
IFN $\gamma$	Interferon gamma
IHD	Ischemic heart disease
IKK	Inhibitor of kappa B Kinase
IL	Interleukin
I $\kappa$ B	Inhibitor of kappa B
JAB1(CSN5)	Jun-activation-domain-binding protein
JAM	Junctional adhesion molecule
JAMM	JAB1/MPN domain metalloenzyme
JNK	C-Jun N-terminal kinase
KLF	Kruppel-like factor
LDL	Low density lipoprotein
LDLR	Low density lipoprotein receptor
LFA-1	Lymphocyte function-associated antigen 1
LOX1	Lectin-like oxldl receptor 1
LPS	Lipopolysaccharide
LRP1	LDL receptor-related protein
LT $\beta$ R	Lymphotoxin $\beta$ -receptor
LXR	Receptor liver X receptor
M-CSF	Macrophage colony-stimulating factor
Mac-1	Macrophage-1-antigen
MAPK	Mitogen-activated protein kinases
MAPK	Mitogen-activated protein kinase
MEF	Myocyte enhancer factor
MEK	MAPK/ERK kinase
MFI	Mean fluorescence intensity
MHC	Major histocompatibility complex
MI	Myocardial infarction
MIF	Macrophage migration inhibitory factor
MKK	MAPK kinase
MKKK	MAPK kinase kinase
mLDL	Modified LDL
MMPs	Matrix metalloproteinases
MPN	MPR1-PAD1-N-terminal domain
MT-MMPs	Membrane type-mmps
NAE	Neddylation activating enzyme
Nedd8	Neural precursor cell-expressed developmentally downregulated-8
NEMO	NF- $\kappa$ B essential modulator
NES	Nuclear export signal
NF- $\kappa$ B	Nuclear factor-kappa B
NKT	Natural killer T

NLRP3	NLR family pyrin domain containing 3
NLS	Nuclear localization sequence
NO	Nitrite oxide
Nrf2	Nuclear factor erythroid 2-related factor 2
PAD	Peripheral artery disease
PAMPs	Pathogen associated molecular patterns
PCI	Proteasome, COP9 signalosome, translation initiation factor
PCR	Polymer chain reaction
PECAM-1	Platelet endothelial cell adhesion molecule
PGI2	Prostaglandin I2
PI3K	Phosphatidylinositol 3-kinase
PIT	Pathologic intimal thickening
PVAT	Perivascular adipose tissue
RANK	Receptor activator for nuclear factor $\kappa$ b
RNA	Ribonucleic acid
SCF	Skp1-culin-Roc1/Rbx1/Hrt-1-F-box
siRNA	Small interfering RNA
SMCs	Smooth muscle cells
SR	Scavenger receptor
T cells	Thymus cells
TAD	Transactivation domain
TCFA	Thin cap fibroatheroma
TCR	T-cell receptor
TH	Helper T cells
TIMP	Tissue inhibitors of matrix metalloproteinases
TLRs	Toll-like receptors
TNF	Tumor necrosis factor
TNF	Tumor necrosis factor
TNFR	Tumor necrosis factor receptor
TRAF	Tumor necrosis factor receptor-associated factor
UPP	Ubiquitin proteasome pathway
UPS	Ubiquitin-proteasome system
VCAM-1	Vascular cell adhesion molecule-1
VEGF	Vascular endothelial growth factor
VLA	Very late antigen
VSMCs	Vascular smooth muscle cells

## Abstract (English):

Cytokines, chemokines, and inflammatory signalling pathways orchestrate the inflammatory process promoting the development of atherosclerosis. Among these, the NF- $\kappa$ B is pivotal in driving vascular inflammation and atherogenesis. NF- $\kappa$ B triggering enhances endothelial adhesion molecule expression and cytokine/chemokine production and amplifies myeloid cell-based inflammatory responses. The COP9 signalosome (CSN) is a multi-functional protein complex that regulates the degradation of critical cell cycle and inflammatory proteins by controlling cullin-RING E3 ligase (CRL) activity via its intrinsic deNEDDylase activity. The endogenous inhibitor of the NF- $\kappa$ B pathway, I $\kappa$ B- $\alpha$ , is a key CRL substrate. Its stability is controlled by the CSN/CRL axis, suggesting that the CSN modulates atherogenic processes. In fact, we have previously shown that CSN subunits are strongly overexpressed in advanced human atherosclerotic lesions. Moreover, we demonstrated that myeloid-specific gene deletion of CSN subunit 5 (CSN5), i.e. the subunit that harbours the deNEDDylase activity of the complex, leads to exacerbated atherosclerotic lesion formation in *Apoe*<sup>-/-</sup> mice. At the same time, the NEDDylation inhibitor MLN4924 attenuates early atherogenesis (Asare et al., *PNAS* 2017). Although the intact CSN holo-complex of all 8 subunits is required for the deNEDDylase activity, the role of the holo-complex and that of other CSN subunits in atherogenesis has remained unknown, as also complex-independent functions have been reported for some subunits.

Here, I assessed whether the arterial-/endothelial-specific *Csn5* knock-out mice in the atherogenic *Apoe*<sup>-/-</sup> background recapitulates the exacerbated atherosclerotic phenotype found in myeloid-specific *Csn5* knock-out mice. Atherogenic mice with a Tamoxifen-inducible arterial *Csn5* deletion (*C57BL/6 Bmx-Cre-ERT2/Csn5flox/flox/Apoe*<sup>-/-</sup> or *Csn5*<sup>Arterial</sup>*Apoe*<sup>-/-</sup>) generated and their atherosclerotic phenotype and vascular inflammatory status studied. Data here indicates a marked exacerbation of atherosclerosis in *Csn5*<sup>Arterial</sup>*Apoe*<sup>-/-</sup> mice compared to control animals and, for the first time, implicate *Csn5* in early atherogenesis. Interestingly, the atherosclerotic phenotype was only found in male *Csn5*<sup>Arterial</sup>*Apoe*<sup>-/-</sup> mice, suggesting sex-specific mechanisms. Applying a cytokine and inflammatory marker screen of proteins potentially involved in atherosclerosis, I showed TIMP-1 as a factor related to plaque vulnerability.

Furthermore, I demonstrate for the first time a role for the smallest CSN subunit, CSN8, in atherosclerosis *in vivo* by studying atherosclerosis-prone *Csn8*<sup>Δmyeloid</sup>*Apoe*<sup>-/-</sup> mice. At the same time, this suggested a role of the CSN holocomplex in atherosclerosis. Accordingly, gene deletion of either *Csn5* or *Csn8* was found to regulate levels of Timp-1 and those of matrix-metalloproteinases (Mmp), in line with an impact on plaque vulnerability. Mechanistically, this mediated the AP-1 and MAP kinase pathways. Lastly, in a translational approach, I studied small molecule compounds that mimic CSN5 hyperactivation by blocking CRL NEDDylation in a pan-cullin manner or a specific cullin-3-dependent manner. These NEDDylation inhibitors were administered in early and advanced atherogenesis models, and initial data suggest that short-term application can convey a long-term “therapeutic” atheroprotective effect. My thesis contributes to the elucidation of mechanisms underlying atheroprotection by the CSN and identifies novel therapeutic targets.

Key words: COP9 signalosome, NEDDylation, AP-1, TIMP-1, Plaque vulnerability



## 1. Introduction

### 1.1 Atherosclerosis

Cardiovascular disease (CVD) is the most dominant cause of mortality worldwide. In the next decade expected to grow to more than 23.6 million deaths worldwide (Mozaffarian et al., 2015). Atherosclerosis is an underlining cause of vascular disease and is well-recognized as an immunoinflammatory disease. It occurs in the arteries, where it enables the formation of lipid pools in their walls in a non-random fashion over time. These lipid deposits in the arterial wall are named atheromas, and they are next to the lipid deposits prototypically consisting of an accumulation of inflammatory cells such as smooth muscle cells (SMCs), endothelial cells (ECs), leukocytes, and foam cells (Libby et al., 2019; Ross, 1999). Atherosclerosis is not a life-threatening event, but under plaque rupture and thrombosis formation, atherosclerosis becomes clinically essential and could lead to grave health complications, often with lethal outcomes. Clinically relevant outcomes of atherosclerosis progression are myocardial infarction and stroke (Falk, 2006).

The sole term atherosclerosis reflects the intimal fatty material accumulation in the arterial wall. Hence its name comes from the Greek word *there*, describing the inner matter of the atherosclerotic vessel as a reflection of the low-density lipoprotein (LDL) accumulation, and the Greek word *sclerosis*, meaning hardening of the tissues, as an elaboration on the vessel narrowing in the sites of the atherosclerotic plaques (Libby et al., 2019; Milutinović et al., 2020; Soehnlein & Libby, 2021).

The aorta and CAs provide the heart with oxygenated blood and structurally consist of three layers: *tunica intima*, which is in direct contact with the circulating blood and vessel lumen, *tunica media*, *majorly composed* of the SMCs, On the vessel's surface is located *tunica externa*; all surrounded by perivascular adipose tissue (PVAT) (Milutinović et al., 2020; Tellides & Pober, 2015; Waller et al., 1992) (Fig. 1).

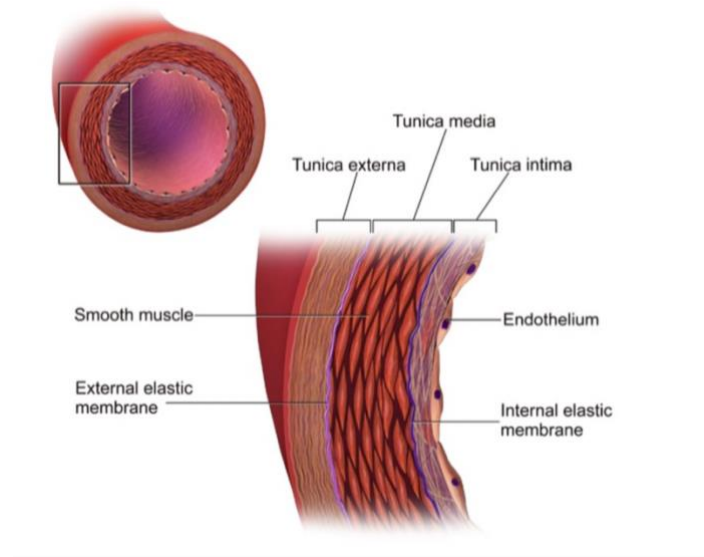


**Figure 1. Schematic representation of the arterial vessel wall structure.** *Tunica intima* comprises the endothelium, and it is at the vessel wall's inner layer. The *tunica media* majorly consists of SMCs. The layers of the vessel are flanked by elastic membranes (internal and external) (Taken from: Mercadante & Raja, 2021).

Although atherosclerotic lesions are defined mainly by structural change in the arterial intimal layer, atherosclerosis induces significant changes in all three blood vessel wall (Milutinović et al., 2020; D. Wang et al., 2017). During the past decade, numerous studies enabled a profound understanding of the molecular mechanism underneath atherosclerosis. Whereby these molecular mechanisms do stand behind the elicitation of the defined changes in the arterial vessel wall phenotype as well as under the regulating the role of inflammatory cells, particularly myeloid cells as well as the endothelial cells, in the disease progression (K.-H. Park & Park, 2015; Woppard & Geissmann, 2010).

The endothelial cell monolayer covers the inner lining of the blood vessels, and it is the main structural component of the *tunica intima*; as such, it represents vessels' crucial interface with the blood (Nakashima et al., 2007, 2008; Soehnlein & Libby, 2021). Between the *intima* and media of the arterial vessel layer stands an elastic membrane, which with age or disease, may be fragmented, duplicated, or lost (Milutinović et al., 2020; Waller et al., 1992). The arterial *media*, as the thickest layer, mainly consists of the VSMCs in several layers, sparsely present fibroblasts, that are all surrounded by an extracellular matrix formed of elastic fibres, collagen fibres, proteoglycans, and glycosaminoglycans (Bobryshev & Lord, 1995; Libby et al., 2019; Soehnlein & Libby, 2021; Waller et al., 1992). The *adventitia* consists mainly of the fibroblasts, small blood vessels, and the sparsely present inflammatory cells surrounded by an extracellular matrix (collagen, elastic fibres) (Moreno et al., 2006; D. Wang et al., 2017). Perivascular adipose tissue and sparsely distributed infiltrating immune cells, such as macrophages and T cells, encircle the arteries (Szasz & Clinton Webb, 2012; D. Wang et al., 2017).

Chronic inflammation drives atherosclerosis progression. It is initiated by the progressive building up and retention of the LDL particles in the subendothelial space of athero-prone sites of the arteries. (Bäck et al., 2019; Tabas et al., 2007). Intimal retention of modified LDL and turbulent blood flow act as a trigger that activates endothelial cells (Skålén et al., 2002). The hallmark of atherosclerotic lesions is built in the interplay of atherosclerosis-relevant cell types and by an infiltration of inflammatory cells, notably blood-derived monocytes and T lymphocytes. With the inflammation progression, gradual foam cell accumulation occurs in the atheroma. That is accompanied by SMC proliferation in the arterial media (Charo & Ransohoff, 2006; Hansson, 2005; Hansson & Libby, 2006; Lahoute et al., 2011; Libby, 2012; Lusis, 2000; Milic et al., 2019; Weber & Noels, 2011).

The initiators of atherosclerosis trigger inflammatory cells in the intima. They, in turn, respond under the pro-inflammatory surrounding of atherosclerotic plaques by extensively producing and secreting chemokines and cytokines. That, moreover, promotes the recruitment of the circulating monocytes and activation of the endothelial cells (Bäck et al., 2019; K. E. Berg et al., 2012; Schiopu et al., 2016; Weber & Noels, 2011).

Inflammatory cells that have been extensively scrutinised for the therapeutical targeting of their underlining pro-inflammatory mechanisms that promote atherosclerosis development are ECs, monocytes, macrophages, foam cells, as well as VSMCs (de Winther et al., 2005; Hansson & Hermansson, 2011; Milic et al., 2019; Navab et al., 1995).

## 1.2 Cellular Mechanism of Atherosclerosis

### 1.2.1 Role of Endothelial Cells in Atherosclerosis

Healthy blood vessel walls are comprised essentially of ECs and VSMCs (M. Li et al., 2018). The endothelial cells are not inert but are a rather highly dynamic and metabolically active interface with the blood with the potential to integrate and transduce blood-derived stimuli (Tabas et al., 2015).

The endothelial layer maintains the vessel wall homeostasis by regulating its permeability, vasomotor tone, hemostatic balance, blood cell trafficking, inflammation, and thrombogenesis (Aird, 2007; Fledderus et al., 2021). Thus, endothelial cells, as the inner liners of the blood vessel ‘sensate’ changes in the blood flow, lipid accumulation, and inflammatory mediators, in turn, generate inflammatory response (Gimbrone & García-Cardeña, 2016; Howe & Fish, 2019; D. Wang et al., 2017).

In healthy vessels, non-active endothelium maintains vascular homeostasis by inhibiting inflammation, blood clotting, vasoconstriction, and sustaining barrier integrity (Fledderus et al., 2021). Endothelial-derived nitrite oxide (NO) production and prostaglandin I2 (PGI2) inhibit platelet adhesion and thus enable blood fluidity. On the other hand, failure of arterial endothelial cells to control blood fluidity, integrity, and leukocyte adhesion are all instances of endothelial cell dysfunction (Pober & Sessa, 2007).

One of the earliest atherosclerotic manifestations is endothelial cell dysfunction (ECD) (D. Wang et al., 2017). The ECD is formed in a ‘non-random fashion’ and is reserved for regions of arterial vasculature. These atherosclerosis prone-regions are mainly localised in the vessel branching and curvature areas, such as arterial tree branch points, vessel bifurcations, and the inner side of the vessel curvatures, where the blood flows disturbance occurs (Chatzizisis et al., 2007). Conversely, areas exposed to the ‘uniform laminar flow’ are atherosclerosis-resistant (Gimbrone & García-Cardeña, 2016). Compared to atherosclerosis-prone areas, the ECs that line the atherosclerosis-resistant regions have unique morphological traits (Tabas et al., 2015). Namely, atherosclerosis-resistant cells have ellipsoidal cells and coaxial alignment in the blood flow direction, while atheroprone endothelial cells have a cuboidal morphology (Tabas et al., 2015). Moreover, the extracellular matrix present on the endothelial lining is different depending on the unique localisation of the blood vessel area. A thick glycocalyx layer can be found on top of the ‘athero-resistant’ ECs. It serves to slow down LDS subendothelial retention into the inflamed intimal vessel space (Koo et al., 2013; B. M. van den Berg et al., 2009). Moreover, ‘atheroprone’ ECs display impaired vessel barrier function, higher rates of overall cell turnover (cell mitosis to cell death rate), cellular senescence, and high expression of the endothelial apoptosis markers (Tabas et al., 2015; Zeng et al., 2009).

Variations of the blood flow, as well as local inflammatory factors such as cytokines and chemokines, determine the localisation of atheroprone sites in the atherosclerosis initiation (Chatzizisis et al., 2007; Cunningham & Gotlieb, 2005). Changes in the hemodynamic forces enable flow-generated endothelial shear stress (ESS) that plays the most fundamental role in the atherosclerosis (Chatzizisis et al., 2007).

Next to the unique morphological arterial wall changes, initial subendothelial retention of the modified LDL, damage- and pathogen-associated molecular pattern, together with the disturbed blood flow, act synergistically to activate the ECS of the intima and induce changes in the endothelial cell gene expression (Salvador et al., 2016). Notably, activation of KLF2 (Kruppel-like factor 2) and KLF4 (Kruppel-like factor 4) via MEK5/ERK5/MEF2 signalling cascade is a trait of the athero-protective

ECs. At the same time, NF- $\kappa$ B induction is reserved for the atheroma-prone-endothelium (G. Zhou et al., 2012). The NF- $\kappa$ B triggering in the ECs elicits gene expression of proatherogenic cell surface receptors such as adhesion molecules (Dai et al., 2004; Mullick et al., 2008). ECs at the focal arterial sites of atherosclerosis initiation by producing cytokine and chemokines contribute to an autocrine or paracrine manner atherogenesis exacerbation (Marin et al., 2013; J. Zhou et al., 2014).

The activated ECs express and synthesise critical drivers of atherosclerosis such as CCL2, CXCL8, CCL5, and CCL3, and as macrophage migration inhibitory factor (MIF), which act as pro-inflammatory triggers at the atherosclerosis-prone vessel sites (Skålén et al., 2002). The markers of the ECD are, furthermore, adhesion molecules. These cell surface glycoproteins are responsible for the recruitment and docking of the inflammatory cells and act as a gateway for their transmigration. They are intracellular adhesion molecule 1 (ICAM-1), vascular cell adhesion molecule (VCAM-1), and E- and P-selectin (Hansson & Hermansson, 2011). Leukocytes cross the EC lining via the para- or transcellular route (Schnoor et al., 2015; Vestweber, 2015).

The capture and ‘rolling’ of the leukocytes onto the ECs occurs via the endothelial (E)- and platelet (P)- selectins (Filippi, 2016). For leukocyte attachment, integrins are required. Notably, lymphocyte function-associated antigen 1 (LFA-1), macrophage antigen 1 (Mac1), and very late antigen-4 (VLA-4) are integrins that enable leukocytes to bind to their corresponding endothelial ligands, such as ICAM-1 and VCAM-1 (Fig. 2).

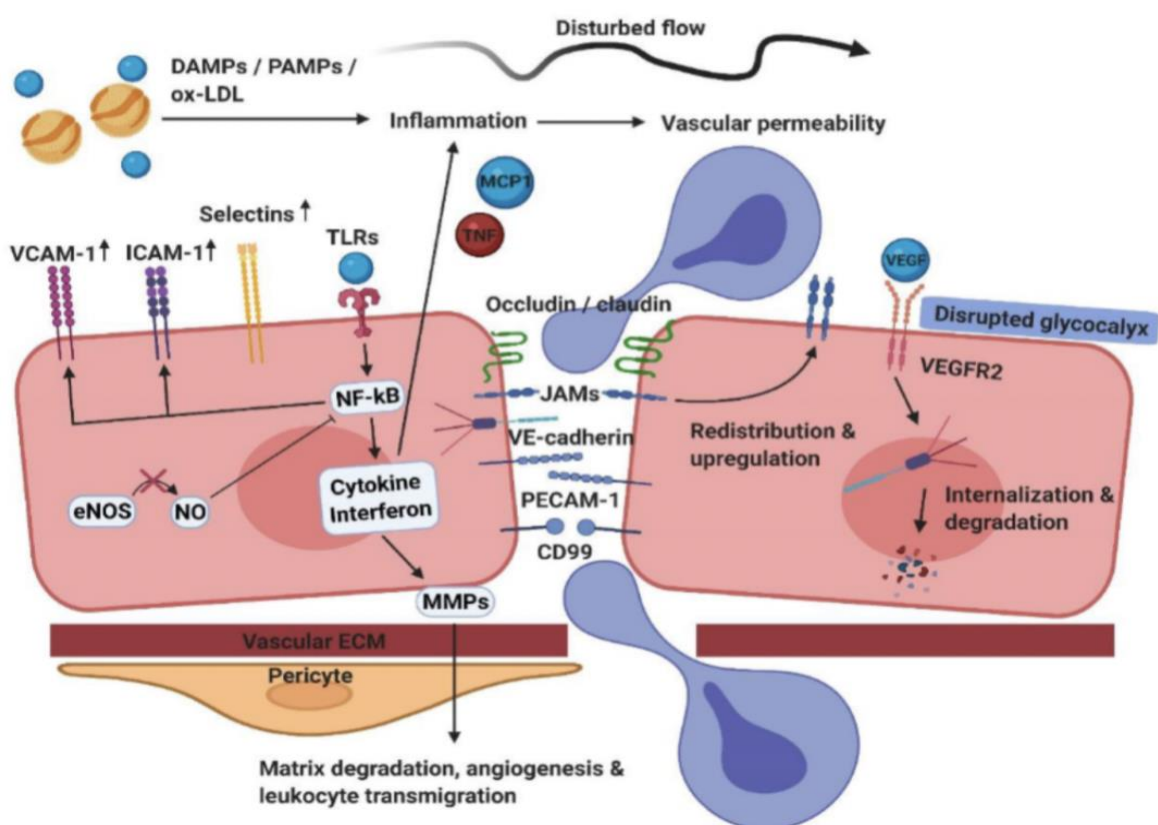


**Figure 2. Leukocyte transmigration into the subendothelial space.** Disturbed laminar flow and ox-LDL stimulation act synergistically with the DAMPs and PAMPs, initiating endothelial cell dysfunction and triggering inflammatory pathway activation via endothelial NF- $\kappa$ B-signaling activation. A pro-

inflammatory environment promotes the elicitation of the VCAM-1, ICAM-1, and Selectins. Endothelial cell dysfunction enables an environment for leukocyte transmigration by displaying vascular permeability and impaired extracellular-matrix degradation (*Taken and modified from: Sluiter et al., 2021*).

The inflammatory cytokines, P- and E-selectins, induce further conformational changes of integrins and enable leukocytes to interact with adhesion molecules on the endothelial cells, thus promoting the slow-rolling and firm adhesion of leukocytes (Alon & Shulman, 2011; Zarbock et al., 2011). Subsequently, leukocytes crawl on the vascular ECs, thus “searching” for the area of the lining where they are going to extravasate. Notably, neutrophils ‘crawl’ by employing the Mac1 integrins. However, monocyte ‘crawl’ on the endothelial lining by employing Mac1- and/or LFA-1 integrins (Phillipson et al., 2006; Sumagin et al., 2010). Transmigration of the leukocytes at the endothelial lining occurs at the extravasation site, the so-called “docking structures” or transmigratory cups (Carman & Springer, 2004). These structures are enriched for adhesion molecules and form marked filopodia enriched in the cytoskeleton, such as actin and microtubules (Barreiro et al., 2002; Carman et al., 2003). The formation of “docking structures” is small Rho-GTPases RhoA, Rac1, and Cdc4 dependent (Schimmel et al., 2016; van Buul et al., 2007). Interestingly by targeting the endothelial docking structure formation, such as inhibition of VCAM-1 and ICAM-1, lesion formation and leukocyte infiltration are impaired (Kitagawa et al., 2002; J.-G. Park et al., 2013). While P- and E-selectin depletion, *in vivo*, does consequently reduce overall plaque size in early and advanced atherosclerotic lesions (Dong et al., 1998). Moreover, since the NF- $\kappa$ B singling regulates expression of the adhesion molecules, ECs-specific inhibition of the ofNF- $\kappa$ B signalling *in vivo* has been shown to impair leukocyte infiltration and thus reduce murine plaque formation (Gareus et al., 2008; Sugama et al., 1992; Xue et al., 2009).

To transmigrate into intimal vessel space, leukocytes move across the endothelial lining (diapedesis) in a transcellular manner, directly through the endothelial cell body, or in a paracellular way, bypassing the endothelial cell junctions (Filippi, 2016).

The endothelial integrity and permeability are guarded by the tight junctions (occludin, claudin family members, and junctional adhesion molecules-), adherence junctions (cadherin and  $\gamma$ -catenin), and gap junctions (Fig. 2) (Dejana, 2004; L.-Z. Zhang & Lei, 2016). Paracellular leukocyte transmigration enables moving through the EC junction (L.-Z. Zhang & Lei, 2016). At the same time, the paracellular leukocyte transmigration route includes a transcellular channel formation by fusion of the membrane of leukocytes and ECs (Carman et al., 2007; Filippi, 2016). Leukocyte diapedesis is tightly regulated and involves complex communication and cell interactions between the leukocyte and the ECs, including selectins, integrins, junctional adhesion molecule (JAM), and other endothelial adhesion molecules such as ICAM-1, platelet endothelial cell adhesion molecule (PECAM-1 or CD31) (Filippi, 2016). Migration through the endothelial monolayer takes 2-5 minutes, while migration through the basement membrane takes 20 to 30 minutes (O. Hoshi & Ushiki, 2004).

Although the passage of leukocytes through the endothelial basement membrane takes longer, it is not well described so far. There is evidence that is dependent on yet another essential function of ECs in atherogenic inflammation, and that is endothelial cells derived matrix metalloproteinases (MMPs) production (Fig. 2) (Pruessmeyer et al., 2014; Sluiter et al., 2021). The ECs are responsible for producing multiple MMPs, MMP-1, -2, -3, -7, and -9 (S. Wang et al., 2006; C. Wu et al., 2009). Moreover, leukocyte transmigration and ECs activation are MMP-2 and MMP-9. While, whereas MMP9 endothelial stimulation consequently induces endothelial apoptosis (Carmona-Rivera et al., 2015).

Next to their complex interaction with the leukocytes, endothelial cells have crucial direct and indirect interaction with the other atherosclerosis-relevant cells contributing to the overall lesion phenotype, such as SMCs (M. Li et al., 2018). Whereby endothelium is a source of factors that either directly/indirectly stimulate or constrain the proliferation of the underlying SMCs guided by a local lesion environment (Scott-Burden & Vanhoutte, 1994). Indeed, *in vivo*, studies show that interventional removal of diseased plaques, such as angioplasty, induces endothelial dysfunction and, consequently, repression of the VSMC proliferation via the MAPK signalling axis (P.-J. Yu et al., 2007).

Finally, increased endothelial turnover and apoptosis are present in atheroma-prone sites of the arteries (Paone et al., 2019; Tricot et al., 2000). Moreover, endothelial turnover is triggered by the factors such as high glucose-induced reactive oxygen species (ROS) production in a c-Jun N-terminal kinase (JNK)-dependent manner (Ho et al., 2000). Moreover, low shear stress in vessel bifurcations could trigger endothelial apoptosis, eventually weakening EC and subsequent exposure to the intimal cellular debris (Paone et al., 2019).

The endothelial lining marks every stage of atherosclerosis progression from initiation to advancement, eventually leading to thrombus formation.

### 1.2.2 Role of Mononuclear Cells in Atherosclerosis

The predictive markers of atherosclerosis development are high-plasma LDL concentrations, endothelial dysfunction, increased permeability, intimal-lipid retention, and subsequent modifications (K. J. Williams & Tabas, 1995).

Subendothelial lipid modification, such as oxidation, glycosylation, carbamylation, and glycoxidation, has been shown *in vitro* and *in vivo* in the atherosclerosis development (Alique et al., 2015). LDL is suspectable to oxidation within the *intima* to become an oxLDL particle, which will be excessively taken up by the resident macrophages in the arterial vessel *intima* (Hansson & Hermansson, 2011). Resident macrophages that engulf oxLDL in the intima eventually undergo a series of changes that converts them into foam cells that initiate the early stage of atherosclerotic lesion formation, fatty streaks (Libby, 2002a). Modified LDL particles, moreover, trigger endothelial cell activation and initiate an inflammatory response and recruitment of different atherosclerosis-relevant cells, such as monocytes and leukocytes, to the site of the atheroma via the employment of a spectrum of different categories of chemokines (Galkina & Ley, 2009b; Hansson & Libby, 2006). Macrophages, endothelial cells, leukocytes, and infiltrating monocyte further impact atherosclerosis lesion progression.

#### 1.2.2.1 Monocytes

Monocytes are recruited from the bone marrow and can reside in the spleen, where before circulating the bloodstream, they undergo rounds of proliferation and activation (Tabas et al., 2015; Woppard & Geissmann, 2010). Monocytes are part of the steady-state immunosurveillance, injury healing, and remodelling under homeostatic conditions. Under atherosclerotic lesion progression, circulating monocytes are elevated (Flynn et al., 2019; Tacke et al., 2007).

Murine monocytes recruited to the atherosclerotic lesions express Ly6C antigen; depending on the antigen level, they are classified as Ly6C<sup>high</sup> or Ly6C<sup>low</sup> monocyte subsets. These monocytes drive inflammatory response and employ CX<sub>3</sub>C motif receptor 1 (CX<sub>3</sub>CR1), C-C motif receptors 2 (CCR2), and C-C motif receptors 5 (CCR5) upon monocyte to macrophage differentiation (Geissmann et al., 2003; Tabas et

al., 2015). These chemokine receptors are particularly crucial, enabling monocyte to migrate to the lesions (Tacke et al., 2007; H. J. Williams et al., 2012). The Ly6C<sup>high</sup> monocyte subsets preferentially migrate into atherosclerosis-prone arteries. In contrast, Ly6C<sup>low</sup>CCR2<sup>low</sup>CX3CR1<sup>high</sup> monocytes represent the homeostatic monocytes, as they regularly patrol the blood vessels and differentiate into alternatively activated (M2-like) macrophages in the lesions (Galkina & Ley, 2009). Murine atherosclerosis progressions can only be ablated upon Ly6<sup>high</sup> and Ly6<sup>low</sup> monocytes not entering the atherosclerotic lesions (Tacke et al., 2007).

The monocyte population circulating the peripheral blood express different signature markers than the mice (Tabas et al., 2015). Namely, they express CD14 and CD16 cell surface markers (Passlick et al., 1989). So far, three populations of human monocytes have been described: classical monocytes (CD14<sup>++</sup>CD16<sup>-</sup>), intermediate monocytes (CD14<sup>++</sup>CD16<sup>+</sup>), and non-classical monocytes (CD14<sup>+</sup>CD16<sup>++</sup>) (L. Ziegler-Heitbrock et al., 2010). Up to 90% of total circulating human monocyte populations are CD14<sup>++</sup>CD16<sup>-</sup> (Aw et al., 2018; L. Ziegler-Heitbrock et al., 2010). These monocytes are more prone to express inflammation-reducing cytokines, such as IL-10 (Ancuta et al., 2003; Aw et al., 2018; K. L. Wong et al., 2011; H. W. Ziegler-Heitbrock et al., 1992). The CD14<sup>+</sup>CD16<sup>++</sup> monocytes subsets are the “pro-inflammatory” monocytes and thus are more prone to produce inflammation-eliciting cytokines such as IL-1 $\beta$ , TNF- $\alpha$ , and IL-6 (Belge et al., 2002). The last human monocyte subset is prone to express TNF- $\alpha$  and IL-10 upon stimulation (Belge et al., 2002; K. E. Berg et al., 2012; Skrzeczyńska-Moncznik et al., 2008).

Overall, monocyte subsets differ in their gene expression patterns, antigen processing and capacity to induce atherosclerosis, their ability of trans-endothelial migration, and phagocytosis (Aw et al., 2018; K. L. Wong et al., 2012; L. Ziegler-Heitbrock & Hofer, 2013). Both murine and human monocytes are driven to the lesion-prone sites in the vessel over/through the endothelial lining. Where they interact with adhesion molecules on the Ecs, such as endothelial selectins (Mestas & Ley, 2008). E-selectin with P-selectin supports the monocyte rolling (Kumar et al., 2001). LFA-1, VLA-4, VCAM and ICAM-1 enable stable adhesions and monocytes monocyte arrest, followed by directional monocyte spread and locomotion laterally (spread) to find the extravasation site (Kamei & Carman, 2010; Phillipson et al., 2009; Schenkel et al., 2004; Woppard & Geissmann, 2010).

### 1.2.2.2 Macrophages

Macrophages are essential in atherogenesis (Murphy et al., 2014). In atherosclerotic lesions, microenvironmental factors, such as cytokines, LDLs, and growth factors, determine the monocyte differentiation of prospective macrophage populations. Monocyte differentiation is triggered by the growth factors present in the atheroma, such as granulocyte-macrophage colony-stimulating factor (GM-CSF) and macrophage colony-stimulating factor (M-CSF) (B. D. Chen et al., 1988). The atherosclerotic lesion's infiltrated monocytes and resident macrophages dynamically respond to the local lesion environment. Based on their function and particular cell surface markers, the heterogeneous macrophage phenotypes encountered in the lesion were traditionally for over 20 years classified as pro-inflammatory, M1-type, and anti-inflammatory M2-type macrophages. More recently, Willemsen and his team in 2020, by employing single-cell RNA sequencing technology combined with the surface macrophage markers (CyTOF), identified three dominant groups of macrophages termed: ‘resident-like macrophages’, ‘pro-inflammatory macrophages’, and ‘foamy TREM2<sup>hi</sup> macrophages’ (Mills et al., 2000; Willemsen & de Winther, 2020). The resident-like macrophages

were not changing with the lesion progression, resembling the previously described M2 type of anti-inflammatory or inflammation resolving like macrophages. These macrophages are mainly found in an abundance of the *tunica adventitia* of the vessel. Moreover, resident-like macrophages proliferate inside of the atherosclerotic lesion and participate in endocytosis while expressing a specific set of markers: *Cx3cr1*, *Lyve1*, *Folr2*, *Cd206*, *F13a1*, *Cbr2*, *Sepp1* and *Pf4* expression (Cochain et al., 2018; Cole et al., 2018; Willemsen & de Winther, 2020).

The dominant population of the macrophages found in the lesion is the non-foamy, intimal M1-like macrophages. The pro-inflammatory macrophage population is enriched in expressing the inflammasome related-genes expression *Nlrp3*, as well as NF- $\kappa$ B signalling-related factors, cytokines *Tnf* and *Il1 $\beta$* , as well as chemokines *Cxcl2* and *Ccl2-5* (Cochain et al., 2018; Cole et al., 2018; K. Kim et al., 2018; J.-D. Lin et al., 2019).

The latest identified subpopulation of macrophages that does not belong to the previously used “colloquial good-bad macrophage paradigm” is the foamy TREM2 high anti-inflammatory macrophages (Turnbull et al., 2006). These foamy macrophages are not enriched in a certain atherosclerotic stage and thus can be found in human or murine early as well as advanced atherosclerotic lesions (Cochain et al., 2018). They are well associated with cholesterol metabolism and oxidative response, hence their annotation as a ‘foamy’ (K. Kim et al., 2018). Moreover, this ‘foamy macrophage’ population is high in expressing the transmembrane glycoprotein Trem2. (Huang et al., 2011, p. 9; Willemsen & de Winther, 2020). They have been heavily reported to reside in the intimal area and the necrotic core of atherosclerotic lesions but not in the healthy lesion.

Although the traditional pro-inflammatory M1 and anti-inflammatory M2 paradigm appear outdated, it is still a solid reference point for this thesis’ topic, as it reflects many findings that relate to the role of the COP9 signalosome in atherosclerosis, (Mills et al., 2000). The diverse atherosclerotic lesion factors determine the heterogeneity of the macrophages. They can either skew them towards the more ‘pro-inflammatory activated -M1 macrophages or the more ‘anti-inflammatory- M2 macrophage’ phenotype (Libby, 2012).

The inflammatory M1 type of macrophages is characterised as more prone to express and synthesise the inflammation eliciting cytokines and thus inflammation exacerbation while being highly phagocytic (MacMicking et al., 1997; Mosser & Handman, 1992). They originate from the Ly6C<sup>high</sup> monocyte population drawn in the lesion via the CCR2 and CX<sub>3</sub>CR1 surface receptors employment (J. L. Johnson & Newby, 2009). Their activation is triggered upon the T-cell-derived IFN- $\gamma$ , followed by the pro-inflammatory stimulation such as TNF $\alpha$ , microbial-derived lipopolysaccharides (LPS), or lesion-derived oxLDL stimuli (Gordon & Martinez, 2010; Martinez et al., 2008). Under the M1 type of cytokine activators, intracellular JAK-STAT signalling, NF- $\kappa$ B and mitogen-activated protein kinases (MAPKs) regulate the inflammatory macrophage gene expression (Mosser & Edwards, 2008).

On the other hand, M2 macrophage populations are usually derived from the Ly6C<sup>low</sup> monocytes and are differentiated under the IL-4 and -13 cytokine stimulation gear to the anti-inflammatory phenotype (Bi et al., 2019). They are prone to express IL-10, scavenger receptors (SR-A1), and arginase -1 (Arg1), thus propagating the inflammation resolution (J. L. Johnson & Newby, 2009). They also encompass a broader heterogeneity subdivision among the anti-inflammatory profiles into M2a, M2b, M2c, and M2d types of macrophages. The JAK-STAT signalling is considered a classical pathway leading to the M2 polarisation *in vitro* and *in vivo* fields (Roy et al., 2002). Analysis of human and murine transcriptome shows that 50% of macrophage

markers determining the macrophage phenotype are species-specific (Martinez et al., 2006).

In early lesions, the murine atherosclerotic plaque cytokine environment is abundant in IL-4 and skews macrophage towards a more anti-inflammatory phenotype, promoting inflammation resolution. With the lesion progression, IFN- $\gamma$  levels have been shown to rise and shift from M2 to a more M1-inflammatory-prone environment (George et al., 2000). Hence *in vivo* IL-4 levels impact the early lesions but not the later stages of atherosclerosis progression (George et al., 2000; Kleemann et al., 2008). Inflammatory and anti-inflammatory types of macrophages reside in a particular area of the lesions. While M1-type of macrophages are often in the surrounding of the lipid core, anti-inflammatory macrophage subtypes reside in the areas surrounding the fibrous cap (Chinetti-Gbaguidi et al., 2011). M1/M2 paradigm is ever-evolving and represents the dynamic state of the found macrophages *in vivo*, and macrophage phenotype heterogeneity potential can be infinite with the atherosclerosis progression/regression (Gordon & Martinez, 2010).

Functionally, macrophages define the plaque environment, ingest the cell debris and the modified LDL particles, and complexly interact with the other atherosclerosis-relevant cells, such as VSMCs, and Ecs, next to interacting with the extracellular matrix of the lesion.

The macrophages have been shown to determine indeed viability of the neighbouring cells, such as VSMCs, whereby their interaction determines the outcome of atherosclerosis, such as the plaque stability (Boyle et al., 2002). Actual plaque rupture has been shown to occur once the macrophage activity is more pronounced, enabling the lowering of the VSMCs lesion count upon their apoptosis (Virmani et al., 2002). Moreover, VSMCs under cell death-apoptosis can synthesise factors of coagulation that promote blood clotting, contributing to the phenotype of vulnerable plaques (H. J. Williams et al., 2012).

Another study has demonstrated that macrophages also interact with endothelial cells. It was shown that endothelial cells synthesise factors that support macrophage proliferation and survival and further differentiate into the M2-like subtype. Consequently, in this interaction, macrophages increase the stability of the EC monolayer by providing a local source of VEGF (He et al., 2012).

Macrophages are known to secrete MMPs that enable extracellular matrix-cleavage, and with atherosclerosis, advancement promotes atheroma rupture, atherothrombosis, and clinically significant outcomes of atherosclerosis (Newby, 2016). Macrophage-derived proteases are either serine/cysteine proteinases (urokinase, cathepsins, plasminogen activator) or MMPs (MMP-2, -7, -9, and -12) (Murdoch et al., 2008). Macrophage-derived MMP-2 and -9 are essential in eliciting ECM remodelling factors that enable ECM network weakening, fibrous cap thinning, and the vulnerable atheromas (Xu & Shi, 2014).

Macrophages also participate in efferocytosis or clearance of the apoptotic cells. Cells that undergo cell death expose plasma membrane-derived phospholipid phosphatidylserine (PS), which upregulates the ABCA1 expression in macrophages (Greenberg et al., 2006; Kiss et al., 2006). Furthermore, macrophages employ cytoskeletal rearrangement machinery through the small Rho GTPases, Rac1 and RhoA (Nakaya et al., 2006). IL-10 and TGF $\beta$  will be released upon effective clearance of apoptotic cells, and inflammation resolution would be locally signalled (Fadok et al., 1998; Kojima et al., 2017). In the atherosclerotic lesion, inflammation resolution signalling is abrogated, and clearance of the apoptotic cells is ablated, leading toward necrotic core size augmentation, eventually causing vulnerability of the plaque lesions (Kojima et al., 2017).

Moreover, the local plaque environment dictates macrophage polarisation. Thus M1 skewed macrophages are less prone to perform efferocytosis, while on the other hand, M2 type of macrophages is more effective in the phagocytosis (Michlewska et al., 2009). Therefore macrophages promote atherosclerosis by ineffective efferocytosis clearance, promoting VSMCs apoptosis, weakening ECM matrix by MMP production, and finally by their apoptosis upon exacerbated oxLDL ingestion, which all, in turn, enables large necrotic core and plaques prone to rupture (H. J. Williams et al., 2012).

### 1.2.2.3 Foam Cells

Although there was substantial evidence in the past that foam cells originating from the macrophages are the hallmark of atherosclerotic plaques, current research suggests that a broad range of cell types can develop into the foam cells, such as VSMCs and ECs (Huff & Pickering, 2015; Kloc et al., 2021; Owsiany et al., 2019; Y. Wang et al., 2019). Moreover, it has been shown recently that up to 70% of foam cells in the mouse atheroma and more than 50% of human foam cells found in lesions are not monocyte-derived (Owsiany et al., 2019; Y. Wang et al., 2019). Moreover, there is substantial heterogeneity in the mechanisms employed under each cell type's lipid modifications process and the disease progression outcome generated from such a heterogeneity (Guerrini & Gennaro, 2019).

As previously described, subendothelial lipid accumulation is an early atherosclerosis initiator. The subendothelial environment nurtures low cell migratory ability and pro-inflammatory conditions, such as the urge of macrophages and dendritic-like cells to phagocytose LDL particles (Xu & Shi, 2014). Monocyte-derived macrophages initially phagocytose the oxLDLs, acetylated-LDLs, and minimally modified-LDLs (Kloc et al., 2021). Mechanisms employed to engulf these subendothelial LDLs are macropinocytosis or phagocytosis. Macrophages, in general, utilise scavenger receptors (SRs), the cluster of differentiation 36 (CD36), and SR-A (CD204) surface receptors to phagocytose oxLDL particles, which are the main surface lesion macrophage markers (Kelley et al., 2014; Libby et al., 2000; Y. M. Park, 2014). CD36 is an important scavenger receptor on the surface of the different cell types next to the lesion macrophages, such as ECs, and platelets (Y. M. Park, 2014). Next to the primary scavenger receptors, other LDL receptors have been described- such as LDL receptor-related protein 1 (LRP1) and lectin-like oxLDL receptor 1 (LOX1), which also leads the lipid take-in (Crucet et al., 2013; Lillis et al., 2016). Interestingly, Kruth and his team found that the foam cell differentiation could be likewise enabled by the native LDL, which is independent of the previously described receptors and occurs via the endocytosis (Kruth et al., 2005).

Upon internalisation of the LDLs, macrophages perform lysosomal-based degradation to free cholesterol and fatty acids. Furthermore, free cholesterol in the endoplasmic reticulum (ER) goes through re-esterification by acetyl-coenzyme A: cholesterol acetyltransferase 1 (ACAT1) (Chistiakov et al., 2016; Maxfield & Tabas, 2005). Excessive cholesterol uptake in this manner, followed by its accumulation in cytoplasm, leads to defective ER-based re-esterification and cholesterol loading, which furthers atherosclerosis progression with the macrophage/foam cell apoptosis (Feng et al., 2003).

Next to the clearance of the ox-LDL particles, macrophages recognise the cells that are undergoing apoptosis in the tissues and can remove them through programmed cell death removal in homeostatic conditions. This process is referred to as efferocytosis, and it is essential in tissue repair. Under atherosclerotic lesion conditions, efferocytosis is impaired by the calreticulin (the so-called "eat me" ligand) being down-regulated

(Kojima et al., 2017; Thorp & Tabas, 2009). The inflammatory conditions favour more foam cells, which are the main component that builds up the necrotic core, and therefore over time, might lead to its increase, finally developing a more vulnerable type of atherosclerotic plaques (Bobryshev et al., 2016).

Macrophages also possess the inflammatory resolving strategy by employing cholesterol discharge led by ABCA1 and/or ABCG1 transporters (Tabas et al., 2015). Spann *et al.* have also shown that macrophages can have lowered inflammatory profile upon employment of yet another described oxLDL receptor, liver X receptor (LXR), that has a beneficial impact on the atherosclerosis (Spann et al., 2012).

VSMCs can undertake cholesterol and differentiate in foam cells (Rong et al., 2003). These smooth-muscle cells decrease their cell surface markers while it elevates macrophage markers, such as CD68 and/or Mac-2. However, these smooth muscle cell-derived macrophages have less phagocytic and efferocytosis capacity (Vengrenyuk et al., 2015).

### 1.3 Atherogenic Inflammation

Atherogenesis involves cross-talk between many inflammatory signalling pathways of the immunity (Hansson et al., 2002). Atherosclerosis “incubation period” can progress over many decades, present clinically later in life, or even pass unnoticed. The balance between atherogenic inflammatory signalling pathways underlining atherosclerosis determines cell life and death, synthetic and degradative processes, and the development speed of the lesion, its progression, complication, and clinical manifestation (Libby, 2002b, 2012; Libby et al., 2019).

Although LDL is the hallmark of atherosclerosis, inflammatory processes underline all phenotypes of atherogenesis: from an EC lining activation by LDLs to the eventual rupture of atheroma. The main distinction between innate and adaptive immune responses lies in the cellular components, mechanisms, and receptors employed for their immune recognition (Medzhitov & Janeway, 2000). Inflammation plays a significant role in all the stages of atherosclerosis, and it underlines different atherosclerosis-relevant cell types of response to various stimuli. NF- $\kappa$ B, MAPKs, and AP-1 intracellular cell signalling are essential in regulating atherogenic inflammation as their therapeutic potential has been heavily investigated over the past decade.

#### 1.3.1 NF- $\kappa$ B Signalling

The immune processes underlining atherogenesis are all orchestrated by the large array of genes regulated by the NF- $\kappa$ B (T. Liu et al., 2017a). Typically, inflammation is favourable and over time, it can be resolved. However, its dysregulation can cause inflammatory diseases. The NF- $\kappa$ B transcriptional factor acts as one of the central mediators of the inflammation elicitation (T. Liu et al., 2017b).

A variety of proinflammatory signals trigger the NF- $\kappa$ B signalling. It controls proinflammatory and anti-inflammatory genes and regulates innate and adaptive immunity pathway activation (Bonomini et al., 2015).

NF- $\kappa$ B family of proteins consists of p50, p52, p65, RelB, and c-Rel. All members have an N-terminal Rel homology domain (RHD) that mediates dimerisation, association with inhibitory proteins, and DNA binding. Only p65 (RelA), c-Rel, and RelB have a transcriptional activation domain (de Winther et al., 2005; Silverman & Maniatis, 2001). Moreover, based on their transactivation potential and carboxy-terminal transactivation domains (TAD) that enable positive regulation of gene

expression, the NF- $\kappa$ B family is further divided. The Rel NF- $\kappa$ B subfamily includes c-Rel, RelB, and p65, as they have a C-terminal TAD. While p105, p100, and the *Drosophila* Relish proteins subfamily have C-terminal domain absent of TAD but replaced by multiples of ankyrin repeats. The NF- $\kappa$ B members can only bind DNA-upon proteolysis of its precursors p105 and p100 to a shorter, active p50 and p52, respectively (Oeckinghaus & Ghosh, 2009). There are two well-described NF- $\kappa$ B signalling pathways, ‘the canonical or classical’ and the ‘non-canonical pathway’ (Fig. 3). There is a third axis as well described named ‘atypical signalling pathways’ initiated only by a DNA-damage that will not be discussed here (Mussbacher et al., 2019; Prashar et al., 2017).

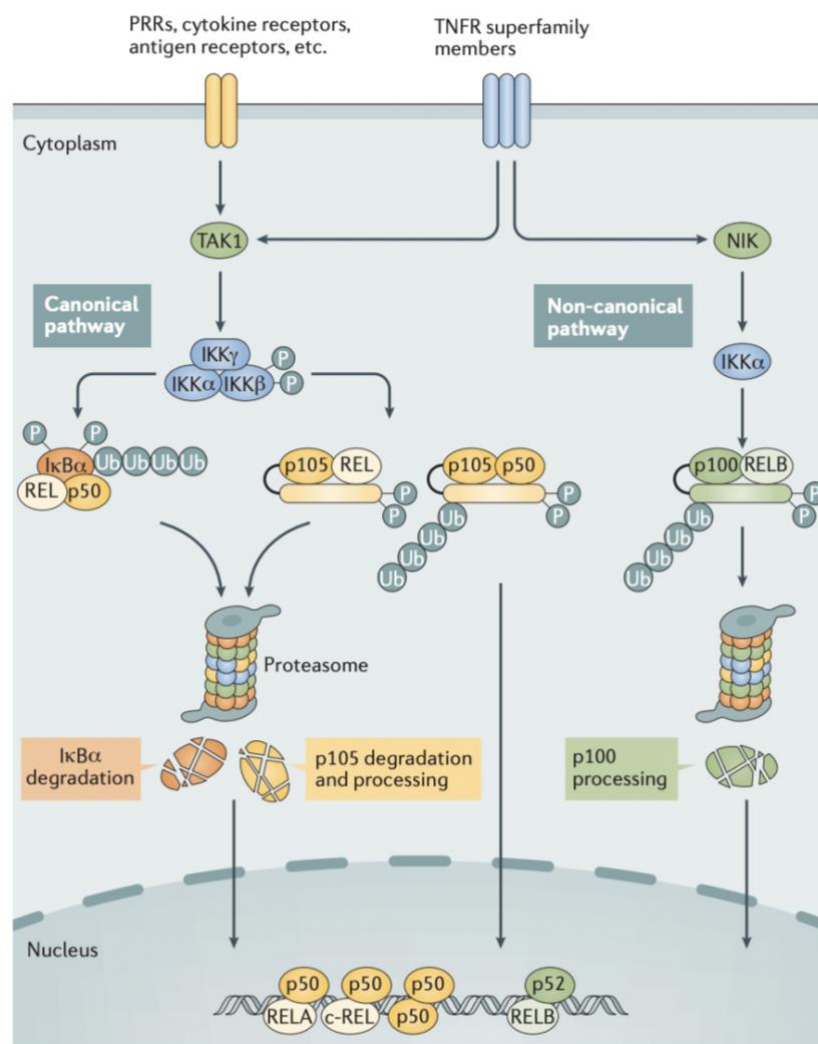


**Figure 3. The major NF- $\kappa$ B signalling pathways.** Canonical: Different triggers initiate canonical pathways, such as cytokines, infectious agents, and stress-inducing factors. All signals are further conveyed into enabling p50/p65 subunits to enter the nucleus and trigger gene expression of its target genes. That is only enabled on one side by phosphorylation of the I $\kappa$ B and its targeting of proteasome-mediated degradation. Conversely, this pathway is enabled by processing the subunits p100/p105 to their shorter active forms p65/p50. Non-canonical: Main executors of the signalling are p52/RelB dimers. Likewise, consecutive phosphorylation of the NIK and IKKs, next to the p100 processing, mediates the signalling. Eventually, both axes convey their signalling into the nucleus, regulating gene expression of multiple atherosclerosis-relevant gene targets (Taken from: S.-C. Sun, 2017).

In steady-state, NF- $\kappa$ B is constrained (Fig. 3) in the cytoplasm by its inhibitory proteins, I $\kappa$ B $\alpha$ , I $\kappa$ B $\beta$ , I $\kappa$ B $\epsilon$ , and *Drosophila* Cactus. Activation of the NF- $\kappa$ B under the

stimulation of cytokines, infectious agents, and stress-inducing factors is possible via phosphorylation and degradation of its inhibitory protein at conserved serine residues at the N-terminus such as Ser-32 and Ser-36 of I $\kappa$ B $\alpha$  by the IKK complex (Bonizzi & Karin, 2004; Karin & Delhase, 2000; E. T. Wong & Tergaonkar, 2009). Recently, it has been shown that the NF- $\kappa$ B pathway is subjected to several control mechanisms. One is the auto-feedback regulation of the NF- $\kappa$ B by its protein, I $\kappa$ B $\alpha$ . Furthermore, I $\kappa$ B $\alpha$  is being ubiquitinated by SCF-type cullin-RING E3 ligase (CRL) and proteasome targeting, which stands under the control of the COP9 signalosome complex (CSN) (Karin & Ben-Neriah, 2000). NF- $\kappa$ B signalling plays a role in every step of the atherogenic process and all atherosclerosis-relevant cell types.

Non-canonical NF- $\kappa$ B activation regulates the pathogenesis of inflammatory diseases (S.-C. Sun, 2017). Initiation and signalling of non-canonical signalling are typically slow, persistent, and tightly regulated (S.-C. Sun, 2017). Typical cell surface responders (Fig. 3) for the non-canonical pathway are ligands responsible for activating tumour necrosis factor receptor (TNFR), B cell-activating factor receptor (BAFFR), CD40, NF- $\kappa$ B (RANK) (Claudio et al., 2002; McPherson et al., 2012; Novack et al., 2012; Saitoh et al., 2003; Z. Wang et al., 2011). The non-canonical receptors bind TNFR-associated factor (TRAF) family members on the cytoplasmic side. This is followed up by the ubiquitination of NIK, thus enabling the negative regulation of the NF- $\kappa$ B non-canonical pathway. Among them, TRAF3 acts as the primary negative regulator, regulating NIK ubiquitination under the steady state. Upon the non-canonical signalling being triggered, TRAF3 degradation occurs, followed by the NIK accumulation and subsequently, the p100 processing is enabled (Liao et al., 2004). Herby, TRAF-mediated proteasomal degradation is facilitated by recruiting the CRLs cellular inhibitor of apoptosis 1 (IAP) to the NIK (Vallabhapurapu et al., 2008; Zarnegar et al., 2008).

Processing of the p100 occurs through its phosphorylation by the  $\beta$ TrCP CRLs recruitment (Fong & Sun, 2002; Liang et al., 2006; Xiao et al., 2001). The non-canonical NF- $\kappa$ B pathway is mediated by the NF- $\kappa$ B-inducing kinase (NIK), which renders the p100 phosphorylation by activation through the recruitment of the kinase IKK $\alpha$  (Xiao et al., 2001). By its activation, the non-canonical axis predominantly employs and acts through NF- $\kappa$ B2 p52 and RelB, although additional NF- $\kappa$ B members, such as RelA, are known to be activated as well (S. C. Sun et al., 1994; Tucker et al., 2007; Zarnegar et al., 2008).

NF- $\kappa$ B signalling regulates different stages of atherosclerosis development, such as subendothelial LDL modification, endothelial activation, and monocyte attraction to the lesion site (de Winther et al., 2005). Enzymes responsible for LDL modification, such as 5-lipoxygenase and 12-lipoxygenase, and secretory phospholipase A<sub>2</sub>, are all under the NF- $\kappa$ B mediated gene expression regulation (Burleigh et al., 2002; Ivandic et al., 1999; L. Zhao & Funk, 2004).

Moreover, the attraction of the monocytes in an early atherosclerotic lesion site is under the NF- $\kappa$ B regulation as it exerts its action via regulating the gene expression of the chemoattractant protein-1 (MCP-1) (Aiello et al., 1999; Gu et al., 1998).

In ECs, NF- $\kappa$ B signalling is in the essence of endothelial activation and its dysfunction, as it has been demonstrated that it exerts its regulation over the adhesion molecules' gene expression, permeability, and survival. The potent inducer of the NF- $\kappa$ B signalling in endothelial cells is TNF $\alpha$ , IL-1 $\beta$ , and IFN $\gamma$ , as well as the oxLDL (Mussbacher et al., 2019). In endothelial lining, NF- $\kappa$ B stands under the expression regulation of several adhesion molecules, including P-and E-selectin, ICAM-1, and VCAM-1, (Collins et al., 2000; Cybulsky et al., 2001; R. C. Johnson et al., 1997).

Prior studies showed that the NF-κB signalling in endothelial cells of the aortic regions atheroma-prone upon LPS stimulation or high-fat diet exposure *in vivo* does have more elevated NF-κB signalling compared to the areas that are less athero-prone (Hajra et al., 2000). Importantly, NF-κB in ECs, by regulating the expression of adhesion molecules, mediates inflammatory cells arrests (Rahman et al., 1999; Sprague & Khalil, 2009; Sugama et al., 1992; Xue et al., 2009). Laminar flow disturbance initiates NF-κB transcriptional activity (Petzold et al., 2009). Prior studies also show that NF-κB acts as a survival factor in LPS-treated ECs under the acute stress (Kisseleva et al., 2006). Thus, NF-κB, by acting as an endothelial cell apoptosis inhibitor, ensures that endothelial lining manages to recover promptly and the endothelial barrier is preserved (G. Liu et al., 2014). Prior *in vivo* studies testify that EC-specific depletion of NEMO or the IκB $\alpha$  overexpression exerts atheroprotective effects over the *Apoe*-deficient mice (Gareus et al., 2008).

Next to its essential role in the ECs, NF-κB signalling also exerts its regulation upon macrophage differentiation by regulating the expression of the M-CSF expression (Brach et al., 1991). Interestingly, upon the absence of the M-CSF, and thereby monocyte-macrophage differentiation axis impairment, there was ablation of the atherosclerosis development (Rajavashisth et al., 1999; J. D. Smith et al., 1995).

Furthermore, monocyte extravasation into the subendothelial space is MMP-9 dependent, which is regulated by the NF-κB transcriptional factors (Bond et al., 1998). Interestingly, loss of the MMP-9 in the *Apoe*<sup>-/-</sup> mice displayed a reduction in an overall atherosclerosis load and impairment of the macrophage infiltration (Luttun et al., 2004). The MMP-9 enables SMC migration, which is the major contributor to the fibrotic cap formation (Galis et al., 2002). Finally, in the atherosclerotic lesions, NF-κB signalling regulates the expression of relevant atherogenic cytokines: TNF, IL-1 $\beta$ , -6, -10, -12, and IFN $\gamma$ , thus determining the overall plaque environment (de Winther et al., 2005).

In the adverse stages of atherosclerosis, SMCs migration and fibrotic cap formation are the factors determining the stability of the atherosclerotic lesion. Prior studies have demonstrated that blocking p65 inhibits SMC proliferation and neo-intima formation *in vivo*, thus elaborating on its protective role in the VSMCs proliferation (Autieri et al., 1995).

Moreover, expression of the NF-κB is elevated in the proliferating SMCs, and its exacerbation of the activation, by inhibiting IκB $\alpha$ , induces intimal hyperplasia *in vivo* (S. Hoshi et al., 2000; Selzman et al., 1999; Zuckerbraun et al., 2003). Since VSMC proliferation may be majorly involved in the fibrous cap formation and, thereby plaque-stabilizing process, the NF-κB may positively as well regulate the adverse stages of atherosclerosis. Overall, the broad-range NF-κB inhibition as a potential therapeutical approach may be too risky.

However, understanding the NF-κB axis may unravel the essence of the inflammatory homeostasis regulation during atherosclerosis progression. While setting focus on a specific atherogenic pathway may yield novel therapeutic targets to modulate the atherosclerosis progression and its adverse outcome (de Winther et al., 2005).

### 1.3.2 MAP Kinases (MAPKs)

MAP-kinases are inflammatory signalling pathways initiated upon many factors present in the atherosclerotic environment, such as oxidative stress, growth factors, various cytokines, and the chemokines (Reustle & Torzewski, 2018). This cascade is led by sequential kinases: MAPK kinase (MKKK), MAPK kinase (MKK), and a terminal

MAPK (Fig. 4). From the cell surface sensing to the transcriptional regulation stand three distinct axes ERK1/2, JNK, and p38 MAP kinases (Fig. 4).

ERKs signalling acts through the MAPKKs (MKK), MEK1, and/or 2. At the same time, JNK signalling is enabled by MKK4 and -7 activation. The MKK3 and -6 activate the p38 MAPKK response (Kaminska, 2005; Pearson et al., 2001; Raingeaud et al., 1996).

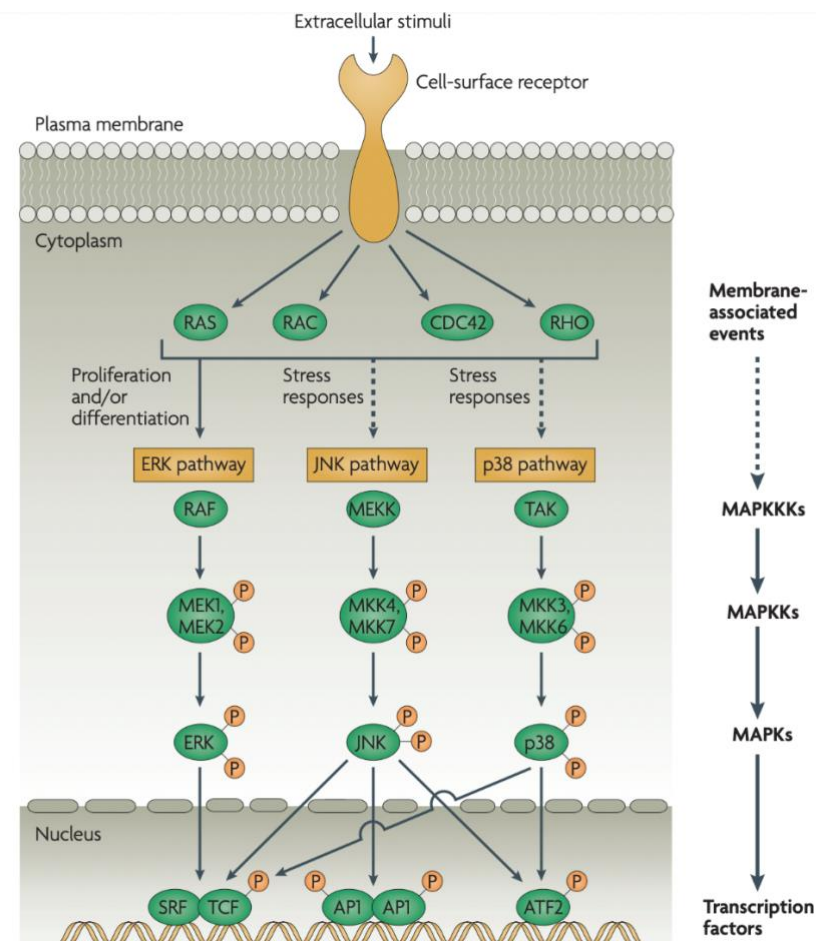


**Figure 4. MAPK signalling pathways.** The pathways signal through the three axes: ERK, JNK, and p38. Cell signalling starts with the sensing of the stress stimuli. That, in turn, exerts activity and activates RAS, RAC, RHO, and CDC42. That is followed by MAPKKK RAF initiating the ERK pathway. At the same time, MEKK initiates the JNK pathway. Finally, p38 acts through the TAK MAPKKs. Dual phosphorylation MAPKs further that. MAPKs exert cascade phosphorylation of the MAPKs. Respective MAPKs can move in the nucleus to phosphorylate (Taken from: Y. Liu et al., 2007).

The MAPKs are the kinases that enable its activity by phosphorylating serine/threonine. They comprise extracellular signal-regulated kinases (ERKs), the c-Jun N-terminal kinases (JNKs), and p38.

The p38 MAPKs are responsive to signalling that elicits inflammation, such as cytokines (IL-1 $\alpha$ , -2, -7, -17, -18; TGF $\beta$ ; TNF $\alpha$ ), or they respond to extracellular stress (ultraviolet radiation, heat shock, or hypoxia) signals (Reustle & Torzewski, 2018). MKK3/6 experience phosphorylation on their Thr-180 and -182, enabling the p38 signalling (Kaminska, 2005; Pearson et al., 2001). p38 triggering involves stimulation and activation of mediators, which promote inflammation that, in turn, enables functions such as leukocyte recruitment. p38 MAPK is responsible for TNF- $\alpha$ , IL-1, -6, -8, COX-2, MMP-1, and -3 (Baldassare et al., 1999; Hommes et al., 2003; Kaminska, 2005; Kyriakis & Avruch, 2001; J. C. Lee et al., 1999; Saklatvala et al., 2003). Most notably, p38 MAPK exerts its activity via TFs (transcription factors), most renowned is

activating transcription factor-2 (ATF-2) (Kaminska, 2005; Pearson et al., 2001; Vermeulen et al., 2003; S. H. Yang et al., 1999).

The JNK family members essentially exert their regulation over CVD injury and underline the disease progression. Murine *in vivo* studies have revealed that the JNK is elicited in arterial intima as a result of the injury response and during the development of aneurysm or atherosclerotic lesions (Amini et al., 2014; Metzler et al., 2000; Ost et al., 2008; Yoshimura et al., 2005). The JNK family consists of JNK-1 and -2 members that are both universally expressed in all cells; JNK3 is only found to be expressed and reported in a brain tissue (Amini et al., 2014; D. D. Yang et al., 1997). Even though JNK1 and JNK2 expression extends along with the same cells, they initiate separate cellular functions and regulate different protein targets (Amini et al., 2014; Kallunki et al., 1994).

JNKs were instigated in atherosclerosis by employing *JNK1<sup>-/-</sup>* and *JNK2<sup>-/-</sup>* in atherogenic *ApoE<sup>-/-</sup>* background. JNK loss was found to be athero-protective in these studies. Interestingly, even upon JNK1/2 signalling inhibitor (SP600125) application *in vivo*, atherogenic mice developed less pronounced atherosclerosis than their control. Moreover, bone marrow (BM) transplant studies have demonstrated the atheroprotective capacity of the macrophage-derived JNK deficiency *in vivo* (Muslin, 2008; Ricci et al., 2004). Interestingly, JNK signalling was also found to underline the foam cell regulation and the ox-LDL uptake in macrophages. The oxLDL has been shown to up-regulate all the MAPKs, JNK, p38 $\alpha$ , and ERK1/2. But the ERK1/2 signalling inhibition doesn't yield fewer foam cells, elevating the importance of the p38 and JNK axes as more relevant in the foam cell formation processes (Muslin, 2008; Rahaman et al., 2006; M. Zhao et al., 2002).

Endothelial JNK signalling loss yields are atheroprotective and only reserved in early atherogenesis, and its effect was lost in the advanced stages of atherogenesis. It was previously demonstrated that particularly JNK1 expression is elevated in the endothelial cells upon exposure to the disturbed blood flow *in vivo* (Amini et al., 2014; Zakkari et al., 2008). Moreover, JNK1 regulates ECs viability as well. Upon the JNK1 deletion, apoptosis of the endothelial lining is reduced. Observed effects have been attributed to the role of the JNK1 in promoting the transcription of the pro-apoptotic mediator's (Amini et al., 2014; Chaudhury et al., 2010). Yet *in vivo*, studies did confirm that JNK1 deletion in *LDLR<sup>-/-</sup>* atherogenic mice plays a significant role in early atherosclerosis development, endothelial cell turnover, and overall lowering of the atherosclerotic lesion load (Amini et al., 2014).

### 1.3.3 AP-1 (Activator Protein-1) Signaling

AP-1 signalling was traditionally assumed to exert a pro-inflammatory role, but more recent publications suggest that it might elicit both pro-and anti-inflammatory responses in atherosclerosis-relevant cells. Yet, most *in vitro* and *in vivo* studies implicate the common inflammatory transcription factor, AP-1, as a critical factor in the initiation and progression of the atherogenesis (Meijer et al., 2012).

The AP-1 is comprised of TFs families: Jun that encompass c-Jun, JunB, v-Jun, JunD); the Fos family that includes c-Fos, FosB, Fra1, Fra2; moreover, Maf TFs and finally also the cyclic AMP-responsive element-binding (CREB) TFs (Eferl & Wagner, 2003; Shaulian & Karin, 2002).

AP-1 transcription factors are either forming homo- or hetero-dimers, and they can exert their activity by binding the DNA via the leucine zipper domain (Chinenov & Kerppola, 2001). AP-1 family members are diverse in affinity towards the DNA-responsive gene elements and their affinity to form homo- or hetero-dimers. Thus, Fos

and Jun TFs have an elevated rate of gene expression capacity compared to the rest of the AP-1 signalling members (Chiu et al., 1989). Their gene expression is stimulated by cytokines, growth factors, infection, UV radiation, and cellular stress (Rai, 2019).

The c-Jun stabilisation is regulated by c-Jun mediated Ser-63 and Ser-73 phosphorylation embodied in their N-terminus, which reduces ubiquitin-dependent degradation of c-Jun. The JNKs are the primary kinase that enables c-Jun stability via phosphorylation. The COP9 signalosome (CSN) kinase activity promotes the stability of the c-Jun and overall elevation in the AP-1 transcriptional activity (Naumann et al., 1999). The c-Jun interaction with the COP9 signalosome is enabled by c-Jun activation domain-binding protein 1 (Jab1), more often referred to as the CSN5 subunit of the COP9 signalosome (Naumann et al., 1999; Wei et al., 1998). Indeed, CSN5/Jab1 was found as an AP-1 transcription factors coactivator that does so by binding directly to c-Jun or JunD (Claret et al., 1996). The function of the COP9 subunit, CSN5, is a serine/threonine kinase activity and specificity for c-Jun was characterised (Seeger et al., 1998). COP9 signalosome formation and its assembly anew *in vitro* stabilise c-Jun and elevate the AP-1 cellular activity (Naumann et al., 1999). This prior study consequently suggests the existence of a CSN-directed c-Jun signalling pathway (Seeger et al., 1998).

Another way of regulating the AP-1 signalling is based upon their destabilisation or targeted degradation. The ubiquitin-proteosome system mediates the c-Jun protein degradation via E3-CRL ligase, COP1 upon MKK1/2-Erk1/2 signalling pathway inactivation (Migliorini et al., 2011; Ouyang & Frucht, 2021). Whereas the COP1 CRLs are destabilised by the deNEDDylases activity of the COP9/Keap1/Usp15 super complex (Sanchez-Barcelo et al., 2016). Thus, COP9 subunits are essential in stabilising c-Jun via phosphorylation and destabilising CRLs responsible for c-Jun degradation.

The AP-1 transcriptional factor controls the gene expression underlining atherogenic inflammation by being responsible for cytokine productions such as the TNF $\alpha$ , IL-1, IL-2, IFN $\gamma$ , GM-CSF, MMPs, and TIMPs. The activator protein-1 directly annealing to their promoter, AP-1 binding motifs, enables their transcriptional regulation (Gutman & Waslyk, 1990; Schöenthal et al., 1988; Sirum-Connolly & Brinckerhoff, 1991; Ye et al., 2014).

The AP-1 signalling is deemed an essential regulator of an atherogenic-related process as the AP-1 activation has been previously shown throughout all the stages of the atherosclerosis (A. Wang et al., 2013).

In the endothelial mechano-sensing systems, LOX-1 expression via fluid shear stress at the atheroprone sites is mediated through the KLF2-AP1 triggering pathway (J. Y. Lee et al., 2018). AP-1 signalling is also an essential TFs that regulate the expression of MMPs (MMP9 and MMP2) as well as its inhibitors (TIMPs) that play a role in plaque remodelling through activating the p-cJun/JNK1 signalling (Sozen et al., 2014). The AP-1 signalling impairment, via JNK2 ablation, acts protectively in endothelial cells against the oxidative stress (Osto et al., 2008). The endothelial-derived AP-1 signalling regulates suppression of the VCAM-1 expression upon IL-35 stimulated inflammation (Sha et al., 2015).

Angiotensin II (Ang II) upregulates the adhesion molecules and thus promotes leukocyte adhesion. *In vivo* study has shown that Ang II-driven inflammation upregulates AP-1 signalling (Y. Chen & Currie, 2005). VSMC proliferation is also regulated via triggering the AP-1 signalling, suggesting its role in the plaque stabilisation (Metzler et al., 2000).

Upon the atherosclerotic lesion formation, its initiator oxLDL has been demonstrated to also stimulate MAPKs, JNK, c-JUN, and AP-1 via CD36-dependent signalling pathway in macrophages (Rahaman et al., 2006; Y. Zhu et al., 1998).

Moreover, macrophage AP-1 heterodimer composition has been shown to determine the macrophage polarisation (Srivastava et al., 2017). Whereby c-Jun has been identified as a regulator that triggers pro-and anti-inflammatory gene expression during macrophage activation (Hannemann et al., 2017). Finally, AP-1-driven regulation might be responsible for the MMP9 upregulation and TIMP1/AP1 disbalance in a human unstable lesions (F. Chen et al., 2005). Hence, AP-1 inhibition is investigated as one of the therapeutical targets in the atherosclerosis prevention (Manning et al., 2003; Muslin, 2008; Osto et al., 2008; J. Wang et al., 2011).

Since AP-1 signalling is deemed important in all stages of vascular inflammation, clinical study trials dampening the AP-1 signalling have been probed in recent years. Clinical trials involving the AP-1 signalling players gave controversial results, suggesting a more complex story behind the AP-1 signalling complex involvement in atherogenic inflammation. One of the known pharmacological inhibitors of the AP-1 signalling, doxycycline exerts an inhibitory effect on JNK1 and JNK2 eliciting.

In one study, doxycycline inhibition has been found to have a beneficial effect only on early atherosclerosis *in vivo*. Here it was demonstrated that AP-1 inhibition lowers IL-6 and IL-8 cytokine levels and yields reduced infiltration of the cells in the intima (Lindeman et al., 2009). While on the other hand, a clinical trial by Meijer et al. excluded AP-1 as a human plaque instability biomarker by evaluating its active form of c-Jun, in advanced atherosclerosis. Interestingly, up-regulation of AP-1 signalling was found to be conveyed to an endothelial lining and SMCs in a lesion but did not markedly show differences in the expression in stable vs unstable plaque lesions (Meijer et al., 2012). Moreover, another study has revealed that in human carotid endarterectomy plaques c-Jun and JunB levels of AP-1 complex are increased while JunB, FosB, and c-Fos were undetectable with the disease progression (Gonçalves et al., 2011).

Mouse studies have reported that doxycycline does have a beneficial effect on an *Apoe*<sup>-/-</sup> mouse atherosclerosis progression (Madan et al., 2007; Pawlowska et al., 2011). As well that, under the high-cholesterol diet, proteasomal activity is decreased, as such is causing elevation of active c-Jun and c-Fos in a murine atherosclerosis progression (Sozen et al., 2014).

## 1.4 Atherosclerotic Pathology

Atherosclerosis is initiated by an increased blood lipoprotein, of which LDL usually is the most prominent. However, the disease develops even at lower levels of LDL in combination with risk factors such as smoking, hypertension, diabetes mellitus, gender, and genetic susceptibility to the disease (Soehnlein & Libby, 2021).

Nevertheless, atherosclerosis is a slow- sometimes life-long progressing disease that involves LDL retention, inflammatory cell recruitment and turnover, foam cell formation, SMC proliferation, media thickening, ECM synthesis and remodelling, calcification, neo-vascularization, vessel wall remodelling, fibrotic cap rupture, and eventually thrombosis. This pleiotropy of processes and phenotypes are in the dynamic of the plaque lesion formation and have different importance on the atherosclerotic lesion development outcome (Fig. 5) and clinical significance (Bentzon et al., 2014).

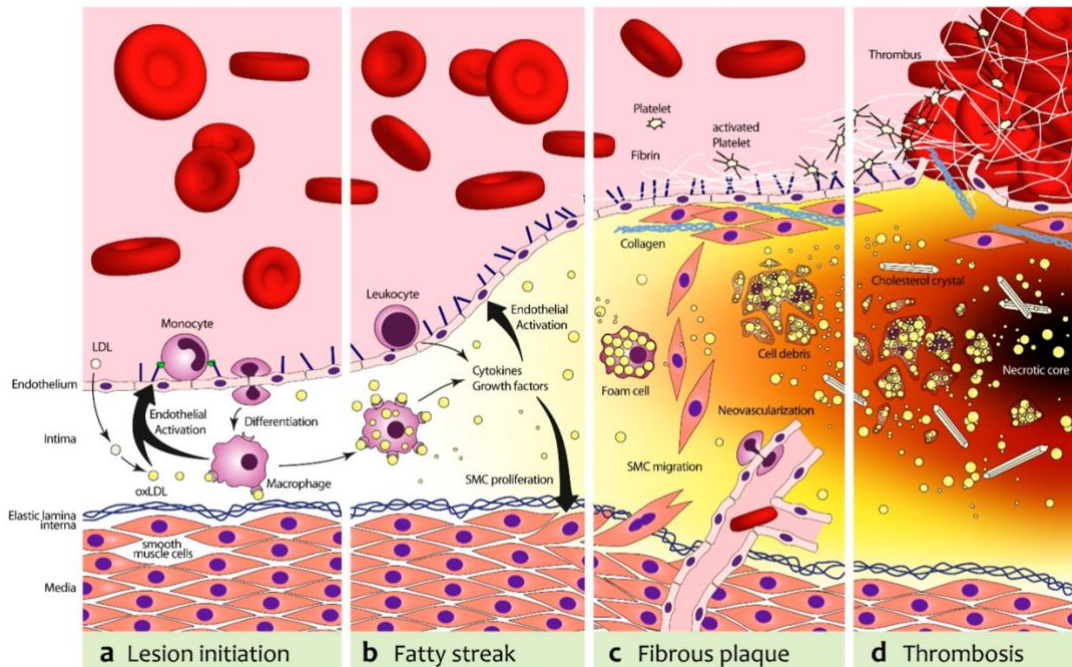


**Figure 5. Atherosclerotic pathology.** (a) Initially, LDL in subendothelial space undergoes oxidative modification to the oxLDL. OxLDL activates ECs and upregulates adhesion molecules (ICAM, VCAM, and selectins) and cytokines ad chemokines, which further recruits inflammatory cells such as monocytes, which in intima where they give rise to macrophages; (b) Macrophages excessively uptake subendothelial modified LDL and cell debris (c) SMCs proliferation stabilise the atheromas(d) Foam cells experience cell death and release cell content resulting in necrotic core formation. Finally, proteases released from SMCs, ECs, and foam cells give rise to fibrotic cap decrease, which leads to adverse effects and possible thrombotic event (Taken from: Steinl & Kaufmann, 2015).

The most atherosclerotic lesion will remain silent and stay clinically asymptomatic. Still, they can evolve from fatty streaks that are possible to tackle and over-turn to a stage of advanced fibrotic lesions that display enlarged necrotic core, ECM, and vessel remodelling that can advance to the plaque instability and/or rupture/erosion, and eventually give rise to the atherothrombosis (Bentzon et al., 2014; Libby, 2012; Milic et al., 2019). Once thrombosis leads to interruption or reduction of the blood supply, it can lead to MI or stroke (Prioreschi, 1967; Stoll et al., 2008). Hence atherosclerosis stands behind myocardial infarction (MI), ischemic stroke, and peripheral artery disease (PAD) (Galkina & Ley, 2009a; Lusis, 2000; Milic et al., 2019).

#### 1.4.1 Plaque Pathology

Atherosclerotic lesions can be characterised and developed in several stages according to histopathology, morphological changes of the vessel wall, general disease advancement, and atherosclerosis-relevant cell players involved in these stages of atherosclerosis.

Stary and his team performed one of the most well-known characterisations of the atherosclerosis (Stary et al., 1994, 1995). Namely, they recognised six development stages of atherosclerosis progression. Additionally, Virmani and his team recently revised Stary's atherosclerosis histopathology classification (Virmani et al., 2000). Notably, patients who have atherosclerosis would have the capacity to develop all the ranges from the atherosclerosis lesion development stages in their vessel wall at the different focal sites (Bentzon et al., 2014).

Coronary atherosclerosis begins with intimal thickening (Fig. 6A), usually near the branch points (Otsuka et al., 2016). Type I atherosclerotic lesions by Stary and his team

are recognised as the initial arterial intimal accumulation of lipid drifts. They are often encountered in early infancy well as in adults. Type II early atherosclerotic lesions have fatty streaks that on a histopathological view, visible as a narrow stretch in the intima (Stary et al., 1994). On the other hand, Virmani and his team recognise so-called “adaptive intimal thickening” (AIT) and “intimal xanthoma” (or so-called “fatty streaks”) (Fig. 6B) as an early display of atherosclerosis development in humans (Virmani et al., 2000). Whereas ‘adaptive intimal thickening’, as a manifestation of an early lesion (Fig. 6A), is built up mainly of SMCs and ECM with the sparse presence of the inflammatory cells. “Intimal xanthoma” is made predominantly of macrophages within the intima (Virmani et al., 2000). These early lesions, over time, progress to ‘pathologic intimal thickening (PIT)’ (Fig. 6C). Thus, the first stage of the progressive lesions are PITs, which have traits of observable lipid accumulation, absents of cells, which are positioned neighbouring the vessel media. PITs’ intimal space comprises SMCs immersed in the ECM, and sparsely, macrophages can be found (Otsuka et al., 2016). Macrophages moving into the lipid accumulation, the PITs represent the changeover and development of necrotic core and fibrotic atheroma formation (Virmani et al., 2000). According to the American Heart Association (Fig. 6D), this is the same as the first stage of advanced lesions (Stary et al., 1995; Virmani et al., 2000). The hallmark of the advanced lesion is a necrotic core buildup of macrophages encompassed by fibrotic tissue. Fibroatheroma is further subdivided (Virmani et al., 2000). Early fibroatheroma has lipid accumulation with the macrophages and experiences loss of the ECM (Nakashima et al., 2007; Otsuka et al., 2016). Late fibroatheromas comprise cells that underwent cell death, elevated free cholesterol, and ECM depletion due to elicited MMPs (Otsuka et al., 2016; Virmani et al., 2000).

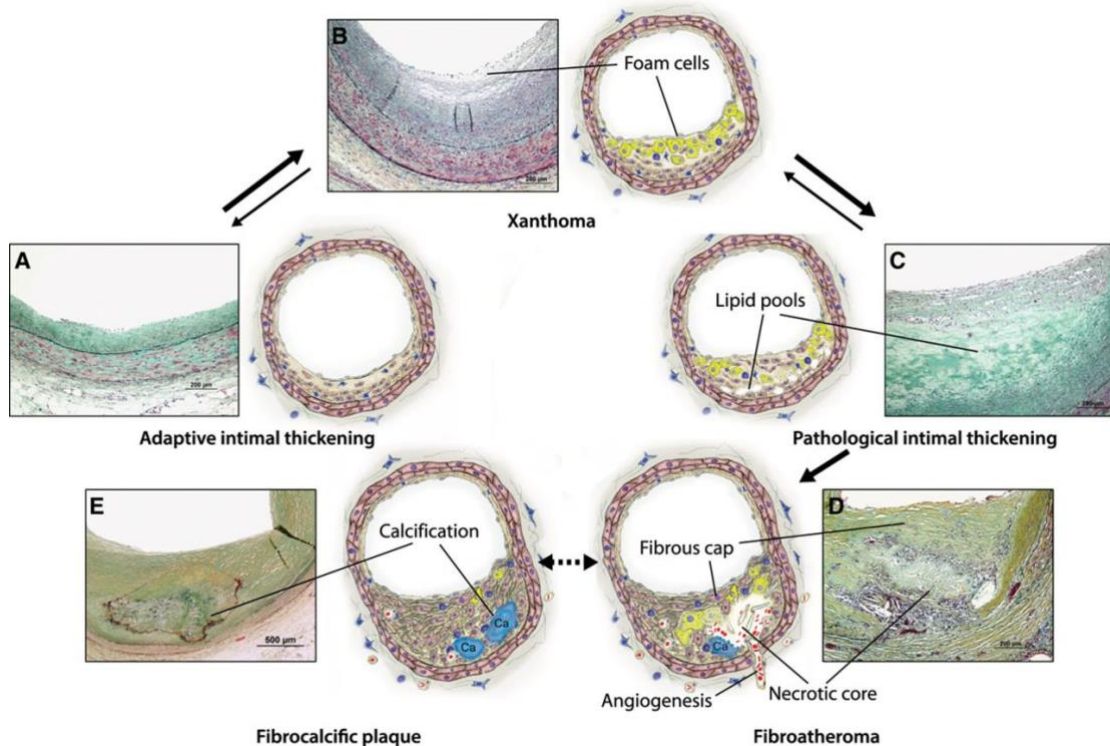


**Figure 6. Lesion types in human atherogenesis** (Based on: Virmani et al., 2000). **A, AIT:** SMCs proliferation forms the AITs. **B, ‘Intimal xanthoma’:** the presence of the foam cell accumulation. **C, PIT:** is lipid accumulation without necrotic core presence. **D, Fibroatheroma:** consists of a necrotic core. At the same time, calcification (**E**) can be present in the late stages of advanced atherosclerosis amounting to the calcified fibro lesions (**E**) representative Movat pentachrome staining is standing next to the individual schematic histopathology characteristics of each described atherosclerotic stages (taken from: Bentzon et al., 2014).

The necrotic core enlargement over time, followed by the fibrotic cap thinning, leads to '*thin-cap fibroatheroma* (TCFA)'; This type of atherosclerotic lesion is prone to rupture (Bentzon et al., 2014; Virmani et al., 2000). The prototypical vulnerable plaques (Fig. 7) have big plaque size, thin-fibrotic cap, augmented necrotic core, abundant macrophage content in fibrous cap, luminal obstruction ('positive remodelling'), high neovascularisation, present adventitial inflammation, and macrophage caused spotty patterns of calcification as well as loss of the SMCs (Otsuka et al., 2016). The cap width of TCFA is pathohistologically defined to be less than 65  $\mu\text{m}$  (Fig. 7). The prevalence of TCFAs or vulnerable plaques and their capacity to rupture as well as the death-induced rate in patients is more significant in males compared to female patients (Burke et al., 1997).

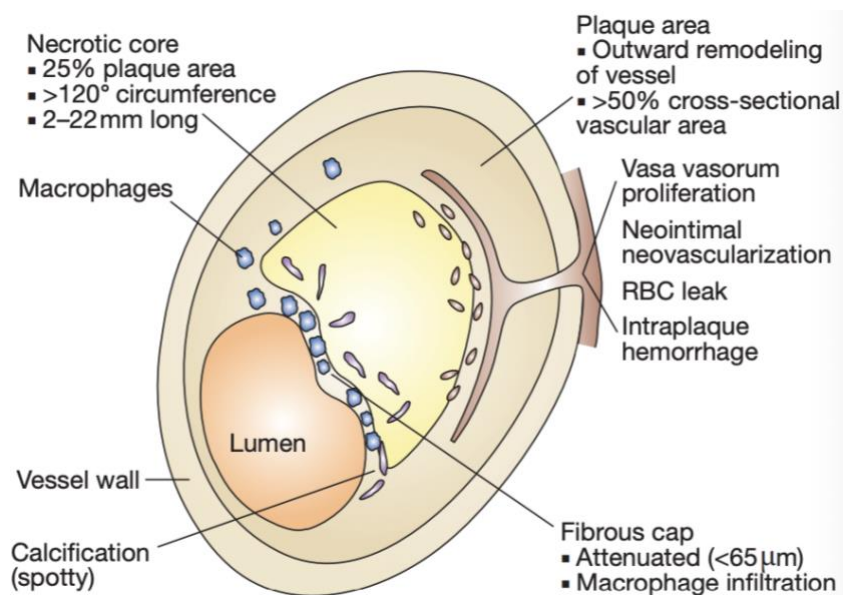


**Figure 7. Schematic representation of plaque vulnerability.** The figure is a schematic representation of the morphologic characteristics of a plaque vulnerable that is prone to rupture. Vulnerable plaques have been characterised by a set of morphological features: large lesions, positive remodelling (more than 50% of the cross-sectional vascular area), thin fibrous caps (less than 65  $\mu\text{m}$  in thickness), large necrotic cores, macrophage infiltration, neointimal neovascularisation and finally leading to the red-blood-cell (RBC) intraplaque haemorrhage (Narula et al., 2008).

Atherosclerosis is not clinically relevant except upon vessel occlusion and/or plaque rupture. Thus, plaque progression in more than 60% of TCFAs is a thrombi formation as a result of their rupture (Virmani et al., 2000). Thus, plaques with a thin fibrous cap can progress into lesions with thrombi caused by plaque erosion, plaque rupture, or calcification.

Plaque rupture and erosion, although similar, have histopathological particularities. Namely, rupture entitles cap wearying, and thrombus material leaks in the vessel lumen. Their fibrous caps are depleted of the SMCs, while they have infiltrated macrophage and foam cells that produce extensive enzymes such as MMPs that digest and weaken further the fibrous caps (Bentzon et al., 2014). Atherosclerotic plaque that is eroded presents loss of endothelial lining. Their intima consists of the sparsely present SMCs and ECM loss, with minimal or no inflammation. Plaque erosion mainly occurs in younger suffering patients below the age of 50 (Bentzon et al., 2014).

Atheroma progression can drive towards their calcification. This process entitles the necrotic core and its surrounding calcification and gives rise to the '*fibrocalcific plaques*' (Bentzon et al., 2014). The vascular calcification process usually comes from the SMC apoptosis in the lipid accumulations of the PIT, which is an early event in the process of the vessel calcification (Kelly-Arnold et al., 2013; Otsuka et al., 2014, 2015; Vengrenyuk et al., 2006). Macrophage apoptosis-induced calcification presents as augmented calcified areas  $\geq 15 \mu\text{m}$ , compared to the SMC derived. Further calcification progression is in the necrotic core's surroundings, while the necrotic's central area is not affected (Otsuka et al., 2016).

In the last couple of years, common histopathological factors that play a role in human atherosclerotic plaque proneness to forming a lesion with thrombi in the short term have been described. Still, it is a still-evolving field (Burke et al., 2001).

#### 1.4.2 Plaque remodelling and atherosclerotic plaque classification

Vascular remodelling encompasses changes in the vessel wall as part of the physiological process of tissue repair and adaptation. Its regulation dysfunction underlines cardiovascular diseases and atherosclerosis (Galis & Khatri, 2002). In the late 1980s, Glagov and his team described that the lumen of the vessel's capacity under the atherosclerosis progression remains unaltered as far as the plaque burden remains below 40% (Wissler & Vesselinovitch, 1968). In the early atherosclerosis disease representation, the vessel wall grows outward in the lumen, described as the positive "arterial remodelling" (Armstrong et al., 1990; Wissler & Vesselinovitch, 1968). Positive "arterial" remodelling of the CA wall is affiliated and attributed to intimal lipid buildup and macrophage infiltration. Overall could give rise to plaque vulnerability/rupture and potentially intraplaque haemorrhage (Schoenhagen et al., 2001). While on the other hand, erosion, vessel occlusion, and fibrocalcific plaques have been shown to exhibit the so-called 'negative vessel remodelling' (Otsuka et al., 2016).

Negative vessel remodelling can be described as plaque lesion formation and disease progression without the overall reduction of the vessel luminal diameter. It is associated with more stable human coronary artery plaques (Schoenhagen et al., 2001). It develops in the later phases as an inward remodelling, causing the protrusion of the atheroma (D. N. Kim et al., 1987; Otsuka et al., 2016). ECM, the regulators of the composition of the ECMs- MMPs, and tissue inhibitors of matrix metalloproteinases (TIMPs) are the key players in plaque remodelling and act as determining factors of the plaque stability (Galis & Khatri, 2002).

##### 1.4.2.1 The ECM

The extracellular matrix (ECM) is a network of structural fibrous proteins (**Fig. 8A**) that comprises collagen fibres, glycoproteins, proteoglycans, elastin, etc. (Holm Nielsen et al., 2020).

The ECM is implicated throughout the atherogenesis, from LDL accumulation to ECs activation to the cap rupture. The extracellular matrix is in a steady state providing structural integrity and a dynamic interactive platform for complex cellular activity – such as attachment, interaction, proliferation, apoptosis, etc. As such, ECM is essential, and its loss and changes are regarded as the biomarkers of the plaque stability (Chistiakov et al., 2013; Holm Nielsen et al., 2020).

The glycocalyx layer comprises various proteoglycans, glycoproteins, and soluble proteins. It acts as a cover on the surface of the endothelial lining as their essential ECM

point of communication. Moreover, endothelial cells participate in synthesising and creating the ECM by giving rise to their basement membrane to which they adhere towards the *media* (Mitra et al., 2017). In the *media* of the arterial vessel, the ECM provides a surrounding for the SMCs, in which the secretory phenotype of the VSMCs produces and secrete ECM proteins (Mohindra et al., 2021). At the same time, intimal ECM composition is mainly comprised of elastin fibres and type I and III collagens (Eble & Niland, 2009). The outer vessel layer is shaped by fibroblastic tissue and is mainly composed of the proteoglycan versican (Eble & Niland, 2009).

The ECM in the arterial *media* originates from the VSMCs, whereas *adventitia* ECM is made at a major by synthesis of fibroblasts (Xu & Shi, 2014). Collagen is architectural and formative in building atherosclerosis and constitutes up to 41% of lesions, whereas they make up to 61% of calcified human lesions (E. B. Smith, 1965). ECM's uncontrolled degradation (Fig. 8B) enables atherosclerosis progression as it is permissive to all the processes governing the atherogenic inflammation (Xu & Shi, 2014).

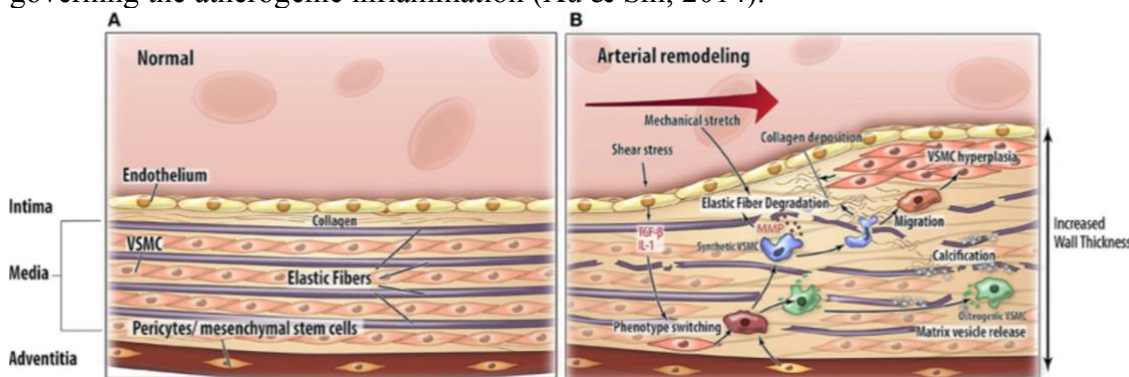


**Figure 8. Arterial remodelling of the ECM under atherosclerotic inflammation.** Schematic view of the arterial wall. A Healthy vessel has an undisturbed arterial wall structure. B, Atherosclerosis disturbs the vessel wall structure as it induces intimal wall expansion, ECM deterioration and calcification, and collagen loss (Taken from: Van Varik et al., 2012).

Within the ECM, MMPs play an essential role as are components of the ECM in a latent form where under the homeostatic conditions, reside inactivated by the tissue inhibitors of MMPs (TIMPs). In contrast, upon the atherosclerosis development MMPs get active and participate in the ECM deterioration (Mohindra et al., 2021).

#### 1.4.2.2 The Matrix Metalloproteinases

The proteinases participating in ECM degradation are the MMPs. (MacColl & Khalil, 2015; Nagase et al., 2006). They are underlining atherosclerosis progression. Besides, prior studies demonstrate their involvement in all the processes, from monocyte infiltration to the atherosclerotic plaque rupture (B. A. Brown et al., 2017). Reports show MMPs regulate important atherosclerosis-related processes such as inflammation, ECD, SMCs migration, arterial calcification, ECM degradation, and atherosclerosis destabilisation (B. A. Brown et al., 2017; Olejarz et al., 2020; Serra et al., 2017).

Matrix metalloproteinases are the family of 28  $Zn^{2+}$  -dependent endopeptidases, (Holm Nielsen et al., 2020; Visse & Nagase, 2003).

They have high domain homology. All the MMPs family members contain an N-terminal pro-domain, whereby Cys- residue binds to the catalytic domain, enabling their inactive/pro-form. MMPs' C-terminal domain contains a hemopexin-like domain of all MMPs, except MMP-7. These two MMP domains are interconnected by a hinge region, which is not conservative among the MMP family members (B. A. Brown et al., 2017; Cauwe et al., 2007; Olejarz et al., 2020).

Thus MMPs are further divided based on their substrate affinity and location (Cauwe et al., 2007). Their classification is still evolving but is, in general, divided into collagenases (MMP-1,-and -13), gelatinases (MMP-2 and -9), stromelysins (MMP-3, -10, and -11), matrilysins (MMP-7and -26), membrane-type MMPs (MMP-14, -15, -16, -17, -25 and -24), and ADAMTS (a disintegrin and metalloproteinase with thrombospondin domains) metalloproteinases (Amin et al., 2016; Olejarz et al., 2020). All MMPs are synthesised in an inactive/proform, and upon their proteolytic processing, their catalytic activity is revealed (B. A. Brown et al., 2017).

MMPs gene expression is managed at the transcription. Gene and its regulatory elements have similar arrangements, although coded on different chromosomes (Zitka et al., 2010). MMP gene promoters contain proximal AP-1, SP-1, and NF- $\kappa$ B transcription factor binding sites (Clark et al., 2008). Promoters of MMP-1, -3, -7, -9, -10, -12, -13, -19, and -26 contain AP-1 binding promoter sites and TATA-binding sites. Just TATA-binding sites belong to MMP8, MMP11, and -2. On the other hand, MMP1, -2, -8, -9, -11, -13, -14, -15, -17, -19, -23, -25, -26, TIMP2, and -4 show canonical NF- $\kappa$ B binding sites in their promotor (Clark et al., 2008).

Elicitors of their active forms are cytokines, which can trigger the TFs, that enable their gene expression. Their protein regulation is also enabled by their processing and generating active forms, which are possible and executed by their inhibitors (TIMPs). The main signalling axis found to be underlining the MMPs' positive regulation has been focused on NF- $\kappa$ B, PI3K, and JNK signalling (B. A. Brown et al., 2017).

Multiple atheromas-relevant inflammatory cells participate in the production and secreting of MMPs (Fig. 9), including ECs, VSMCs, neutrophils, lymphocytes, and at large fibroblasts and macrophages, (MacColl & Khalil, 2015).

Atherosclerosis-relevant cells, ECs, and VSMCs express MMP-1, MMP-2, MMP-3, MMP-7, and MMP-9. Fibroblasts and smooth muscle cells express MMP-12 (Sansilvestri-Morel et al., 2006). Platelets are found to be the source of MMP-1 and -2 (Seizer & May, 2013).

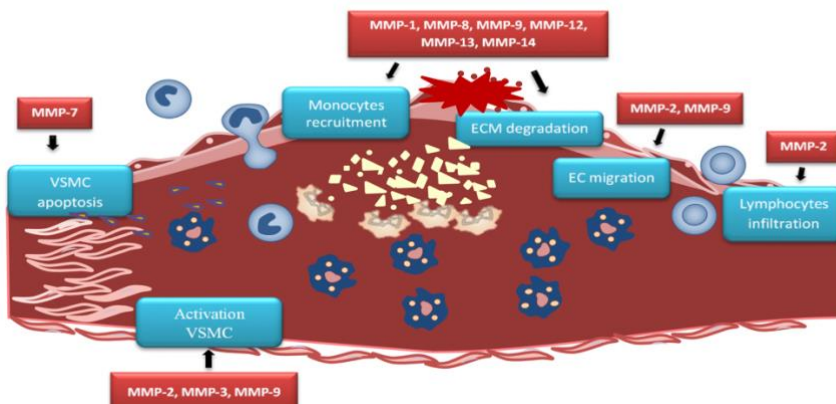


**Figure 9. MMPs in atherosclerotic plaque.** MMP-7 activity elicits VSMC apoptosis, giving rise to atheroma instability. MMP-1, MMP-8, MMP-9, MMP-12, MMP-13, and MMP-14 enable ECM degradation. MMP-2 and MMP-9 regulate endothelial cell (EC) migration. MMP-2 enables lymphocyte infiltration. MMP-2, MMP-3, and MMP-9 activate VSMCs (Olejarz et al., 2020).

MMPs have been heavily implicated in the arterial wall ECM remodelling and, thus, atherosclerosis (Fig. 9) through the inflammation elicitation (J. L. Johnson, 2017). EC-derived MMP-2 synthesis can induce endothelial dysfunction (Carmona-Rivera et al., 2015). Moreover, by synthesising MMP2 upon reactive-oxygen species (ROS) stimulation, it has been shown that endothelial cells are enabled to digest the basement membrane (Belkhiri et al., 1997). Lozito and his team demonstrated that MMP-2 secreted from ECs instigates remodelling of the ECM (Lozito & Tuan, 2012).

Moreover, EC-derived MMP-2 vesicles also stimulate the blood vessel formation and development of the atheroma vulnerability (Moreno et al., 2004). Studies performed on atherogenic prone-*ApoE*<sup>-/-</sup> mice have shown that reducing the activity of MMP-2 limits the formation of atherosclerotic lesions in the aorta (X. W. Cheng et al., 2011). Moreover, another endothelial-derived protease, MMP-1, is paramount in remodelling atherosclerosis lesions as its expression is initiated in ECs upon their interaction with monocytes and stability (Hojo et al., 2000).

Macrophages are the biggest producers of the MMPs in atherosclerotic lesions. MMP media mediates several macrophage functions, such as intimal invasion, ECM deterioration, and atherosclerotic rupture. Enhancement of MMPs expression in macrophage-rich lesion areas suggests their essential role in developing vulnerable regions of atherosclerotic plaques (Shah et al., 1995). Upon differentiation of human monocytes to non-foamy macrophages, increases of MMP-7, -8, -9, -14, and -19 and tissue inhibitors of MMP (TIMPs), -1 to -3 are observed (Newby, 2016). GM-CSF, a differentiation factor, elicits macrophage MMPs such as MMP-12, whereas IFN- $\gamma$  stimulates MMP-12, -14, and -25 production and negatively regulates TIMP-3 in human macrophages. At the same time, M2 skewing has been shown to stimulate the expression of murine and human MMPs, which emphasises their role not just in elicitation but in inflammation resolution as well (Newby, 2016).

Finally, MMPs, by remodelling the extracellular matrix, impact VSMC cells by instigating their migration and proliferation. Namely, MMP2 upon the cytokine stimulation such as IL-1 $\beta$  and oxLDL stimulation triggers the VSMCs proliferation (M.-S. Chen et al., 2018). While TNF- $\alpha$  stimulation induces the MMP9 upregulation and enables the VSMC migration (R. Guo et al., 2008).

Most of the vascular wall atheroma-contributing cells can modify their local surrounding by ECM remodelling through the MMPs production that affects their signalling or aim to alternate local cell interactions that all eventually does indeed, therefore, impact atherosclerosis development, plaque stability, and plaque remodelling (Olejarz et al., 2020).

### 1.4.2.3 Tissue inhibitors of metalloproteinases

An imbalanced ratio amidst the synthesis of MMP enzymes and their endogenous inhibitors (TIMPs) can potentially exacerbate pathological phenotype encountered in lesions under the atherogenic inflammation (Brew & Nagase, 2010).

Tissue inhibitors of metalloproteinases (TIMPs) are directly broad-spectrum endogenous inhibitors of MMPs and indirectly atherosclerosis development regulators (Brew & Nagase, 2010). The first inhibitor of MMPs to be discovered was TIMP-1 in the early 1970s, and it was described as a collagenase inhibitor in the media of cultured human skin fibroblasts (Bauer et al., 1975). Since then, four more TIMPs with different inhibition spectrums have been discovered. There are four described TIMPs. They have two distinct domains, an N-terminal domain that interacts with the catalytical domain of MMPs and a C-terminal domain with an unknown long-term function (**Fig. 10**) (Williamson et al., 1990).

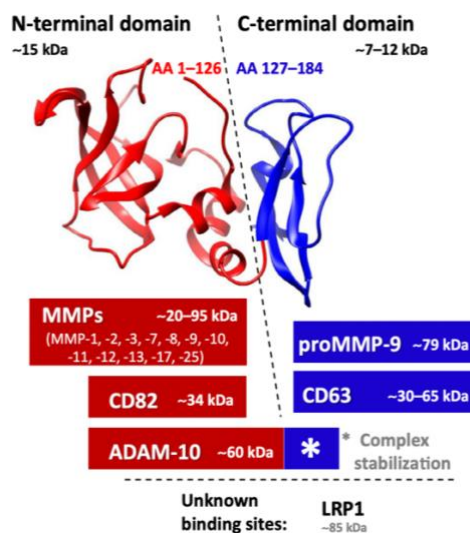


**Figure 10. The structure of the TIMP-1.** The N-terminal domain inhibits several MMPs and membrane-located metalloproteinase ADAM-10 and enables CD82 interaction. The C-terminus: interacts with prompt-9 and cell receptor CD63. (Grünwald et al., 2019).

The four TIMPs effectively inhibit 28 MMPs (Brew & Nagase, 2010). TIMP1 is a potent inhibitor of many MMPs except for some membrane-type (MT)-MMPs, including MMP-14, -15, -16, -19, and -24 (Baker et al., 2002). TIMP-1 and -3 are structurally glycoproteins, whereas TIMP-2 and -4 do not contain carbohydrates (Murphy & Nagase, 2008). Moreover, the structures of full-length TIMP-1 and TIMP-2 have been determined by X-ray crystallography, thus their interaction with the MMPs as well (Brew & Nagase, 2010; Fernandez-Catalan et al., 1998; Iyer et al., 2007). The TIMPs are extracellular/secreted proteins but can be bound to a cell membrane-associated proteins (Baker et al., 2002). TIMPs, next to being MMPs inhibitors, also enable the processing of the cytokines, chemokines, and growth factors, thus regulating the inflammatory state of the plaques (Ries, 2014). Their network includes regulating the MMPs that modulate the functions of cytokines (CCL7, CCL13, CCL13, CCL25, CXCL2, and CXCL5) through precise processing and regulate the inflammatory response, as well as MMPs that cleave cytokines and enable their release (IFN1 $\alpha$ , TNF $\alpha$ , IL-1 $\beta$ , TGF $\beta$ ) (Young et al., 2019).

Particularly the TIMP-1 molecule has a part of a highly unexplored, large network of interactions (Grünwald et al., 2019). Firstly, TIMP-1 inhibits activity via its N-terminal domain binding to at least 14 MMPs, regulating important biological activities

of 10-60 substrates of each MMP target (Jobin et al., 2017). Secondly, cell surface TIMP-1, by inhibiting surface metalloprotease Adams, such as ADAM-10, regulates processes such as shedding cell surface molecules and thus might participate in governing leukocyte recruitment, cell interactions, and endothelial permeability (Ponnuchamy & Khalil, 2008).

Adenoviral administration and TIMP-1 addition ablate the incidence of atherosclerosis (Silence et al., 2002). At the same time, the loss of TIMP-1 expression reduces SMCs content in the brachiocephalic artery of ApoE-depleted mice (Di Gregoli et al., 2016a). Moreover, macrophage and lipid elevation in the atheroma of the atherogenic-prone mice that were *TIMP-1* depleted have been demonstrated (Silence et al., 2002). Yet another study has shown a decrease in atherosclerosis in the aortic root upon *Timp1* depletion *in vivo* (Rouis et al., 1999). Finally, what makes the TIMP-1 a possible biomarker in the progression of atherosclerosis is that its levels were shown to be impaired in the patient's plasma that had instigated a vulnerable type of lesion compared to those with the stable atheroma (Sapienza et al., 2005).

Moreover, TIMP-1 can trigger downstream cell signalling by interacting with two cell-surface integrins, CD63 and CD82, which downstream trigger either PI3K and/or MAPK cell signalling that will mediate intracellular cell signalling that can regulate the cells' survival or trigger fibrosis (Grünwald et al., 2019). TIMP-1, by triggering the CD63/PI3K, downregulates the processes underlining the EC apoptosis, thus regulating atherosclerosis relevant EC turnover (Boulday et al., 2004).

*TIMP-2* gene loss *in vivo* causes plaque vulnerability and atherosclerotic plaque size in brachiocephalic arteries, as well as eases up the monocyte/macrophage accumulation increase via the MMP-14 activity enhancement (Di Gregoli et al., 2016a).

In human atherosclerosis progression, modulation of the MMPs/ TIMPs ratio is critical in the pathogenesis outcome of CVDs, and it is a possible underlining cause of human plaque vulnerability (Raffetto & Khalil, 2008; Sapienza et al., 2005). Increased serum-derived MMP-2 and MMP-9 as a consequence of the inability of TIMPs to regulate their levels and activity are predictive biomarkers in the detection of vulnerable plaques as well as adverse cardiovascular events, response to the therapy as well as mortality rate (Koenig & Khuseyinova, 2007; Loftus et al., 2000; Olejarz et al., 2020; Sapienza et al., 2005).

LRP1 is a universal cell surface receptor that recognises and internalises multiple ligands and regulates the process of endocytosis. LRP1 transduces multiple intracellular signal pathways, thus regulating the inflammation and tissue repair in various tissues and the vasculature (Potere et al., 2019). In atherosclerosis studies, its role can be dual in macrophages and VSMC cells *in vitro* and *in vivo*. The LRP1 can be either atheroprotective, as it aids macrophages to export excess cholesterol. Still, it can also skew and trigger inflammations and athero-progressive effects as it promotes foam cell formation and efferocytosis in macrophages. LRP1 is also expressed in endothelial cells and controls hypoxia-induced proliferation and migration, and it has anti-inflammatory effects (J. Chen et al., 2021). LRP1 is an important surface interaction partner of TIMP1, as it binds TIMP-1/pro-MMP9 and TIMP-1/MMP9 hetero-complex and causes their degradation upon endocytosis. At the same time, TIMP-1-LRP1 interaction exerts TIMP-1 cytokine-like properties (Thevenard et al., 2014).

TIMP-1 possesses multiple regulatory elements in its promoters such as AP-1 proximal cis-acting elements, retinoic acid-responsive elements, GC-rich binding sites, ETS, SRE regulatory elements as well as NF- $\kappa$ B responsive elements (Clark et al., 2008; S. Lin et al., 2006; Logan et al., 1996; L. Tong et al., 2004; Wilczynska et al., 2006a). C-Jun, c-Fos, and Jun-B are the transcriptional regulators of the proximal non-canonical TIMP-1 gene expression. While delayed canonical AP-1 response is

attributed to the TIMP-2 and TIMP-3 gene expression (Sampieri et al., 2008). TIMP1, TIMP3, and TIMP4 promoters also bind Runx1 and Runx2. TIMP2, TIMP-3, and TIMP4 promoters have canonical NF- $\kappa$ B regulatory binding sites. (Sampieri et al., 2008).

### 1.4.3 Current Therapy Approaches in Atherosclerosis

The underlining cause of cardiovascular events remains to be atherosclerosis. Therefore, the current therapeutical focus in primary and secondary prevention of main cardiovascular diseases aims towards reducing its incidence and stimulating its regression (Libby & Everett, 2019).

The main conventional risk factors for atherosclerosis are bad lifestyle choices (e.g. tobacco exposure, obesity, physical inactivity, and high alcohol use).

Non-conventional risk factors include medical conditions such as familial hypercholesterolemia, diabetes mellitus, and chronic inflammatory diseases (for example, rheumatoid arthritis-RA) (Libby et al., 2019).

Atherosclerosis onset or progression is reversible by taking up a healthier lifestyle as an act of a primary prevention measure. Prevention is effective in combating any stage of atherosclerotic disease. (Libby et al., 2019; Piepoli et al., 2016).

Dyslipidemia is a hallmark in instigating atherosclerosis. Lipid-lowering therapy remains the most important therapeutic strategy in the atherosclerotic disease management (Soehnlein & Libby, 2021). Several clinical trials corroborated that lipoprotein decreasing lowers the incidence rate and the risk of CVD events, while with its increased serum levels, atherosclerotic lesions are initiated (X. Su et al., 2021).

Statins are up-to-date the leading therapy in the management of CVDs in a daily practice (X. Su et al., 2021). They are essential for inhibiting the enzymes in the cholesterol production (Libby et al., 2019). Several clinical trials over the years have demonstrated the benefits of statin therapy in CVD prevention, such as the study termed ‘4S’, ‘LIPID’, as well as ‘JUPITER’ (Novack et al., 2012; Simes et al., 2002; X. Su et al., 2021).

Next to lowering LDL levels, statins also improve EC function and reduce inflammation (Wagner et al., 2000). Moreover, lipid-lowering therapy has effectively decreased interactions between ICAM-1 and T cells and reduced the neutrophil transmigration (Weitz-Schmidt et al., 2001; Y.-C. Zhu et al., 2019). Although the efficacy of statins enables a 30–50% reduction in LDL levels, the efficacy of treating patients with familial hypercholesterolemia or statin intolerance can be challenging and may demand therapy combination in preventing cardiovascular events and anti-inflammatory therapies have given rise to a new secondary prevention (Libby & Everett, 2019). Hence several randomised human trials have demonstrated that CVD patients could benefit further from lipid-lowering therapies if they also tackle the incidence rate of inflammation (Bohula et al., 2015; Ma & Chen, 2021; Nissen et al., 2005; Ridker, 2019; Ridker et al., 2005).

Many anti-inflammatory clinical trials have been conducted over the years. All existing therapies can be classified into two categories, therapies with clear targets and broad-spectrum anti-inflammatory approaches (Ma & Chen, 2021). Interestingly most successful anti-inflammatory therapies in the past have all focused on targeting NLRP3 (NOD-like receptor family, pyrin domain-containing protein 3) inflammasome as a therapeutic target (Libby & Everett, 2019).

Therapies with a clear target include tocilizumab, anakinra, and canakinumab. CANTOS was the first clinical trial to demonstrate effectiveness in targeting

inflammation as therapeutically relevant in tackling atherosclerosis (Ridker et al., 2017; Soehnlein & Libby, 2021).

The IL-1 family of cytokines is composed of IL-1 $\alpha$  and IL-1 $\beta$ . IL-1 $\alpha$  exerts its activity through the annealing to and cell surface-bound IL-1R. (Isoda & Ohsuzu, 2006; Tousoulis, 2017). IL-1 $\alpha$  is at large acts bound at the plasma membrane, whereas IL-1 $\beta$  acts systemically (Dinarello, 2009). IL-1 $\beta$  is important in developing the atherosclerosis (Bevilacqua et al., 1985; Khan et al., 2015; Tamaru et al., 1998).

Canakinumab was developed as a selective human monoclonal IL-1 $\beta$  antibody tested in the CANTOS trial on patients that sustained acute myocardial infarction. This trial employed patients with persistently elevated inflammatory markers such as CRP (Ridker, 2013; Ridker et al., 2017; Soehnlein & Libby, 2021). Canakinumab enables the IL-6 lowering and fibrinogen in patients suffering from diabetes (Ridker et al., 2012). The results show that canakinumab significantly reduced markers of inflammation and lowered cardiovascular events (Ridker et al., 2017). Although showing promising results, Canakinumab has not been approved in general clinical practice so far. Its high price largely determines this, and the application invoked a possible risk of elevated infection (Ma & Chen, 2021; Ridker et al., 2017).

Yet another anti-inflammatory therapy aimed at targeting IL-1 signalling. Anakinra is developed as an inhibitor of IL-1 $\beta$  activity. Although it benefited the patients with RA, CAD events were significantly improved compared to the placebo group (Ikonomidis et al., 2008). The clinical MRC-ILA-HEART Study showed that therapy with anakinra did not reduce inflammatory markers or subsequent cardiac events (Khan et al., 2015).

IL-6 levels were also found to be crucial in determining the incidence and rate of CVDs. IL-6 originates from macrophages, ECs, fibroblasts, and adipose tissue (Recinos et al., 2007; Sukovich et al., 1998). IL-6 cytokine exerts its activation via MAPK signalling systems, and it promotes ECD, VSMC migration, and macrophage to foam cells differentiation (Keidar et al., 2001; Khan et al., 2015). Thus, researchers have been set on investigating the anti-IL-6 antibody therapeutic strategy, named tocilizumab, and its effects on CVDs in several clinical trials.

The effect of tocilizumab was evaluated in the 'STEMI' clinical trial (Anstensrud et al., 2019). The trial results publicised in 2020 demonstrated that tocilizumab therapy acted beneficially on MI patients. Therefore, IL-6 is considered a good candidate for developing anti-inflammatory therapeutics (Ma & Chen, 2021).

Broad-spectrum inhibitors include employing methotrexate and colchicine.

Methotrexate in higher doses serves as chemotherapy, but it has anti-inflammatory properties at lower doses (Ridker et al., 2019). Although methotrexate is effective in RA patients by reducing inflammatory markers, mortality, and overall cardiovascular events of atherosclerosis, recently published results of the CIRT show that the clinical trial did not yield fewer cardiovascular events (Khan et al., 2015; Ridker et al., 2019).

The most promising broad-spectrum anti-inflammatory drug in clinical use currently is colchicine. Colchicine inhibits the NLRP3 inflammasome (Slobodnick et al., 2018). NLRP3 inflammasome has been studied extensively in CADs and the atherosclerosis (Arbel et al., 2018; Martínez et al., 2018; Toldo & Abbate, 2018). Colchicine has been previously used to treat inflammatory disorders such as pericarditis (Lorenzatti, 2021). The mechanism underneath the colchicine affects the NLRP3 assembly inhibition (Gorp et al., 2016; Martinon et al., 2006; Misawa et al., 2013). In the LoDoCo study, colchicine has been shown to reduce the incidence of cardiovascular events (Nidorf et al., 2013). A recently publicised COPS clinical trial report in 2020 dismissed the use of colchicine as an addition to the classical therapy as it didn't yield promising effects and

lowering of CVD events but was strikingly associated with an elevated mortality rate (Ma & Chen, 2021; D. C. Tong et al., 2020).

## 1.5 COP9 Signalosome<sup>1</sup>

### 1.5.1 Structure and Function

The CSN is a protein complex found in all species, with an isopeptidase and docking platform functions, comprising 8 subunits designated as CSN1–CSN8 by decreasing molecular weight from 57 to 22 kDa (Lingaraju et al., 2014; Milic et al., 2019). Chamovitz and his team originally described the CSN multi-protein complex in cauliflower. It has been described as a regulator of the plant photo-morphogenesis development patterns necessary for its dark-grown growth phases. Hence it was appropriately termed constitutive photomorphogenesis 9 (COP9) (Chamovitz et al., 1996). The CSN was described initially in mammals in pig spleen and human erythrocytes (Seeger et al., 1998; Wei & Deng, 1998).

The CSN (**Fig. 11A**) is a 400 kDa molecular size complex. Its subunits CSN1, -2, -3, -4, -7, and -8 have structurally a PCI (proteasome, COP9 signalosome, translation initiation factor) domain, while CSN5 and -6 have an MPN (MPR1/Pad1-N-terminal) domain (**Fig. 11C**) (Hofmann & Bucher, 1998; Wei et al., 2008). These structural characteristics exist next to the CSN holo-complex in the 19S lid of the proteasome complex and eukaryotic translational initiation factor 3 (Hofmann & Bucher, 1998).

CSN's crystal structure was only published in 2014 at a resolution of 3.8 Å, and it shed light on its assembly. Whereas the CSN complex harbours two organisational centres. Therefore, the PCI domain provides a scaffolding function and a fully assembled catalytical centre. They are all organised as previously described in a 'horseshoe shaped-open ring' formation in a 'CSN7–CSN4–CSN2–CSN1–CSN3–CSN8 manner', associated by their PCI winged-helix (WH) subdomains to form WH subdomain 'composite β-sheet' at the centre of the CSN complex (**Fig. 11B**). While their C-terminal helices, formed a second organisational centre, a helical bundle, over the PCI ring. While the CSN5 and CSN6 MPN domains form a pseudo-dimer and interact before entering and interacting with the helical bundle of the rest of the subunits, interestingly, in the assembly, CSN5 can enter an already organised and formed seven-subunit complex. Interestingly, in mammals, the absence of CSN8 and CSN3 was permissive for CSN5 to integrate into the complex, while the absence of the rest of the four subunits didn't permit it (Lingaraju et al., 2014). The CSN5 and CSN6 are in the centre of the PCI, forming six subunit-bundle. CSN5, as a carrier of an isopeptidase function of the complex, is a metalloprotease with a conserved JAB1 MPN domain metalloenzyme (JAMM) motif and requires a zinc ion as an activator in its catalytical centre for demethylase activity (**Fig. 11D**) (Cope et al., 2002; Peng et al., 2001). All eight subunits are required for the complex to function *in vitro* (Sharon et al., 2009). The loss of any subunit of the complex is lethal in the development of plants or lethal at the embryonic stage in mice (Wei et al., 2008).

---

<sup>1</sup> Part of this introductory chapter has been published in my first author review article Milic, J., Tian, Y., & Bernhagen, J. (2019). Role of the COP9 Signalosome (CSN) in Cardiovascular Diseases. *Biomolecules*, 9(6), 217.

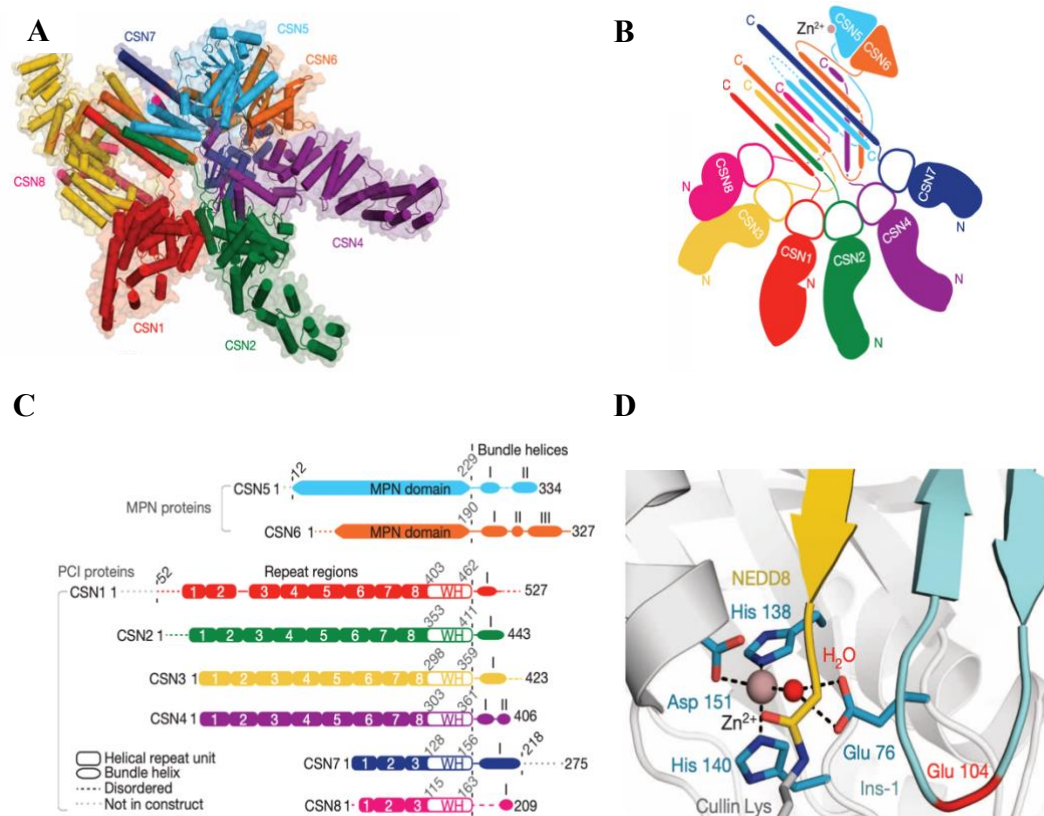


**Figure 11. COP9 signalosome structure.** **A** Schematic representation of the CSN holo-complex. **B**, 2D CSN structure representation. The WH subdomains forming the 'PCI ring' are shown as white rings. Two-component organisational centres of the complex stand in the CSN5–CSN6 dimer, while the remaining subunits surround them, forming the CSN holo-complex. **C**, Domain organisation of the CSN subunits (detailed descriptions are found in the main text). **D**, Schematic representation of the CSN5 catalytical centre, JAB1 MPN domain metalloenzyme (JAMM) motif, where the CRL–NEDD8 isopeptide bond (yellow) is being cleaved on a zinc ion-dependent manner (Lingaraju et al., 2014).

The CSN has been shown to regulate different biological functions: embryonic development, cell cycle progression, cell signalling transmitting, T-cell development, autophagy and circadian rhythm (Kato & Yoneda-Kato, 2009). Its involvement in inflammatory processes upon atherogenic and cancerogenic progression has also been demonstrated (Asare et al., 2017; Deng et al., 2011).

The CSN has 3D- structural similarity to the 19S proteasome lid (Cope & Deshaies, 2003; L. Li & Deng, 2003; Lingaraju et al., 2014). The most recognised intracellular function linked to the CSN it is its capacity to regulate protein stability by governing the activity of CRLs, i.e.ubiquitin ligase, by deNEDDylation.

CRLs are a family of proteins that are an essential part of the UPS(ubiquitin-proteasome system).The proteasome is accountable for 90% of all intracellular protein degradation in eukaryotic cells (Powell, 2006). Although some of these proteins will bind directly to the proteasome, some of the proteins need ubiquitination labelling and will be only in such a manner directed to the proteasome. Ubiquitination (Fig. 13A) involves three successive processes for successful proteasome targeting: ubiquitin-activating enzyme-E1 mediated activation, ubiquitin-conjugating enzymes E2 mediated-transfer, and ubiquitin-protein ligase family E3 mediated conjugation (Ciechanover & Schwartz, 1998; Powell et al., 2012). Whereas humans possess two E1- enzymes

(UBA1 and -6), 30 E2 enzymes, and over 600 different E3 ligases (Nguyen et al., 2017; van Wijk & Timmers, 2010). The big diversity in E3 ligases, compared to the rest of the ubiquitination cascade, is the result of their necessary selectivity towards the substrate, which will be degraded. E3 ligases belong to one of the three families: HECT E3 ligases, RING and U box E3 ligases, or the RBR E3 ligases (Berndsen & Wolberger, 2014).

The RING family E3 ligases are the most dominant (Deshaies & Joazeiro, 2009). Almost 20% of cell ubiquitination happens by employing RING-type CRLs (Petroski & Deshaies, 2005; Soucy et al., 2009). Overall CRLs have a modular and exchangeable structure (Fig. 12) consisting of four essential components: a cullin scaffold; a ‘RING protein’ that harbours E2 enzyme; a ‘substrate receptor’ that enables specific recognition of its substrates; ‘adaptor’ protein that stands amid the ‘substrate receptor’ and the cullin scaffold (Nguyen et al., 2017).

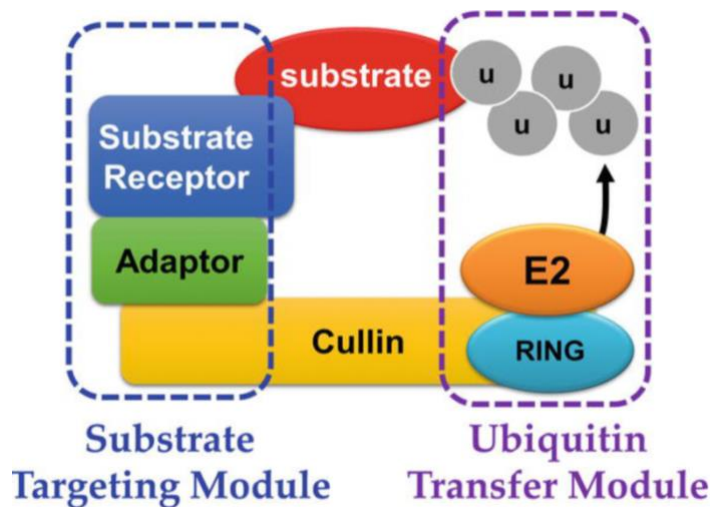


**Figure 12. The modular structure of the CRL E3 ligases.** Dotted outlines show the substrate hosting (blue) section and ubiquitin transfer (purple) modules of CRLs. Overall CRLs have a modular structure consisting of a cullin scaffold, RING protein, substrate receptor, and adaptor proteins. U- ubiquitin. (Taken from: Emanuele & Enrico, 2019).

In mammals, there are 7 known cullin proteins: Cul1, -2, -3, -4A, -4B, -5, and -7. RING proteins (Rbx1 or Rbx2) bind to the C-terminus of the cullins (Nguyen et al., 2017). The cullin N-terminus scaffold docks the adaptors (Skp1, Elongin BC, BTB proteins, DDB1). Each adaptor has the capacity to bind to a family of ‘substrate receptors’ (Nguyen et al., 2017; Sarikas et al., 2011).

To serve the dynamic demands of the intracellular signalling environment and homeostasis maintenance, CRLs are regulated by post-translational modification and the exchange of the 4 CRL subunit modules (cullins, RING proteins, adaptors, receptors) (Nguyen et al., 2017).

CRLs are only active with a covalent attachment of the Neural precursor cell Expressed Developmentally Down-regulated protein 8 (NEDD8). NEDDylation (Fig. 13A) is enabled by employing three sequential enzymes similar to the ubiquitination cascade, ‘E1 NEDDylation activating enzyme’ (NAE), a heterodimer of NAE1(APPBP1)/UBA3, an ‘E2 NEDDylation -conjugating enzyme’ (UBC12/UBE2M and UBE2F), and one of the several E3 NEDDylation ligases (Hori et al., 1999). A distinctive step between NEDDylation and ubiquitination is the NEDD8 ligation step (Fig. 13) as NEDDylation E3 ligase (Rbx1 or Rbx2) demands a co-E3 ligase termed ‘Defective in Cullin Neddylation 1’ (DCN1) (Kurz et al., 2005). CRLs require NEDD8

conjugation occurring at the C-terminal -Lys, which enables their structural-conformational change, which detaches the CRLs from its negative regulators (Duda et al., 2008; Zheng et al., 2002; L. Zhou, Jiang, Luo, et al., 2019). Cul1, -2, -3, -4A, and -5 of a CRL bind CAND1, which is their negative regulator, and which acts as their assembly inhibitor that blocks their N- and C-terminus, and thus enables assembly of only functional CRLs promptly (Duda et al., 2008; Goldenberg et al., 2004; J. Liu et al., 2002; Wolf et al., 2003; Zheng et al., 2002).

DeNEDDylation opposes the process of NEDDylation. It is carried out by isopeptidases termed deNEDDylases (Enchev et al., 2015). The CSN's best-studied function is its deNEDDylase activity.

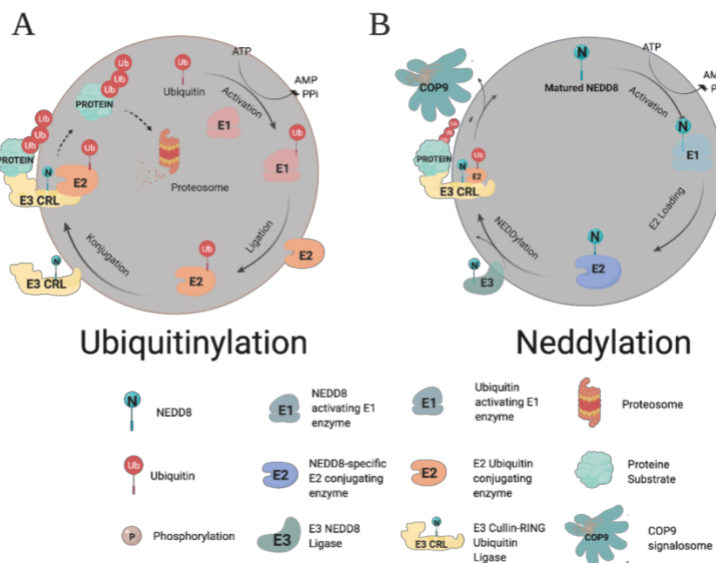


**Figure 13. Comparable ubiquitination and neddylation cascades.** **A,** Ubiquitination: Cascade is enabled, and acts through E1, E2, and E3 enzymes, eventually giving rise to ubiquitin (Ub) ligation to a target substrate that is about to undergo degradation via the proteasome. **B,** The NEDDylation Cascade. NEDD8 ligation to a target substrate acts through E1, E2, and E3 enzymes. DeNEDDylation is enabled by COP9 signalosome, which cleaves NEDD8 from its targets (CRLs), releasing NEDD8. Legends are presented at the bottom of the figures (Created with BioRender.com).

Next to the CSN holo-complex are several other deNEDDylases (Kandala et al., 2014; Watson et al., 2011). NEDP1 (DEN1/SENP8), next to the CSN holo-complex, can recognise NEDD8-specific substrates; all the others are also catalysing deNEDDylation deubiquitylation (Kandala et al., 2014; Rabut & Peter, 2008; Xirodimas, 2008). The other deNEDDylases operate under homeostatic cellular conditions and are considered the canonical pathway of the neddylation (Lobato-Gil et al., 2021). Non-canonical neddylation pathways have been recently described in a certain pathological setting. It has been shown that neddylation can occur on non-cullin targets outside of the previously described cellular proteome and regulate different cellular functions such as transcriptional factors, synaptic plasticity, and DNA damage response. It is still under investigation (Lobato-Gil et al., 2021).

NEDD8 shares 58% homology with ubiquitin. Hence it is referred to as a ubiquitin-like modifier (UBL), and it covalently binds to a conserved lysine (Lys- 720 in CUL1) at the C-terminal cullins (Lydeard et al., 2013).

The CSN5 subunit is the subunit of the CSN that has a catalytic centre to perform deNEDDylase activity, which only is possible as part of the CSN holo-complex (Lingaraju et al., 2014). In that manner, the CSN holo-complex inhibits CRLs by

removing the NEDD8 from its axis. CSN also has low-affinity binding to deNEDDylated CRLs, but on the other hand, favours NEDDylated CRLs. COP9 can also bind the CRL assembly inhibitor CAND1, which is related to the exchange between the active and inactive state of CRLs and their modular structure exchange (Pierce et al., 2013; Zheng et al., 2002).

The targets affected by disturbing the NEDDylation regulation process are previously under the immune regulation of cancer, CVDs, as well neuroinflammation, and metabolic disorders (Asare et al., 2017; H.-S. Park et al., 2016; Soucy et al., 2010; Vogl et al., 2015; X. Zhang et al., 2020). NEDDylation was identified in regulating atherosclerosis-relevant cells such as neutrophils, myeloid cells, VSMCs, ECs and T cells, where it impacts their cell metabolism, survival, autophagy, cytokine production, maturation, proliferation, mitochondrial turnover (J. Li et al., 2020; Lu & Yang, 2020; Milic et al., 2019). Proteosome-mediated degradation in atherogenic inflammation dependent on the neddylation/de-neddylation cycle of CRL regulation. One of the renowned CRLs is the  $\text{SCF}^{\beta\text{-TRCP}}$  E3 ligase complex, which targets  $\text{I}\kappa\text{B-}\alpha$ , as well as checkpoint control proteins such as Wee1 and Cdc25A. Nrf2 is another target and an anti-inflammatory regulator recognised by the Keap1 adaptor of CRLs (Cul3KEAP1), inhibiting its gene expression and targeting it for the proteasome (Cullinan et al., 2004). Moreover, p27KIP1, as cell proliferation and vascular remodelling factors in atherosclerosis, is targeted to degradation via active  $\text{SCF}^{\text{Skp2}}$  E3 ligase (Breitenstein et al., 2013; Suzuki et al., 2014). HIF-1 $\alpha$ , an important regulator and promoter of atherosclerosis under hypoxic atherosclerosis conditions, is also UPS-degraded via the Cul2<sup>VHL</sup> E3 ligase (Aarup et al., 2016). CSN also stands behind the degradation of the inflammatory proteins such as p53, 14-3-3 $\sigma$ , or c-Jun by regulating the stability of the CRLs, as MDM2 and COP1 (Bianchi et al., 2003; H. H. Choi et al., 2011; Milic et al., 2019; X.-C. Zhang et al., 2008).

The CSN also can serve as a scaffold for several important, including casein kinase II (CK-2) or protein kinase D (PKD). Thus it participates in their kinetic activity and control (Seeger et al., 2001; Uhle et al., 2003). Furthermore, COP9 binds directly to inflammatory mediators such as MIF, p53, c-Jun, Smad4, and LFA (Bianchi et al., 2000; Claret et al., 1996; Kleemann et al., 2000). Moreover, CSN can recruit USP15 and thus regulate deubiquitinase (DUB) in the NF- $\kappa$ B signalling (Schweitzer et al., 2007). Finally, as previously mentioned, an essential interacting partner of the Csn5 outside the complex is AP-1 signalling, where Csn5 stabilises the AP-1 signalling axis (Claret et al., 1996; Echalier et al., 2013). Thus, the CSN is deemed important in regulating atherogenic inflammation by governing neddylation/de-neddylation of the CRLs and consequently determines the proteosome-mediated degradation by controlling the ubiquitination and deubiquitinating of target proteins by docking kinases and controlling the stability of pro-inflammatory and anti-inflammatory signalling axis and by regulating gene expression and stability of its interacting partners.

### 1.5.2 Function in atherosclerosis

#### 1.5.2.1 CSN5 in atherogenic inflammation

CSN5 is the CSN subunit that carries catalytical activity and can act as a part of the complex or as a transcriptional coactivator (Wei & Deng, 2003).

Besides, a reduction of NF- $\kappa$ B activation, an increase in the phosphorylation of its inhibitor  $\text{I}\kappa\text{B}\alpha$ , and consequently a reduction in the inflammatory response has been observed in ECs upon loss of the CSN5 unit of COP9 signalosome (Asare et al., 2013b;

F.-M. Chang et al., 2012; Ehrentraut et al., 2013; Swords et al., 2015). This suggests that CSN5 negatively governs NF- $\kappa$ B-regulated gene expression and monocyte capture on ECs *in vitro*. Still, *more* importantly, its loss in a myeloid-specific manner exacerbates atheroprotection *in vivo* (Asare et al., 2017).

CSN5 is abundantly found in the EC lining of human CEA plaque, and with the atheroprotection *in vivo*, CSN5 levels were found to be elevated in the intima (Asare et al., 2013b). *Csn5* *in vitro* siRNA silencing in human endothelial cells causes destabilisation of the CSN holo-complex, impaired CRL deNEDDylation, I $\kappa$ B $\alpha$  degradation, enhanced NF- $\kappa$ B activity, thus untimely increased adhesion molecules gene expression and consequently more pronounced monocyte arrest *in vitro* (Asare et al., 2013b).

Moreover, CSN5 also is significant in regulating the endothelial barrier and its integrity by regulating actin dynamics via RhoGTPases. Namely, loss of E3 CRL functions results in F-actin stress fibres in the endothelial lining and RhoB-dependent loss of endothelial barrier function. Thus, pharmacological CSN5 inhibition *in vitro* has shown a loss of endothelial barrier function in human endothelial cells (Majolée et al., 2019).

Nitric oxide and endothelin released from ECs are prominent regulators of the vascular function (Masaki & Sawamura, 2006). During atherosclerosis development, endothelial dysfunction enhances the synthesis and circulatory levels of, ET-1 which, in turn, acts in a paracrine manner, inducing vasoconstriction by signalling on the smooth muscle cells. CSN5 overexpression in HEK293 cells stimulates the ubiquitin-mediated degradation of ET(A)R after the protein synthesis (Nishimoto et al., 2010). These receptors were found abundantly on medial vascular smooth muscle cells, which is how ET-1 exerts its vasoconstrictive function (Rich & McLaughlin, 2003). As ET-1 aggravates atherosclerosis, the inability to exert its effects might be athero-protective upon CSN5 overexpression. Therefore, *in vitro* studies have shown CSN5 overexpression to be beneficial and its loss to compromise endothelial integrity and activation.

More is known and studied about the role of the CSN's subunit CSN5 *in vivo* in myeloid cells upon atherosclerosis progression. As the macrophages are leading the atherosclerosis progression, loss of CSN5 was studied on their cellular inflammatory signalling. It has been reported that myeloid specific-CSN5 loss lowers the levels of I $\kappa$ B $\alpha$  and instigates p65 transcription, lowering the HIF-1 $\alpha$  transcription in murine myeloid cells *in vivo*. While on the other hand, 'CSN5 hyperactivity' abolishes cytokine and chemokine expression (Asare et al., 2017). Thus proposing that CSN5 is an important regulator of the inflammatory response in myeloid cells and essentially controls the atherosclerosis progression *in vivo*.

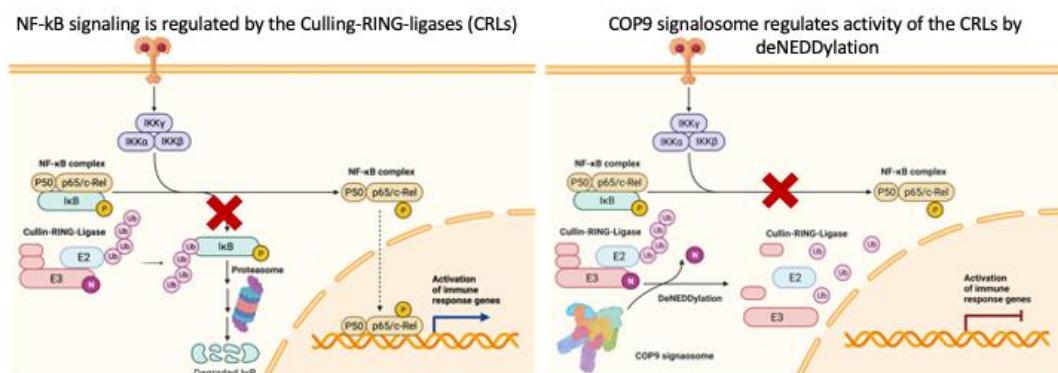


**Figure 14. COP9 regulates NF-κB signalling.** **A** Receptor on the surface is responsive to different stress signals and acts by positive regulation of the IKK complex activity. That is followed by the proteasomal degradation IκB $\alpha$  and positive regulation of NF-κB. **B**, Similarly, upon COP9 signalosome, exerted deNEDDylase upon E3-CRL activity, thus destabilising E3-CRL SCF $\beta$ -TrCP, inducing their disassembly attenuates proteasome-mediated IκB $\alpha$  degradation, thus ablation of NF-κB signalling. Abbreviations: IKK-, kinase complex; p50/p65- NF-κB heterodimer; E3- cullin-RING E3 ligase; E2- ubiquitin-conjugating enzyme; IκB $\alpha$ -inhibitor of NF-κB; Ub-Ubiquitin; N-NEDD8; (Created with BioRender.com)

Schwarz and his team further corroborated this. They studied the role of the CSN in macrophage-to-foam cell development and its effects on the NF-κB and MAPK signalling axis in macrophages upon oxLDL stimulation. Interestingly, it has been shown that under the oxLDL stimulation, expression of the CSN5 in macrophages/foam cells is altered upon p38 MAPK signalling employment, which for the first time emphasised in myeloid-derived CSN5's role in atherogenic stimulation. Conversely, previous studies for the first time showed that CSN5 silencing affects myeloid cells and depletes secreted levels of IL-6 and TNF $\alpha$  (Schwarz et al., 2017). This study also outlined the abundance of the CSN5 positive cells in a shoulder region of the atherosclerotic plaques of the hypercholesterolemic *ApoE*<sup>-/-</sup> mice, which might indicate its involvement in plaque stability as well (Schwarz et al., 2017).

As previously described, foam cell formation is mediated by scavenger receptors and several influx/efflux pumps. The macrophage cellular free cholesterol removal is enabled via HDL-mediated export, which requires the activity of ATP-binding cassette protein A1 (ABCA1) (Hsieh et al., 2014). Murine ABCA1 is degraded via proteasome (Nagelin et al., 2009; Ogura et al., 2011). The study by Azuma and co-workers has shown that CSN controls the ubiquitination and deubiquitylation of ABCA1. Both CSN2 and -5 subunits of the CSN were shown to be the players in poly-ubiquitinating ABCA1, and their over-expression has decreased ABCA1 degradation in murine foam cells (Azuma et al., 2009). Interestingly, another study corroborated this and found that another subunit of the CSN complex, Csn3, stabilises macrophage and smooth-muscle cells ABCA1 expression, rescues cholesterol discharge and reduces foam cell generation in atherosclerosis. The overall novel study suggests that COP9 holo-complex might be a relevant player rather than individual subunits of the CSN complex (Boro et al., 2021).

CSN5 subunit and the CSN, as previously mentioned, are the signalling platform of the regulators of the cell cycle mediators, proliferation factor, protein kinases, and deubiquitinates (DUBs) (Dubiel et al., 2020). The most important DUBs that interact with the COP9 signalosome are the ubiquitin-specific proteases USP48 and USP15. USP15 deubiquitylates IκB $\alpha$ , enhances its stability, and essentially contributes to the resolution of the NF-κB signalling (Schweitzer et al., 2007). In contrast, USP48 deubiquitinase has been shown to stabilise NF-κB transcriptional factor RelA nuclear pool (Ghanem et al., 2019).

Yet another important DUB has been found to interact with the CSN in macrophages named USP36 (ubiquitin-specific protease 36). USP36 has been shown to promote the macrophage antioxidative pathway by prompting CSN and SOD2 (superoxide dismutase 2) interaction (Pariano et al., 2021). The anakinra application Field promotes COP9/USP36/SOD2 interaction (Banda et al., 2005). Anakinra targets the inflammasome NLRP3 activity (Banda et al., 2005; Pariano et al., 2021). The inflammasome mediates cytokine production and contributes to the vascular inflammation driving atherosclerosis development and progression (Grebe et al., 2018). As anakinra promotes sustained COP9/USP36/SOD2 activity, thus inhibiting cytokine signalling and the inflammasome activity, it also exerts an overall strong anti-inflammatory response by inhibiting the p38 MAPK signal transduction pathway in

macrophages (Banda et al., 2005). Thus, the CSN could still promote the anti-inflammatory effects even by inverting the classical promotion of ubiquitination.

### 1.5.2.2 CSN8 in atherogenic inflammation

The CSN8 subunit, by being 21kDa in size, is the smallest subunit of the CSN complexes (C. Liu et al., 2013; J. Wang et al., 2010; Wee et al., 2002).

It was reported that loss of CSN8 *in vivo* impaired CSN complex assembly. CSN8, as an essential component of the CSN holo-complex, is deemed important for the fully functioning complex. For instance, it has been shown that germline loss of the CSN8 causes early murine embryonic lethality (C. Liu et al., 2013; Menon et al., 2007). Also, Csn8 conditional deletion throughout T-cell development has revealed its involvement in T-cell activation. It is crucial for quiescent T-cells response to the immune stimulation (Menon et al., 2007). In contrast, conditional deletion of CSN8 in the liver causes cell death and impedes liver regeneration (Lei et al., 2011). Additionally, a prior study testified that depletion of CSN8 is linked to UPS-mediated proteolysis in cardiomyocytes and severe defects in the autophagosome maturation (H. Su, Li, Menon, et al., 2011; H. Su, Li, Ranek, et al., 2011). Recent studies reinstated the myocardial transcriptome of CSN8-conditional knock-out mice and have outlined CSN8 importance as a transcription regulator of multiple cellular networks was revealed in oxidative stress, cytoskeleton dynamics, and intracellular vesicle maturation. Curiously, also it was outlined that CSN8 deficiency impairs histone gene expression. Hence, CSN8 might govern transcription via the chromatin remodelling (Abdullah et al., 2017).

Thus, although not previously explored in atherosclerosis, it could be hypothesised that CSN8 is essential in maintaining the structural integrity of the COP9 complex and the regulatory network behind the inflammatory process of atherosclerosis.

### 1.5.2.3 Potential therapies based on the CSN

Dysfunction of the UPS has been shown to alter atherosclerosis development, as proteasome activity is increased in early atherosclerotic plaques and unstable atherosclerotic lesions (Herrmann et al., 2002; Marfella et al., 2006). UPS dysfunction is specific to certain atherosclerosis stages (Wilck et al., 2017). As the proteasome regulates the degradation of 90% of all the cellular proteins, especially encompassing the signalling cascades underlying inflammatory pathways and regulators of oxidative stress, it has been investigated as a valid therapeutic target by employing its inhibitor bortezomib (Wilck et al., 2017).

Proteasome inhibitors have been investigated for their anti-inflammatory therapeutic potential. Their probing *in vitro* demonstrated application they impede NF-κB and their target genes (Ludwig et al., 2009). However, the *in vivo* application of bortezomib has revealed controversial effects in atherogenesis. Namely, inhibitor positively hinders an early lesion formation (Wilck et al., 2012). On the other hand, in explanted murine atherosclerotic plaques, the application of proteasome inhibitors bortezomib lowers SMC and macrophage content. *In vivo* application of the bortezomib promotes features of destabilising plaque phenotype in advanced plaques of *ApoE*<sup>-/-</sup> mice (Van Herck et al., 2010). Therefore, the therapeutic potential of UPS modulation in atherosclerosis treatment is still unclear. At the same time, it enables furthering the understanding of ubiquitin-proteasome axis-associated targets as a therapeutic option in the early lesion formation treatment. In comparison, most studies concluded that inhibition of

proteasome activity suppresses bulk intracellular protein turnover and can lead to adverse effects.

Among the ubiquitination-related players, the CSN, a critical UPS regulator and UBL post-translational modification regulator of neddylation/deneddylation, has emerged as a valid therapeutic target for probing atherosclerosis.

Currently, the therapeutic potential of targeting the CSN is mostly based on cancer trials, its underlying inflammatory pathways, and cardiovascular and neuronal diseases (Milic et al., 2019). This is due to its governing role in the cell cycle, apoptosis, UPS axis regulation, and complex interactome relationships that partly underly inflammatory responses.

One of the therapeutic approaches of modulating the UPS axis relates to modulating the neddylation cascade and leads to reductions in the degree of ubiquitination of certain substrates by impairing the neddylation of the responsible E3 ubiquitin ligase. In fact, the small molecule pharmacological inhibitor MLN4924 (Pevonedistat or 1S,2S,4R)-4-(4-(((S)-2,3-dihydro-1H-inden-1-yl)amino)-7H-pyrrolo [2,3-d] pyrimidine-7-yl)-2 hydroxy cyclopentyl methyl sulfamate) has been described in 2009 and has been shown to effectively ablate cullin NEDDylation by inhibiting NAE (Soucy et al., 2009). MLN4924 has been employed in cancer (non-haematological malignancies, acute myeloid leukaemia, and myelodysplastic syndromes) and, more recently, murine atherogenic inflammation (Asare et al., 2017; Sarantopoulos et al., 2016; Soucy et al., 2009; Swords et al., 2015). MLN4924 is structurally analogue to adenosine 5'-monophosphate and competitively binds the NAE enzyme's ATP sites. Thus, downstream degradation of CRL-mediated ubiquitination is impaired by the inhibition of NAEs (Soucy et al., 2009).

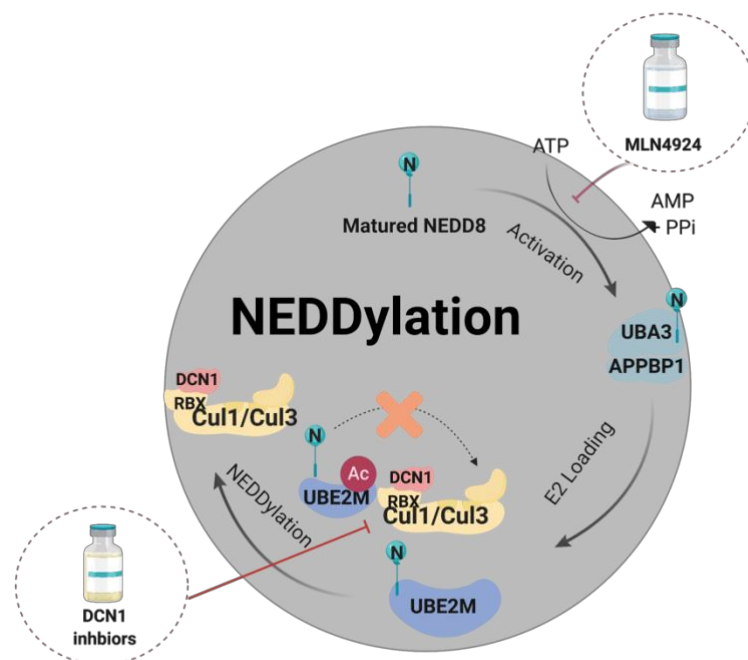


**Figure 15. NEDDylation inhibitors activity.** Free NEDD8(N) conjugation occurs on an ATP-dependent to an NAE(E1). MLN4924, as an analogue of ATP, competitively binds the ATP-binding site in the E1 enzyme and enables ablation of neddylation. DCN1 inhibitors exert activity on a NEDD8-E3 ligase complex, which blocks N-terminal acetylation of the E2-conjugating enzyme for NEDD8) with the DCN1, thus blocking the NEDDylation downstream cycle (Created with BioRender.com).

MLN4924 also has been explored in modulating the inflammatory response in atherogenesis-relevant cells and atherosclerosis *in vivo*. My laboratory has been instrumental in important parts of this preliminary work, an important basis for this PhD thesis.

MLN4924 treatment has been evaluated in atherosclerosis in *ApoE*<sup>-/-</sup> mouse model, and it has been shown that it leads to a decrease of mouse lesion size in the overall aorta and inhibits the growth of early lesions of the aortic root but not in advanced lesions (Asare et al., 2017). Moreover, a recent study has shown that MLN4924 application can potentially target endothelial dysfunction and atherosclerosis, as *in vivo* MLN4924 administration inhibits human neointimal hyperplasia while it increases VSMC intimal apoptosis (Ai et al., 2018). Another study scrutinised the signalling cascade involved in the MLN4924 treated TNF $\alpha$ -activated endothelial cells, as it destabilises the NF- $\kappa$ B signalling triggering upon the atherogenic stimulation *in vitro* (Asare et al., 2013b). As a result, NF- $\kappa$ B regulated genes are downregulated due to reduced NF- $\kappa$ B activation (Asare et al., 2013b, 2017). Therefore, MLN4924 reduced adhesion molecule expression levels and monocyte arrest in the endothelium (Asare et al., 2013b). The protective activity of MLN4924 in HAoECs is also confirmed by its effects on improved endothelial barrier integrity and NEDDylation-dependent endothelial dysfunction regulation (Nomura et al., 2021; Pandey et al., 2015). Conversely, one other study reveals controversial study shows that impairment of CRLs, Cullin-3–Rbx1–KCTD10 E3 ligase, by employing small molecule inhibitor MLN4924, impairs endothelial barrier function by inhibiting Rho GTPases ubiquitination (RhoB) and its degradation. Thus showing two sides of the neddylation impairment in the endothelial activation (Kovačević et al., 2018).

MLN4924 effects were also probed in another atherogenic relevant driver cells-neutrophils. It was corroborated that NF- $\kappa$ B axis is being ablated upon neddylation inhibition of the SCF $\beta$ -TRCP E3 ligase activation. Consequently, IkBa/p-IkBa accumulation ablates the underlining atherogenic inflammation (Jin et al., 2018; Y. Wang et al., 2015). Hence, this study revealed the essential role of neddylation in neutrophil recruitment to the lesion site (Asare et al., 2017; Z. Zhu et al., 2017).

Mononuclear-phagocytic cells such as monocyte and macrophages were heavily investigated under the effects of the MLN4924 treatments and have revealed intriguing effects of employing this small molecule inhibitor in their immunoregulation, as neddylation has been observed as a critical mechanism in their proliferation recruitment as well polarisation regulation (Jiang et al., 2021). Asare and colleagues show that MLN4924 ablates atherogenic stimulated bone marrow-derived macrophage synthesis of pro-inflammatory cytokine (Asare et al., 2017; Jiang et al., 2021). Moreover, MLN4924-stimulated RAW264.2 cells have shown that next to the NF- $\kappa$ B driven gene expression ablation, there is broad down-regulation of the gene expression affecting classical inflammatory cytokines (IL-6, TNF- $\alpha$ , IFN- $\gamma$ , IL-1 $\beta$ , and CRP), chemokines (CCL-1, -2, -3, -4, -5, -7, -8, -12, -17, -19, -20, -22) and C-X-C type of chemokines (CXCL1, CXCL5, CXCL10, CXCL11) and the related receptors (CCR1, CCR3, CCR7, CXCR4) (Jiang et al., 2021).

Moreover, MLN4924 treatment by diminishing the levels of IL-1 $\beta$  led to the ablation of an important atherogenic driver- inflammasome (Segovia et al., 2015). The chemokines such as CCL2 are downregulated in the MLN4924 stimulated bone-marrow-derived macrophages, consequently monocyte recruitment into the atherosclerotic lesions was reported (Asare et al., 2017; L. Zhou, Jiang, Liu, et al., 2019). Although the cancer studies do suggest that MLN4924 treated macrophages have lower anti-apoptotic protein Bcl-2 expression, thus challenging the cell proliferation,

this was not shown to be the fact for the atherogenic stimulated MLN4924 pretreated BMDMs proliferation (Asare et al., 2017; S. C. Chang & Ding, 2014). Interestingly MLN4924 can decrease MAPK signalling in pro-inflammatory stimulated macrophages, as ERK1/2 and p38 phosphorylation partially are shown to be downregulated in the macrophages (Asare et al., 2017; X. Zhou et al., 2010). Interestingly, MLN4924 treatment drives BMDM macrophage skewing towards the anti-inflammatory M2 phenotype by elevating arginase-1 and IL-13 gene expression while on the other hand, pro-inflammatory "M1" type of markers, e.g. IL-6, and -12 are decreasing under the neddylation ablation, urging thereby resolving inflammation in atherosclerotic plaques (Asare et al., 2017). Moreover, next to M2-like-gene expression being elevated, overall cell population counts have been skewed under the MLN4924 treatment by CD11b<sup>+</sup>/F4/80<sup>+</sup>/CD206<sup>+</sup> expression of typical "M2" anti-inflammatory markers in BMDMs being stimulated (Jiang et al., 2021). Thus collectively, neddylation ablation by employing small molecule inhibitor MLN4924 mimics "CSN5 overexpression" by inverting effects observed upon Csn5 depletion, and it regulating macrophage polarisation, survival, and the inflammatory responses generated under the atherogenic inflammation.

Next to innate immunity, adaptive immunity is affected by neddylation inhibition. For example, NF- $\kappa$ B axis ablation by phospho-I $\kappa$ B $\alpha$  accumulation, decreased p65/p52 nuclear translocation, and pro-apoptotic effects ablation upon MLN4924 treatment of the B-cells (Godbersen et al., 2014). As part of adaptive immunity, T cells are crucial players in atherogenesis. Naive T cells- named Th cells, are present in lesions, and they are athero-promoting (Th manner) or athero-protective (Treg) depending on the antigen-presenting cells (APCs) (Koltsova et al., 2012). Most T-cells in atherosclerotic lesions are T<sub>H</sub>1 cells (Fernandez et al., 2019). Hence colloquially, T helper 1 (T<sub>H</sub>1) cells have atherosclerosis-promoting, and regulatory T (T<sub>reg</sub>) cells have anti-atherogenic roles. MLN4924 treated T-cells shift toward the Th1 cytotoxic type of T-cells in cancer patients, and neddylation ablation tends to downregulate Treg cell type (Best et al., 2021). This remains to be elucidated in atherogenic inflammation, and it is unclear, not reported so far if it holds in atherosclerotic plaque lesions.

Finally, a significant therapeutic potential of MLN4924 lies in its potential to elicit HIF-1 $\alpha$  (Asare et al., 2017). In steady-state conditions, HIF-1 $\alpha$  is hydroxylated. Hydroxylated HIF-1 $\alpha$  regularly interacts with the CRLs' VHL protein to be targeted for the proteasomal degradation (Lu & Yang, 2020). HIF-1 $\alpha$  is strongly associated with the pro-inflammatory response in inflammatory cells, angiogenesis, ECs, macrophages, and VCMCs proliferation (X. Li et al., 2020; Tabata et al., 2019). Conversely, HIF-1 $\alpha$  has a dual role and can mediate adaptive responses under compromised oxygen conditions and was described as providing the myocardial ischemia/reperfusion injury protection (X. Li et al., 2020; Loor & Schumacker, 2008; Veith et al., 2016).

Although well over ten years of research have yielded significant beneficial data and extensive knowledge on the role of NEDDylation in different cell models and murine and human inflammatory signalling regulation, complete neddylation inhibition may have significant side effects. This has triggered the search for druggable targets downstream of the NEDD8 E2 conjugates and/or E3 ligases to target more specific NEDD8-ablation effects and reduce adverse signalling effects. Moreover, MLN4924 has been described to already at nanomolar concentrations, lead to activation of MAPK and stimulate stem cell proliferation, self-renewal, and differentiation in both tumours and normal stem cell models. On the other hand, MLN4924 activates and promotes mitochondrial oxidative phosphorylation (OXPHOS) as a non-specific targets (Q. Yu et al., 2020).

The success of MLN4924 therapy led to the development of novel small molecule inhibitors that target the DCN1 protein of the NEDDylation axis (Fig.15) (Hammill et al., 2018).

DCN1 inhibitors target multi-protein E3 ligase complexes. It does so by inhibiting the N-terminal acetylation of the E2-conjugating enzyme with DCN1 (the E3-co ligase) and, consequently, blocking NEDD8 from being ligated to the cullin proteins (Hammill et al., 2018; Scott et al., 2017).

DCN1 inhibiting compound has been so far probed in murine cancer but has not yet been used in combating inflammation or atherogenic processes (Hammill et al., 2018).

The CSN and its subunits have a complex role in inflammation regulation. Therefore, a therapeutic compound, CSN5i-3, has been recently developed, which specifically targets CSN5, and inhibits deNEDDylation activity over the CRLs, hence keeping them NEDDylated and consequently active- CRL (Schlierf et al., 2016). This small molecule inhibitor exerts sustained neddylation of Cullin RING-ligases and thus excessive activations of the NF- $\kappa$ B pathway. In ECs, it has been shown to elevate the expression of RhoGTPases via Rho/ROCK-dependent activation, cause disruption of the endothelial barrier, and increase the macromolecule leakage (Majolée et al., 2019).

Several other small molecule inhibitors of neddylation were generated over well over 10 years. Still, none yielded solid evidence in atherosclerosis studies or clinical trials in cardiovascular patients.

In recent years anti-inflammatory therapies have set the ground for further exploration of the inflammatory pathways modulation and confirmed the anti-inflammatory theory underlining cardiovascular disease.

## 2. Material and Methods

### 2.1 Materials

#### 2.1.1 Chemical and reagents

Chemicals	Manufacturer
10% formalin	Sigma Aldrich (St. Louis, USA)
30% acrylamide/ bis solution 29:1	Biorad (Hercules, USA)
Acetone	Merck (Darmstadt, Germany )
Acrylamide (30%)	Biorad, (Hercules, USA)
Ammonium persulfate (APS)	Sigma Aldrich (St. Louis, USA)
Albumin bovine serum (BSA)	Carl Roth (Karlsruhe, Germany)
DAPI	Sigma Aldrich (St. Louis, USA)
DMSO	Carl Roth (Karlsruhe, Germany)
DTT	Sigma Aldrich (St. Louis, USA)
EDTA	AppliChem Panreac (Chicago, USA)
Eosin Y	Sigma Aldrich (St. Louis, USA)
Ethanol	Carl Roth (Karlsruhe, Germany)
Fetal calf serum (FCS)	Invitrogen (Waltham, USA)
Glycine	Fluka Chemie (Buchs, Switzerland )
GoTaq® qPCR Master Mix	Promega (Madison, USA)
Hanks Buffered Saline Solution (HBSS)	Sigma Aldrich (St. Louis, USA)
Heparin	Ratiopharm (Ulm, Germany)
Hydrochloric acid (HCl)	Fluka Chemie (Buchs, Switzerland)
Isopropanol	KMF Laborchemie (Lohmar, Germany)
Mayer hematoxylin solution	Sigma Aldrich (St. Louis, USA)
Methanol	Carl Roth (Karlsruhe, Germany)
Miglyol	Caelo (Hilden, Germany)
Na <sub>2</sub> HPO <sub>4</sub>	Sigma Aldrich (St. Louis, USA)
Novex Tris-glycin-SDS running buffer	Invitrogen (Waltham, USA)
Novex zymogram developing buffer	Invitrogen (Waltham, USA)
Novex Zymogram renaturing buffer	Invitrogen (Waltham, USA)
NuPAGE LDS sample buffer (4x)	Novex (Hochdorf, Switzerland)
Oil-red-O solution	Sigma Aldrich (St. Louis, USA)
Penicillin-streptomycin	Gibco (Carlsbad, USA)
PFA	Morphisto (Hessen, Germany)
Phosphate-buffered saline (PBS)	Invitrogen (Waltham, USA)
PhosStop	Roche (Basel, Switzerland)
Pico-sirius red solution	Sigma Aldrich (St. Louis, USA)
Potassium chloride (KCl)	Sigma Aldrich (St. Louis, USA)
Potassium dihydrogen phosphate	Sigma Aldrich (St. Louis, USA)
Propylene glycol	Sigma Aldrich (St. Louis, USA)
RBC lysis buffer	BioLegend (San Diego, USA)
Recombinant human M-CSF	PreproTech (Rocky Hill, USA)
RNAiMAX transfection reagent	Invitrogen (Waltham, USA)
SimplyBlue safestain	Invitrogen (Waltham, USA)
Sodium chloride (NaCl)	Sigma Aldrich (St. Louis, USA)
Sodium dodecylsulfate (SDS)	Sigma Aldrich (St. Louis, USA)
Sodium hydroxide (NaOH)	Sigma Aldrich (St. Louis, USA)

SuperSignal west pico substrate	Thermo Fischer (Waltham, USA)
Tissue-Tek O.C.T	Sakura Finetek (Tokyo, Japan)
TMB substrate	Thermo Fisher (Waltham, MA, USA)
TNF $\alpha$ (human)	PeproTech (Rocky Hill, USA)
TNF $\alpha$ (murine)	PeproTech (Rocky Hill, USA)
Tris	Carl Roth (Karlsruhe, Germany)
Tris-HCl	Carl Roth (Karlsruhe, Germany)
Triton X-100	Fluka Chemie (Buchs, Switzerland)
Trypan blue	Biorad (Hercules, USA)
Tween 20	Fluka Chemie (Buchs, Switzerland)
Weigert's hematoxylin solution	Sigma Aldrich (St. Louis, USA)

### 2.1.3. Enzymes and buffers for the enzymes

Description	Manufacturer
Green GoTaq Flexi buffer	Promega (Madison, USA)
GoTaq polymerase	Promega (Madison, USA)
Revert Aid RT (200 U/ $\mu$ L)	Thermo Scientific (Waltham, USA)
5X reaction buffer	Thermo Scientific (Waltham, USA)
250 mM Tris-HCl (pH 8.3),	Invitrogen (Waltham, USA)
250 mM KCl	Sigma Aldrich (St. Louis, USA)
20 mM MgCl <sub>2</sub>	Invitrogen (Waltham, USA)
50 mM DTT	Sigma Aldrich (St. Louis, USA)

### 2.1.2 Primer pairs for qPCR

#### 2.1.2.1 Mouse primers

Primers used	Sequence 5'→3'
Mouse <i>Timp1</i>	<i>Left Primer</i> gcaaagagcttctcaaagacc <i>Right Primer</i> agggatagataaacaggaaacact
Mouse <i>Timp2</i>	<i>Left Primer</i> cccagaatcaacgaga <i>Right Primer</i> tgggacttgtggcata
Mouse <i>Mmp2</i>	<i>Left Primer</i> gcctcatacacacagcgtcaatctt <i>Right Primer</i> cggttatttggcgacagt
Mouse <i>Mmp9</i>	<i>Left Primer</i> cgtgtcggagatcgcacttga <i>Right Primer</i> tggaaatgtcggtgagttcc
Mouse <i>c-Jun</i>	<i>Left Primer</i> tggcacatcaccactacac <i>Right Primer</i> tcggctatgcagtcagcc
Mouse <i>c-Fos</i>	<i>Left Primer</i> cgaaggaaacggaataag <i>Right Primer</i> ctctggaaagccaaggc
Mouse <i>JunB</i>	<i>Left Primer</i> cctgcgccagtcctcc <i>Right Primer</i> caatatgaattcagtcctttgc
Mouse <i>Csn5</i>	<i>Left Primer</i> tcacctccggctcaagtg <i>Right Primer</i> ccaatgcgtggatgtcgag
Mouse <i>Csn8</i>	<i>Left Primer</i> gccagtgacggcagtc <i>Right Primer</i> ttccacagatacttgcattattcat
Mouse <i>Csn1</i>	<i>Left Primer</i> caggagctgcaacgaaatg <i>Right Primer</i> agatgtgtctgacctgtgg
Mouse <i>Csn2</i>	<i>Left Primer</i> ttgctggcagtgcatact <i>Right Primer</i> accccttctgtatgatcca

Mouse <i>Csn3</i>	Left Primer <i>catgtttcataacatcgacca</i> Right Primer <i>tcctggccatagccctcag</i>
Mouse <i>Csn4</i>	Left Primer <i>aaatgcagcccaagtgttg</i> Right Primer <i>gcaaatttcaggttaagtctccag</i>
Mouse <i>Csn6</i>	Left Primer <i>cagcactgacaagttcaagacag</i> Right Primer <i>caaactggttcattgtgtgc</i>
Mouse <i>Csn7</i>	Left Primer <i>aagcagcagatcggaaagtggag</i> Right Primer <i>ctgtcagggttgcgtcagga</i>
Mouse <i>Tnfa</i>	Left Primer <i>catttctcaaaattcgagtgaca</i> Right Primer <i>tgggagtagacaaggtaaac</i>
Mouse <i>Ccl2</i>	Left Primer <i>catccacgtgttggctca</i> Right Primer <i>gatcatcttgctggtaatgagt</i>
Mouse <i>Il-6</i>	Left Primer <i>atggatgttaccaaactg gat</i> Right Primer <i>tgaaggactctggctttgtct</i>
Mouse <i>Rplp0</i>	Left <i>actggcttaggaccggagaag</i> Right <i>ctcccaccttgcgtccagtc</i>
Mouse <i>Actin</i>	Left <i>Ggagggggtttggaggtgtt</i> Right <i>gtgtgcactttattggctcaa</i>

### 2.1.2.2 Human primers

Primers used	Sequences 5'→3'
Human <i>TIMP1</i>	Left Primer <i>ctgttgttgcgtgtggcgtat</i> Right Primer <i>aacttggccctgtatgcacg</i>
Human <i>C-JUN</i>	Left Primer <i>ggaaacgacccatctatgcacgtgcctcaa</i> Right Primer <i>gaaccctccgtcatctgtcacgttctt</i>
Human <i>C-FOS</i>	Left Primer <i>ggaggaggaggagctgactgata</i> Right Primer <i>ggcaatctcggtctgcaa</i>
Human <i>JUNB</i>	Left Primer <i>gtcaccggaggaggcaggagg</i> Right Primer <i>tcttgtcagatcgccagg</i>
Human <i>MMP2</i>	Left Primer <i>gcagatgcctggaaatgcct</i> Right Primer <i>agggtctgtgagccacaga</i>
Human <i>MMP9</i>	Left Primer <i>ttcaaggctggaaagtactg</i> Right Primer <i>tccggaggggcccggtcacct</i>
Human <i>CSN5</i>	Left Primer <i>cgaaggccctggactaaggat</i> Right Primer <i>tggcatgcatacaccatct</i>
Human <i>CSN8</i>	Left Primer <i>ccagccaaattatggaaagcac</i> Right Primer <i>gcgtatgttgaagtatacgccttg</i>
Human <i>TNF<math>\alpha</math></i>	Left Primer <i>agcccatgtttagcaaacc</i> Right Primer <i>tctcagctccacgcccatt</i>
Human <i>CCL2</i>	Left Primer <i>agtctctgcggcccttct</i> Right Primer <i>gtgactggggcatgttgg</i>
Human <i>RPLP0</i>	Left Primer <i>ttggcaccattgaaatcctgag</i> Right Primer <i>gaccagcccaaaggagaag</i>
Human <i>ACTIN</i>	Left Primer <i>agagctacgagctgcctgac</i> Right Primer <i>cgtggatgccacaggact</i>

All primers above were manufactured by Euorfins, Germany.

### 2.1.3 Antibodies

#### 2.1.3.1 Primary Antibodies

Description	Species	Manufacturer and catalog #	Use
Anti- $\beta$ -actin	mouse	Santa Cruz (sc-47778)	WB 1:1000
Anti- $\alpha$ -tubulin	rabbit	Invitrogen (T5168)	WB 1:100
Anti-CSN5	mouse	Santa Cruz Biotechnolog (sc-13157)	WB 1:1000 IHC 1:100
Anti-Jab1	mouse	Gentex (GTX70207)	IHC 1:100
Anti-CSN8	rabbit	Enzo (BML-PW8290)	WB 1:1000 IHC 1:100
Anti-CSN8	rabbit	Abcam (EPR5139)	WB 1:1000 IHC 1:100
Anti-TIMP-1	mouse	Thermo Fisher (MA5- 13688)	WB 1:100 IHC 1:50
Anti- c-Jun (60A8)	rabbit	Cell Signaling (9165)	WB 1:1000
Anti-Phospho-c-Jun (Ser63)	rabbit	Cell Signaling (9261)	WB 1:1000
Anti-JunB	rabbit	Cell Signaling (3753)	WB 1:1000
Anti-c-Fos	rabbit	Cell Signaling (2250)	WB 1:1000
Anti-ERK1/2	rabbit	Cell Signaling (9120)	WB 1:1000
Anti-p-ERK1/2 (Thr202/Tyr204)	rabbit	Cell Signaling (9101S)	WB 1:1000
Anti-p38	rabbit	Cell Signaling (9212)	WB 1:1000
Anti-p-p38 (Thr180/Tyr182)	rabbit	Cell Signaling (9211)	WB 1:1000
Anti-Cd68	rabbit	Sigma Aldrich (HPA048982)	IHC 1:200
Anti-Mac2	rat	Cedarlane (CL8942AP)	IHC 1:200
Anti-SMC akin-Cy3	mouse	Sigma Aldrich (C6198)	IHC 1:200
Anti-CD31	rabbit	Thermo Scientific (PA5-32321)	IHC 1:200

CD3, anti-mouse, FITC, REAfinity, clone REA641	Milteny Biotec (130-119-798)	FACS 1:100
APC/Cyanine7 anti-mouse CD19 Antibody, Clone 6D5	BioLegend (115530)	FACS 1:100
APC anti-mouse Ly-6C, Clone HK1.4	BioLegend (128016)	FACS 1:100
PE/Cyanin7 anti-mouse/human Cd11b, Clone M1/70	BioLegend (101216)	FACS 1:100
PerCP anti-mouse Ly-6G, Clone1A8	BioLegend (127654)	FACS 1:100
PE anti-mouse CD11c, Clone N418,	BioLegend (17308)	FACS 1:100
V450 Rat Anti-Mouse CD45	BD Biosciences (560501)	FACS 1:100

Detailed antibodies application is described in the methods section.

### 2.1.3.2 Secondary Antibodies

Description	Host	Manufacturer and catalog #	Use
Anti-Mouse IgG -HRP	Goat	Abcam (ab97023)	WB 1:5000
Anti-Rabbit IgG -HRP	goat	Abcam (ab6721)	WB 1:5000
Anti-Rat IgG- Alexa Fluor 488	goat	Thermo Fisher (A-11006)	IHC 1:500
Anti-Rat IgG- Alexa Fluor 647	goat	Thermo Fisher (A-21247)	IHC 1:500
Anti-Mouse IgG -Alexa Fluor 647	goat	Thermo Fisher (A-21235)	IHC 1:500
Anti-Mouse IgG-Alexa Fluor 488	goat	Thermo Fisher (A-11001)	IHC 1:500
Anti-Rabbit IgG -Alexa Fluor 555	goat	Thermo Fisher (A27039)	IHC 1:500
anti-Mouse IgG -IRDye® 800CW	donkey	Licor (926-32212)	WB 1:5000
anti-Rabbit-IgG IRDye® 800CW	donkey	Licor (926-32213)	WB 1:5000
anti-Mouse IgG-IRDye® 680RD	donkey	Licor (926-68072)	WB 1:5000
anti-Rabbit IgG-IRDye® 680RD	donkey	Licor (926-68073)	WB 1:5000

Detailed antibodies application is described in the methods section.

## 2.1.4 Media, buffers, and solutions

### 2.1.4.1 Cell culture media

Cell culture media	Formulation	Used for culturing	Manufacturer and catalog #
EGM-2 Endothelial Cell Growth Medium-2 Bullet Kit	EBM-2 basal medium (Lonza, CC-3156) Single Quotes Supplements (Lonza, CC-4176)	MAEC HUVEC HAoEC	Lonza (CC-3162)
Dulbecco's Modified Eagle Medium nutrient mixture F-12 (DMEM/ F12)	DMEM-F12, Glutamax (Gibco, 31331093) 10% fetal bovine serum (FBS) (Gibco, 26140079) 1% Penicillin-streptomycin (10.000 U/ml) (Gibco, 15140-163)	NIH/3T3 MEFs	Thermo Fisher (31331093)
Gibco Roswell Park Memorial Institute (RPMI 1640)	RPMI 1640 (Gibco, 21875034,) 10% Fetal bovine serum (FBS) (Gibco, 26140079) 1% Penicillin-streptomycin (10.000 U/ml) (Gibco, 15140-163)	PBMCs BMDMs	Thermo Fisher (21875034)
Opti-MEM I Reduced Serum Medium	Opti-MEM I reduced serum medium (Gibco, 31985962) 10% Fetal bovine serum (FBS) (Gibco, 26140079) 1% penicillin-streptomycin (10.000 U/ml) (Gibco, 15140-163)	MAEC HAoEC BMDMs	Thermo Fisher (31985962)

### 2.1.4.2 Buffers and solutions

#### GENERAL BUFFERS

Description	Concentration
PBS	137 mM NaCl 2.7 mM KCl 1.5 mM KH <sub>2</sub> PO <sub>4</sub> 8.1 mM Na <sub>2</sub> HPO <sub>4</sub>
TBS (pH 7.3)	20 mM Tris-HCl 150 mM NaCl

TE buffer (pH 8)	10 mM Tris 1 mM EDTA
TBE	8.9 mM Tris-HCl 8.9 mM Boric acid 0.2 mM EDTA

**GENOTYPING**

Description	Concentration
1 M Tris-Cl (pH 7.0)	30,275 g Tris-Cl
	100 ml ddH <sub>2</sub> O
	21 ml HCl (pH: 7.0),
5 M NaOH	250 ml ddH <sub>2</sub> O 50,01 g NaOH
	250 ml ddH <sub>2</sub> O

**WESTERN BLOTTING**

Description	Concentration
Resolving gel	12% (w/v) acrylamide/Bis 375 mM Tris-HCl, pH 8.8 0.1% (w/v) SDS 0.1% (w/v) ammonium persulfate 0.1% (v/v) TEMED
Stacking gel	5% (w/v) Acrylamid/ bis-solution 125 mM Tris-HCL 1M pH 6.8 7.8 ml ddH <sub>2</sub> O 0.1% (w/v) SDS (sodium-dodecyl sulfate) 0.1% (w/v) ammonium persulfate (APS) 0.1% (v/v) TEMED
Running buffer (5x)	15,14g Tris 72,05g glycine 50 ml 10% SDS 950 ml ddH <sub>2</sub> O
1x LDS buffer	500 µL 4x Nu-PAGE LDS 250 µL 1M DTT 1250 µL distilled H <sub>2</sub> O
Blocking buffer	1-5% BSA in TBS-T
Washing buffer (TBS-T)	0.05% Tween dissolved in TBS buffer

**ELISA**

Description	Concentration
Reagent diluent	1% BSA in PBS
Washing buffer	0.05% Tween dissolved in PBS buffer
Stop solution	2 M H <sub>2</sub> SO <sub>4</sub> in ddH <sub>2</sub> O

**2.1.5 Inhibitors**

Inhibitor	Use	Manufacturer
-----------	-----	--------------

MLN4924	NEDD8-Activating Enzyme Inhibitor	Chemgood (Glen Allen, USA)
JNK inhibitor II	JNK signaling inhibitor	Calbiochem (San Diego, USA)

### 2.1.6 Multi-component systems

Description	Manufacturer
Human Pan Monocyte Isolation Kit	Miltenyi Biotec (USA)
First Strand cDNA Synthesis Kit	Thermo Scientific (Germany)
TIMP-1 mouse DuoSet ELISA kit	R&D (USA)
TIMP-1 human DuoSet ELISA kit	R&D (USA)
Proteome Profiler Mouse XL Cytokine Array	R&D (USA)
MMP Activity assay Kit (Fluorometric-green)	Abcam (UK)
Cholesterol	Cayman (USA)
Triglyceride	Cayman (USA)
GoTaq® qPCR Master Mix	Promega (USA)
siPOOL-5 kit Cops5	Biotech siTOOLS (Germany)
siPOOL-5 kit Cops8	Biotech siTOOLS (Germany)

### 2.1.7 Equipment and consumables

Equipment	Manufacturer
-152 °C Freezer ULT	Thermo Scientific (USA)
-20 °C Freezer Premium NoFrost	Liebherr (Switzerland)
-80 °C Freezer HeraFreeze HFU T	Thermo Scientific (USA)
4 °C Fridge Premium BioFresh	Liebherr (Switzerland)
Analytic balance Analytical	Mettler Toledo (USA)
Analytic balance PCB	Kern&Sohn (Germany)
Automatic blood counter Scil Vet ABC™Hematology Analyze	Scil Animal Care (Germany)
Biometra TRIO PCR Thermocycler	Analytik Jena AG (Germany)
Centrifuge accuSpin Micro 17	Thermo Fisher (USA)
Centrifuge Heraeus Megafuge 16R	Thermo Fisher (USA)
Clean bench HERAsafe	Heraeus (Germany)
Clean bench Biowizard Silverline	Kojair (Finland)
DMi8 Fluorescent Microscope	Leica (Germany)
DMIL LED Microscope	Leica (Germany)
Elmasonic S40	Elma Electronics AG (Germany)
EnSpire Plate Reader	Perkin Elmer (USA)
FACSVerser™ Flow Cytometer	BD Bioscience (USA)
Heating magnetic stirrer	VELP Scientifica (Italy)
Heracell™ VIOS 160i CO2 Incubator	Thermo Fisher (USA)
Ice machine	Manitowoc (USA)
Microbiological Safety Cabinet class II	Kojair (Finland)
Mini Blot Modul	Life Technologies (USA)
Mini Gel Tank	Life Technologies (USA)
Nanodrop™ ONE	Thermo Fisher Scientific (USA)

Oddysey Fc Imaging System	LI-COR (USA)
Olympus IX81 (fluorescent microscope)	Olympus (Japan)
Ph meter FiveEasy	Mettler Toledo (USA)
Pipettes	Gilson, Middleton (USA)
Pipettor accu-jet® pro	Brand, Wertheim (Germany)
Quadro MACS Separator	Miltenyi Biotec (USA)
Real-Time PCR machine Rotorgene Q	Quiagen (Germany)
Rocking shaker VIBRAX VXR basic	Janke&Kunkel (Germany)
Roller Mixer SRT6D	Stuart Equipment (USA)
TC20TM - Automated Cell Counter	Biorad (USA)
Thermo Shaker 7001200	4 more Labor (Germany)
Vortex VV3	VWR(USA)
Water bath type 1004	GFL (Germany)

### 2.1.8 Consumables

Equipment	Manufacturer
Cell counting slides	Biorad (USA)
Cell scrapers	Falcon (USA)
Cell strainers (40µm Nylon)	Corning Incorporated (Germany)
FACS tubes	Corning Incorporated (Germany)
Falcon tubes 15 ml and 50 ml	Corning Incorporated (Germany)
Flasks 25 cm <sup>2</sup>	Corning Incorporated (Germany)
Flasks 75 cm <sup>2</sup>	Thermo Fisher Scientific (USA)
LS columns	Miltenyi Biotec (USA)
Rotor-Gene Strip Tubes	Starlab (Germany)
Syringe 10 ml/ 30 ml	Braun (Germany)
Microtube	Eppendorf (Germany)
Cryotubes	Nalgene (USA)
Parafilm "M" – Laboratory Film	American National Can (USA)
Pipette tips (200 µl, 10 µl and 1000 µl)	Sarstedt (Germany)
Plastic vials	Sarstedt (Germany)
12/ 24/ 96 well cell culture plates	Corning Incorporatedcity Germany)
Empty gel cassettes, Mini, 1.0 Mm	Thermo Fisher Scientific (USA)
Amicon® Ultra 0.5ml filters	Merck (Germany)
PCR Soft tubes 0,2ml	Biozym Scientific Gmbh (Germany)
Roti-PVDF membranes (0,45µm)	Carl Roth (Germany)
Reaction tubes (0.5 ml, 1.5 ml; 2ml)	Carl Roth (Germany)
6.5 mm transwell ,5.0 µm pore	Corning Incorporated (Germany)
polycarbonate membrane inserts	

### 2.1.9 Software

Software	Company
FIJI	(Created by: Schindelin et al., 2012)
FlowJo	Becton, Dickinson & Company (USA)
Leica Application Suite X (LAS X)	Leica Microsystems (Germany)
Q-Rex	Qiagen (Germany)
GraphPad Prism 9.3.1	GraphPad Prism 9.0 (USA)
Image Studio Ver. 5.2.	LI-COR Biosciences, (USA)

### 2.1.10 Cell lines

Cell line	Origin	Manufacturer
Bone marrow derived macrophages (BMDM)	mouse	Bernhagen lab this thesis
Human aortic endothelial cells (HAoEC)	human	Promocell, C-12272
Human umbilical vein cord cells (HUVEC)	human	Provided by Prof. Hans Schnittler, Universität Münster
Mouse aortic endothelial cells (MAEC)	mouse	Innoprot, P10427
Mouse embryonic fibroblasts (MEF CSN5 <sup>+/−</sup> )	mouse	Kindly provided by Prof. Junya Kato, Japan
Mouse embryonic fibroblasts (MEF WT)	mouse	Kindly provided by Prof. Junya Kato, Japan
Mouse embryonic fibroblasts (NIH/3T3 CSN5 <sup>+++</sup> )	mouse	Kindly provided by Prof. Johannes Schmid, University of Vienna, Austria
Mouse embryonic fibroblasts (NIH/3T3 CSN5 <sup>wt</sup> )	mouse	Kindly provided by Prof. Johannes Schmid, University of Vienna, Austria
Peripheral blood mononuclear cells (PBMCs)	human	Healthy blood donors (Blutbank LMU Klinikum)

### 2.1.11 Mice

Description of the mouse line	Source
<i>C57BL/6 Apoe<sup>−/−</sup></i> (Termed <i>Apoe<sup>−/−</sup></i> or <i>Csn5<sup>wt</sup> Apoe<sup>−/−</sup></i> )	The Jackson Laboratory
<i>C57BL/6 LysM-Cre/Csn5<sup>fl/fl</sup> Apoe<sup>−/−</sup></i> (Termed <i>Csn5<sup>Δmyeloid</sup> Apoe<sup>−/−</sup></i> )	Dr. Ruggero Pardi, San Raffaele, School of Medicine, Milano, Italy
<i>C57BL/6 Tg(Bmx-cre/ERT2) Mif<sup>fl/fl</sup> Apoe<sup>−/−</sup></i> (Termed <i>Mif<sup>Δarterial</sup> Apoe<sup>−/−</sup></i> )	Bernhagen lab
<i>C57BL/6 Tg(Bmx-cre/ERT2) Csn5<sup>fl/fl</sup> Apoe<sup>−/−</sup></i> (Termed <i>Csn5<sup>Δarterial</sup> Apoe<sup>−/−</sup></i> )	CRC1123 This thesis
<i>Csn8-flox flox</i>	Dr. Ning Wei, Yale University, Molecular, Cellular and Developmental Biology
<i>C57Bl/6 Tg(Vill-Cre<sup>+/−</sup>)/Csn8<sup>fl/fl</sup></i> <i>C57Bl/6 LysM-Cre/ Csn8<sup>fl/fl</sup>/Apoe<sup>−/−</sup></i> (Termed <i>Csn8<sup>Δmyeloid</sup> Apoe<sup>−/−</sup></i> )	Bernhagen lab this thesis

## 2.2 Methods

### 2.2.1 Primary cell culture and Csn5/Csn8 siPOOL depletion in vitro

All the employed primary cells and cell lines were cultured in their appropriate medium in 75 cm<sup>2</sup> or 25 cm<sup>2</sup> flasks. All the cell culturing was done under sterile conditions in a laminar flow hood. The flasks were stored in a tissue culture incubator under a humidified atmosphere, 5% CO<sub>2</sub> at 37°C. Cells were subcultured once they reached 80% confluency. To perform passaging, cells were washed initially with cold PBS, and their detachment from the culturing dish was enabled by using TrypLE. Trypsin enabled

cleavage of the protein bonds, encouraging adherence to the flask. Adding a complete growth media stopped the process. Cells were further diluted and transferred into a new culture flask depending on the cell culturing protocols.

Mouse aortic endothelial cells (MAoEC) (Innoprot, P10427) were cultured as adherent monolayers on collagen (Gibco) plated dishes (Sarstedt) in EGM-2 endothelial growth media (Lonza, CC-3162) supplemented with 1% Pen/Strep. There were subcultured and used between passages 3 and 8.

Usually, 120,000 cells per well were seeded into 12-well tissue culture plates. To achieve *Csn5* or *Csn8* down-regulation, transfection of MAoECs with the *siPOOL-5 kit* (Biotech siTOOLs) was employed. Overall, 10 nM *siPOOL-5 kit Cops5* (Biotech siTOOLs, 26754) or 15 nM *siPOOL-5 kit Cops8* (Biotech siTOOLs, 108679) solution were mixed with Opti-MEM® I medium for each well. Non-targeting scrambled control (scrRNA, Biotech siTOOLs) was used per the manufacturer's protocol for both treatments. To efficiently deliver a solution of the 30 siRNAs demonstrated to remove off-target effects, *siPOOL Csn5 and Csn8*, Invitrogen 4 µL Lipofectamine RNAiMAX Transfection Reagent™ (Thermo Fisher, 13778100) in the OptiMEM® I Reduced Serum Medium (Gibco™) was added per well. 48 to 72 h later, transfected cells were further treated or harvested.

Mouse aortic endothelial cells were stimulated with 20 ng/ml human TNF- $\alpha$  (PeproTech) at different indicated time intervals.

Neddylation activation inhibition was achieved in MAECs by applying 500nM MLN4924 treatment as indicated for 4h or 16 h or DMSO, vehicle treatment was used as a control.

The human umbilical vein chord primary cell line (HUVEC) was kindly provided by Prof. Prof. Hans Schnittler (Universität Münster). HUVECs were cultured on collagen (Gibco)-plated dishes (Sarstedt) in EGM-2 endothelial growth media (Lonza, CC-3162) and were used between passages 2 and 7. Endothelial cells were exposed to the 20 ng/ml human TNF- $\alpha$  (PeproTech) stimulation at indicated time intervals.

Human aortic endothelial cells (HAoECs) were obtained from Promocell and were cultured in T75 flasks at a density of 500.000 cells in 10 ml. They were cultured on collagen (Gibco)-pre-coated dishes (Sarstedt) and were grown in EGM-2 endothelial growth media (Lonza, CC-3162) and 1% Pen/Strep. They were cultured and used between passages 3 and 6. To achieve effective *CSN5* depletion, *CSN5 siTOOL* (Biotech siTOOLs, 10987) technology was employed. Or on the other hand, scrambled RNA control was used as a control. Where indicated, 500 nM MLN4924 was used for 4h or 16 h.

To further understand the mechanism underlying the *Csn5* overexpression, primary mouse embryonic fibroblast cells (*NIH/3T3 CSN5<sup>+++</sup>*) were used. *NIH/3T3 CSN5<sup>wt</sup>* and *NIH/3T3 CSN5<sup>+++</sup>* were kindly provided by Prof. Junya Kato (Japan). NIH/3T3s were cultured in Dulbecco's Modified Eagle's Medium containing 10% FCS and 1% Pen/Strep. Mouse primary fibroblastic cells were used in the experiment at passage 9 at the latest.

To inhibit JNK signalling, 10 µM, JNK inhibitor II (Calbiochem, 420119) was used on mouse embryonic fibroblast cells cultured in a low serum media (1% FCS) for 1h. Moreover, TNF (20ng/ml) stimulation was applied to investigate atherogenic signalling. Mouse primary fibroblastic cell lines used to decipher the signalling mechanisms underlining the *Csn5* depletion were MEF *CSN5<sup>wt</sup>* and MEF *CSN5<sup>+/−</sup>*, kindly provided by Prof. Johannes Schmid (University of Vienna, Austria). MEFs were cultured in Dulbecco's Modified Eagle's Medium containing 10% FCS and 1% Pen/Strep. Primary mouse embryonic fibroblast cells were exposed to the 20 ng/ml human TNF- $\alpha$  (PeproTech) at the indicated time intervals.

### 2.2.1.1 Freezing and thawing

For long-term storage, frozen cells were stored in cryovials in a cryogenic freezer (-150°C).

Upon harvesting cells, they were resuspended, usually at the concentration of 0.5-1x10<sup>6</sup> cells/ml in a medium containing 5% DMSO and 20% FCS. The cryovials were temporarily stored at -80°C and in a 150°C freezer for long-term storage.

Thawing of the cells included placing a cryovial briefly in a 37°C water bath, followed by adding a warm growth medium and finally centrifuging at 300xg for 5 min before resuspending and culturing in their respective growth medium.

### 2.2.2 Cell lysis and Western blot

The cells were initially washed with cold PBS, and total cell lysates were prepared by lysis in LDS-DTT buffer, containing phosphatase inhibitors (PhosSTOP, Roche) if necessary. Total cell lysates were prepared by lysis in 1x NuPAGE-LDS sample buffer (Thermo Scientific, NP0008) containing 1 mmol/L DTT, protease, and phosphatase inhibitors for immunoblotting analysis. Before usage, the samples were boiled (95°C for 5min), syringed, and sonicated. The Western Blots were performed using the standard protocols using homemade gels (7.5% and 11%) and running- buffers. The transfer buffer was purchased from Invitrogen (Novex™ Tris-Glycine SDS Running Buffer, Thermos Scientific).

Running of the gels was performed at 120V for 90 min. The transfer was performed at 20V for 90 min by using polyvinylidendifluorid (PVDF) membranes (Invitrogen) that were first activated in pure Methanol (Carl Roth). After the transfer, the membranes were blocked in sterile-filtered blocking buffer, 1%- 5% BSA in TBS for 1hr at room temperature or overnight at 4°C. Antibodies were diluted according to the manufacturer's recommendations in 1% BSA in TBS-T.

Signals from the cell lysates were developed by employing the following primary antibodies: CSN5 (Santa Cruz, B-7), CSN8 (Enzo, BML-PW8290), Timp-1 (Thermo Fisher, MA5-13688,), c-Jun (Cell Signaling, 9165), p-c-Jun (cell Signaling, 9261), JunB (Cell Signaling, 3753), c-FOS (Cell Signaling, 2250), ERK1/2 (Cell Signaling, 9120), p38 (Cell Signaling, 9212), p-p38 (Cell Signaling, 9211), Actin (Santa Cruz, sc-47778).

While secondary antibodies used were IRDye 800CW donkey anti-mouse (Licor, 926-32212), IRDye 800CW donkey anti-rabbit (Licor, 926-32213), IRDye® 680RD donkey anti-mouse (Licor, 926-68072), IRDye® 680RD donkey anti-rabbit (Licor, 926-68073). Rabbit anti-mouse-HRP (Abcam, ab97023), donkey anti-rabbit-HRP (Abcam, ab6721).

The membranes were incubated with primary antibodies overnight at 4°C, then washed 3x15min with TBS-T and incubated with secondary antibodies for 1hr at room temperature. Before imaging, the membranes were washed 3x15min with TBS-T. The blots were developed using SuperSignal™ West Femto- substrate. Protein bands were obtained with a LICOR Odyssey FC and visualised and quantified using Image Studio Version 5.2.

### 2.2.3 Real-time qPCR

Trisol reagent (Invitrogen, Germany) was used according to the standard protocol to isolate high-quality RNA. Briefly, after removal of the growth media, cells in monolayer (approximately 200 000 cells/12 well) were lysed in 300 µl TRIzol™ Reagent. Lysates were either snap-frozen or immediately used in the RNA isolation

procedure. After a brief incubation period to allow complete dissociation of the nucleoproteins complex, 0.2 mL of chloroform per 1 mL of TRIzol™ Reagent was used for lysis. After centrifugation, the mixture separates into a lower red phenol chloroform, interphase, and a colourless upper aqueous phase. RNA is in the upper aqueous phase. The Upper colourless phase is used further in isolation, and RNA is precipitated by adding 0.5 mL of isopropanol to the aqueous phase per 1 mL of TRIzol™. After brief incubation and centrifugation, total RNA precipitates and forms a white gel-like pellet, washed in 1 mL of 75% ethanol per 1 mL of TRIzol™. To solubilise the pellet at the bottom after washing, RNA is resuspended in 20–30 µL of RNase-free water, 0.1 mM EDTA, and exposed to the heat block at 60°C for 15 minutes. Finally, to determine the RNA yield absorbance at 260 nm and 280 nm without prior dilution is managed by using NanoDrop™ Spectrophotometer (Thermo Fisher, USA). Absorbance at 260 nm provides total nucleic acid content, while absorbance at 280 nm determines sample purity as such, only high-quality RNA is used further on.

To isolate RNA from the paraffin-embedded human CEA sections, 10 sections from the same patient were used per one RNA isolation. Herby, High Pure FFPE RNA Isolation Kit was used (Roche, Germany). Briefly, the deparaffinisation step includes exposure of the sections collected in a 1.5 ml Eppendorf tube to the xylene, and 2 changes of absolute ethanol, before air drying the pellet. Pellets were further exposed to the RNA Tissue Lysis Buffer, 10% SDS, and Proteinase K working solution and were incubated for 30 minutes at +85°C. Further, RNA Binding Buffer and absolute ethanol were applied to the pellets to be finally separated by the High Pure Filter Tube. Whereby centrifuged material was discarded, whereas columns with the remaining sample were exposed to the working DNaseI working solution. After three steps of washing, RNA elution buffer was applied to the columns to gain high-purity RNA from CEA paraffin sections, which was further evaluated using NanoDrop™ Spectrophotometer (Thermo Fisher, USA).

RNA was employed in the cDNA synthesis reaction and the real-time PCR gene expression analysis to proceed with the analysis. Quantitative real-time PCR analysis was performed with primers, as listed in Table 1 (Methabion). Quantitative PCR was performed by using the RevertAid First Strand cDNA Synthesis Kit (Thermo Scientific, K1621), GoTaq® qPCR Master Mix (Promega, A6002) on a Rotor-Gene Q real-time PCR cycler (Qiagen). Data obtained was analysed in a Q-Rex operating and analysis software (Qiagen).

### cDNA synthesis reaction

Components	Amount (µL)
5X Reaction Buffer	4 µL
Oligo (dT)18 Primer	1 µL
RiboLock RNase Inhibitor (20 U/µL)	1 µL
10mM dNTP Mix	2 µL
RevertAid RT (200 U/µL)	1 µL
Water, nuclease-free	9 µL

### cDNA synthesis program

Step	Temperature, °C	Time	Number of cycles
------	-----------------	------	------------------

<b>Initial denaturation</b>	94	3 min	1 cycle
<b>Denaturation</b>	94	30 s	35 cycles
<b>Annealing</b>	58	30 s	
<b>Extension</b>	72	45 s	

### Real-time PCR mix reaction contained

<b>Components</b>	<b>Amount (µL)</b>
GoTaq® qPCR Master Mix (Promega, A6002)	7.5 µL
Forward primer (0.2 µM)	1.25 µL
Reverse primer (0.2 µM)	1.25 µL
cDNA	To a final concentration of 100 ng/µL
Water, nuclease-free	To a final volume of 20 µL

### RT-PCR programme

<b>Step</b>	<b>Temperature, °C</b>	<b>Duration</b>	<b>Cycles</b>
Denaturation	95°C	10 min	1
Amplification	95°C	30 sec	40
	60°C	1 min	
Melting curve	95°C	10 sec	1
	60°C	10sec	
	95°C	Continuous	

The relative mRNA expression was estimated as relative mRNA expression:  $2^{(-\Delta\Delta Ct)}$

### 2.2.4 The mouse cytokine array

Cytokine Multiplex Assay Kits (R&D, ARY006) enabled simultaneous detection and screening of the levels of multiple cytokines in a single sample. It utilises capture antibodies spotted onto a nitrocellulose membrane to allow high-throughput multi-analyte profiling of 40-120 cytokines and chemokines in a single sample as a membrane-based sandwich immunoassay. Mouse plasma was used here upon allowing blood samples to clot for 30 minutes at room temperature before centrifuging for 15 minutes at approximately 2000 x g. Plasma was immediately used to detect store samples at  $\leq -80$  °C. Mouse plasma was initially diluted with a biotinylated detection antibody. That was followed by incubation with the Mouse Cytokine Array. Finally, membranes were incubated with streptavidin-horseradish peroxidase. The signal was detected via chemiluminescence. (Licor). After detection, the signal found on the membranes was quantitated to generate a protein profile (histogram) using FIJI. The table (Fig. 16) shows the organisation of the cytokines and chemokines in both kits used one is Mouse Cytokine Antibody Array, Panel A (R&D, ARY006), allowing 40 cytokine analysis and the other one is Proteome Profiler Mouse XL Cytokine Array (R&D, ARY028) allowing 111 simultaneous cytokine analysis per one plasma sample used.

List of analysed cytokines and chemokines in this assay:

	1	2	3	4	5	6	7	8	9	10	11	12	13	14	15	16	17	18	19	20	21	22	23	24
A	Ref																							Ref
B	Cxcl13	C5/Ca	G-csf	Gm-csf	Ccl1	Ccl11	slcam-1	Ifn- $\gamma$	Il-1 $\alpha$	Il-1 $\beta$	Il-1ra													Il-2
C	Il-3	Il-4	Il-5	Il-6	Il-7	Il-10	Il-13	Il-12p70	Il-16	Il-17	Il-23													Il-27
D	Cxcl10	Cxcl11	Cxcl1	M-csf	Ccl2	Ccl12	Cxcl9	Ccl3	Ccl4	Cxcl2	Ccl5													Cxcl12
E	Ccl17	Timp-1	Tnfa	Trem-1																				
F	Ref																							-

	1	2	3	4	5	6	7	8	9	10	11	12	13	14	15	16	17	18	19	20	21	22	23	24
A	Ref		Adipoq	SDG F	Ang-1	Ang-2	Angpt-13	CD257	CD93	Ccl2	Ccl3	Ccl5												Ref
B			Ccl6	Ccl11	Ccl12	Ccl17	Ccl19	Ccl20	Ccl21	Ccl22	Cd14	Cd40												
C			Cd160	Tig-2	Chi3l1	TF	C5/C5a	CFD	CRP	Cx3cl1	Cxcl1	Cxcl2												
D	Cxcl9	Cxcl10	Cxcl11	Cxcl13	Cxcl16	Cst3	Dkk-1	Cd26	Egf	Cd105	Col18a1	Ahsg												
E	Fgf-1	Fgf-21	Flt3iG	Gas6	G-csf	Gdf-15	Gm-csf	Hgf	Icam1	Ifn- $\gamma$	Igfbp-1	Igfbp-2												
F	Igfbp-3	Igfbp-5	Igfbp-6	Il-1 $\alpha$	Il-1 $\beta$	Il-1ra	Il-2	Il-3	Il-4	Il-5	Il-6	Il-7												
G	Il-10	Il-11	Il-12p40	Il-13	Il-15	Il-17a	Il-22	Il-23	Il-27p28	Il-28	Il-33	Ldlr												
H	Ob	Lif	Ngal	Cxcl5	M-csf	Mmp-2	Mmp-3	Mmp-9	Mpo	Spp1	Opg	Pdecgf												
I	Pdgf-bb	Ptx2	Ptx3	Osf-2	Pref-1	Mrp	PCS K9	RAGE	RBP4	Reg3g	Fizz3													
J	Ref	E-sel	P-sel	Pai-1	Pedf	Mgdf	Tim-1	Tnf- $\alpha$	Vcam-1	Vegf	Wisp-1	Neg.												

**Figure 16. List of analysed cytokines and chemokines in this assay.** The upper grid is the organisation of the Mouse Cytokine Antibody Array, Panel A, allowing 40 cytokine analyses. Below is the Proteome Profiler Mouse XL Cytokine Array grid allowing 111 cytokine analyses. Red labelled cytokines from the table are the cytokine shown in the analysis in the results. Acronyms of the individual cytokine are discussed in the main text.

## 2.2.5 Zymography

Zymography was used to evaluate whether the enzymatic activity of the MMP9 and/or MMP2 was impacted in the cell supernatant of MAECS and HAoECS, after the MLN4924 treatment or CSN5 depletion by using CSN5 siPOOL kit. Cell supernatants from the mouse aortic endothelial cells and human aortic endothelial cells after the treatment with 500 nM MLN4924 or CSN5 siPOOL (10 nM/15 nM), as previously described, were collected. Cell supernatants were concentrated using Amicon® Ultra 0.5ml filters (Merck) for protein concentration according to the manufacturer's protocol. Concentrated cell supernatants (16  $\mu$ L) together with the Nu-PAGE LDS sample buffer (Thermo Fischer Sci xxx) were loaded on the pre-made Zymography gels (Novex 10% gelatin zymogram gels 1.0mm, 12 wells, Invitrogen). They could develop on a stable current and 120V for 90 min in the 1X running buffer (Novex Tris-Glycin-SDS running

buffer, Invitrogen). Gels were further incubated in renaturing buffer (Novex Zymogram renaturing buffer, Invitrogen for 30 minutes, followed by 30 minutes of developing buffer (Novex zymogram developing buffer, Invitrogen) a room temperature and overnight (16-18h) at 37 degrees. Gels were stained by using SimplyBlue Safestain (Invitrogen) for one hour. De-staining was performed in deionised water (3x15 min). Images were scanned, and data analysis was performed in ImageJ as previously described (Hu & Beeton, 2010).

### 2.2.6 MMP activity assay

The MMP activity assay kit (fluorometric-green) (Abcam, ab112146) is used to evaluate general MMP enzyme activity in human and mouse aortic cell supernatants and was purchased from Abcam. Per the manufacturer's instruction, the protocol was used to analyse MMP activity changes over time in an endothelial cell culture supernatant. Briefly, HAoECs and MAECs were seeded in the 500  $\mu$ l cell culture media at a total density of 60 000 cells in a 12-well plate format. Before being used in the experiment, HAoECs/MAECS were treated with either (500nM) MLN4924 Vs. Vehicle for 4h or human or mouse CSN5/CSN8 siPOOL kit vs scrRNA for 48h. 1M AMPA (4-Aminophenylmecrcuric Acetate) was diluted (1:500) in a provided assay buffer. That was followed by cell supernatants (25  $\mu$ l) being activated with (25 $\mu$ l) 2mM AMPA in a black 96-well plate for 20-30 min on a 37 °C. MMP green (1:100) substrate was further applied to the wells. Kinetic reading was performed on every 10 minutes for 60 minutes on a microplate reader (EnSpire Plate Reader) to give readouts regarding the total MMP activity in each well.

### 2.2.7 ELISA

The ELISA assay is an antibody-based technique to identify proteins quantitatively and qualitatively in solutions. TIMP-1 mouse (R&D, DY970) or human (R&D, DY980) DuoSet ELISA kit capture antibody was incubated in the indicated working concentration overnight at room temperature on a 96-well microplate. After washing the plates, they were blocked for unspecific binding with the reagent diluent (1% BSA in PBS, pH 7.2-7.4, 0.2  $\mu$ m filtered). That was followed by the 100  $\mu$ l/well sample and standards addition. Samples were collected in mouse serums (1:500) or cell culture supernatants (1:100) diluted in a cell culture grade PBS. Afterwards, plates were washed (400  $\mu$ l/well) with wash buffer, and detection antibody solution was added to each well. After an incubation time at RT, the plate was rewashed. Before adding the substrate solution, each well was exposed to a Streptavidin-HRP conjugate for 20 min at RT in the dark. After washing, a substrate solution (Thermo Scientific) was added. The reaction was stopped by applying a stop solution (2N H<sub>2</sub>SO<sub>4</sub>). Each well's optical density was determined using a microplate reader (EnSpire Plate Reader) set to 450 nm. And the wavelength correction is enabled by using a microplate reader set to 540 nm or 570 nm. Generating standard curve concentrations of available mouse and human TIMP-1 in supernatants and serums was evaluated.

### 2.2.8 Mouse work

All mice had access to food and water and were housed in a pathogen-free animal facility under a 12 h light-dark cycle. We conducted a gender-balanced study. Data were excluded for mice with broken aortic root valves after sectioning of the heart. All animal experiments were approved by the institutional animal care committee of

Regierung von Oberbayern (ROB- 55.2-2532.Vet\_02-16-165; ROB-55.2-2532.Vet\_02-18-84).

Mice were anaesthetised using medetomidine-midazolam-fentanyl. Blood was collected via cardiac puncture. Upon sacrifice, blood was collected in the EDTA-coated Microtube, K3 EDTA (Sarstedt). Mice were perfused through the left ventricle consecutively with sterile, cold PBS containing 5 IU/ml heparin and 2 mM EDTA. Hearts were directly embedded in Tissue-Tek® O.C.T. compound to perform frozen section procedure of the heart tissue and later analyse atherosclerotic lesion load in their aortic roots. At the same time, aortas were directly fixed in the cold 1% PFA (Morphisto).

### 2.2.8.1 Generation of tamoxifen-inducible arterial endothelial cell-specific deletion of *Csn5*

*C57BL/6 Csn5<sup>flox/flox</sup>* mice were kindly provided by Dr. Ruggero Pardi (San Raffaele, School of Medicine, Milano, Italy). They were crossed with *C57BL/6 LysM-Cre/ Apoe<sup>-/-</sup>* mice to obtain a myeloid-specific deletion of *Csn5* on an atherogenic *Apoe<sup>-/-</sup>* background (termed *Csn5<sup>Δmyeloid</sup> Apoe<sup>-/-</sup>*) as previously described (Asare et al., 2017). To achieve a tamoxifen-inducible arterial endothelial cell-specific deletion of *Csn5*, *Csn5<sup>Δmyeloid</sup> Apoe<sup>-/-</sup>* mice were crossed with *Tg(Bmx-cre/ERT2)* expressing mice (termed *Bmx-Cre*) (kindly provided by the CRC1123) for > 10 generations. Finally, the genotyping verified cohort was *C57BL/6 Tg(Bmx-Cre/ERT2)/ Csn5<sup>flox/flox</sup> Apoe<sup>-/-</sup>* was out of convenience termed herein the thesis *Csn5<sup>Δarterial</sup> Apoe<sup>-/-</sup>* mice. *C57BL/6 Csn5<sup>flox/flox</sup> Apoe<sup>-/-</sup>* were used as a control littermate group. To induce *Csn5* deletion, 6-7 weeks-old mice were intraperitoneally injected with 50 mg/kg (per mouse body weight) with the tamoxifen (Sigma-Aldrich) dissolved in Miglyol, Caelo). All mice received one for 5 consecutive days one injection. Mice were fed a Western-type high-fat diet (HFD) containing 21% fat and 0.21% cholesterol (TD88137, Sniff) for 4 weeks to induce early atherosclerosis or 12 weeks to achieve medium to advanced atherosclerosis.

### 2.2.9 Generation of myeloid-specific deletion of *Csn8*

To investigate the role of the CSN holo-complex, mice with the myeloid-specific deletion of yet another CSN subunit, i.e. *Csn8*, were studied. *C57Bl/6 Tg(Vil-Cre<sup>+/</sup>)/Csn8<sup>fl/fl</sup>* were developed in the Bernhagen Lab, whereas *C57Bl/6 Csn8<sup>flox/flox</sup>* mice were kindly provided by Dr. Ning Wei (Yale University, USA). *C57Bl/6 Tg(Vil-Cre<sup>+/</sup>)/Csn8<sup>fl/fl</sup>* were crossed with atherosclerosis prone *C57Bl/6 LysM-Cre/Csn5<sup>wt/wt</sup>/ Apoe<sup>-/-</sup>* in order to generate myeloid-specific *Csn8<sup>fl/fl</sup> Apoe<sup>-/-</sup>* mice (termed *Csn8<sup>Δmyeloid</sup> Apoe<sup>-/-</sup>*). Mice were fed a Western-type high-fat diet (HFD) containing 21% fat and 0.21% cholesterol (TD88137, Sniff) for 12 weeks to evaluate atherosclerosis load.

### 2.2.9.1 MLN4924 treatment of mice

Neddylation activation inhibitor MLN4924 (Pevonedistat, MCE, HY-70062) was evaluated on an early atherosclerotic lesion in *Apoe<sup>-/-</sup>* mice. 6 weeks old male and female *Apoe<sup>-/-</sup>* mice were injected with the MLN4924 i.p. by administering 15 mg/kg MLN4924 or control solvent twice per day on two days per week for 4 weeks under continued HFD as previously reported (Asare et al., 2017). MLN4924 was diluted in 10% DMSO (AppliChem, No: A3672)/45% PG (Sigma-Aldrich, P50404)/45% PBS). Finally, bone marrow, heart and aorta were harvested upon mice being sacrificed for processing. A cohort of *Apoe<sup>-/-</sup>* mice was further evaluated in a long-term study as after

the initial 4-week MLN4924 treatment. They were continued on a further 8 weeks HFD without the MLN4924 application.

### 2.2.9.2 Genotyping of mice

To examine the genotype of newly generated genetically modified mouse lines, DNA was isolated from mouse-ear punch biopsies and analysed via PCR.

#### 2.2.9.2.1 DNA isolation protocol

Three to five weeks old mice were mouse-ear punch tissue was lysed in 25 µl 50 mM NaOH after brief centrifugation. The mouse biopsies were exposed to NaOH on a heating block for 30 min at 95°C and 300 x g. This was followed by the addition of 7.5 µl 1 M Tris-HCl (pH 7.0). Finally, the solution was centrifuged at the room temperature for 1 minute at full speed in accuSpin Micro 17 centrifuge (Thermo Scientific) and supernatants containing DNA were either temporary stored on -20°C or directly used for the PCR reaction.

#### 2.2.9.2.2 Genotyping primers

Primer name	Sequences 5'→3'
IMRO180	gcctagccgagggagagccg
IMRO181	tgtgacttgggagctctgcagc
IMRO182	gccgc(cccgactgcac)ct
Bmx-s7	aaataccttcagtttcatct
PAC-Cre-as1	ttgcgaacctcatcactcgtt
E5D	gactccaccacaagaatggtt
C916R	gttaggtgacccatcaatgtcac
In II for	ggtcagaaagcttaggcctaagaag g
Ex II rev	ggcatgcatcaccatttcagtag
MLys1	cttgggctgccagaatttctc
MLys2	ttacagtggccaggctgac
Cre8	cccagaaaatgccagattacg
MIF-B1	tctcactgttctgggtgtgagg
MIF-C1	ggctccctggctcagtcagg
VilCre1	caagcctggctcgacggcc
VilCre2	cgcgaacatcttcaggttct

All primers above were manufactured by Euorfins Germany.

#### 2.2.9.2.3 Genotyping protocols

The DNA isolated from mouse biopsies was checked for status of the genes *Apoe*, *LysM-Cre*, *BmxCre*, *Csn5* and *Csn8* respectively. Whether mice contained genes from the parental breeding line *VillCre* or *Mif* was also analyzed.

##### 1. *Apoe tm* protocol

Components	Volume
2x GoTaq Master Mix	12.5 µl
PCR H <sub>2</sub> O	2.5 µl

---

Primer IMRO 180	4.0 $\mu$ l
Primer IMRO 181	2.0 $\mu$ l
Primer IMRO 182	2.0 $\mu$ l
DNA – Mouse	2.0 $\mu$ l

2. *LysMCre protocol*

<b>Components</b>	<b>Volume</b>
2x GoTaq Master Mix	12.5 $\mu$ l
PCR H <sub>2</sub> O	6.5 $\mu$ l
Primer MLys 1	4.0 $\mu$ l
Primer MLys 2	2.0 $\mu$ l
Primer Cre8	2.0 $\mu$ l
DNA – Mouse	2.1 $\mu$ l

3. *BmxCre protocol*

<b>Components</b>	<b>Volume</b>
2x GoTaq Master Mix	12.5 $\mu$ l
PCR H <sub>2</sub> O	8.5 $\mu$ l
Primer BMx-s7	1.0 $\mu$ l
Primer PAC-Cre-as1	1.0 $\mu$ l
DNA – Mouse	2.0 $\mu$ l

4. *Csn5 flox protocol*

<b>Components</b>	<b>Volume</b>
2x GoTaq Master Mix	12.5 $\mu$ l
PCR H <sub>2</sub> O	6.5 $\mu$ l
Primer InIIFor	2.0 $\mu$ l
Primer IniiREV	2.0 $\mu$ l
DNA – Mouse	2.0 $\mu$ l

5. *Csn8 flox protocol*

<b>Components</b>	<b>Volume</b>
2x GoTaq Master Mix	12.5 $\mu$ l
PCR H <sub>2</sub> O	6.5 $\mu$ l
Primer C9/6R	2.0 $\mu$ l
Primer E5D	2.0 $\mu$ l
DNA – Mouse	2.0 $\mu$ l

6. *VilllCre protocol*

<b>Components</b>	<b>Volume</b>
2x GoTaq Master Mix	12.5 $\mu$ l
PCR H <sub>2</sub> O	6.5 $\mu$ l
Primer VilllCre 1	2.0 $\mu$ l
Primer VilllCre 2	2.0 $\mu$ l
DNA – Mouse	2.0 $\mu$ l

### 7. *Mifflox protocol*

Components	Volume
2x GoTaq Master Mix	12.5 $\mu$ l
PCR H <sub>2</sub> O	6.5 $\mu$ l
Primer MIF-B1	2.0 $\mu$ l
Primer MIF-C1	2.0 $\mu$ l
DNA – Mouse	2.0 $\mu$ l

#### 2.2.9.2.4 *Genotyping PCR programme*

##### 1. *ApoE* tm PCR programme:

Step	Temperature (°C)	Time	Number of cycles
Initial denaturation	95°C	1 min	1x
Denaturation	95°C	20 sec	35 x
Annealing	58°C	20 sec	
Extension	72°C	20 sec	
Extension	72°C	5 min	

**Results: ApoE WT- 155bp; ApoE KO- 245 bp**

##### 2. *LysM-Cre* PCR programme

Step	Temperature, (°C)	Time	Number of cycles
Initial denaturation	94°C	3 min	
Denaturation	94°C	30 sec	35 x
Annealing	58°C	30sec	
Extension	72°C	5 sec	
Extension	72°C	3min	

**Results: LysMCre WT- 350 bp; LysMCre KO- 700 bp**

##### 3. *Bmx-Cre* PCR programme

Step	Temperature, (°C)	Time	Number of cycles
Initial denaturation	94°C	2 min	
Denaturation	94°C	30 sec	35 x
Annealing	58°C	4.5sec	
Extension	72°C	1 min	

Extension	72°C	5 min
<b>Results: Bmx-Cre +/- or +/- 770 bp;</b>		

4. *Csn5 flox* PCR programme

Step	Temperature, (°C)	Time	Number of cycles
Initial denaturation	94°C	1 min	
Denaturation	94°C	45 sec	35 x
Annealing	60°C	30 sec	
Extension	72°C	30 sec	
Extension	72°C	5 min	

**Results: Csn5 WT- 400 bp; Csn5 flox- 500 bp**5. *Csn8 flox* PCR programme

Step	Temperature (°C)	Time	Number of cycles
Initial denaturation	94°C	2 min	
Denaturation	94°C	35 sec	35 x
Annealing	56°C	45 sec	
Extension	72°C	1 min	
Extension	72°C	5 min	

**Results: Csn8 WT- 130 bp; Csn5 flox- 190 bp**6. *Vill-Cre* PCR programme

Step	Temperature (°C)	Time	Number of cycles
Initial denaturation	94°C	5 min	
Denaturation	94°C	45 sec	35 x
Annealing	55°C	45 sec	
Extension	72°C	45 sec	
Extension	72°C	5 min	

---

**Results: Vill-Cre 300 bp**
**7. *Mif*<sup>fl</sup>ox PCR program**

Step	Temperature (°C)	Time	Number of cycles	
Initial denaturation	94°C	2 min		
Denaturation	94°C	1 min	35 x	<b>2.2.9.2.5 Agarose gel</b>
Annealing	62°C	45 sec		
Extension	72°C	45 sec		PCR products were analysed in gel electrophoresis. To enable visualisation, gels were stained with SYBR™ Safe
Extension	72°C	10 min		DNA Gel Stain (Thermo Fischer, S33102). DNA gels were made by exposing the different concentrated gels to a high temperature, moulding them, and allowing them to polymerise in a gel chamber dish (Biorad). Polymerised gels were run in a TBE buffer. 1 kB or 500 bp DNA marker (Thermo Fisher) was used to evaluate the band size of the amplified products. Gels were running under constant current conditions and voltage set to 110 V.
<b>Results: MIF WT- 544 bp; MIF flox- 683 bp</b>				

Fischer, S33102). DNA gels were made by exposing the different concentrated gels to a high temperature, moulding them, and allowing them to polymerise in a gel chamber dish (Biorad). Polymerised gels were run in a TBE buffer. 1 kB or 500 bp DNA marker (Thermo Fisher) was used to evaluate the band size of the amplified products. Gels were running under constant current conditions and voltage set to 110 V.

The Oddysey Fc Imaging System (Licor) monitored and recorded DNA bands. Indicated band size was placed under each PCR programme.

### 2.2.10 Mouse model of atherosclerotic disease progression

After the previously described mouse models were sacrificed by employing isoflurane flowed my midazolam/meDETomidine/fentanyl, the heart and its vasculature were rinsed with PBS until the liver was uncoloured.

Spleen, liver, lung, kidney, femur, and tibia were harvested, flash-frozen, and stored at -80°C for further use. After harvesting these organs, the heart and its vasculature were rinsed with a 4% PFA solution. The heart, aortic arch, and descending aorta were harvested by *in situ* perfusion fixation with 4% PFA. The heart was sectioned with a microtome to access the aortic root.

The extent of atherosclerosis was assessed in the aortic roots and the descending aorta by either staining transversal sections or the prepared aorta, respectively for lipid deposition with Oil-red-O. All animal experiments were conducted according to German animal protection law.

## 2.2.11 Phenotyping mouse atherosclerosis

### 2.2.11.1 *En-face* aorta preparation

The whole aorta ('en-face) preparation enables staining of the aorta for the atherosclerotic lesions *in situ*, from the aortic root to the common iliac arteries. It can also give solid information on the regio-specificity and atheroprone sites in the vessel and the locus of potential disturbed blood flow effects and mechano-signalling in endothelial cells. Upon removal, the aorta was placed in a fixative solution containing 4% PFA and incubated for 48 h at +4 °C. Finally, the vessel was briefly incubated in cold ethanol for a couple of hours and washed in PBS. Upon fixation, vessels were transferred into the Petri dishes and carefully removed under a dissecting stereomicroscope (Leica) and the adventitia, perivascular fat, and connective tissue. The aorta and carotid arteries were longitudinally opened, and endothelium was exposed and pinned on the surface. Vessels were pinned down on the rubber surface coated with the black isolation tape and were preincubated with the absolute Propylene glycol (Sigma Aldrich, 54347) for 15 minutes and then were stained in pre-warmed Oil-red-O (ORO) (Sigma Aldrich, 01516) solution on the 37°C for 3 hours. Staining was finally differentiated in 85 % propylene glycol. Finally, pins were removed, and aortas were mounted (Sigma, F4680) on the glass side and imaged under the microscope for lesions (Dmi8, Leica).

### 2.2.11.2 ORO staining of aortic root

The aortic roots assessed the atherosclerosis burden in general by staining lipid depositions with ORO solution (Sigma Aldrich, 01516).

Murine hearts were embedded in Tissue-Tek® O.C.T. Compound (Sakura Finetek USA Inc, 4583) for cryo-sectioning. Atherosclerotic lesions were quantified in 8 µm transverse serial sections, and averages were calculated from 2-3 sections.

Aortic roots were preincubated with the absolute Propylene-glycol (Sigma Aldrich, 54347) for 15 minutes and stained in pre-warmed ORO (Sigma Aldrich, 01516) solution at 37°C for 1 hour. Staining was finally differentiated in 85% propylene glycol. Subsequently, tissue slices were differentiated in 85% propylene glycol. Fresh frozen tissues were stained in Mayer's hematoxylin solution, mounted on the slides, and imaged (Dmi8, Leica).

### 2.2.11.3 Pico-Sirius red staining

To evaluate the total collagen and fibrous cap thickness, pico-Sirius red staining was performed on a fresh frozen aortic root section. Pico-Sirius red method used here was previously described (Junqueira et al., 1979; Puchtler et al., 1973).

After briefly drying the aortic root sections for 30 minutes, slides were fixed in a neutral buffered formaldehyde solution at +4°C for 30 minutes. This was followed by nuclei staining with Weigert's hematoxylin for 8 minutes. Sirius red/Direct Red 80 (Sigma-Aldrich, 365548) was diluted in the saturated aqueous solution of picric acid, as such, was applied upon aortic roots for 1h at room temperature. Finally, excess Sirius red was washed in two changes of acidified water. Upon this step, slides were mounted and imaged under the bright field modality as well as the polarisation light filter of the fluorescent microscope (Leica, Dmi8).

### 2.2.11.4 Hematoxylin and Eosin staining

To evaluate total lesion size and necrotic core size in atheroprone-mice, fresh frozen aortic root tissues were stained with Hematoxylin (Sigma Aldrich, 51275) and Eosin Y (Sigma, E4009) solutions according to the manufacturer's protocols. Briefly, slides with the frozen aortic tissue slices were immersed in a water-based hematoxylin for 8 minutes to stain the cell nuclei. After the washing step, hematoxylin was applied for another 2 minutes. Finally, slides were mounted and imaged under the fluorescent microscope (Leica, Dmi8).

### 2.2.12 Immunohistochemistry and immunofluorescence

The immunohistochemical methods were applied to stain specific proteins in tissue and sections by antibody binding or chemical reactions.

After briefly drying the slides containing mouse aortic root slices on a hot plate at 37 degrees, slides were fixed in cold 10% formalin. That was followed by employing 1h of blocking solution containing 3% BSA and serum of donkey/goat (depending on the secondary antibody host). Slides were either stained for 16 h on +4°C with the corresponding antibody or were stained with the vehicle, 3% BSA in PBS as a control of the staining. After the washing step of the primary antibody, the slide was all exposed to the corresponding secondary antibody. Finally, after washing the secondary access antibody, slides containing the mouse aortic root cross-sections were mounted in a water-based mounting media and covered with the coverslips to be imaged.

The aortic roots of female and male mice after 12 weeks of an HFD were visualised by immunofluorescent staining for the macrophage and smooth muscle cell (SMC) content. Macrophages were stained with the anti-CD68 (1:200, Sigma, HPA048982) or anti-Mac2 (1:200, Cedarlane, CL8942AP) primary antibodies. Smooth muscle cells were visualised using an anti-Sma-cy3 conjugated primary antibody (1:200 Sigma, C6198). The endothelial layer was effectively visualised by using the anti-CD31 antibody (Thermo Scientific, PA5-32321). Cre recombinase was visualised in the aortic cross-sections by using an anti-Cre antibody (1:100) (Novus Biologicals, NB100-56133)

To evaluate the efficiency of the COP9 subunit depletion in the lesion, fresh frozen tissues were stained with the Csn5 antibody (B-7, Santa Cruz) and Csn8 (Enzo, BML-PW8290) antibody. Anti-TIMP-1 (Thermo Fisher, MA5-13688) (1:50) antibody was used to determine the levels of the MMP inhibitor in the frozen aortic cross-section.

Secondary antibodies employed following primary antibody staining were Alexa 488- and Alexa 647- secondary antibodies conjugated (1:500, Thermo Fisher). Nuclei were counterstained by 4', 6-diamidino-2-phenylindol (DAPI) (Thermo Fisher, D1306). Incubation with secondary antibody alone without prior primary antibody use served as a negative staining control.

All images were recorded with a Dmi8 fluorescence microscope (Leica). The software used to visualise stained aortic root cross-sections was Leica Application Suite X (Leica). Lesion size and composition were quantified using Fiji analysis software (Schindelin et al., 2012).

### 2.2.13 Analysis of vulnerability

Plenty of studies are conducted on mouse atherosclerotic vulnerability in the existing literature. Although many new markers are being discovered, there is no single way of approximating mouse atherosclerotic plaque vulnerability. Here I used histological sections and analysed them by using ImageJ software (Schindelin et al., 2012). Several factors were considered. Lesion size as a factor was quantified by employing the Oil-

red-O staining as well as Hematoxylin and Eosin-stained tissues as previously described (Fig. 17). Lesion size was quantified by using FIJI software as area ( $\mu\text{m}^2$ ). Necrotic core (NC) size was defined as an area without nuclei underneath a formed fibrous cap (FC). FC thickness was defined as the average length measurements from the lumen to an underlining necrotic core.

The Vulnerability Index (VI) was used to evaluate the overall degree of lesion vulnerability by integrating all plaque features analysed in the prior study (Shiomi et al., 2001). To calculate the vulnerability index ( $VI$ ) relation between the analysed unstable ( $U$ ) and stable ( $S$ ) features of the plaque was evaluated. The formula for VI was expressed as:

$$VI_{c(i)} = (U_{(i)}/S_{(i)})$$

*i*- individual mouse

$U = \text{NC area } (\% \text{ of intima}) \times \text{CD68+ area } (\% \text{ of intima})$ .

$S = \text{SMA+ area } (\% \text{ of intima}) \times \text{collagen+ area } (\% \text{ of intima})$ .

Analysis of vulnerability and respective cross-section frozen slices staining was performed on lesions with the same lesion severity.

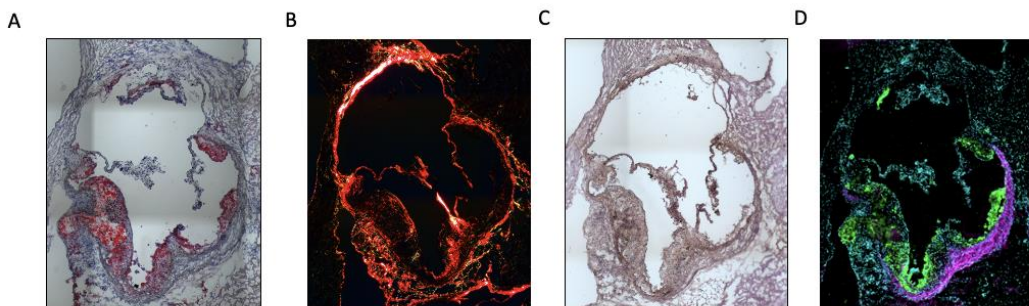


**Figure 17. Images of a single lesion.** Representative views of ORO (A) Sirius Red (B) and H&E (C); D, MAC-2(green), and SMC (cyan).

### 2.2.14 FACS

To analyse blood cell content and cell subtypes, an EDTA-buffered blood samples vial was used. To achieve a single-cell suspension blood sample was prepared and filtered over a 70  $\mu\text{m}$  cell strainer (Corning, CLS431751). Cells were treated with erythrocyte lysis buffer and RBC lysis buffer (BioLegend, 420301). Finally, cell suspensions were stained with FACS staining buffer and combinations of antibodies against Cd45 (BD Biosciences 560501), Cd19 (BioLegend, 115530), Cd11b (BioLegend, 101216), Cd11c (BioLegend, 17308), Ly-6C (BioLegend, 128016), Ly-6G (BioLegend, 127654) and Cd3 (Milteny Biotec, 130-119-798) was used. Flow cytometry was performed using FACSVerse and FACSuite software (BD Biosciences). Leukocyte subsets were gated using FlowJo software (Treestar). B cells were identified as Cd45 $^+$ Cd19 $^+$ ; T cells as Cd45 $^+$ Cd3 $^+$ ; neutrophils as Cd45 $^+$ CD11b $^+$ , Ly6G $^+$ ; monocytes as Cd45 $^+$  Cd11b $^+$  Ly6C $^+$ .

## 2.3 Blood analysis

Upon sacrificing the mice by cardiac puncture and blood collection in the EDTA-coated Microtube, K3 EDTA (Sarstedt), mouse blood was used to collect plasma and for the blood cell count analysis. Blood cell count was performed by using the Automatic blood

counter Scil Vet ABC™Hematology Analyze (Scil Animal Care). The generated parameters are summed up in a table in the results section. Each of the blood cell result tables contains the same parameters acronyms: WBC-White blood cell; RBC-Red blood cell, HGB- Hemoglobin; HCT- Hematocrit; MCV- Mean corpuscular volume; MCH- Mean corpuscular haemoglobin; MCHC- Mean corpuscular haemoglobin concentration; PLT- Platelet count; MPV- Mean platelet volume; RDW- Red cell distribution width; LYM- Lymphocytes; MO- Monocytes; GRA- Granulocytes—SD-standard deviation; N- number of individual experiments. Units are written in a table.

Cholesterol and triglyceride (Cayman) levels in plasma were quantified using enzymatic assays (Cayman) according to the manufacturer's protocol, and the signal from the perspective plates was developed by using Plate reader EnSpire™ Multimode Plate Reader (PerkinElmer, Inc).

## 2.4 Isolation of bone marrow cells and generation of bone marrow-derived macrophages

Bone marrow-derived macrophages (BMDMs) were generated by flushing them from the bone marrow of mice femurs and tibiae with ice-cold PBS. Bone marrow flushes were resuspended in PBS and filtered through a 40 µm cell strainer (Corning). The cell suspension was exposed to centrifugation at 300 g for 10 min. Finally, the pellet was resuspended in a culture medium RPMI 1640 containing L929-conditioned medium (LCM) and was plated on 12 well-culture plates. 15 % fresh L929-conditioned medium (LCM) was added again on days 3 and 6 of culturing.

Once macrophages were used in a simulation experiment as indicated, macrophages were left for 24h in a full RPMI 1640 media without the LCM. Cells were then stimulated with 20 ng/ml mouse recombinant Tnf $\alpha$  (Peprotech) at different intervals or left untreated.

## 2.5 Immunohistochemistry and immunofluorescence on human lesions

The collection of human carotid artery sections from autopsied individuals and early and advanced human carotid artery lesions from patients undergoing endarterectomy was approved by an institutional review committee and, with the patient's informed consent, by institutional guidelines.

Tissue sections on microscopic slides were deparaffinised by three changes and 10 min incubation in xylene. Sections of incubation follow that in a descending alcohol series (100% / 96% / 70% ethanol / deionised water). Sodium Citrate Buffer (10mM Sodium Citrate, 0.05% Tween 20, pH 6.0) was used for heat-induced antigen retraval in a water bath at 60°C. All further incubations were carried out in a humidified chamber. Peroxide solution (0.3% H<sub>2</sub>O<sub>2</sub>) in TBS for 15 min was used to block endogenous peroxidase. After the washing step, the slides were immersed in TBS /0.025% Triton X-100 with gentle agitation. Human CEAs were blocked in 10% normal serum with 1% BSA in TBS for 2 hours at room temperature Primary antibody was applied and diluted in TBS with 1% BSA overnight at 4°C, which was followed by enzyme-conjugated secondary antibody in TBS with 1% BSA for 2h on a room temperature. Where fluorescent signal was developed, fluorophore-conjugated secondary antibody in TBS with 1% BSA was incubated for 1 hour at room temperature. In the DAB staining development, chromogen was added to the samples to visualise the tissues. This was followed by counterstain with Mayer's Hematoxylin solution (Sigma Aldrich). After

staining, the sections were exposed to an ascending alcohol series (70 % / 96 % / 100 % EtOH). After incubation in xylene, coverslips were mounted on the sections using Roti®-Histokitt.

On the other hand, if using fluorescent detection, the end step is counterstaining by using DAPI, dehydrating, clearing, and applying a coverslip with a mounting medium.

For immunohistochemistry, an antibody against CSN5 (FL-337, Santa Cruz Biotechnology), TIMP-1(Thermo Fisher, MA5-13688), or an appropriate isotype control antibody was used and visualized by the avidin-biotin complex method with alkaline phosphatase enzyme development by employing Dako REAL EnVDetectSys Perox/DAB+, Rb/M from Agilent Technologies (DAKO REAL, Agilent, USA). Secondary antibodies were either HRP (Abcam) or fluorophore AF-488/-647 conjugated (Thermo Fisher). Nuclei were counterstained by either 4', 6-diamidino-2-phenylindole (DAPI, Thermo Fisher), or Mayer's hematoxylin solution. Images were recorded with a Leica DMi8 fluorescence microscope and charge-coupled device camera, and image analysis was performed with FIJI software.

### 2.5.1 Isolation of human PBMCs

Monocytes were isolated from Peripheral Blood Mononuclear Cells (PBMCs) using a Human Pan Monocyte Isolation Kit (Miltenyi Biotec).

The cells were centrifuged and resuspended in MACS buffer (40 $\mu$ l per 10<sup>7</sup> cells). Blocking reagent (10 $\mu$ l per 10<sup>7</sup> cells) and Biotin- Antibody Cocktail (10 $\mu$ l per 10<sup>7</sup> cells) were added. The cell suspension was incubated at 4°C for 20min. After that, MACS buffer (30 $\mu$ l per 10<sup>7</sup> cells) and Anti-Biotin Micro Beads (20 $\mu$ l per 10<sup>7</sup> cells) were added, and the mixture was put at 4°C for 30min. After that, another 500 $\mu$ l of MACS- buffer per 10<sup>7</sup> cells was added.

Magnetic cell separation was performed using LS columns (Miltenyi Biotec). The columns were placed in the magnetic field of a MACS separator and prepared by rinsing them with 3ml of MACS buffer. After that, the cell suspension was added to the columns, and they were washed with 3x3ml of MACS buffer. The flow-through was collected and centrifuged (300 x g, 5min). The cell pellet was resuspended in RPMI-media containing 10% FCS and 1% Pen-Strep and the cells were used for the following experiments.

PBMCs were obtained from healthy donors. The cells were placed in RPMI-media containing 10% FCS, 1% Pen-Strep and MCSF (100ng/ml). Half of the media was replaced with fresh media every other day to guarantee stable levels of MCSF. After seven days, the macrophages were adherent and could be used for the following experiments.

## 2.6 Statistical analysis

Statistical analysis was performed with GraphPad Prism 9 (GraphPad Software Inc.). Data are represented as means  $\pm$  SD. After testing for normality with the Shapiro-Wilks test and visual inspection of the QQ-plots, data were analyzed by Two-tailed t-test Two-sided Mann-Whitney test, or One-way ANOVA with Newman-Keuls post-test as appropriate. P-value was rated: \*p<0.05, \*\*p<0.01, \*\*\*p<0.001. N- represents a number of biological replicates(mice, patients, and experimental biological replicates).

### 3. Aims

Atherosclerosis is a lipid-driven, progressive, chronic inflammatory disease that starts with EC dysfunction and activation at the focal area of disturbed shear stress or laminar flow. It is followed by multiple processes, such as inflammation, vascular proliferation, and extracellular matrix (ECM) degradation. While the atherogenic process is initially clinically asymptomatic, it can evolve into an irreversible advanced fibrous lesion and a necrotic core, which can potentially lead to vessel occlusion and adverse cardiovascular events over time. In many cases, atherosclerosis is, therefore, not life-threatening or clinically symptomatic unless there is an event of plaque rupture. The permissive requirement for this to occur is the development of lesions defined as thin-cap fibroatheroma. Identifying the mechanisms that lead to plaques prone to rupturing would be key to understanding which therapies would effectively prevent major life-threatening events such as heart attacks and ischemic strokes. On the other hand, understanding the inflammatory mechanisms underlying vulnerable atherosclerotic plaques would enable the establishment of effective screening marker panels.

The CSN is a multi-functional protein complex that regulates the degradation of critical cell cycle and inflammatory proteins by controlling another family of proteins named the CRLs, via the removal of the ubiquitin-like modifier NEDD8, by a posttranslational modification process called “NEDDylation”. So far, studies on the role of the CSN as a regulator of inflammatory mechanisms involved in atherosclerosis development have focused on investigating the NF- $\kappa$ B signalling axis. The catalytical centre of the CSN5 subunit carries out the function of the CSN complex. Also, CSN5 has been described to act as a negative regulator of NF- $\kappa$ B-dependent pro-inflammatory gene expression, which aligns with its potential beneficial role in atheroprotection.

Hence, the focus of my thesis has been to understand the role of the COP9 signalosome in atherosclerosis development and decipher the mechanism(s) through which the COP9 signalosome controls inflammatory mechanisms in atherogenesis. Also, I wanted to evaluate if the COP9 signalosome is a reliable biomarker in preventing the devastating outcome of atherosclerosis and cardiovascular diseases. I sought to investigate if arterial-/endothelial-specific *Csn5* knock-out mice in the atherogenic *ApoE*<sup>-/-</sup> background recapitulated the exacerbated atherosclerotic phenotype found previously in myeloid-specific *Csn5* knock-out mice and what inflammatory mechanism stands behind it. Since the intact holo complex of all 8 subunits of the CSN appears necessary to exert deNEDDylation activity, the loss of one of the CSN subunits destabilises the CSN complex structure and leads to impaired deNEDDylation activity. I aimed to evaluate if CSN5 solely confers the atheroprotection or if it is a function of the CSN holo-complex. The smallest subunit, CSN8, has been studied in the context of heart failure but hasn't been investigated in atherosclerosis, although it can be found overexpressed in advanced human lesions. Accordingly, the study of CSN8 and the holo-complex is one of the key questions I am addressing in my PhD thesis.

Recent studies have identified and described a first-in-class potent pharmacological inhibitor of the NEDD8 system that has been in trials for cancer therapy, MLN4924. MLN4924 mimics CSN hyperactivity in atherosclerosis-relevant mouse models and shows a strong anti-atherogenic effect, as demonstrated by previous studies. Thus, I also investigated the therapeutic potential and the mechanism of the small molecule inhibitor on early lesion formation.

## 4. Results

### 4.1 Arterial-endothelial *Csn5* deletion

The global deletion of the *Csn5* gene is embryonically lethal (Tomoda et al., 2004). For the functional study of the *Csn5* in arterial endothelial cells and vascular inflammation, we developed a conditional atherosclerosis-prone mouse model in which CSN5 was tissue-specifically deleted in arterial endothelial cells only in an inducible manner.

We generated mice with a tamoxifen-inducible arterial endothelial *Csn5* deletion, *C57BL/6 Bmx-Cre-ERT2/Csn5<sup>flox/flox</sup>/Apoe<sup>-/-</sup>tm* (*Csn5<sup>Δarterial</sup>Apoe<sup>-/-</sup>*). Bone marrow x (*Bmx-Cre*) promoter -under the estrogen receptor (*ERT2*) conditional expression enables arterial-endothelial tissue-specific recombinase activity. Tamoxifen administration induces nuclear translocation of the Cre-ERT2 fusion protein and activation of the Cre recombinase, allowing the knockout of loxP-flanked genes in endothelial cells. The loxP-flanked gene used here was *Csn5*, which was efficiently excised in arterial endothelial cells upon five days of continuous tamoxifen induction in *Apoe<sup>-/-</sup>* mice. The most widely used murine models to study atherosclerosis, as they can develop hypercholesterolemia, are apolipoprotein E knockout (*Apoe<sup>-/-</sup>*) and low-density lipoprotein (LDL) receptor-deficient *Ldlr<sup>-/-</sup>* mice. Hence, in generating an appropriate mouse model, *Apoe<sup>-/-</sup>* mice were found to be more suitable for this study. To verify if the breeding strategy was successful and if mice indeed did express the *Bmx-Cre ERT2* gene and *Csn5 floxP* gene and were *Apoe* knock-out mice, PCR was performed on the mouse biopsies. PCR-based genotyping did verify that the mice exhibited the appropriate genotype and that arterial-specific *Csn5* gene excision was efficient (Fig. 18 and 19).

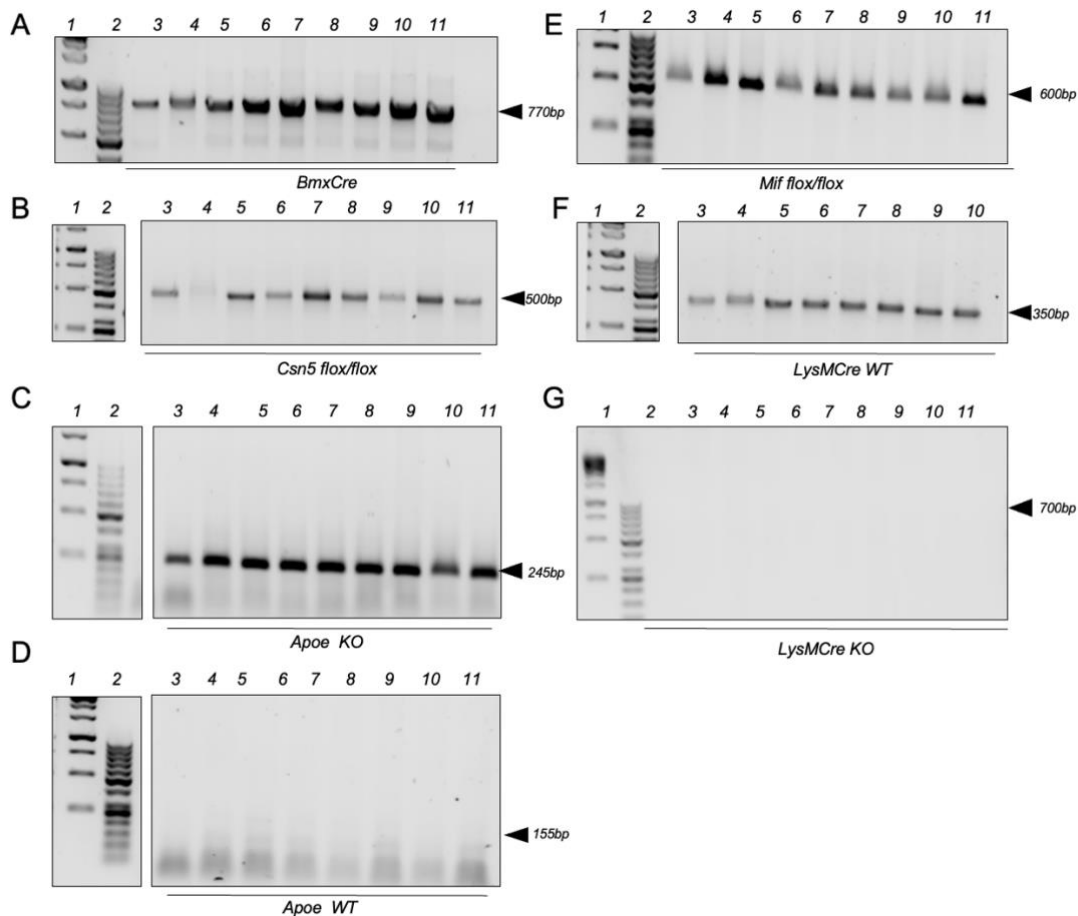


**Figure 18. PCR products of genomic DNA of *Csn5<sup>Δarterial</sup>Apoe<sup>-/-</sup>* mice run on an agarose gel.** Genomic DNA samples of the *Csn5<sup>Δarterial</sup>Apoe<sup>-/-</sup>* mice were used to investigate mouse genotypes. **A**, *Bmx-Cre-ERT2* conditional expression was confirmed on a gel-electrophoresis development as a PCR amplified product size of 770 bp. **B**, *Csn5* floxed (*flox/flox*) gene presence was observed as an amplified PCR product size of 500 bp (*knock-out*) or as a 400 bp band (*wild-type*)\*. **C**, *Apoe* *knock-out* was confirmed on a gel as a single PCR amplified product of 245 bp size. **D**, *Apoe* *wild-type* band was investigated as a 155 bp PCR product size. **E**, *MIF* floxed (*flox/flox*) gene was investigated as an amplified PCR gene product of 544 bp (*wild-type*) or 683 bp (*knock-out*) size. **F-G**, *LysM-Cre* expression was evaluated on the gel as PCR amplified gene product size of 350 bp (*wild-type*) (**F**) as well as 700 bp (*knock-out*)\* (**G**). Black arrowheads indicate the respective sizes of the amplified gene products according to DNA gene ladders. The first two lanes in each electrophoresis-gel development are DNA gene ladders of 100 bp (1) and 50 bp (2). 3-11, PCR samples of the first generated *Csn5<sup>Δarterial</sup>Apoe<sup>-/-</sup>* mouse cohort. bp- base pairs; PCR- polymerase chain reaction; *Bmx*- Bone marrow X; *Apoe*- apolipoprotein E; WT-*wild-type*; *LysM* - lysozyme M gene; *Cre*- Cre recombinase; *MIF*- migration inhibitory factor; KO- *knock-out*.

\*Gene knock-out (KO) indicates the loss of the respective gene, while *wild-type* indicates unaltered gene expression (in the case of LoxP genes, it indicates the absence of the gene floxing).

At six weeks, mice were treated with tamoxifen (50 mg/kg of mouse BW) and consumed an HFD for 4 or 12 weeks, only to be sacrificed at the age of 10 or 18 weeks. Atherosclerosis lesion development was evaluated in the aortic root and aorta or the *Csn5<sup>Δarterial</sup>Apoe<sup>-/-</sup>* mice and compared to their littermate control mice, *Csn5<sup>wt</sup>Apoe<sup>-/-</sup>*. Next, to confirm the genotypes of mice (Fig. 18), immunohistochemical staining was employed to confirm the successful generation of the appropriate mouse model. CSN5 positive area was evaluated in the CD31(PECAM-1)<sup>+</sup> cells in the aortic roots (Fig. 19). PECAM-1 is well-known to be exclusively expressed on the surface of the ECs, hence here, it is used as an endothelial-specific marker. The general tyrosine recombinase enzyme derived from the P1 bacteriophage (Cre-recombinase) expression in the endothelial-tissue specific expression was also validated in the mouse aortic roots (Fig. 20). The aortic root endothelial layer of the tamoxifen-treated *Csn5<sup>Δarterial</sup>Apoe<sup>-/-</sup>* and control *Csn5<sup>wt</sup>Apoe<sup>-/-</sup>* mice were investigated (Fig. 19).

The CSN5<sup>+</sup> area was depleted in the endothelial layer of the *Csn5<sup>Δarterial</sup>Apoe<sup>-/-</sup>* mouse aortic roots, compared to the *Csn5<sup>wt</sup>Apoe<sup>-/-</sup>* mouse aortic roots (Fig. 19, A-C).

The activity of Cre recombinase in the endothelial lining was detected only in the mice receiving tamoxifen (*Csn5<sup>Δarterial</sup>Apoe<sup>-/-</sup>*) and was absent in the control mouse group (*Csn5<sup>wt</sup>Apoe<sup>-/-</sup>*) (Fig. 19, D-F). Thus, general observations sufficed to conclude the efficacy of the CSN5 loss in an arterial-endothelial manner *in situ*.

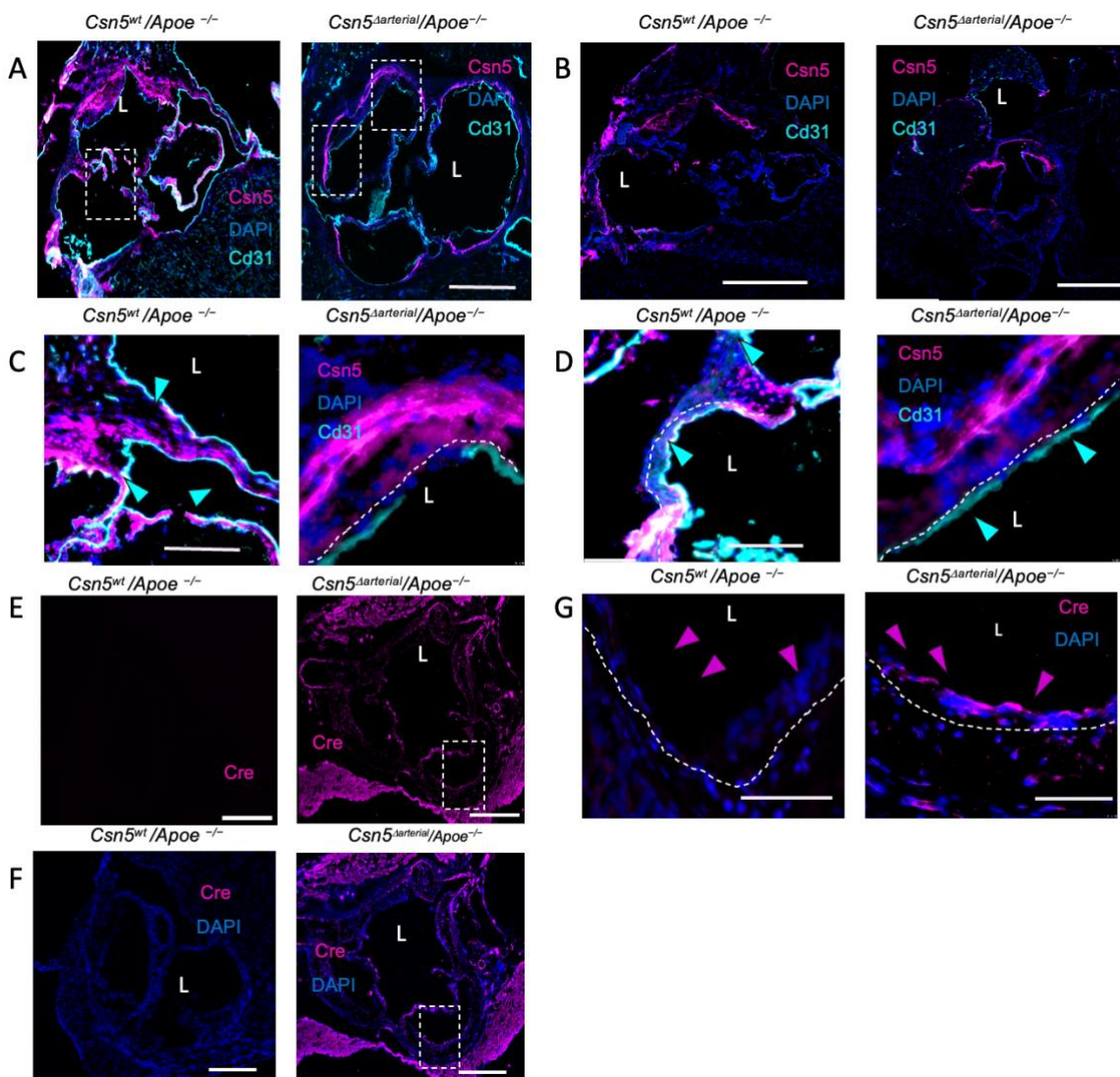


**Figure 19. Csn5 depletion in the endothelial lining of the *Csn5<sup>Arterial</sup>Apoe<sup>-/-</sup>* mice.** *Csn5<sup>Arterial</sup>Apoe<sup>-/-</sup>* mice were injected with tamoxifen or vehicle to induce Csn5 depletion in the arterial endothelial lining and early atherosclerosis. Representative immunostaining of the aortic roots shows the efficacy of the depletion of the CSN5<sup>+</sup> area (magenta) in the CD31<sup>+</sup> endothelial area lining (cyan). **B**, Representative control staining of the aortic roots of the CSN5 area (magenta) and CD31 (cyan) of the *Csn5<sup>Arterial</sup>Apoe<sup>-/-</sup>* and *Csn5<sup>wt</sup>Apoe<sup>-/-</sup>* mice. **C-D**, Magnified area of the *Csn5<sup>Arterial</sup>Apoe<sup>-/-</sup>* aortic roots compared to their *Csn5<sup>wt</sup>Apoe<sup>-/-</sup>* controls. **A-D**, Arrowheads indicate CD31<sup>+</sup> area in *Csn5<sup>Arterial</sup>Apoe<sup>-/-</sup>* aortic roots and *Csn5<sup>wt</sup>Apoe<sup>-/-</sup>* control aortic roots; Magenta is distinct CSN5<sup>+</sup> area. Dotted squares represent enlarged areas of the root. Scale bar, 50  $\mu$ m. **E-F**, Representative Cre recombinase staining activity (magenta) in the aortic root of *Csn5<sup>Arterial</sup>Apoe<sup>-/-</sup>* and control littermates *Csn5<sup>wt</sup>Apoe<sup>-/-</sup>*. **E-G**, Cre recombinase positive area (magenta) in aortic roots with (**D**) or without DAPI staining (**E**). Scale bar, 500  $\mu$ m. **F**, Representative enlarged Cre recombinase staining. Magenta arrowheads show the Cre recombinase-positive areas reside in the endothelial lining (intercepted white line) of the *Csn5<sup>Arterial</sup>Apoe<sup>-/-</sup>* aortic roots are absent in the *Csn5<sup>wt</sup>Apoe<sup>-/-</sup>* control aortic roots: scale bar, 50  $\mu$ m.

## 4.2 Arterial-specific deletion of Csn5 enhances early atherosclerosis

The role of the COP9 signalosome or its subunit CSN5 has yet to be explored explicitly in early lesion development. The previous study has shown that the MLN4924 might effectively treat the small atherosclerotic lesion progression by mimicking the Csn5 hyperactivity intracellular conditions. Conversely, Csn5 loss of functions accelerates vascular inflammation by triggering the NF- $\kappa$ B signalling in endothelial cells *in vitro* (Asare et al., 2017). Since endothelial dysfunction is an early event that initiates atherosclerosis progression, we aimed to determine the role of Csn5 loss in arterial-endothelial cells in early lesion development.

Lesion size in the aortic root and aorta was assessed by lipid staining. The ORO area was accounted for as the percentage of the total lesion area (**Fig. 20A**). In the aorta of a male cohort of mice, it could be observed that already after four weeks of HFD *Csn5<sup>Arterial</sup>Apoe<sup>-/-</sup>* had higher plaque load in the aortic arch as well as abdominal aorta, while this wasn't observed on thoracic aorta compared to the control mice (**Fig. 20, B-C**). Moreover, *Csn5<sup>Arterial</sup>Apoe<sup>-/-</sup>* already in early atherosclerotic lesions had higher plaque load (ORO<sup>+</sup> area) in the aortic roots than the vehicle-treated controls *Csn5<sup>wt</sup>Apoe<sup>-/-</sup>* (**Fig. 20, D-E**). There was no significant impact of *Csn5* endothelial loss on lipid metabolism, e.g. triglyceride or cholesterol circulating levels (**Fig. 20, F-G**). Conversely, female *Csn5<sup>Arterial</sup>Apoe<sup>-/-</sup>* mice showed no differences in an overall aortic root atherosclerotic lesion size after 4 weeks HFD (**Fig. 20 H-I**). They suggested that there is a potential *Csn5* dependent gender-specific effect on an early lesion progression.

Overall, arterial-endothelial CSN5 loss exacerbates early atherosclerosis in the aortic root and aorta, and it does so in a gender-specific manner.

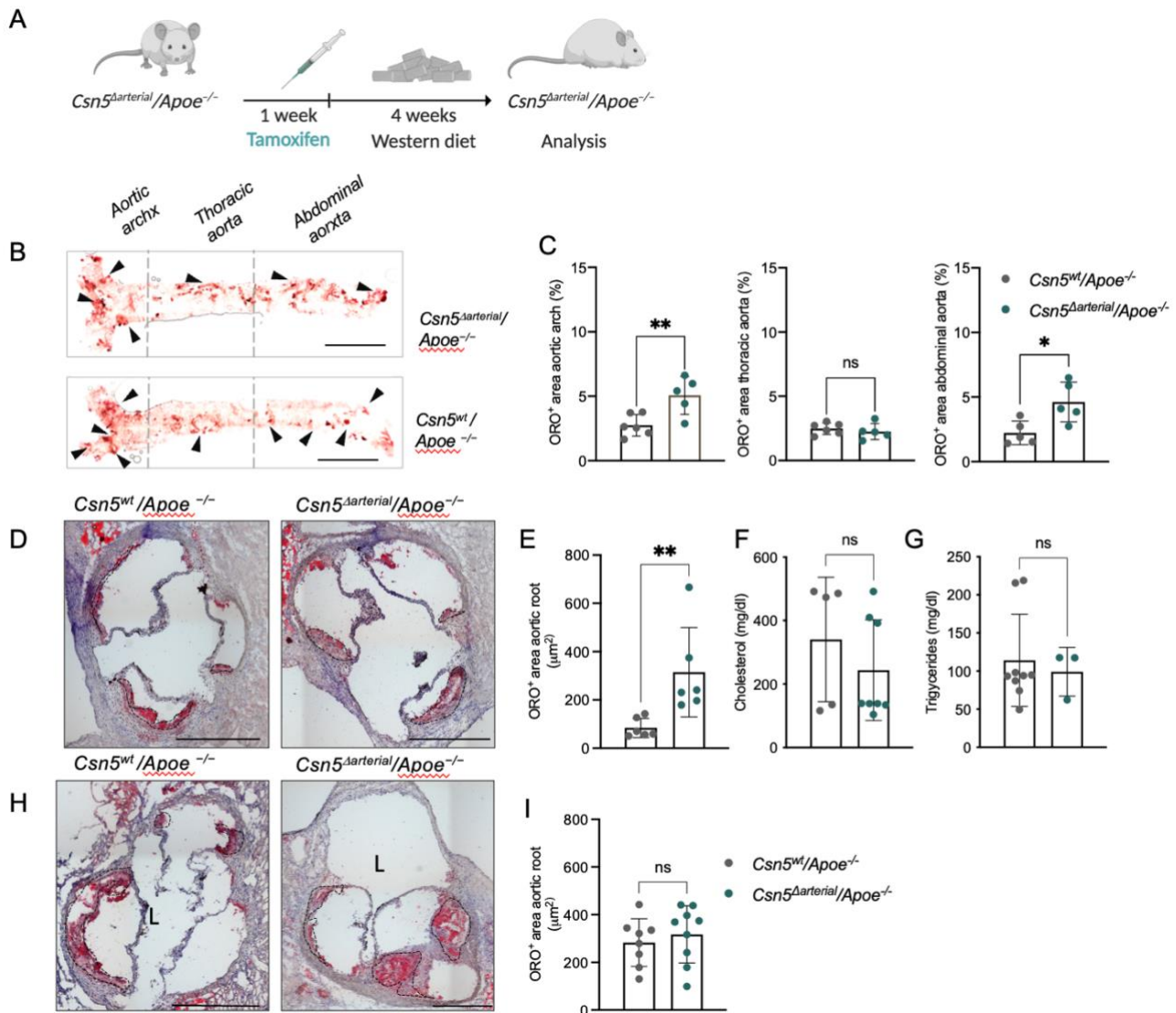


**Figure 20. Arterial-endothelial specific depletion of Csn5 enhances early atherosclerosis.** **A**, An experimental outline. *Csn5<sup>Arterial</sup>Apoe<sup>-/-</sup>* mice were injected with tamoxifen to induce *Csn5* depletion in the arterial endothelial lining and were consuming HFD for 4 weeks to elicit early atherosclerosis. **B**, Representative images of *en-face* murine aortas of *Csn5<sup>Arterial</sup>Apoe<sup>-/-</sup>* and *Csn5<sup>wt</sup>Apoe<sup>-/-</sup>* mice. Black arrowheads indicated Oil-red-O positive areas (ORO<sup>+</sup>). Scale bars, 3 mm. **C**, Quantification of the lesion sizes (ORO<sup>+</sup> area) in the *Csn5<sup>Arterial</sup>Apoe<sup>-/-</sup>* (n=5) and vehicle-treated *Csn5<sup>wt</sup>Apoe<sup>-/-</sup>* (n= 5- 6) aorta. **D**, Representative image of the ORO-stained aortic root of male *Csn5<sup>Arterial</sup>Apoe<sup>-/-</sup>* and *Csn5<sup>wt</sup>Apoe<sup>-/-</sup>* mice after 4 weeks of HFD consumption. Scale bars, 500 μm. **E**, Quantification of the male atherosclerotic plaque load in *Csn5<sup>Arterial</sup>Apoe<sup>-/-</sup>* (n= 6-7) and *Csn5<sup>wt</sup>Apoe<sup>-/-</sup>* (n= 6-9) aortic roots. Cholesterol (**F**) and triglyceride (**G**) levels of *Csn5<sup>Arterial</sup>Apoe<sup>-/-</sup>* (n=3-8) and *Csn5<sup>wt</sup>Apoe<sup>-/-</sup>* (n=5-9) male mice. **H**, Representative image of the ORO-stained aortic root of female *Csn5<sup>Arterial</sup>Apoe<sup>-/-</sup>* and *Csn5<sup>wt</sup>Apoe<sup>-/-</sup>* mice after the 4 weeks of HFD consumption. **I**, Quantification of the male atherosclerotic plaque load in *Csn5<sup>Arterial</sup>Apoe<sup>-/-</sup>* (n= 6-7) and *Csn5<sup>wt</sup>Apoe<sup>-/-</sup>* (n= 6-9) aortic roots. These data represent means ± SD.

### 4.3 MLN4924 mimics athero-protection by CSN5 in vivo after 4 weeks of the Western diet

MLN4924, a novel therapeutical approach to treating inflammatory disease, has been at the essence of this thesis. Prior work has established its beneficial effects on small lesion progression and determined its limitation in combating the advanced stages of atherosclerosis (Asare et al., 2017). Moreover, as an ATP analogue, its ablates neddylation, and in that manner, MLN4924 simulates Csn5 overexpression conditions (Asare et al., 2013b, 2017). To clarify the effects of the ‘Csn5 overexpression’ on an early lesion progression, we employed the pharmacological modelling approach and treated the *Apoe*<sup>−/−</sup> mice with the small molecule inhibitor, MLN4924 (Pevonedistat), as previously described (Asare et al., 2017), MLN4924 was applied for 4 weeks, while atherogenic-prone *Apoe*<sup>−/−</sup> mice consumed HFD (Fig.21A). Atherosclerosis was evaluated in a gender-equal study.

In the aorta of the MLN4924 treated males, we could observe that neddylation ablation lowered the lesion size in the aortic arch and the thoracic aorta. In contrast, the abdominal aorta was unaffected compared to their vehicle-treated littermate controls (Fig.21, B-C). Atherosclerosis progression in the male aortic root (Fig.21, D-E) revealed that MLN4924-treated male mice had less pronounced atherosclerotic lesions in the aortic root. Moreover, no impact of the NAE inhibitor was observed on cholesterol or triglyceride blood content (Fig.21, F-G, Table 1). Also, blood analysis has revealed no effect on the monocyte blood count, while there was a decline in the lymphocyte count observed and elevated granulocyte percentage (Fig. 21H). Thus, MLN4924 has a protective role on early lesion atherosclerosis in male mice and might exert its effects by lowering the lymphocyte count.

To further understand if the MLN4924 application has only a short-term effect, a preliminary experiment has been set to evaluate the long-term effects of the inhibitor of male atherosclerosis. Namely, after the 4-week MLN4924 application or a vehicle treatment application, mice receiving the treatment were continued on a high-fat diet regimen for 8 more weeks without the MLN4924 or vehicle treatments. Intriguingly, it has been shown that MLN4924 lowers the lesion size in the aortic arch and the abdominal aorta. On the other hand, MLN4924 protective effects are lost in the male thoracic aorta (Fig. 21I). Thus, suggesting that the short-term application of neddylation inhibitor might have long-term protective consequences on atherosclerosis progression.

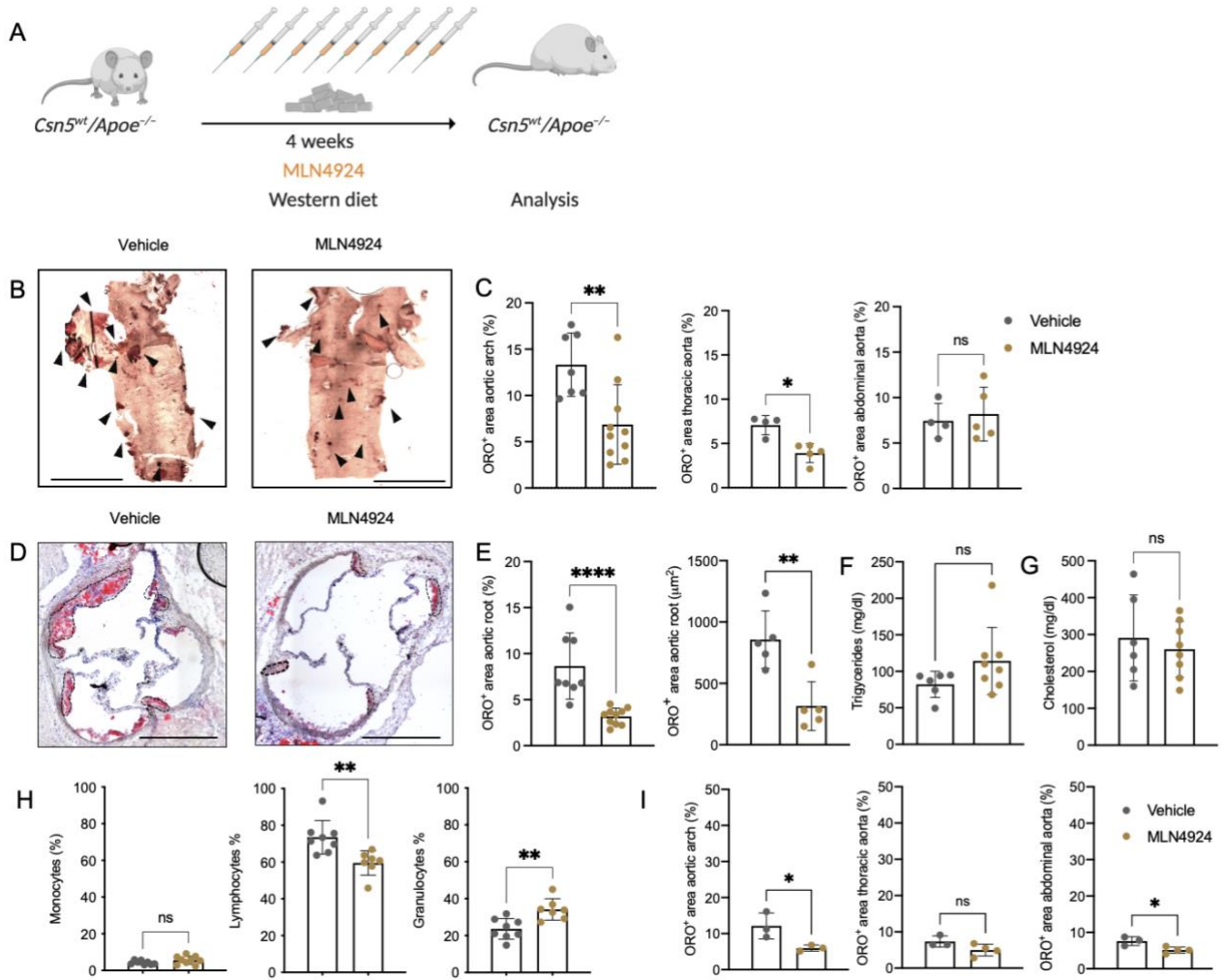


**Figure 21. MLN4924 mimics atheroprotection by Csn5 after 4 weeks of HFD and impacts small lesions.** **A**, Experimental Outline. Male *Apoe*<sup>-/-</sup> mice were fed HFD in parallel and received MLN4924 or vehicle treatment. **B**, Representative images of ORO-stained aortic arches. Black arrowheads indicate the ORO<sup>+</sup> areas. Scale bars, 3 mm. **C**, Quantification of lesion sizes in the mouse aorta after the MLN4924 treatment (n=4-7) compared to the vehicle-treated mouse aortas (n=5-10). **D**, Representative image of the ORO-stained aortic root of male MLN4924 (n=5-10) or vehicle-treated (n=5-8) mice. Scale bars, 500  $\mu$ m. **F-G**, Triglyceride, and cholesterol levels of mice receiving MLN4924 (n=8) or vehicle (n=6) treatment. **H**, Blood cell count of MLN4924 (n=7) treated male *Apoe*<sup>-/-</sup> mice compared to the vehicle-treated (n=8) controls. Male *Apoe*<sup>-/-</sup> mice consumed HFD for 12 weeks while receiving MLN4924 (n=3-4) or vehicle (n=3) treatment only for the first 4 weeks. **I**, Quantification of lesion sizes in aortas of MLN4924 treatment compared to the controls. Two-sided Mann-Whitney test was used. Data are mean  $\pm$  SD: \*p<0.05, \*\*p<0.01, \*\*\*p<0.001. These data represent means  $\pm$  SD.

**Table 1. Male *Apoe*<sup>-/-</sup> blood cell count after receiving the MLN4924 or Vehicle treatment**

Parameters*	Vehicle			MLN4924			P-value
	Mean	SD	N	Mean	SD	N	
<b>WBC (/mm<sup>3</sup>)</b>	5,757143	5,42582	7	3,211429	1,763778	7	0,053078
<b>RBC (/mm<sup>3</sup> l)</b>	2,802625	2,779181	8	2,943333	2,206122	9	0,506174
<b>HGB (g/dl)</b>	15,18571	6,027832	7	9,267778	5,178667	9	0,360028
<b>HCT (%)</b>	25,02857	9,550866	7	41,62222	63,3011	9	0,954541
<b>MCV</b>	136,125	82,58751	8	97,73333	84,62155	9	0,169700
<b>MCH</b>	103,9429	80,36948	7	106,4111	87,28954	9	0,934073
<b>MCHC</b>	57,2	22,4153	8	93,76667	68,2855	9	0,183060
<b>PLT (10<sup>3</sup> /µl)</b>	189,95	232,619	8	199,8556	250,5307	9	0,211686
<b>MPV</b>	6	3,000476	8	30,43333	49,24505	9	0,146075
<b>RDW</b>	13,86667	1,457166	3	10,31667	4,222519	6	0,007569
<b>LYM (%)</b>	72,18571	11,13664	7	60,76667	16,92011	9	0,210391
<b>MO (%)</b>	3,942857	1,213613	7	6,344444	1,727796	9	0,655413
<b>GRA (%)</b>	23,87143	10,35273	7	32,93333	15,74738	9	0,451855
<b>LYM (/mm<sup>3</sup>)</b>	4,514286	5,386226	7	8,088889	20,04379	9	0,539125
<b>MO (/mm<sup>3</sup>)</b>	0,157143	0,113389	7	0,333333	0,589491	9	0,053078
<b>GRA (/mm<sup>3</sup>)</b>	1,085714	0,313202	7	1,377778	1,1872	9	0,506174

\* Acronyms are explained in the Material and methods.

The previous study demonstrated that MLN4924 only exerts its athero-protectiveness on male mice (Asare et al., 2017). Hence it might not have any beneficial outcome for the female atherogenic mice. The reason might stand behind that CSN5/Jab1 stimulates estrogen-receptor degradation, and estrogen receptors are known to mediate several athero-protective effects on cells and molecules implicated in the vascular inflammation (Calligé et al., 2005; Kassi et al., 2015). Hence, we here aimed to investigate if MLN4924 treatment benefits an early lesion progression in female mice (Figure 22).

MLN4924 treatment of the *Apoe*<sup>-/-</sup> female mice didn't yield less pronounced atherosclerotic lesions than their vehicle-treated controls, the athero-protective effect previously observed in the equally treated *Apoe*<sup>-/-</sup> males. *Apoe*<sup>-/-</sup> females, after receiving the MLN4924 treatment, didn't show a less pronounced lesion found in their aortic root (Fig. 22, A-B), or the plaque load in the aorta (Fig. 22, C-D) compared to their vehicle-treated controls, after the 4 weeks of HFD consumption. In conclusion, suggesting yet again that MLN4924, as previously observed, has only a beneficial effect in a gender-specific manner, as it seems it is ineffective in combating early lesion progression in female atherogenic, *Apoe*<sup>-/-</sup> mice.

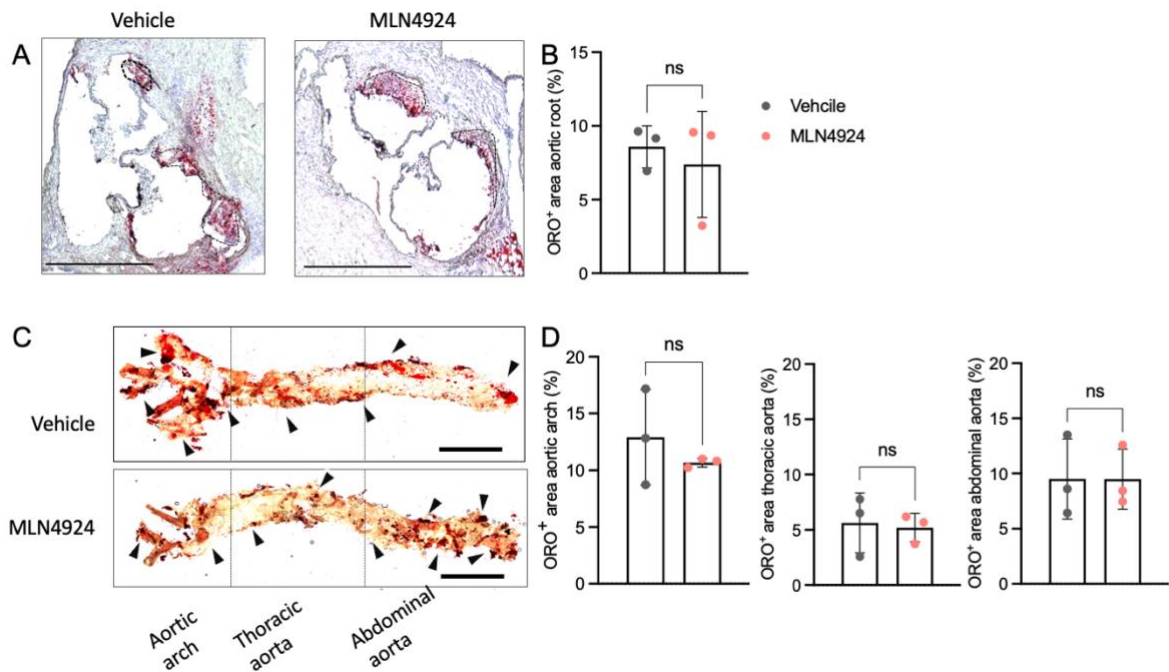


**Figure 22. MLN4924 does not confer atheroprotection in female *Apoe*<sup>-/-</sup> mice.** Six weeks old female *Apoe*<sup>-/-</sup> mice were fed an HFD for 4 weeks and received MLN4924 or vehicle treatment. **A** Representative ORO-stained aortic roots of females *Apoe*<sup>-/-</sup> mice receiving MLN4924 or vehicle treatment. The black intercepted line outlines the lesion area. Scale bar, 500  $\mu$ m. **B**, Quantification of the percentage of the ORO-stained lesion area of the female aortic roots after receiving MLN4924 treatment ( $n = 3$ ) or vehicle treatment ( $n = 3$ ). **C**, Representative images of the *en-face* ORO-stained aortas, with indicated (black arrowheads) lesion sites. Scale bars, 3 mm. **D**, Quantification of lesion sizes in mouse aorta after the MLN4924 treatment ( $n = 3$ ) compared to the vehicle-treated mouse aortas ( $n = 3$ ). These data represent means  $\pm$  SD.

#### 4.4 Csn5 depletion in arterial endothelial cells promotes advanced atherosclerosis

Starry and his team define atherosclerotic lesions advanced by several marked phenotypes. Firstly, advanced stages as every stage of atherosclerosis have notable lipid accumulations. Matrix components of the advanced lesion, together with the cells of the vessel, are structurally disorganized, causing significant structural changes in the vessel wall formation. Advanced lesions have significant intimal thickening, with lumen narrowing and possible histologically visible clinical manifestations (Starry et al., 1994, 1995). Previous studies have demonstrated that the Csn3 depletion and myeloid-specific-Csn5 depletion in athero-prone *Apoe*<sup>-/-</sup> mice exacerbate advanced atherosclerosis (Asare et al., 2017; Boro et al., 2021). Hence, I wanted to investigate if arterial-/endothelial-specific *Csn5* knock-out (KO) in an atherogenic *Apoe*<sup>-/-</sup> background (*Csn5*<sup>Arterial</sup>*Apoe*<sup>-/-</sup>) upon Western-type diet recapitulates the exacerbated atherosclerotic phenotype *in vivo*. Atherosclerosis progression of the *Csn5*<sup>Arterial</sup>*Apoe*<sup>-/-</sup> male (Fig. 23) and female mice (Fig. 23) was investigated after 12 weeks of HFD consumption.

Initially, I could conclude that the body weight, blood count, and lipid levels showed no differences in *Csn5*<sup>Arterial</sup>/*Apoe*<sup>-/-</sup> compared to the *Csn5*<sup>WT</sup>/*Apoe*<sup>-/-</sup> male mice (Fig. 23, A-B, Table 2). Atherosclerotic lesion size found in the male aorta was exacerbated

in the whole aorta of the *Csn5<sup>Arterial</sup>/Apoe<sup>-/-</sup>* mice (Fig. 23, C-D) compared to the vehicle-treated male mice, *Csn5<sup>wt</sup>/Apoe<sup>-/-</sup>*. Investigation of the lesion prone-sites in the total aorta revealed that *Csn5* deletion in the endothelial lining was affecting lesion size more profoundly in the aortic arch and abdominal aorta (Fig. 23 C-D).

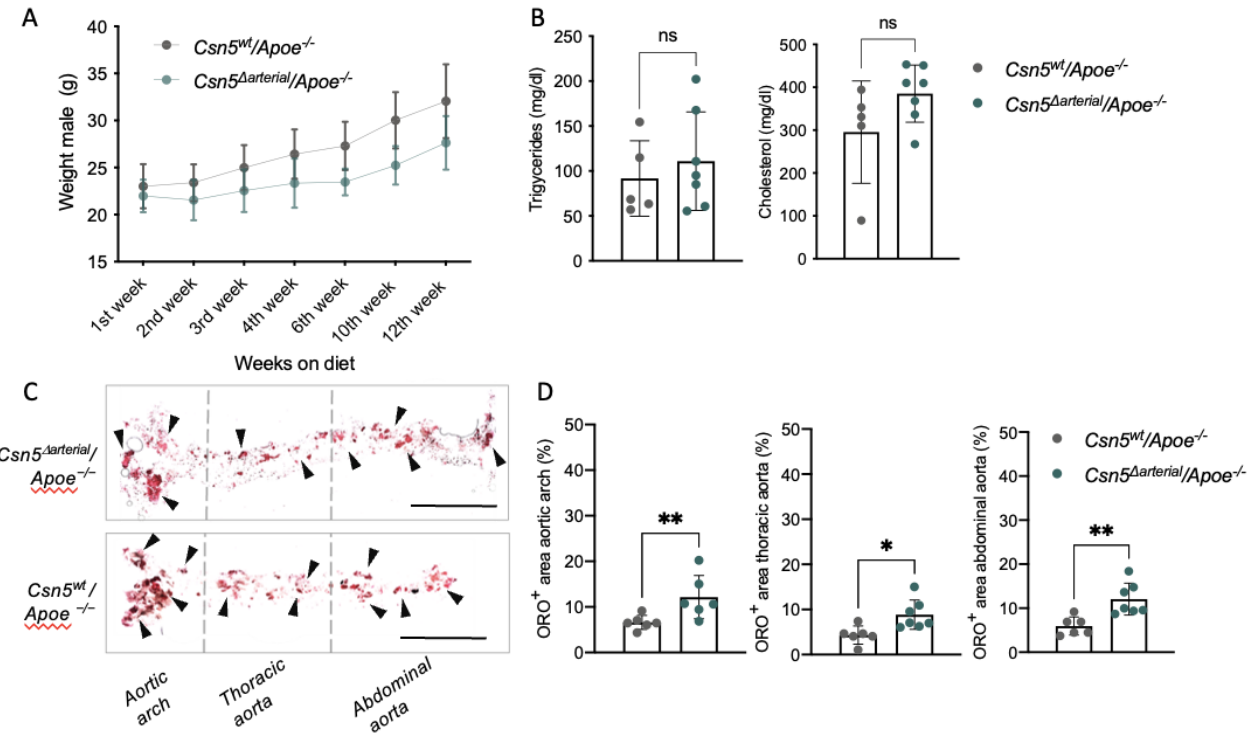


**Figure 23. Arterial-endothelial specific depletion of *Csn5* promotes advanced atherosclerosis in the aorta but doesn't impact mouse well-being and lipid mouse metabolism.** *Csn5<sup>Arterial</sup>/Apoe<sup>-/-</sup>* male mice were injected with tamoxifen or vehicle to induce *Csn5* depletion in the arterial endothelial lining. They were fed a high-fat diet for 12 weeks to cause advanced-stage atherosclerosis. **A**, Male *Csn5<sup>Arterial</sup>/Apoe<sup>-/-</sup>* (n = 7) weight over the 12 weeks compared to the *Csn5<sup>wt</sup>/Apoe<sup>-/-</sup>* controls (n = 7). **B**, Triglyceride and cholesterol levels are shown. *Csn5<sup>Arterial</sup>/Apoe<sup>-/-</sup>* (n = 7), *Csn5<sup>wt</sup>/Apoe<sup>-/-</sup>* (n = 5). **C**, Representative images of aortic arches of *Csn5<sup>Arterial</sup>/Apoe<sup>-/-</sup>* and *Csn5<sup>wt</sup>/Apoe<sup>-/-</sup>* mice. Black arrowheads indicate the Oil-red-O positive areas. Scale bars, 3 mm. **D**, Quantification of lesion sizes in mouse aorta of the *Csn5<sup>Arterial</sup>/Apoe<sup>-/-</sup>* (n = 6-7) compared to the vehicle-treated mouse *Csn5<sup>wt</sup>/Apoe<sup>-/-</sup>* aortas (n = 6). These data represent means  $\pm$  SD.

**Table 2. Blood cell count of male *Csn5<sup>Arterial</sup>/Apoe<sup>-/-</sup>* compared to the *Csn5<sup>wt</sup>/Apoe<sup>-/-</sup>* controls**

Parameters*	<i>Csn5<sup>wt</sup>/Apoe<sup>-/-</sup></i>			<i>Csn5<sup>Arterial</sup>/Apoe<sup>-/-</sup></i>			p- value
	Mean	SD	N	Mean	SD	N	
<b>WBC (/mm<sup>3</sup>)</b>	4,017	1,447	6	5,53	7,145	6	0,621343
<b>RBC (/mm<sup>3</sup>)</b>	3,917	2,051	3	5,8	1,451	6	0,148390
<b>HGB (g/dl)</b>	10,4	5,381	5	10,612	3,073	6	0,934844
<b>HCT (%)</b>	21,8	11,677	3	29,433	6,15	6	0,225482
<b>MCV</b>	55,3	1,155	3	51,167	3,126	6	0,066377
<b>MCH</b>	18,067	5,977	3	18,517	4,039	6	0,895555
<b>MCHC</b>	32,53	10,22	3	98,517	156,13	6	0,502689
<b>PLT (10<sup>3</sup> /<math>\mu</math>l)</b>	131,33	69,3	6	145	150,4	6	0,843849
<b>MPV</b>	5,933	1,93	6	6,8	0,87	6	0,338013
<b>RDW</b>	13,3	1,34	3	15,683	3,397	6	0,292357

<b>LYM (%)</b>	67,083	9,521	6	71,417	7,225	6	0,395359
<b>MO (%)</b>	4,367	0,773	6	4,867	1,109	6	0,342579
<b>GRA (%)</b>	28,6	9,203	6	23,717	7,524	6	0,337996
<b>LYM (/mm<sup>3</sup>)</b>	2,55	0,872	6	1,75	0,6	6	0,093538
<b>MO (/mm<sup>3</sup>)</b>	0,15	0,084	6	0,083	0,040	6	0,109946
<b>GRA (/mm<sup>3</sup>)</b>	1,317	0,686	6	0,7	0,364	6	0,080097

\* Acronyms are described in material and methods.

Once the role of *Csn5* loss in the endothelial lining was investigated in female *Csn5<sup>Arterial</sup>/Apoe<sup>-/-</sup>* mice after 12 weeks HFD, no differences could be observed in lesion size in the aorta (Fig. 24, B-C) or aortic root (Fig. 24, D, E-F) compared to their *Csn5<sup>wt</sup>/Apoe<sup>-/-</sup>* control. Furthermore, advanced marking of arterial remodelling was investigated, and no collagen content or fibrous cap thickness changes were observed (Fig. 24, G-H) between the

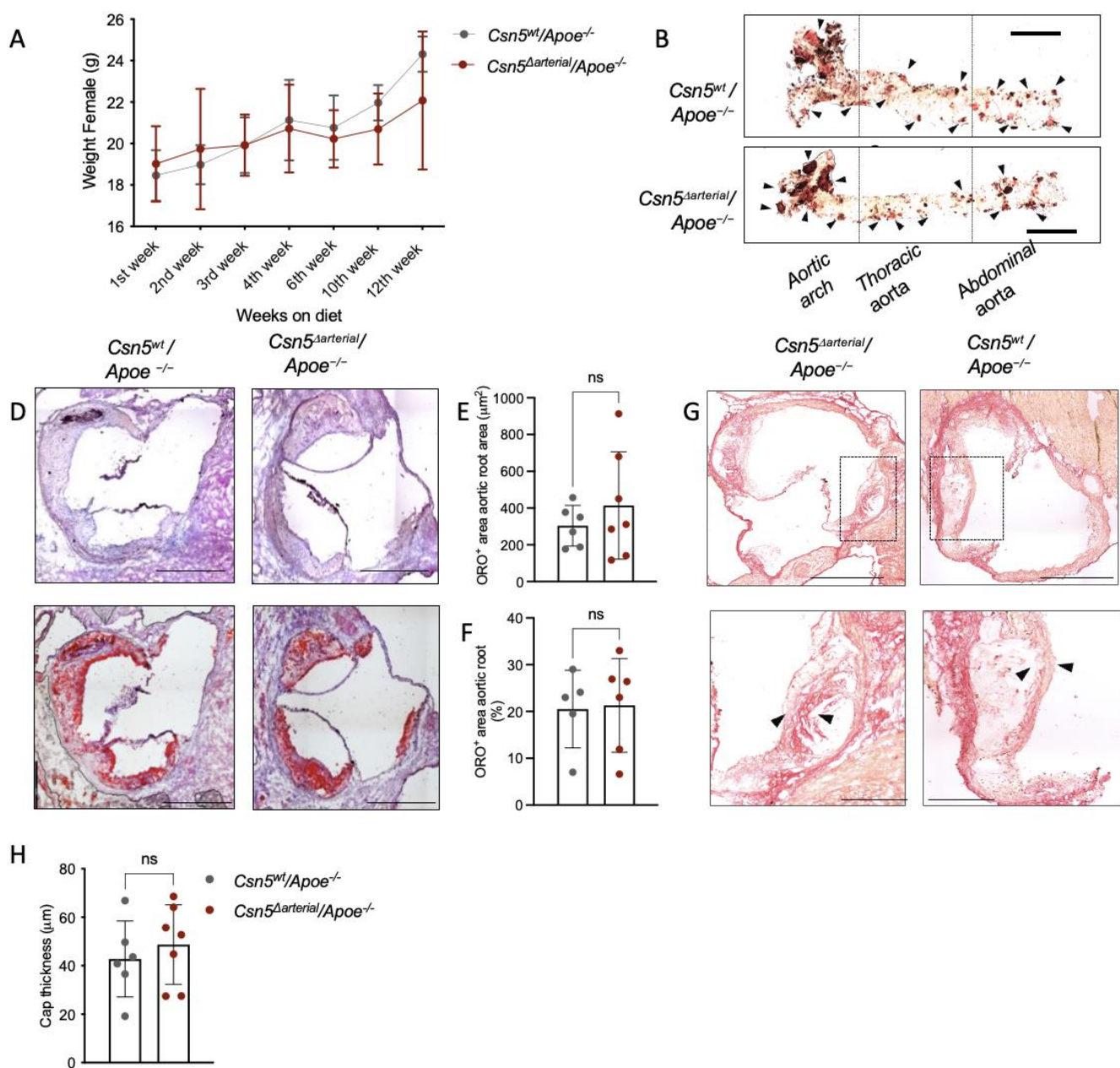


**Figure 24. Arterial-endothelial specific depletion of Csn5 isn't affecting atherosclerosis progression in female mice after 12 weeks of HFD.** Six weeks old, *Csn5<sup>Arterial</sup>/Apoe<sup>-/-</sup>* female mice were injected with tamoxifen or vehicle to induce Csn5 depletion in the endothelial lining. They were consuming a high-fat diet for 12 weeks to induce advanced atherosclerosis. A Female's well-being was evaluated on their weight progression over the 12 weeks. *Csn5<sup>Arterial</sup>/Apoe<sup>-/-</sup>* (n = 8) and *Csn5<sup>wt</sup>/Apoe<sup>-/-</sup>* (n = 6) B, Representative female ORO-stained aortas are shown. Black arrowheads outline the lesion sites in the aortic arch, aortic root, and abdominal aorta. Scale size, 3mm. D, Representative hematoxylin and eosin-stained female aortic roots (up) and ORO-stained aortic root areas (down). Scale size, 500  $\mu$ m. E-F, Quantification of the females ORO<sup>+</sup> aortic root area and lesion size. *Csn5<sup>Arterial</sup>/Apoe<sup>-/-</sup>* (n= 6- 7) and *Csn5<sup>wt</sup>/Apoe<sup>-/-</sup>* (n= 5- 6) controls. G, Sirius red collagen staining of the female aortic roots after 12 weeks of HFD is shown in lower (up, scale size bar 500  $\mu$ m) and higher magnification (down, scale size bar 50  $\mu$ m). Black arrowheads outline the fibrous cap. H, Quantification of the total collagen lesion fibrous cap thickens is shown. *Csn5<sup>Arterial</sup>/Apoe<sup>-/-</sup>* (n = 7) and *Csn5<sup>wt</sup>/Apoe<sup>-/-</sup>* (n = 6) controls. These data represent means  $\pm$  SD.

*Csn5<sup>Arterial</sup>/Apoe<sup>-/-</sup>* and *Csn5<sup>wt</sup>/Apoe<sup>-/-</sup>* female mice. Female weight showed no significant differences change over the period of 12 weeks western type of diet (Fig. 24A), nor was the blood cell count altered between the *Csn5<sup>Arterial</sup>/Apoe<sup>-/-</sup>* and *Csn5<sup>wt</sup>/Apoe<sup>-/-</sup>* female mice (Table 3).

**Table 3. Blood cell count of female *Csn5<sup>Arterial</sup>/Apoe<sup>-/-</sup>* compared to the *Csn5<sup>wt</sup>/Apoe<sup>-/-</sup>*-controls.**

*Prametars	<i>Csn5<sup>wt</sup>/Apoe<sup>-/-</sup></i>			<i>Csn5<sup>Arterial</sup>/Apoe<sup>-/-</sup></i>		
	MEAN	SD	N	MEAN	SD	N
<b>WBC (/mm<sup>3</sup>)</b>	3,4	0,72	3	5,1	2,82	4
<b>RBC (/mm<sup>3</sup>)</b>	7,81	1,90	3	6,96	2,41	4
<b>HGB (g/dl)</b>	12,6	2,70	3	11,75	5,72	4
<b>HCT (%)</b>	38	7,9	3	36,62	11,98	4
<b>MCV</b>	49	1,73	3	53	2,45	4
<b>MCH</b>	17,03	5,92	3	16,37	5,01	4
<b>MCHC</b>	34,5	11,01	3	30,85	9,28	4
<b>PLT (10<sup>3</sup> /<math>\mu</math>l)</b>	109,3	18,15	3	140,5	57,49	4
<b>MPV</b>	7,3	1,05	3	6,62	0,56	4
<b>RDW</b>	15,27	2,89	3	14,05	0,87	4
<b>LYM (%)</b>	69,37	3,70	3	71,97	4,29	4
<b>MO (%)</b>	5,53	0,23	3	5,32	1,34	4
<b>GRA (%)</b>	25,1	3,57	3	22,7	4,18	4
<b>LYM (/mm<sup>3</sup>)</b>	2,3	0,5	3	9,65	11,69	4
<b>MO (/mm<sup>3</sup>)</b>	0,13	0,06	3	0,275	0,22	4
<b>GRA (/mm<sup>3</sup>)</b>	0,96	0,21	3	1,25	0,75	4

\* Acronyms are described in material and methods.

#### 4.5 Csn5 loss in arterial endothelial lining enhances atherosclerotic plaque vulnerability

Atherosclerosis can evolve over a lifetime, and often enough, it cannot be clinically symptomatic unless there is an event of plaque rupture and, thus, exposure to thrombus material. One of the necessities for advanced lesions to become clinically relevant is the thinning of the fibrous cap. The mechanism behind plaques being prone to rupture is largely unknown. But understanding the players and factors contributing to its

vulnerable atherosclerotic phenotype would be crucial in preventing major life-threatening events as a consequence of adverse atherosclerosis. Several studies have previously demonstrated that the loss of COP9 function promotes lesion advancement *in vivo* (Asare et al., 2017; Boro et al., 2021). So far there to our knowledge, there is no available data on the atherosclerotic plaque's content and phenotype upon the COP9 signalosome loss of function described in the literature. Hence, I aimed here to decipher for the first time the contributing factor and mechanism behind observed advanced lesion size exacerbation and plaque lesion cell content and phenotype. Moreover, as many cell-derived factors determine atherosclerosis development, I aimed to investigate the most crucial ones, such as overall lesion size and lesion macrophage content, and smooth muscle cell content.

Firstly, atherosclerotic lesion size upon arterial-endothelial specific depletion of *Csn5* in *Apoe*<sup>-/-</sup> mice after 12 weeks of HFD is significantly more elevated than controls *Csn5*<sup>wt</sup> / *Apoe*<sup>-/-</sup>. This was testified by the percentage of the ORO-stained lesion area (Fig. 25, C-D) and via overall lesion size by employing H&E staining (Fig. 25, A-B). H&E staining is also an effective tool to analyse necrotic core size (Fig. 26D). As necrotic core enlargement is effectively impacting the thinning of the fibrous cap. Also, the necrotic core is formed mainly by the macrophage population, whereby macrophages and the SMCs are the major producers of matrix remodelling factors. SMCs loss plays a big role in the loss of plaque stability (Bentzon et al., 2014; Virmani et al., 2000). Mouse lesions with advanced atherosclerosis after consuming 12 weeks of HFD were probed for these vulnerability factors. Hereby, it could be observed that macrophage content was elevated in the *Csn5*<sup>Arterial</sup> / *Apoe*<sup>-/-</sup> mice (Fig. 25, E-F). In contrast, the smooth muscle cell (<sup>+</sup>SMC) content in a lesion of arterial-endothelial specific *Csn5* knockout mice was significantly reduced compared to the vehicle-treated mice (Fig. 25, G-H).

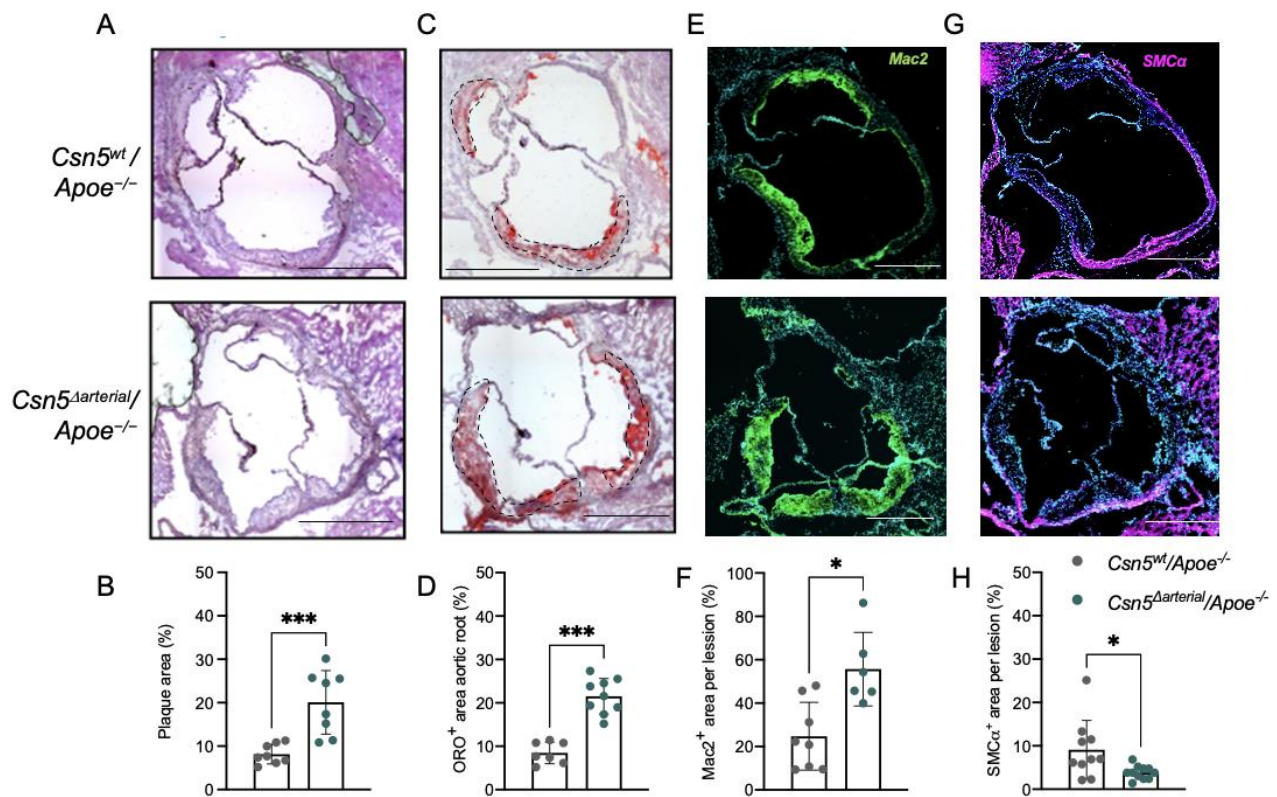


**Figure 25. Arterial-endothelial specific depletion of Csn5 promotes advanced atherosclerosis and enhances factors of atherosclerotic plaque vulnerability after 12 weeks of HFD.** **A, C**, Representative image of Hematoxylin and Eosin (A) and ORO stained (C) aortic root lesion. Scale bars, 500  $\mu$ m. **B, D**, Quantification of lesion sizes in the aortic root of *Csn5<sup>wt</sup>/Apoe<sup>-/-</sup>* (n=4 - 7), *Csn5<sup>Arterial</sup>/Apoe<sup>-/-</sup>* (n= 6 - 9 mice). **E, G**, Representative immunostainings of the lesion MAC2<sup>+</sup> area (E) in green and (F) SMA<sup>+</sup> cell area in magenta. **F, H**, Quantification of immunostainings *Csn5<sup>Arterial</sup>/Apoe<sup>-/-</sup>* (n=6 -11 mice) *Csn5<sup>wt</sup>/Apoe<sup>-/-</sup>* (n=8 - 10 mice). These data represent means  $\pm$  SD.

Lesion phenotype with elevated macrophage and SMCs content could be more prone to plaque vulnerability. To further evaluate plaque vulnerability, atherosclerotic lesions of the *Csn5<sup>Arterial</sup>/Apoe<sup>-/-</sup>* mice were analyzed for total collagen content (Fig. 26B) and cap thickness (Fig. 26, A-C), by employing the Sirius red staining. Although total collagen content was not significantly different among the *Csn5<sup>Arterial</sup>/Apoe<sup>-/-</sup>* mice, and its control littermates (Fig. 26, A-C), fibrous cap thickness was significantly decreased in arterial-endothelial *Csn5* depleted mice (Fig. 26C). Collectively, factors of vulnerability were combined, and we could determine that *Csn5<sup>Arterial</sup>/Apoe<sup>-/-</sup>* male mice have more vulnerable plaques and more pronounced advanced atherosclerosis compared to the *Csn5<sup>wt</sup>/Apoe<sup>-/-</sup>* mice (Fig. 26E).

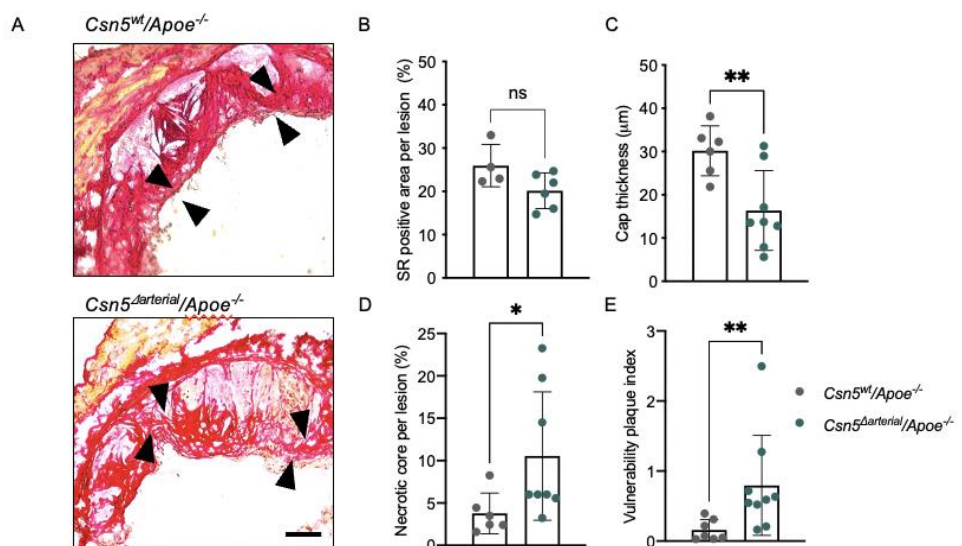


**Figure 26. Csn5 depletion in arterial endothelial lining enhances atherosclerotic plaque vulnerability after 12 weeks of HFD.** **A** Representative Sirius red-stained lesions with fibrous cap indicated with black arrowheads. Scale bars, 50  $\mu$ m. **B-C**, Quantification of collagen content and FC thickness. *Csn5<sup>Arterial</sup>/Apoe<sup>-/-</sup>* (n= 6-8 mice) *Csn5<sup>wt</sup>/Apoe<sup>-/-</sup>* (n=4-6 mice). **D**, Quantification of the necrotic core size of the *Csn5<sup>Arterial</sup>/Apoe<sup>-/-</sup>* (n= 8 mice) and *Csn5<sup>wt</sup>/Apoe<sup>-/-</sup>* (n=6 mice). **E**, Vulnerability plaque index quantification of *Csn5<sup>Arterial</sup>/Apoe<sup>-/-</sup>* (n= 9 mice) compared to the *Csn5<sup>wt</sup>/Apoe<sup>-/-</sup>* (n=7 mice). These data represent means  $\pm$  SD.

#### 4.6 Arterial-endothelial specific depletion of Csn5 downregulates TIMP1 levels in vivo

Much effort has been invested in understanding the vulnerability phenotype in the last couple of years (Bentzon et al., 2014; Otsuka et al., 2016;). Many circulatory markers have been evaluated over the years to predict the atherosclerosis outcome and/or investigate the appropriate therapy. Hereby, we aimed to perform unbiased screening for the markers of atherogenic inflammation, endothelial-derived factors, and

factors of plaque vulnerability to understand the signalling pathways elicited upon arterial-endothelial specific CSN5 deletion (**Fig. 27, A-G**).

The multiplex cytokine panel enabled us to evaluate systemically inflammatory cytokines in the mouse serums (**Fig. 27, A-B**). Firstly, we could observe arterial-endothelial specific CSN5 deletion caused an upregulation of atherogenic markers, such as M-CSF and a system of complement component C5-C5a, which are well established in the lesion promotion (**Fig. 27C**). Surprisingly, levels of TIMP-1 were strikingly low upon *Csn5* depletion. Thus, for the first-time involving matrix remodelling component and potentially justifying encountered plaque vulnerability of the phenotype (**Fig. 27G**). Atherosclerosis is led by endothelial dysfunction and, consequently, adhesion molecules up-regulation. Moreover, *Csn5* in the endothelial cells negatively regulates the gene expression of the adhesion molecules by regulating the NF- $\kappa$ B signalling axis *in vitro* (Asare et al., 2013b). Hence here we wanted to verify this for the first time *in vivo*. Adhesion molecules, such as ICAM-1 and VCAM-1, have been up-regulated in *Csn5<sup>Aarterial</sup>/Apoe<sup>-/-</sup>* mice compared to the serums of their controls (**Fig. 27D**). Furthermore, circulating chemokines such as CX3CL, CXCL13 and CXCL10 were elevated signalling more pronounced atherogenic inflammation (**Fig. 27E**). Moreover, cytokines such as IL1- $\alpha$ , IL-4, IL-6, IL-10, and IL-13 are more elevated. At the same time, IL-12p40 is seemingly less expressed upon CSN5 depletion in the endothelial lining suggesting a more complex picture in systemic atherogenic inflammation (**Fig. 27F**).

As the systemic murine Timp-1 levels were impaired with the arterial-endothelial *Csn5* depletion, its functionality was probed on the systemic levels of the MMPs as TIMP-1 known substrates. Interestingly, the most pronounced effects could be seen systemically on the MMP3 elevated levels, while MMP2 and MMP9 were unchanged (**Fig. 27H**). Vascular cell types that upregulate and secrete OPN include ECs, VSMCs, and macrophages (Lok & Lyle, 2019). OPN (osteopontin) is a secreted multifunctional glycol-phospho-protein and is one of the predictive markers of adverse atherosclerotic events as it accelerates the cardiovascular remodelling process through TGF $\beta$  signalling and MMPs. Myeloperoxidase (MPO) and its end product HOCl activate MMP and deactivate inhibitors of MMPs, thus promoting untimely the weakening of the fibrous cap and destabilisation of atherosclerotic plaque (**Fig. 27H**) (Koenig & Khuseyinova, 2007; Okamoto, 2007).

After analysing more than 150 biomarkers in the serums of *Csn5<sup>Aarterial</sup>/Apoe<sup>-/-</sup>* and *Csn5<sup>wt</sup>/Apoe<sup>-/-</sup>* mice, markers were sorted according to the existing literature either marker of plaque vulnerability (**Fig. 27H**) or endothelial-derived factors (**Fig. 26G**).

Cytokines such as TNF $\alpha$ , IL-6, RAGE, and CCL2 are majorly produced by either monocyte/macrophages or endothelial cells, as they amplify atherogenic inflammation. TNF $\alpha$  is well known pro-atherogenic stimulus, but as it has been shown, it can also elevate the expression of the MMPs (Y. Y. Li et al., 2000). Circulatory TNF $\alpha$  levels didn't change upon *Csn5* depletion in the endothelial lining (**Fig. 27G**). IL-6 expression is elevated in atherosclerotic lesions and coincides with the TIMP-1 depletion while favouring MMP elicited activity (Schieffer et al., 2004). Once *Csn5* was depleted in the endothelial lining of atherosclerotic *Apoe<sup>-/-</sup>* male mice, it could be observed that there is a slight trendline towards IL-6 cytokine elevation in these mouse serums (**Fig. 27G**).

Pentraxin-related protein (PTX3) is elevated by IL-1 or TNF in ECs (Breviario et al., 1992; G. W. Lee et al., 1993). State-of-the-art suggests PTX3 protects the atherosclerosis development (Norata et al., 2010). Herby, PTX3 is noticeably elevated in mice upon loss of CSN5 in the endothelial lining and 12 weeks of HFD consumption (**Fig. 27G**).

The most widely used marker for evaluating adverse atherosclerosis effects, atherosclerotic plaque vulnerability, and the main factor for evaluating atherogenic inflammation in mice and humans is C-reactive protein (CRP) (Koenig & Khuseyinova, 2007). Interestingly, although there were few biological replicates, the significance wasn't achieved. I could determine much higher CRP levels in *Csn5<sup>Δarterial</sup>/Apoe<sup>-/-</sup>* compared to the *Csn5<sup>wt</sup>/Apoe<sup>-/-</sup>* mice, representing the elevated atherogenic inflammation status (**Fig. 27G**).

oxLDL stimulation, proinflammatory environment, and endothelial activation up-regulate the adhesion molecules expression of VCAM-1, ICAM-1, P-sel, and E-sel, which in turn participate in cell recruitment of the blood-derived leukocytes and monocytes into the subendothelial space (Koenig & Khuseyinova, 2007). Once their shedding was evaluated in serums of the CSN5-depleted mice, adhesion molecules were elevated, suggesting more pronounced atherosclerosis (**Fig. 27G**).

One of the ECs dysfunction promoters is the platelet-derived growth factor (PDGF-BB). Upon CSN5 depletion in the endothelial lining, mice responded by noticeably higher expression of PDGF-BB circulatory levels compared to their vehicle-treated vehicle-treated controls (**Fig. 27F**). Finally, proprotein convertase subtilisin/Kexin 9 (PCSK9) is up-regulated in endothelial cells under the pro-inflammatory stimuli *in vivo*, as such is a strong promotes of the ECs apoptosis which can lead to a disturbed endothelial barrier (Leucker et al., 2021; J. Li et al., 2017). Interestingly, PCSK9 is trend-line elevated in serums of *Csn5<sup>Δarterial</sup>/Apoe<sup>-/-</sup>* mice compared to their *Csn5<sup>wt</sup>/Apoe<sup>-/-</sup>* controls.

Overall, several markers of plaque vulnerability are elevated in mice upon endothelial *CSN5* loss elaborating on the systemic response and more complex mechanism underlining endothelial activation. I analysed here as well endothelial-derived biomarkers as COP9 has been associated with endothelial dysfunction *in vivo* (**Fig. 27G**). Among the more pronounced endothelial-derived factors are Angiotensin II and -L3, which might be, as previously shown, one of the driving forces behind NF- $\kappa$ B regulation of the VCAM-1, as well as a direct inducer of endothelial dysfunction via regulation of RhoA/ROCK pathway (Piqueras & Sanz, 2020; Pueyo et al., 2000; Silva et al., 2020)

CD93 is majorly expressed in ECs, but also neutrophils and monocytes (Fonseca et al., 2001). A matrix metalloproteinase that mediates soluble CD93 cleavage in human patients was associated with adverse clinical outcomes (Newby, 2007; Youn et al., 2014). CD93 is strongly elevated in mouse serums upon arterial-endothelial specific depletion of *Csn5* (**Fig. 27H**).

Endothelial homeostatic CCL21 chemokine dysregulation has been shown to enable T-cell mediated atherosclerosis progression (Damås et al., 2007). We could observe that the CCL21 chemokine is upregulated in *Csn5<sup>Δarterial</sup>/Apoe<sup>-/-</sup>* mouse serums (**Fig. 27H**). Insulin-like growth factor-binding protein showed diverse profiles in male mouse serums upon *CSN5* loss in an endothelial arterial manner. Namely, IGFBP1 plays a crucial protective role in vascular remodelling and stimulates EC regeneration, and has been demonstrated to possibly play a role in the plaque stability (Martin et al., 2008; C.-M. Wu et al., 2021). IGFBP-2 concentrations correlate negatively with arterial intima-media thickness (Martin et al., 2008). In contrast, IGFBP-3 plays a role in angiogenesis-related gene expression and modulating matrix remodelling by increasing the MMP2 and MMP9 activation (Forbes et al., 2012; Granata et al., 2007). Thereby, in serums of the *Csn5<sup>Δarterial</sup>/Apoe<sup>-/-</sup>* mice, insulin-like growth factors 1 and 2 were decreased, while on the other hand, IGFBP-3 was increased compared to the *Csn5<sup>wt</sup>/Apoe<sup>-/-</sup>* suggesting possible adverse effects upon matrix remodelling players and induce higher intimal vessel thickness (**Fig. 27H**). Adipokine, chemerin, also known as tazarotene-induced

gene 2 (TIG2), is shown to be elevated here upon CSN5 depletions (**Fig. 27H**). Previous studies have shown that chemerin inductions worsen the atherosclerosis progression in vivo and promote endothelial angiogenesis and MMP production and activity (Kaur et al., 2010; H. Liu et al., 2019). Chitinase-3-like protein 1 (CHI3L1) Chi3l1 mediates EC inflammation and VSMC activation, accelerating the atherosclerosis progression (Jung et al., 2018).

Overall many of the outlined factors triggered by the arterial-endothelial Csn5 deletion can be endothelial-derived or systemic. Their plausible contribution to the plaque vulnerability can be only speculated as there is not enough evidence to outline their importance. Future studies might be designed to investigate them individually.

As one of the most strikingly affected factors to be altered by this unbiased assay is the TIMP-1 levels, I strived to validate this observation by evaluating its systemic levels in serums of the *Csn5<sup>Δarterial</sup>/Apoe<sup>-/-</sup>* by employing ELISA. Indeed, TIMP-1 levels were significantly lower in the *Csn5<sup>Δarterial</sup>/Apoe<sup>-/-</sup>* mice compared to the serums of their controls (**Fig. 27K**). Moreover, as seemingly systemic levels of TIMP-1 are altered, I wanted to evaluate if its loss in circulation can be recorded in the atherosclerotic lesions of the *Csn5<sup>Δarterial</sup>/Apoe<sup>-/-</sup>* mice. Immunofluorescence staining against TIMP-1 was performed on the aortic roots of the arterial-endothelial CSN5 mice and their respective controls. Interestingly, it was shown that there is less TIMP-1<sup>+</sup> area in the mice's plaque with down-regulated endothelial Csn5 levels (**Fig. 27, I-K**). On the other hand, this was only observed on the male lesions, while female atherosclerotic lesions were not affected, and their atherosclerotic plaque Timp-1 levels were non-altered (**Fig. 27L**).

Overall, initial unbiased screening of the *Csn5<sup>Δarterial</sup>/Apoe<sup>-/-</sup>* atherosclerotic lesions and mouse serum has revealed that matrix remodelling factor and biomarkers determining the vulnerable atherosclerotic phenotype has been somewhat affected, and for the first time link between endothelial-CSN5 and systemic Timp-1 has been demonstrated.

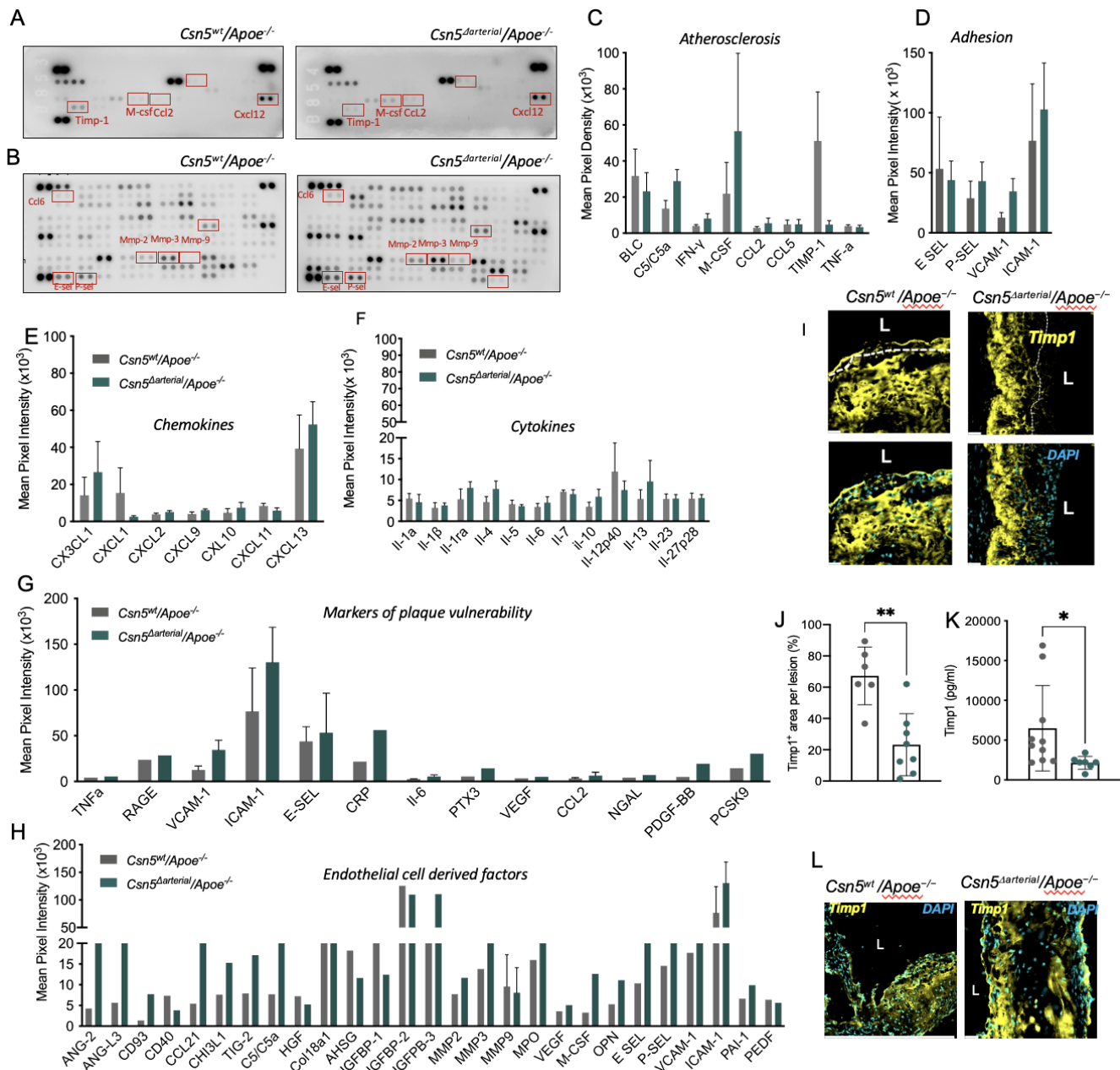


**Figure 27. Arterial-endothelial Csn5 depletion downregulates the systemic TIMP1 levels in vivo.** Tamoxifen treated *Csn5<sup>arterial</sup>/Apoe<sup>-/-</sup>* mice and their respective control, vehicle-treated *Csn5<sup>wt</sup>/Apoe<sup>-/-</sup>* littermates were exposed to the HFD diet for 12 weeks and their serums were probed on the multiplex mouse cytokine panel. **A-B**, Representative immuno-blots of the cytokine panels of the *Csn5<sup>arterial</sup>/Apoe<sup>-/-</sup>* (n= 2 - 3) and *Csn5<sup>wt</sup>/Apoe<sup>-/-</sup>* (n= 2 - 3) male mouse serums. Red rectangles outline the signal areas of the atherosclerosis-relevant cytokines measured in serums. **C-H**, Immuno-blot quantification of the cytokine panel signals of the processed mouse plasma. *Csn5<sup>arterial</sup>/Apoe<sup>-/-</sup>* (n= 2- 3), *Csn5<sup>wt</sup>/Apoe<sup>-/-</sup>* (n= 2 - 3). **I**, Representative immunostainings of the TIMP1+ area (yellow), in the lesions of the male aortic roots. Scale bars, 50  $\mu$ m. **J**, Quantification of the TIMP1+ area in the plaque lesions of the male *Csn5<sup>arterial</sup>/Apoe<sup>-/-</sup>* (n = 8 mice) and *Csn5<sup>wt</sup>/Apoe<sup>-/-</sup>* (n= 6 mice) after the 12 weeks HFD. **K**, Quantification of the TIMP1 in the male mouse serums of *Csn5<sup>arterial</sup>/Apoe<sup>-/-</sup>* (n= 7 mice) and *Csn5<sup>wt</sup>/Apoe<sup>-/-</sup>* (n= 10 mice) mice. **L**, Representative immunostainings of the TIMP1+ area in the aortic root (yellow) of the *Csn5<sup>arterial</sup>/Apoe<sup>-/-</sup>* and *Csn5<sup>wt</sup>/Apoe<sup>-/-</sup>* female mice, after 12 weeks of HFD. These data represent means  $\pm$  SD.

#### 4.7 Timp1 is downregulated in mouse aortic endothelial cells upon arterial-endothelial specific depletion of Csn5 in vitro

The endothelial-derived CSN5 is previously described as a negative regulator of human atherosclerosis. It suppresses NF- $\kappa$ B-driven pro-inflammatory gene expression and inhibits monocyte arrest *in vitro* (Asare et al., 2013b). A previous study did report that COP9 regulates certain groups of NF- $\kappa$ B-driven gene sets, as some of the NF- $\kappa$ B gene targets don't seem to be affected upon *Csn5* depletion *in vitro* (Asare et al., 2017). Thus, I aimed to describe the underlining mechanism for the observed phenotype by employing the mouse aortic endothelial cells and confirming *in vivo* obtained data, and tackling the underlining mechanism (Fig. 28). MAECs were used to comprehend the role of Timp-1lesional and systemic depletion and comprehend its interaction between the *Csn5* depletion and Timp-1 levels in the endothelial lining (Fig. 28). The mechanism that interplays between *Csn5* and Timp1 in aortic endothelial cells is unknown. Although, Timp-1 target, *Mmp9* gene expression elevation was reported in the *Csn5*-KO macrophages (Asare et al., 2017).

As isolating primary arterial endothelial cells from the *Csn5*<sup>Δendothelial</sup>*Apoe*<sup>-/-</sup> mouse aorta was shown to be deemed an inconsistent method in our hands, *Csn5* knock-down was enabled by employing the *Csn5* *siPOOL* technology, while its *wild-type* controls were scrambled RNA (scrRNA) treated cells (Fig. 28A). The efficacy of the CSN5 knock-down was evaluated on the qPCR gene expression and showed a reduction of more than 60% *CSN5* gene expression in MAECs compared to their *scrRNA* controls (Fig. 28B). *Csn5* lowering down induced 10-20 % *Timp1* mRNA gene expression (Fig. 28C), which yet again aligned with the previously obtained *in vivo* data. To confirm that observed Timp-1 and *Csn5* gene expression reflects on the protein expression levels, total MAEC cell lysates were analysed by employing Western blot (Fig. 28C). We could confirm as well that there is a Timp1 protein depletion (Fig. 28, D, F) upon *Csn5* effective protein depletion *in vitro* (Fig. 28D, E). Moreover, I could evaluate that mouse aortic endothelial cell (MAEC) supernatants, upon *siPOOL*-induced *Csn5* depletion, decreased secretion of the extracellular levels of Timp-1 compared to the scrambled control (Fig 28G).

Tissue inhibitor of matrix-metalloproteinase expression has previously been described in endothelial cells as it was shown to up-regulated upon low shear stress (Uchida & Haas, 2014). While the majority of studies on the TIMP-1 expression regulation have been shown on macrophages and fibroblasts in cancer inflammation and tissue-remodelling (Di Gregoli et al., 2016a; L. Tong et al., 2004), only recently has been described to figure in atherosclerosis progression (Di Gregoli et al., 2016a; Silence et al., 2002). Interestingly, *Timp-1* loss has been shown to suppress VSMC proliferation *in vivo* (Di Gregoli et al., 2016a). Yet another study has shown that *Timp-1*<sup>-/-</sup> significantly increased atherosclerotic burden in *Apoe*<sup>-/-</sup> mice after 36 weeks of HFD (Kremastiotis et al., 2021). Hence, in the interest of this study, we wanted to understand how CSN5 depletion affects secretory TIMP-1 levels.

TIMP-1 functions as an endogenous inhibitor of MMPs (Introduction). *Timp1*, the *MMP9*, and *MMP2* are governed by NF- $\kappa$ B (Clark et al., 2008). Thus, I have tested if the expression of *Mmps* and *Timp1* changes upon *CSN5* loss (Fig. 28, H-L). TIMP-2 loss has been shown to elevate the atherosclerosis lesion progression in *Apoe*<sup>-/-</sup> mice (Di Gregoli et al., 2016a). On that basis, I aimed to investigate whether its gene expression levels are also changing with the *Csn5* depletion in ECs, which I couldn't detect (Fig. 28H). From the analysed MMPs, only *MMP9* has been shown to be a significantly up-regulated gene in *CSN5* *siPOOL*- treated endothelial cells, while *MMP2* gene expression was not changing.

In an effort to understand how the gene expression of elevated MMP9 and lowered TIMP-1 could be explained upon CSN5 depletion in ECs, I have investigated the expression of transcriptional factor c-Jun (**Fig. 28H**). Namely, c-Jun is known to be stabilised by the Csn5 of the COP9 signalosome. While on the other hand as AP-1 homo- or heterodimer regulates the *Timp-1* gene expression, suggesting it might stand between Csn5-Timp1 non-interacting partners (Chamovitz & Segal, 2001; Clark et al., 2008; L. Tong et al., 2004). c-Jun mRNA gene expression was lowered upon the Csn5 depletion (**Fig. 28H**). Henceforward, c-Jun and AP-1 might be responsible for the vulnerable phenotype and NF- $\kappa$ B pro-inflammatory atherogenic signalling.

A reported mechanism underneath the vulnerable atherosclerotic lesion is a disturbed ratio amid MMPs/TIMPs levels, which leads to dysregulated proteolytic activity and a commonly unfavourable ECM remodelling (Spinale & Villarreal, 2014). That urged me to investigate if the observed lowering of TIMP-1 levels in MAECs supernatants upon *CSN5 siPOOL* treatment could be responsible for the overall MMP activity modulation. The activity of the ECS-derived-MMPs secreted in their supernatants upon *CSN5 siPOOL* treatment or scrRNA has been evaluated on an MMP fluorometric assay. Endothelial cells' MMPs capacity to digest their substrates was measured every 10 minutes for 60 minutes. We could demonstrate that already after 20 minutes, there is a significant decline in MMP activity under the Csn5 depletion in vivo (**Fig. 28I**). Moreover, in the deciphering of the MMP activity and pinpointing responsible parties, gelatinases activity (matrix-metalloproteinase -2 and -9) was addressed on the zymography assay (**Fig. 28J**). Significant elevation in the activity of Mmp2 and Mmp9 upon Csn5 loss was shown (**Fig. 28, K-L**). In conclusion, obtained data suggested that endothelial-*Csn5* depletion triggers destabilisation of the c-Jun levels, which is at least partially responsible for the downregulation of the *Timp-1* levels, elevating the overall MMP activity.

In general, it is known that Csn5 acts as deNEDDylase as part of the CSN holo complex (Cope & Deshaies, 2003; Kato & Yoneda-Kato, 2009; Wei & Deng, 2003). On the other hand, Csn5 has been described to have functions outside of the complex independently of the CSN complex (Kato & Yoneda-Kato, 2009; Sharon et al., 2009). To investigate whether the CSN holo-complex plays a role in determining the *Timp-1* levels or the sole function of the Csn5 subunit outside of the complex, the smallest subunit of the complex, Csn8, has been depleted in the mouse-aortic endothelial cells by employing Csn8 siPOOL (**Fig. 28M**).

Although *Timp-1* gene expression seemingly was affected upon Csn8 depletion in MAECs (**Fig. 28, N-O**), no changes in the total MMP activity changes were observed except at the zero time-point (**Fig. 28P**). Suggesting that Csn8 and the CSN holo-complex might contribute to the gene expression changes but not the overall MMP activity changes are CSN5 dependent in ECs *in vitro*.

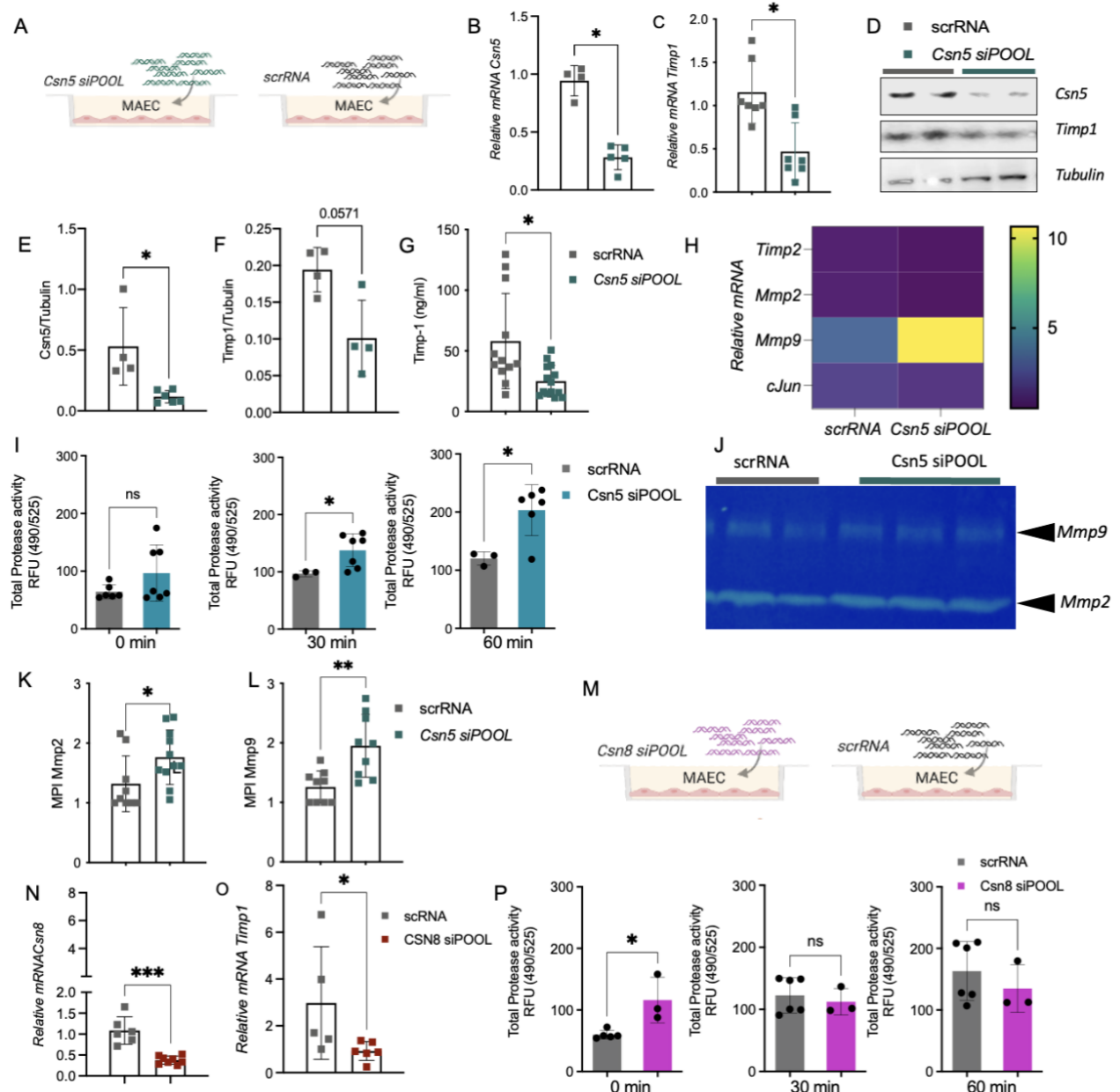


**Figure 28. Arterial-endothelial *Csn5* depletion downregulates the TIMP1 levels in vitro.** **A**, Graphical representation of the experimental setup. Mouse aortic endothelial cells (MAECs) depletion of the *Csn5* was achieved by employing 30 highly specific CSN5 targeting siRNA strand solution (*siPOOL* technology) (blue-green), and non-annealing siRNA-scrambled RNA (*scrRNA*) was employed as control (grey). **B-C**, Relative mRNA gene expression of *Csn5* and *Timp1* in MAECs *in vitro*. *Csn5 siPOOL* (n=5-7), *scrRNA* controls (n=4-7). **D**, Representative immuno-blots of CSN5 and TIMP1 protein levels in MAECs upon *Csn5 siPOOL* knock-down compared to their *scrRNA* controls *in vitro*. **E-F**, Quantification of the *Csn5* and *Timp1* protein levels in MAECs upon *Csn5* depletion (*Csn5 siPOOL*) (n=4-6) compared to the scrambled RNA controls (*scrRNA*) (n=4). **G**, *Timp1* secreted levels in MAEC supernatants upon *Csn5* depletion (n=13) compared to the supernatants of the mouse aortic endothelial cells exposed to the *scrRNA* control (n=12). **H**, Relative mRNA gene expression histogram of *Timp2*, *Mmp2*, *Mmp9*, and *c-Jun* in MAECs with *Csn5* depletion (n=5) or treated with the *scrRNA* controls (n=5). **I**, Quantification of the total MMP activity in MAEC supernatants of the controls *scrRNA* (n=3-6) and *Csn5 siPOOL* (n=6-7) at the indicated time-points. **J**, Representative zymogram gel of *Csn5 siPOOL* treated MAECs supernatants compared to the RNA scrambled controls (*scrRNA*). **K-L**, Bar charts of MMP2 and MMP9 levels.

**L**, Quantification of the MPI of the MMP2 (**I**) and MMP9 (**J**) enzyme activity upon *Csn5 siPOOL* treatment (n=9-11) versus *scrRNA* control treatment (n=8). **M**, Graphical representation of experimental setup. MAECs and *Csn8* specific depletion was enabled by employing *CSN8 siPOOL* technology (magenta) and was compared to their scrambled RNA (*scrRNA*) controls (grey) *in vitro*. **N-O**, Relative mRNA *Csn8* and *Timp1* gene expression in MEAC upon *Csn8* depletion (*Csn8 siPOOL*) (n=6-7) compared to the scrambled RNA controls (*scrRNA*) (n=5-6). **P**, Quantification of the total MMP activity in MAEC supernatants. *scrRNA* (n=6) and *Csn8 siPOOL* (n=3). These data represent means  $\pm$  SD.

#### 4.8 MLN4924 treatment up-regulates TIMP1 levels in vivo and in vitro

As TIMP-1 levels are seemingly being lowered down upon CSN5 depletion *in vitro* and *in vivo*, I wanted to investigate if the elevating CSN5 levels trigger the TIMP-1 elevation *in vivo*.

*In vivo* study was performed by employing the blood serum analysis and aortic roots immunohistochemical staining of mouse aortic roots that have received MLN4924 or vehicle treatment for 4 weeks while consuming the HFD, as previously described.

In the aortic roots of the MLN4924 treated mice could be observed that TIMP-1 is more overall expressed in their atherosclerotic lesions, compared to the lesion of the vehicle-treated mice (**Fig. 29A**). Specifically, TIMP-1 is more expressed in the shoulder of the MLN4924 treated atherosclerotic lesions (**Fig. 29B**). Moreover, receiving the neddylation inhibitor treatment had elevated systemic levels of the circulatory TIMP-1 levels, suggesting a protective mechanism of the small molecule inhibitor (**Fig. 29C**).

To investigate how ‘*Csn5* overexpression mimics’ impacts, specifically endothelial lining, MAECs were treated with the small molecule inhibitor (500 nM), MLN4924, for 16h or DMSO vehicle control *in vitro* (**Fig. 29D**). Firstly, MAECs upon MLN4924 application showed higher gene expression of *Timp-1* compared to the vehicle-treated controls, suggesting the involvement of stabilisation of the transcriptional regulators (**Fig. 29E**). Secondly, secretory *Timp1* levels detected in the supernatants of mouse aortic endothelial cells upon MLN4924 treatment were as well significantly elevated (**Fig. 29F**). Finally, the total intracellular content of the TIMP-1 in MAEC treated cells was evaluated in their lysate on the immunoblotting, and we couldn’t observe significant changes, but the trendline (**Fig. 29H**).

The balance between the protease inhibitor *Timp1* and its MMPs target is deemed important for the lesion progression clinically significant outcome (Kremastiotis et al., 2021). To probe total matrix-metalloproteinase enzymatic activity in cell endothelial supernatants, we have employed an MMP activity assay. Depletion of MMP activity was observed already after 20 min of the substrate digestion upon MLN4924 (**Fig. 29J**). Finally, collagenase zymography was developed to pinpoint which MMPs were driving the enhanced activity after the MLN4924 treatment (**Fig. 29K**). Neddylation-activation enzyme inhibition in the mouse aortic endothelial cells has demonstrated only a significant impact on the *Mmp9* cell supernatant activity, while *Mmp2* activity hasn’t changed (**Fig. 29, L-M**).

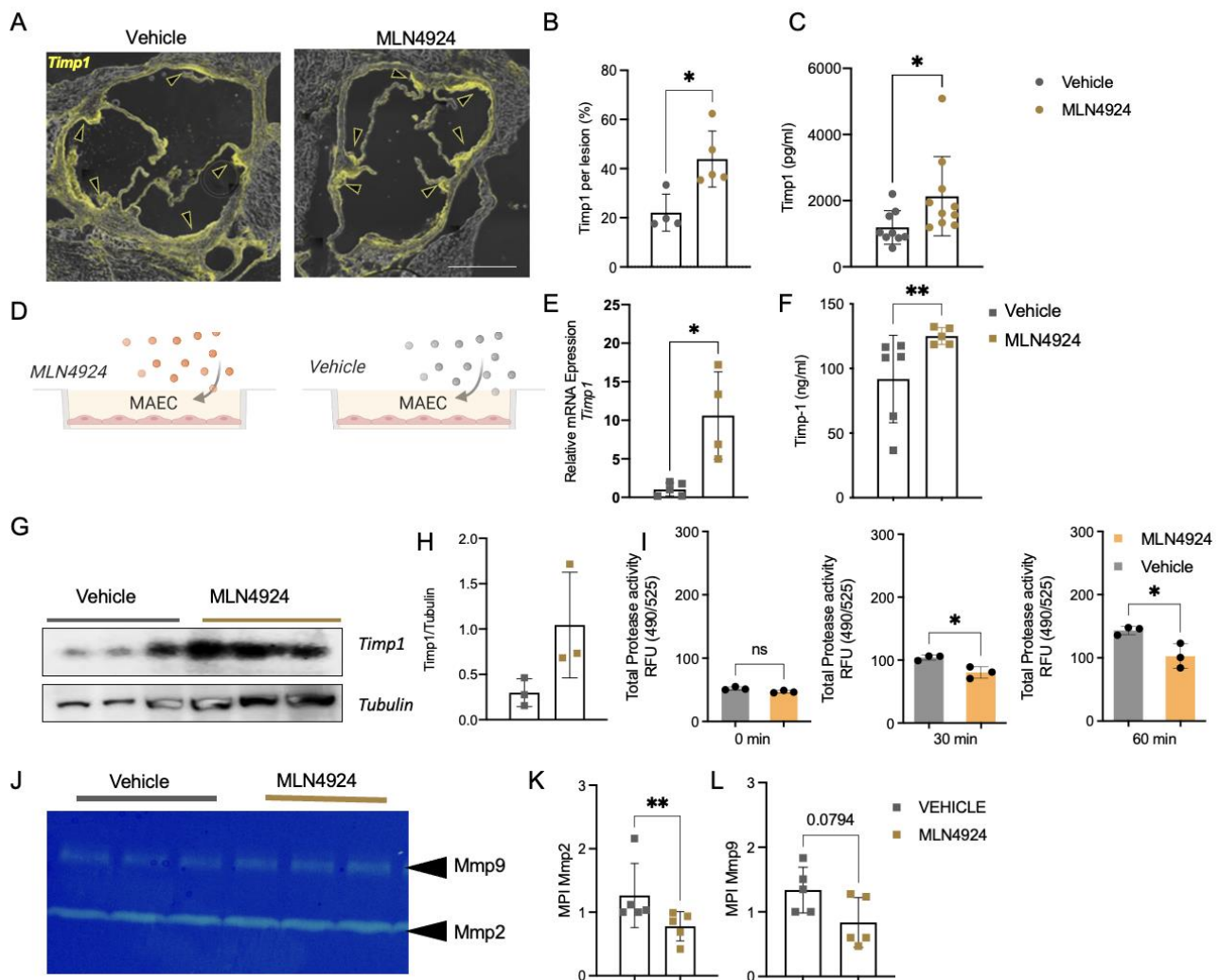


**Figure 29. MLN4924 treatment up-regulates TIMP1 levels and impacts the activity of the matrix-metalloproteinase *in vivo* and *in vitro*.** Representative immunostaining of the TIMP1<sup>+</sup> positive area in the aortic root (stained yellow) of the MLN4924 and vehicle-treated mice after 4 weeks of HFD. Scale bars, 500  $\mu$ m. **B**, Quantification of the TIMP1<sup>+</sup> area in the lesion. MLN4924 treated mice (n=10 mice) compared to the vehicle-treated mice (n=9). **C**, Quantification of the TIMP1 circulatory levels of MLN4924 (n=10) and Vehicle treated mice (n=9). **D**, Experimental outline *in vitro*. MAECs were either MLN4924 or vehicle-treated. **E**, Relative mRNA *Tim1* expression in MEAC after MLN4924 (n=4-6) stimulation compared to the vehicle (n=4-5) treated control. **F**, Relative mRNA *Tim1* expression in MEAC after MLN4924 stimulation compared to the vehicle control after the TNF $\alpha$  co-stimulation. **G**, Representative immunoblots of the *Tim1* levels compared to the vehicle treatment of the MAECS. **H**, Quantification of the *Tim1* protein levels in MACES upon MLN4924 (n=3) treatment compared to the vehicle-treated (n=3) control. **I**, Quantification of the total MMP activity in supernatants of the vehicle-treated (n=3) and MLN4924 (n=3) MAECS at the indicated time points. **J**, Representative zymogram gel of MLN4924 treated MAECs supernatants compared to the vehicle controls. **K-L** Quantification of the MMP2 (K) and MMP9 (L) enzymatic activity of MLN4924 (n=5) treated MAEC supernatants compared to the vehicle (n=5) treatments. These data represent means  $\pm$  SD.

#### 4.9 Csn5 overexpression reveals the involvement of MAPKs and the AP-1 signalling axis in determining the Timp-1 levels

In the previous studies in this thesis, systemic effects upon MLN4924 ‘Csn5 overexpression mimics’ were evaluated, which wouldn’t yield true intracellular state conditions of the Csn5 overexpression, only partially mimic conditions as such. Csn5’s capacity to act independently of the CSN and signalling underneath was aimed here to investigate how it impacts the TIMP-1 regulation and the matrix-remodelling system.

Firstly, mouse fibroblasts (NIH/3T3 or MEFs) were used here, as they are well-described major cellular producers of MMPs and Timp-1 (Boucherat et al., 2007; L. Tong et al., 2004). Secondly, AP-1, NF- $\kappa$ B, p38 MAPK, ERK1/2, and Akt signalling have been shown to regulate the TIMP-1 gene expression (L. Tong et al., 2004). In the same time, TIMP1 gene expression is extensively regulated by the homo- or heterodimers of AP-1, one of them being c-Jun (L. Tong et al., 2004). Csn5 stabilising c-Jun is well described and is shown to be a JNK signalling-independent (Kleemann et al., 2000; Naumann et al., 1999; Tsuge et al., 2001). Hence, by employing mouse fibroblasts over-expressing Csn5 compared to their non-cloned constitutively Csn5 expressing fibroblast controls (**Fig. 30 A, up**), we could manage to investigate the role of the Csn5 overexpression (NIH/3T3 *Csn5<sup>+++</sup>*) and mechanisms underneath the Timp-1 gene regulation.

Initial mRNA gene expression studies have shown that elevated Csn5 (**Fig. 30, B**) levels do mirror the Timp1 elevated gene expression (**Fig. 30C**) in the NIH/3T3 *Csn5<sup>+++</sup>* compared to their controls (NIH/3T3 *Csn5<sup>wt</sup>*). As the regulators underneath the Timp-1 gene expression next to the c-Jun are c-Fos and Jun-B, their gene expression was investigated under the Csn5 overexpression without (**Fig. 30, D-F**) or under the TNF $\alpha$  pro-atherogenic stimulation (**Fig. 30, G-I**). At the same time, all the AP-1 signalling players were found to be up-regulated upon Csn5 over-expression in the NIH/3T3 *Csn5<sup>+++</sup>* compared to their constitutive Csn5 expressing NIH/3T3 *Csn5<sup>wt</sup>* (**Fig. 30, D-I**). Once protein levels were investigated in these mouse fibroblasts, I could see that Csn5 overexpression is paralleled by the c-Jun levels (**Fig. 30J**). The same higher Timp-1 levels could be seen in the NIH/3T3 *Csn5<sup>+++</sup>* compared to the NIH/3T3 *Csn5<sup>wt</sup>* (**Fig. 30K**).

JNK inhibitor II was used to block JNK signalling in the NIH/3T3 cell lines, hence evaluating the CSN5-derived function. Up-regulation of the c-Jun was present already without the TNF $\alpha$  (20ng/ml) stimulation in the NIH/3T3 *Csn5<sup>+++</sup>* (**Fig. 30L**). On the other hand, JunB and c-Fos were up-regulated under the TNF $\alpha$  stimulation after 15 min compared to their NIH/3T3 *Csn5<sup>wt</sup>* stimulated controls (**Fig. 30L**).

Active phosphorylated c-Jun levels were investigated as well once JNK signalling was blocked. I could observe higher active c-Jun levels already after 15 min in the Csn5 overexpressing cells (**Fig. 30L**).

To verify if the Csn5 depletion in the mouse fibroblasts (MEF *Csn5<sup>+-</sup>*) parallels the Timp-1 lowering levels previously observed on endothelial cells, we analysed mouse fibroblasts with an endogenous heterozygous loss of the Csn5. Their effects were analysed next to the constitutively expressing mouse fibroblasts, MEF *Csn5<sup>wt</sup>* (**Fig. 30A right**). The lowering of the *Csn5* gene expression lowered the *Timp-1* levels in these mouse fibroblasts (**Fig. 30M**). The same protein lowering was observed in the Timp-1 and Csn5 protein levels in the MEF *Csn5<sup>+-</sup>* compared to the MEF *Csn5<sup>wt</sup>* cell clones (**Fig. 30P**). While curiously, c-Jun protein levels remained unchanged in this condition, suggesting another signalling player potentially being involved in regulating the Timp-1 gene expression (**Fig. 30P**).

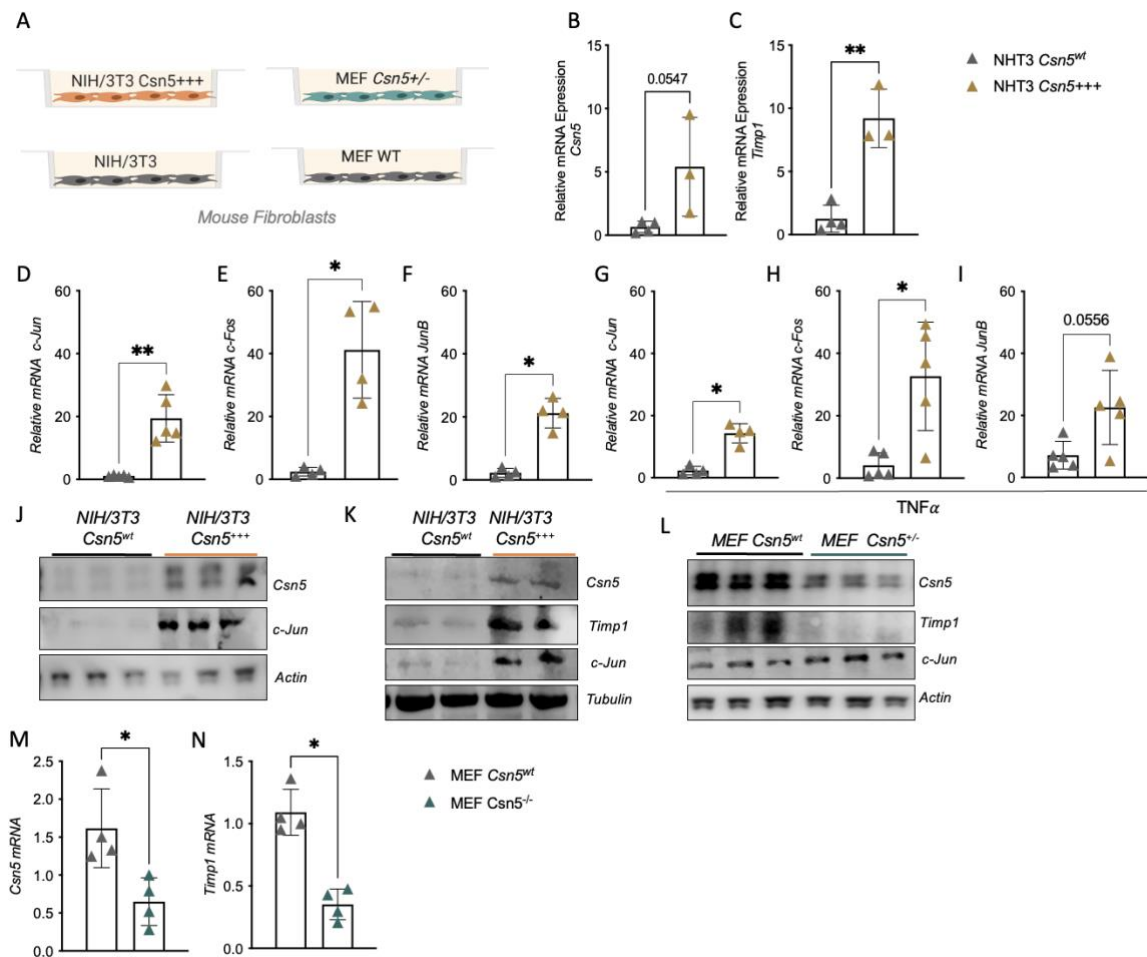


**Figure 30. Csn5 regulates TIMP-1 via stabilising the AP-1 signalling axis independently of the JNK signalling in a mouse fibroblast *in vitro*.** Schematic representation of experimental design employing mouse fibroblastic cell line; **Left:** NIH/3T3 cell clones (left) overexpressing *Csn5* (NIH/3T3 *Csn5*<sup>+++</sup>) compared to the control cell clones, NIH/3T3 cell line expressing stable levels of *Csn5* (NIH/3T3 *Csn5*<sup>wt</sup>); **Right:** mouse embryonic fibroblasts (MEF) cell clones with the depletion of *Csn5* expression (MEF *Csn5*<sup>-/-</sup>) compared to their native *Csn5* expressing cell clones MEF *Csn5*<sup>wt</sup>. **B-C:** Relative mRNA levels of *Csn5* and *Timp1* gene expression in the NIH/3T3 *Csn5*<sup>+++</sup> (n=5) compared to the *Csn5*<sup>wt</sup> (n=4) controls. **D-I:** Relative mRNA gene expression of *c-Jun* (**D**), *c-Fos* (**E**), *JunB* (**F**) without (**D-F**) or with (**G-I**) overnight  $\text{TNF}\alpha$  (20ng/ml) stimulation. NIH/3T3 *Csn5*<sup>+++</sup> (n=4-5), *Csn5*<sup>wt</sup> (n=4-5) controls. **J-K:** Representative immunoblots of *Csn5*, *Timp1*, and *c-Jun* protein levels in the NIH/3T3 *Csn5* overexpressing cells compared to their control NIH/3T3 *Csn5*<sup>wt</sup> cells (n=2-3 individual experiments). **L:** Representative immunoblots of *Csn5*, *Timp1*, and *c-Jun* protein levels in the MEF *Csn5*<sup>-/-</sup> compared to their MEF *Csn5*<sup>wt</sup> controls. **M-N:** Relative mRNA of *Csn5* and *Timp1* gene expression in the MEF *Csn5*<sup>-/-</sup> (n=4) compared to the MEF *Csn5*<sup>wt</sup> (n=4) controls (n=3 individual experiments). Data represent means  $\pm$  SD.

To investigate under which signalling axis AP-1 signalling is triggered, we analysed MAPKs, p-p38, and p-ERK1/2, and we could observe that while p-ERK1/2 doesn't seem to be affected but depleted in the *Csn5* overexpressing fibroblasts, p-38 might be responsible for the observed AP-1 signalling (**Fig. 31B**). To verify this claim, non-active p-38 and ERK1/2 protein levels were investigated with and without the  $\text{TNF}\alpha$  (20ng/ml) stimulation as well as under the effects of the JNK inhibitor II. I could evaluate that ERK1/2 signalling was only impacted with the  $\text{TNF}\alpha$  (20ng/ml)

stimulation in the NIH/3T3 *Csn5*<sup>+++</sup> cells, while this was not the case once the JNK II inhibitor was employed. While on the other hand, MAPK p38 signalling was triggered only upon TNF $\alpha$  (20ng/ml) stimulation in the NIH/3T3 *Csn5*<sup>+++</sup>, while that was not the case in the *Csn5* *wild-type* expressing NIH/3T3 fibroblasts (Fig. 30A). Overall data was suggesting that Timp1 elevated levels under the *Csn5* overexpressing conditions, enabled AP-1 gene expression stabilisation via p38 triggered signalling.

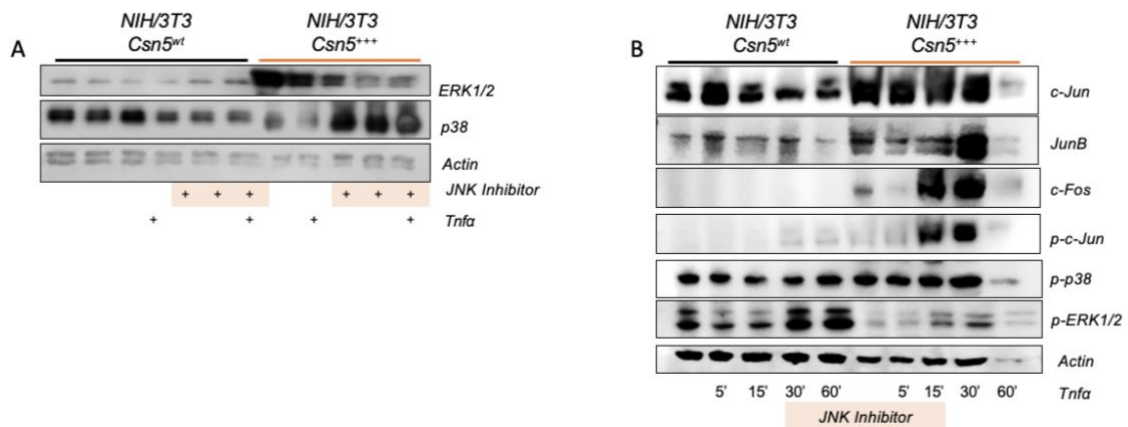


**Figure 31. *Csn5* regulates the AP-1 signalling axis independently of the JNK signalling in a mouse fibroblast *in vitro*.** An Immunoblots of AP-1 signaling (c-Jun, JunB, c-Fos, and p-c-Jun) and MAPK activation (p-p38 and p-ERK1/2) upon TNF $\alpha$  stimulation for indicated time points of NIH/3T3 *Csn5*<sup>+++</sup> compared to the NIH/3T3 *Csn5*<sup>wt</sup> under the JNK II inhibitor treatment. **B**, Immunoblot of MAPK levels (ERK1/2 and p38) under or without TNF $\alpha$  stimulation, with or without JNK II inhibitor treatment as indicated. \NIH/3T3 *Csn5* overexpressing cells (NIH/3T3 *Csn5*<sup>+++</sup>) compared to their control NIH/3T3 *Csn5*<sup>wt</sup> cells (n=3 individual experiments).

#### 4.10 The CSN holo-complex plays a role in atherosclerosis progression in vivo

The role of the *Csn5* subunit has been investigated in atherosclerosis development by employing *Csn5*<sup>amyloid</sup>*Apoe*<sup>-/-</sup> *in vivo* (Asare et al., 2013b, 2017). Moreover, the role of the *Csn3* has been recently probed *in vivo* (Boro et al., 2021; Schwarz et al., 2017). These studies suggest the important role of the CSN holo-complex in atherosclerosis progression in different cell types. Since the CSN holo complex holo-complex of 8 subunits, I wondered if depletion of the small CSN subunit 8 (CSN8) in an atherosclerosis model *in vivo*, i.e. by studying *Csn8*<sup>amyloid</sup>*Apoe*<sup>-/-</sup> mice, would similarly impact atherosclerosis progression as the myeloid knockouts of subunit *Csn5*. As removing one subunit of the CSN holo-complex would lead to its disassembly, I aimed to investigate the role of the COP9 holo-complex in atherosclerosis for the first time here.

We conditionally deleted the *Csn8* gene in myeloid cells in mice by employing the Cre-loxP system. This was achieved by crossbreeding *LysMCre*/*Apoe*<sup>-/-</sup> expressing mouse line with the established *Csn8*<sup>fl/fl</sup> mice. Thus, I generated an addressed *Csn8*<sup>amyloid</sup>*Apoe*<sup>-/-</sup> mouse line.

Analysis of genomic DNA from the ear-tissue biopsied (Fig. 32, A-D), as well as protein levels (Fig. 32F) and mRNA gene expression (Fig. 32G) of *Csn8* in BMDMs, confirmed the appropriate genotype, and by that effective depletion of the *Csn8* in myeloid cells.

Moreover, mouse weight progression (Fig. 32E) and blood cholesterol levels (Fig. 32F) of the *Csn8<sup>Δamyloid</sup>Apoe<sup>-/-</sup>* mouse line showed no differences over the time of 12 weeks of the HFD. consumption, compared to their *Csn8<sup>wt</sup>Apoe<sup>-/-</sup>* control littermates. Finally, to verify if *Csn8* indeed is expressed in *Apoe<sup>-/-</sup>* mouse atherosclerotic lesions, the *Mac2<sup>+</sup>* area of the lesion has been probed for the *Csn8* expression where we could observe that, indeed, macrophage in the advanced atherosclerotic lesion do express *Csn8* (Fig. 32H).

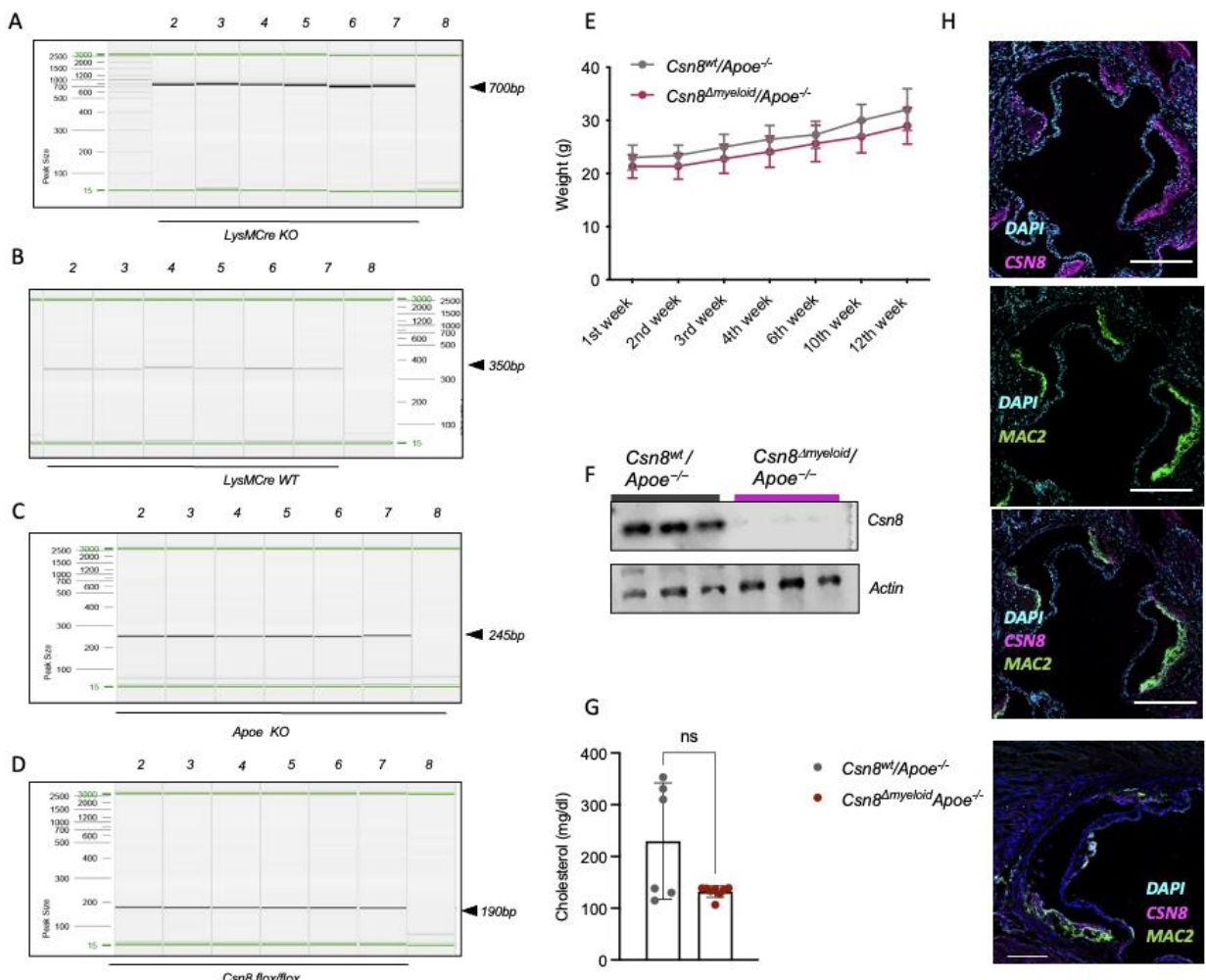


**Figure 32. Targeted deletion of the *Csn8* gene in mouse macrophages.** A-D, PCR amplified gene products of the mouse genomic DNA were analysed on the gel-electrophoresis. *LysMCre* (A-B), *Csn8* floxed (*flox/flox*), and *Apoe* knock-out (B) PCR gene products are shown. The size of the PCR product is indicated with the black arrowhead. E, Male mouse weight progression over the 12 weeks of HFD consumption. *Csn8<sup>Δamyloid</sup>Apoe<sup>-/-</sup>* (*n*=7) *Csn8<sup>wt</sup>Apoe<sup>-/-</sup>* (*n*=7). F, Representative immunoblots of *Csn8* protein levels in the *Csn8<sup>Δamyloid</sup>Apoe<sup>-/-</sup>* (*n*=3) and *Csn8<sup>wt</sup>Apoe<sup>-/-</sup>* (*n*=3) mice. G, Cholesterol levels of the *Csn8<sup>Δamyloid</sup>Apoe<sup>-/-</sup>* (*n*=3) and *Csn8<sup>wt</sup>Apoe<sup>-/-</sup>* (*n*=3) male mice. Data represent means $\pm$ SD. H, Representative immunostainings of the mouse aortic roots showing *CSN8<sup>+</sup>* area in magenta, *MAC2<sup>+</sup>* area in green, of the aortic roots (*Apoe<sup>-/-</sup>* mice) after the 10 weeks HFD. DAPI-nuclear staining in cyan. Scale bar 200  $\mu$ m. These data represent means $\pm$ SD.

As previously shown, *Csn5<sup>Δamyloid</sup>Apoe<sup>-/-</sup>* after 12 weeks of HFD consumption had more pronounced atherosclerosis than their control mice *Csn5<sup>wt</sup>Apoe<sup>-/-</sup>* (Asare et al.,

2017). Thus, *LysMCre/Csn8<sup>fl/fl</sup> /Apoe<sup>-/-</sup>* (*Csn8<sup>Δmyeloid</sup>Apoe<sup>-/-</sup>*) atherosclerosis progression in the aorta and aortic root in male and female atherogenic mice has been put to the test and compared to the atherosclerosis phenotype of the *Csn8<sup>wt</sup>Apoe<sup>-/-</sup>* littermates after the 12 weeks of Western type of diet (Fig. 33A).

Male myeloid-*Csn8* depleted atherogenic mice have shown more pronounced lesion sizes in aortic roots (Fig. 33, B-C) and abdominal aorta (Fig. 33, B- E). In contrast, the thoracic aorta (Fig. 33, B-D) showed no significant differences in the lesion size compared to their *Csn8* expressing atherogenic controls. Atherosclerosis progression was significantly elevated in the *Csn8<sup>Δmyeloid</sup>Apoe<sup>-/-</sup>* male aortic root compared to the aortic roots of the *Csn8<sup>wt</sup>Apoe<sup>-/-</sup>* controls (Fig. 33, F- G).

The lesion of the *Csn8<sup>Δmyeloid</sup>Apoe<sup>-/-</sup>* mice was profiled. Namely, atherosclerotic lesion size was attributed to the variation in the plaque cell content (Fig. 33H). There was a trendline of lowering the smooth muscle cell content upon the myeloid *Csn8* loss in male mice, but overall SMCs content in the lesion didn't change (Fig. 33, H- I). Macrophage percentage (CD68<sup>+</sup> area) in the male *Csn8<sup>Δmyeloid</sup>Apoe<sup>-/-</sup>* mice lesions has been significantly elevated after the 12 weeks of HFD (Fig. 33, H- J).

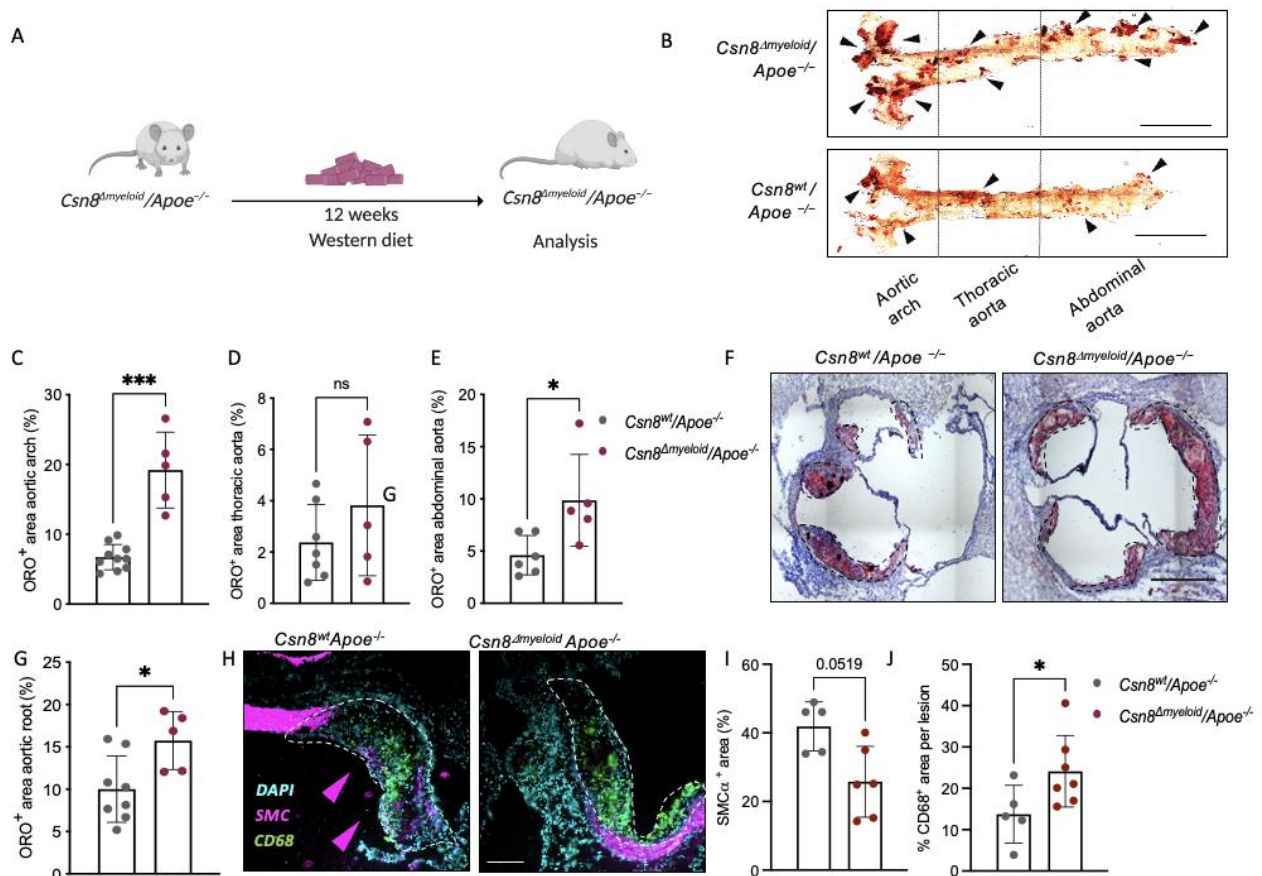


**Figure 33. Macrophage-specific deletion of Csn8 accelerates atherosclerosis.** Experimental outline. *Csn8<sup>Δmyeloid</sup>Apoe<sup>-/-</sup>* male mice were set on an HFD for 12 weeks. (A). B, Representative male ORO-stained aortas are shown. Black arrowheads outline the lesion sites in the aortic arch, aortic root, and abdominal aorta. Scale size, 3mm. C-E, Quantification of the ORO percentage in the aortic arch, thoracic aorta, and abdominal aorta *Csn8<sup>wt</sup>Apoe<sup>-/-</sup>* (n=9 mice), *Csn8<sup>Δmyeloid</sup>Apoe<sup>-/-</sup>* (n=5 mice). F, Representative ORO staining in the aortic arch of *Csn8<sup>wt</sup>Apoe<sup>-/-</sup>*, *Csn8<sup>Δmyeloid</sup>Apoe<sup>-/-</sup>* after 12 weeks of HFD. Scale bar 500  $\mu$ m. G, Quantification of the ORO<sup>+</sup> area in the aortic root of *Csn8<sup>wt</sup>Apoe<sup>-/-</sup>* (n=8 mice) compared to *Csn8<sup>Δmyeloid</sup>Apoe<sup>-/-</sup>* (n=5 mice). H, Representative immunostainings (J) showing CD68<sup>+</sup> area in green and (I) SMA<sup>+</sup> area in

magenta, scale bar 50  $\mu$ m. **I-J**, Quantification of immunostainings  $Csn8^{\Delta myeloid} Apoe^{-/-}$  (n=9-10 mice)  $Csn8^w Apoe^{-/-}$  (n=8-9 mice). Data represent mean  $\pm$  SD.

As macrophages are a major producer of collagenases, we have investigated the collagen content of the lesions by employing Sirius red staining (SR<sup>+</sup> area) (**Fig. 34A, C**). Interestingly, collagen content has been lowered down in myeloid-specific  $Csn8$  depleted male mice, compared to their  $Csn8^w Apoe^{-/-}$  controls (**Fig. 34 B, D**), but that didn't affect the fibrous cap thickness (**Fig. 34M**) nor overall necrotic core size (**Fig. 33J**).

Since we have demonstrated previously that changes in  $Csn5$  expression did affect *in vitro* and *in vivo* systemic Timp1 levels, and as macrophages are known producers of the Timp1 in the atherosclerotic lesion-Timp1 levels were investigated as well. As both Timp-1 serum levels (**Fig. 34H**) and lesion content (**Fig. 34I**) have been lowered, we have speculated that the COP9, not just the  $Csn5$  subunit of the complex, play a role in its expression regulation, thus potentially impacting vulnerability.

Consequently, the vulnerability index of the  $Csn8^{\Delta myeloid} Apoe^{-/-}$  male mice and their controls were analysed by employing previously described factors of cell content, necrotic size, collagen content, and lesion size (Material and Methods). Although there is a strong trendline towards elevating the overall vulnerability index of the  $Csn8$ -depleted mice, no significance was found compared to their littermate  $Csn8$ -expressing male mice (**Fig. 34J**). Thus overall,  $Csn8^{\Delta myeloid} Apoe^{-/-}$  male mice had a bigger lesion size found in the aortic root and aorta as well as the altered phenotype of the atherosclerotic lesions, but no lesions prone to vulnerability, as previously shown with the endothelial  $Csn5$  loss.

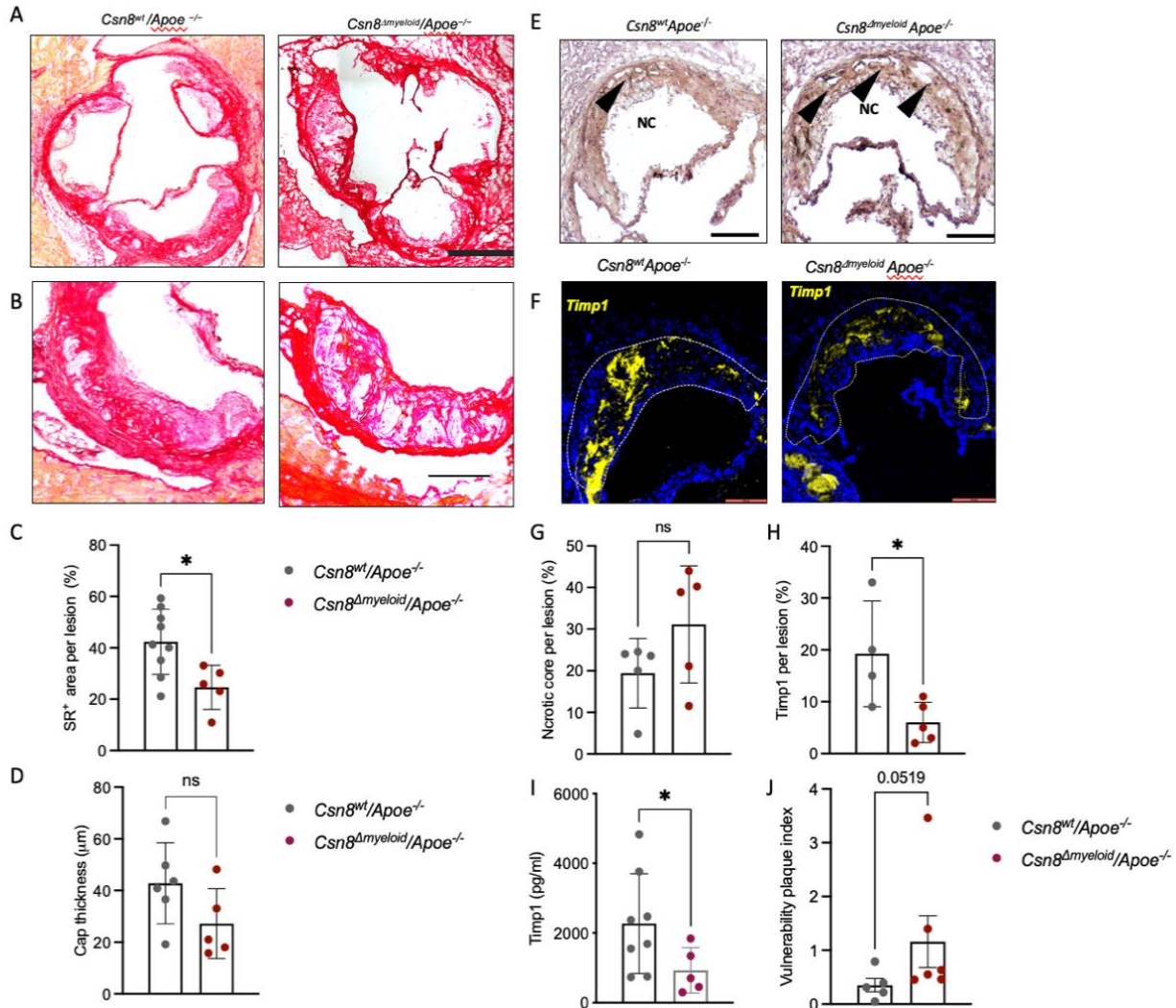


**Figure 34. Macrophage-specific deletion of Csn8 doesn't promote atherosclerotic plaque vulnerability.** **A** Representative Sirius red (SR<sup>+</sup>) stained lesions. Scale bars, 50  $\mu$ m. **C-D**, Quantification of collagen content (Sirius red positive area) (**C**) and fibrous cap (FC) thickness (**D**). *Csn8<sup>Δmyeloid</sup>Apoe<sup>-/-</sup>* (n= 6-8 mice) *Csn8<sup>wt</sup>Apoe<sup>-/-</sup>* (n=4-6 mice). Representative images of H and E (**E**) stained aortic roots and Timp1<sup>+</sup> areas (**F**) in the aortic root lesion. Scale bars, 200  $\mu$ m. **G**, Necrotic core size of the male *Csn8<sup>Δmyeloid</sup>Apoe<sup>-/-</sup>* (n=5 mice) and *Csn8<sup>wt</sup>Apoe<sup>-/-</sup>* (n=8 mice) mice. **H**, Quantification of the Timp1<sup>+</sup> area of the plaque lesions. Male *Csn8<sup>Δmyeloid</sup>Apoe<sup>-/-</sup>* (n=5 mice) and *Csn8<sup>wt</sup>Apoe<sup>-/-</sup>* (n=8 mice) mice. **I**, Quantification of the Timp1 circulatory levels of the *Csn8<sup>Δmyeloid</sup>Apoe<sup>-/-</sup>* (n=5 mice) and *Csn8<sup>wt</sup>Apoe<sup>-/-</sup>* (n=8 mice). **J**, Vulnerability index was calculated for the *Csn8<sup>Δmyeloid</sup>Apoe<sup>-/-</sup>* (n=6 mice) and *Csn8<sup>wt</sup>Apoe<sup>-/-</sup>* (n=5 mice). These data represent means  $\pm$  SD.

If exacerbated lesion size observed in the *Csn8<sup>Δmyeloid</sup>Apoe<sup>-/-</sup>* male mice could have been attributed to the blood cells, it was investigated. In the *Csn8<sup>Δmyeloid</sup>Apoe<sup>-/-</sup>* male mice, no changes have been found in the total lymphocyte count, whereas slightly elevated blood cell count has been shown upon the myeloid *Csn8* loss (Table 4).

**Table 4. Blood cell count of male *Csn8<sup>Δmyeloid</sup>Apoe<sup>-/-</sup>* compared to the *Csn8<sup>wt</sup>Apoe<sup>-/-</sup>***

*Parameters	<i>Csn8<sup>wt</sup>Apoe<sup>-/-</sup></i>			<i>Csn8<sup>Δmyeloid</sup>Apoe<sup>-/-</sup></i>			P-values
	Mean	SD	N	Mean	SD	N	
WBC (/ $\mu$ L)	4,79	3,35	11	2,8	0,87	13	0,051769

<b>HGB (g/dl)</b>	12,26	5,11	11	14,1	5,18	12	0,404248
<b>PLT (<math>10^3</math> /<math>\mu</math>L)</b>	95,34	68,58	10	93,75	105,45	12	0,967761
<b>LYM (%)</b>	65,57	8,43	11	62,054	7,58	13	0,293459
<b>MO (%)</b>	5,50	1,52	11	5,07	1,074	13	0,415842
<b>GRA (%)</b>	28,9	7,64	11	32,57	6,434	13	0,216659
<b>LYM (/<math>\mu</math>L)</b>	2,94	1,87	11	1,68	0,545	13	0,030637
<b>MO (/<math>\mu</math>L)</b>	0,31	0,49	11	0,11	0,027	13	0,149074
<b>GRA (/<math>\mu</math>L)</b>	1,61	1,26	11	1,06	0,46	13	0,173222

\* Acronyms are shown in material and methods.

A possible error in the automated blood cell count was addressed by employing the FACS analysis of the blood cell count (Figure 35). T-cell count is elevated while the remaining blood cells were unaltered upon myeloid-*Csn8* depletion, compared to their *Csn8<sup>wt</sup>Apoe<sup>-/-</sup>* controls (Fig 35B).

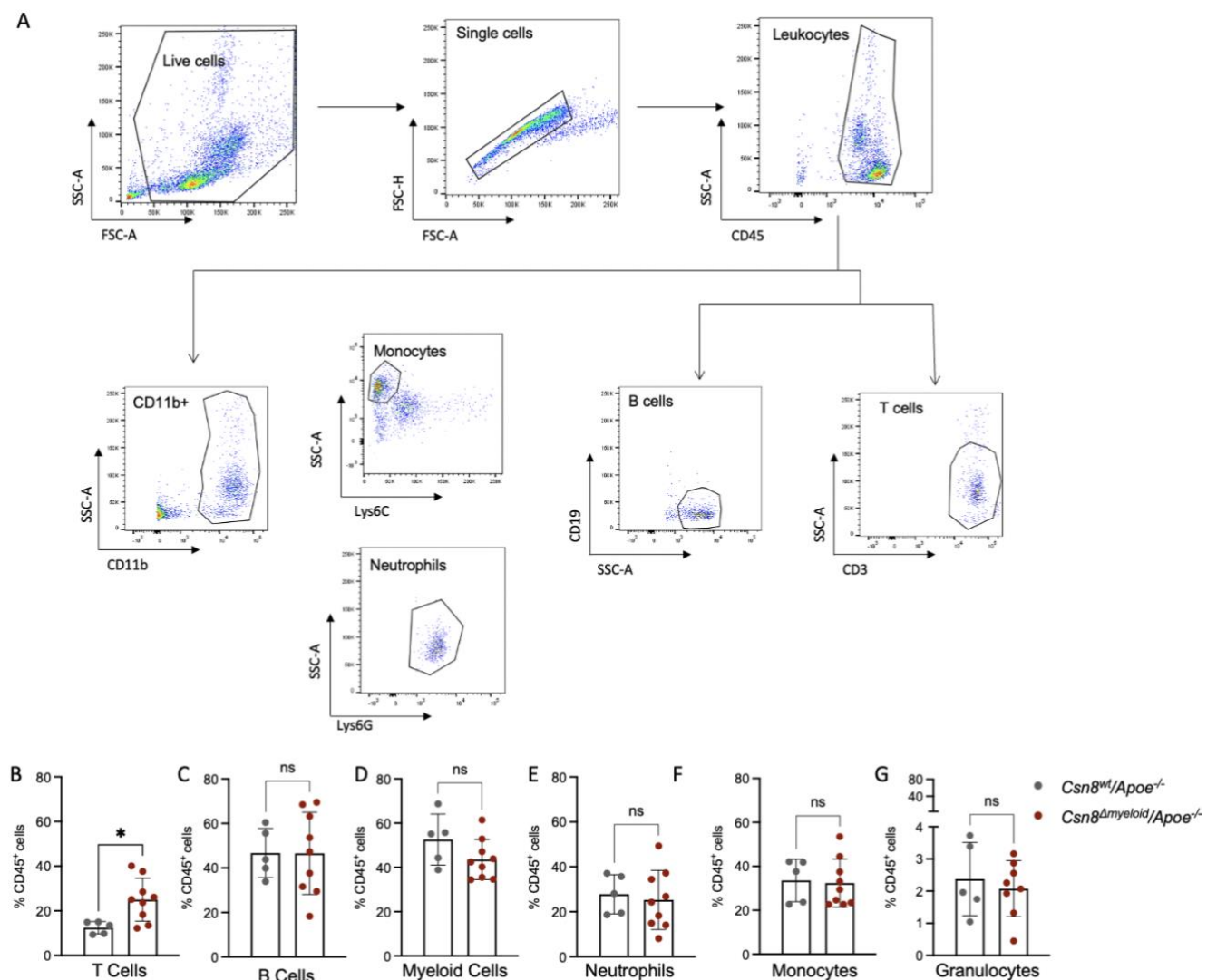


**Figure 35. FACS analysis of the male *Csn8<sup>myeloid</sup>Apoe<sup>-/-</sup>* and their littermate controls *Csn8<sup>wt</sup>Apoe<sup>-/-</sup>* whole blood after the 12 weeks of HFD. A** Gating strategy was employed to analyse the whole blood of mice. **B-G**, Quantification of the percentage of the CD19<sup>+</sup> T-cells (B), CD3<sup>+</sup> B-cells (C) CD11b<sup>+</sup> myeloid cells (D), Lys6G<sup>+</sup> Neutrophils (E) Lys6G<sup>+</sup> monocytes

(F), Granulocytes (G) of the male *Csn8<sup>myeloid</sup>Apoe<sup>-/-</sup>* (n=9 mice) compared to the *Csn8<sup>wt</sup>Apoe<sup>-/-</sup>* (n=5 mice) counted as the percentage of the CD45<sup>+</sup> cells. These data represent means  $\pm$  SD.

COP9 loss of function shows an atheroprotective effect in a gender-specific manner (Asare et al., 2017, this thesis). Hence, I wanted to investigate here if myeloid-specific *Csn8* deletion affects atherosclerosis in female mice upon 12 of HFD (Figure 36). Namely, atherosclerosis of *Csn8<sup>myeloid</sup>Apoe<sup>-/-</sup>* female mice was evaluated in the aortic roots (Fig. 36A) and aorta (Fig. 36C) after 12 weeks of HFD consumption.

Interestingly, no changes in the lesion size were observed after the ORO staining of the intimal lipid deposits of the *Csn8<sup>myeloid</sup>Apoe<sup>-/-</sup>* female aortic roots (Fig. 36B). Although seemingly aortic arch and abdominal aortic lesion are seemingly elevated upon the myeloid-specific *Csn8* deletion (Fig. 36D). The other advanced lesion characteristics, such as fibrous cap thickness (Fig. 36E) didn't seem to be affected.

*Timp-1* systemic levels were unaltered in female mice that are in the *Csn8<sup>myeloid</sup>Apoe<sup>-/-</sup>* compared to their controls *Csn8<sup>wt</sup>Apoe<sup>-/-</sup>* (Fig. 36F). Cholesterol levels in the *Csn8<sup>myeloid</sup>Apoe<sup>-/-</sup>* female were not significantly different after the 12 weeks of HFD compared to their controls *Csn8<sup>wt</sup>Apoe<sup>-/-</sup>*, (Fig. 36G).

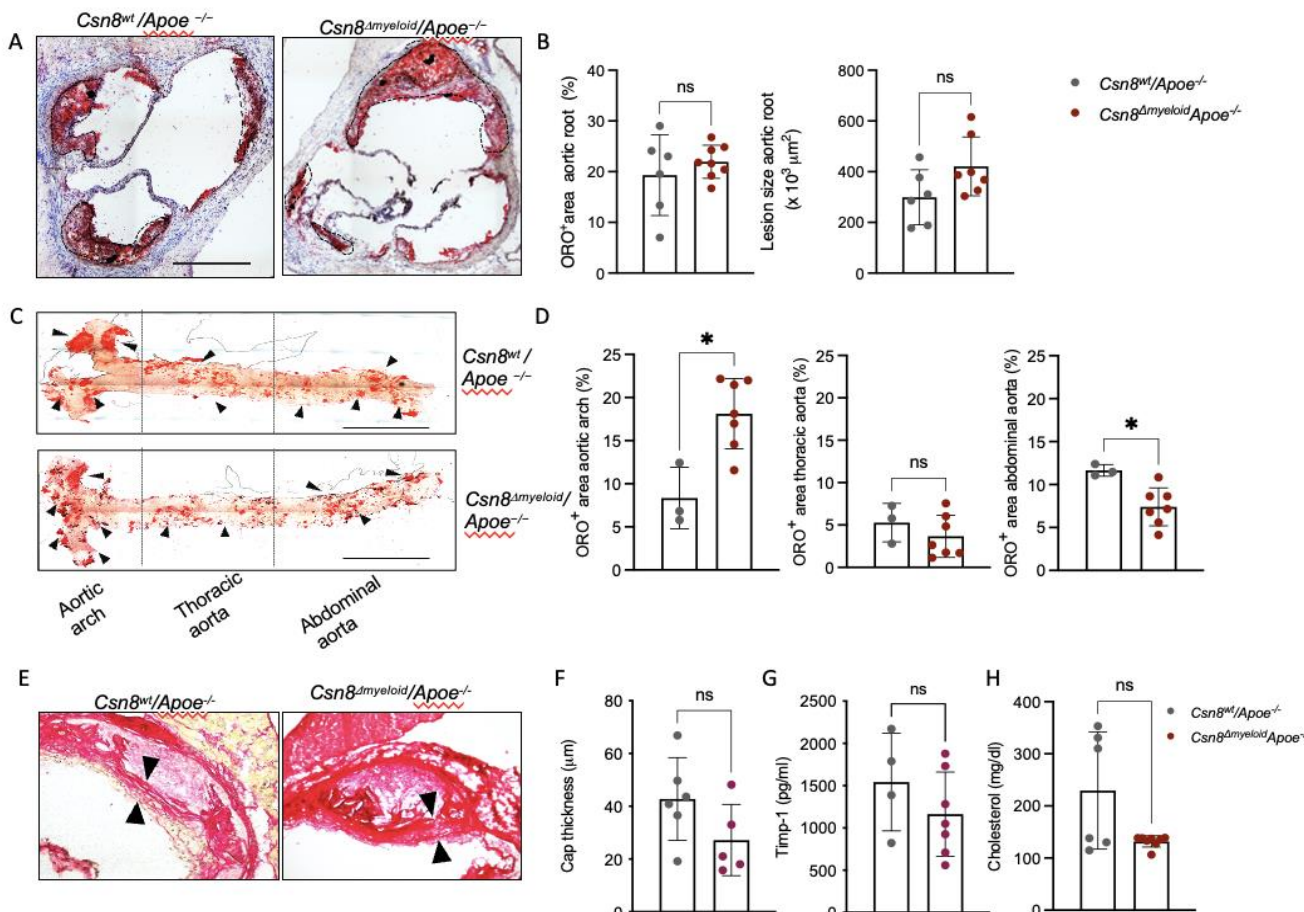


**Figure 36. Myeloid-specific deletion of Csn8 has no adverse effects on female mouse atherosclerosis.** *Csn8<sup>myeloid</sup>Apoe<sup>-/-</sup>* female mice were fed an HFD for 12 weeks. A Representative ORO staining of the aortic arch of *Csn8<sup>wt</sup>Apoe<sup>-/-</sup>*, *Csn8<sup>myeloid</sup>Apoe<sup>-/-</sup>*. Scale bar 500  $\mu$ m. B, Quantification of the ORO lesion size and percentage of the aortic root of *Csn8<sup>wt</sup>Apoe<sup>-/-</sup>* (n=6 mice) compared to *Csn8<sup>myeloid</sup>Apoe<sup>-/-</sup>* (n=7 mice). C, Representative female ORO-stained aortas are shown. Black arrowheads outline the lesion sites in the aortic arch, aortic root, and abdominal aorta. Scale size, 3mm. D, Quantification of the ORO lesion

percentage in the aortic arch, thoracic aorta, and abdominal aorta *Csn8<sup>wt</sup>Apoe<sup>-/-</sup>* (n=3 mice), *Csn8<sup>Amyloid</sup>Apoe<sup>-/-</sup>* (n=6 mice). **E**, Representative Sirius red (SR<sup>+</sup>) stained lesions with fibrotic cap indicated with black arrowheads. Scale bars, 50  $\mu$ m. **F**, Quantification cap thickness of *Csn8<sup>Amyloid</sup>Apoe<sup>-/-</sup>* (n= 5 mice) *Csn8<sup>wt</sup>Apoe<sup>-/-</sup>* (n=6 mice) of female mice. **G**, TIMP1 circulatory levels of the *Csn8<sup>Amyloid</sup>Apoe<sup>-/-</sup>* (n=7 mice) and *Csn8<sup>wt</sup>Apoe<sup>-/-</sup>* (n=4 mice). **G**, Cholesterol levels of the female *Csn8<sup>Amyloid</sup>Apoe<sup>-/-</sup>* (n=8) and *Csn8<sup>wt</sup>Apoe<sup>-/-</sup>* (n=6) after the 12 weeks of HFD. These data represent means  $\pm$  SD.

Overall female blood cell analysis didn't reveal changes in the blood cell count compared to their *Csn8<sup>wt</sup>Apoe<sup>-/-</sup>* control littermates (**Table 5**).

**Table 5. Blood cell count of female *Csn8<sup>Amyloid</sup>Apoe<sup>-/-</sup>* compared to the *Csn8<sup>wt</sup>Apoe<sup>-/-</sup>***

*Parameters	<i>Csn8<sup>wt</sup>Apoe<sup>-/-</sup></i>			<i>Csn8<sup>Amyloid</sup>Apoe<sup>-/-</sup></i>			P- values
	Mean	SD	N	Mean	SD	N	
<b>WBC (/<math>\mu</math>L)</b>	4,79	3,35	11	2,8	0,87	13	0,051769
<b>HGB (g/dl)</b>	12,26	5,11	11	14,1	5,18	12	0,404248
<b>PLT (10<sup>3</sup> /<math>\mu</math>L)</b>	95,34	68,58	10	93,75	105,45	12	0,967761
<b>LYM (%)</b>	65,57	8,43	11	62,054	7,58	13	0,293459
<b>MO (%)</b>	5,50	1,52	11	5,07	1,074	13	0,415842
<b>GRA (%)</b>	28,9	7,64	11	32,57	6,434	13	0,216659
<b>LYM (/<math>\mu</math>L)</b>	2,94	1,87	11	1,68	0,545	13	0,030637
<b>MO (/<math>\mu</math>L)</b>	0,31	0,49	11	0,11	0,027	13	0,149074
<b>GRA (/<math>\mu</math>L)</b>	1,61	1,26	11	1,06	0,46	13	0,173222

\* Acronyms are described in material and methods.

#### 4.11 The CSN holo-complex plays a role in regulating the levels of the TIMP1 via the AP-1 signalling axis in BMDMs

To further the understanding of whether only endothelial-specific *Csn5* loss or, as in earlier studies, myeloid *Csn5* loss has a profound impact on the atherosclerosis progression. Bone marrow has been harvested from *Csn8<sup>Amyloid</sup>Apoe<sup>-/-</sup>* mice after 12 weeks HFD and differentiated and cultured into macrophages by employing L929 conditioned media (LCM) as previously described (**Fig. 37A**).

Total mRNA of unstimulated M0 type of macrophages has been used to profile and confirm the *Csn8* depletion *in vitro* (**Fig. 37B**). Besides, I aimed to verify if other subunits of the CSN, such as *Csn5* gene expression, are affected as well in the *Csn8* depleted BM-derived macrophages (**Fig. 37B**). I could observe that *Csn8* loss of function does lead to the lowering of the *Csn5* gene expression (**Fig. 37C**). Moreover, *Timp-1* gene expression was lowered as well upon the loss of the *Csn8* in the M0-derived macrophages (**Fig. 37C**). Hence, interestingly gene expression of *Timp-1* is yet again lowered upon the complex disassembly (**Fig. 37D**). Once the BMDMs of the *Csn8<sup>Amyloid</sup>Apoe<sup>-/-</sup>* was analysed for the markers of extracellular matrix remodelling, with or without atherogenic stimulation (20ng/ml *Tnf $\alpha$*  for 16h), *Mmp2* and *Mmp9* gene

expression were trendlines elevated upon the COP9 signalosome loss and pro-atherogenic stimulation (**Fig. 37E**).

As there were several reports on the COP9 complex dynamics, I investigated the state of the rest of the subunit's gene expression upon Csn8 loss, with or without the Tnfa stimulation. Whereas only Csn3 gene expression has been elevated upon the Tnfa stimulation (**Fig. 37F**). The previously encountered lowering of the Timp-1 gene expression levels upon Csn8 loss remained true on the protein levels in the BMDMs (**Fig. 37F**). It is seemingly as well affected by the lowering of the AP-1 signaling, and destabilising c-Jun (**Fig. 37H**).

As the COP9 signalosome has been shown to negatively regulate the I $\kappa$ B $\alpha$ , the effects of the Csn8 loss were investigated on the NF- $\kappa$ B signalling as well. Whereby *CCl2* and *IL-6* gene expression is elevated in the *Csn8<sup>Δamyloid</sup>Apoe<sup>-/-</sup>* BMDMs (**Fig. 37I**). While on the other hand, I $\kappa$ B $\alpha$  levels were in the line with previous reports, lowered down with the Csn8 loss in BMDMs of *Csn8<sup>Δamyloid</sup>Apoe<sup>-/-</sup>* (**Fig. 37J**).

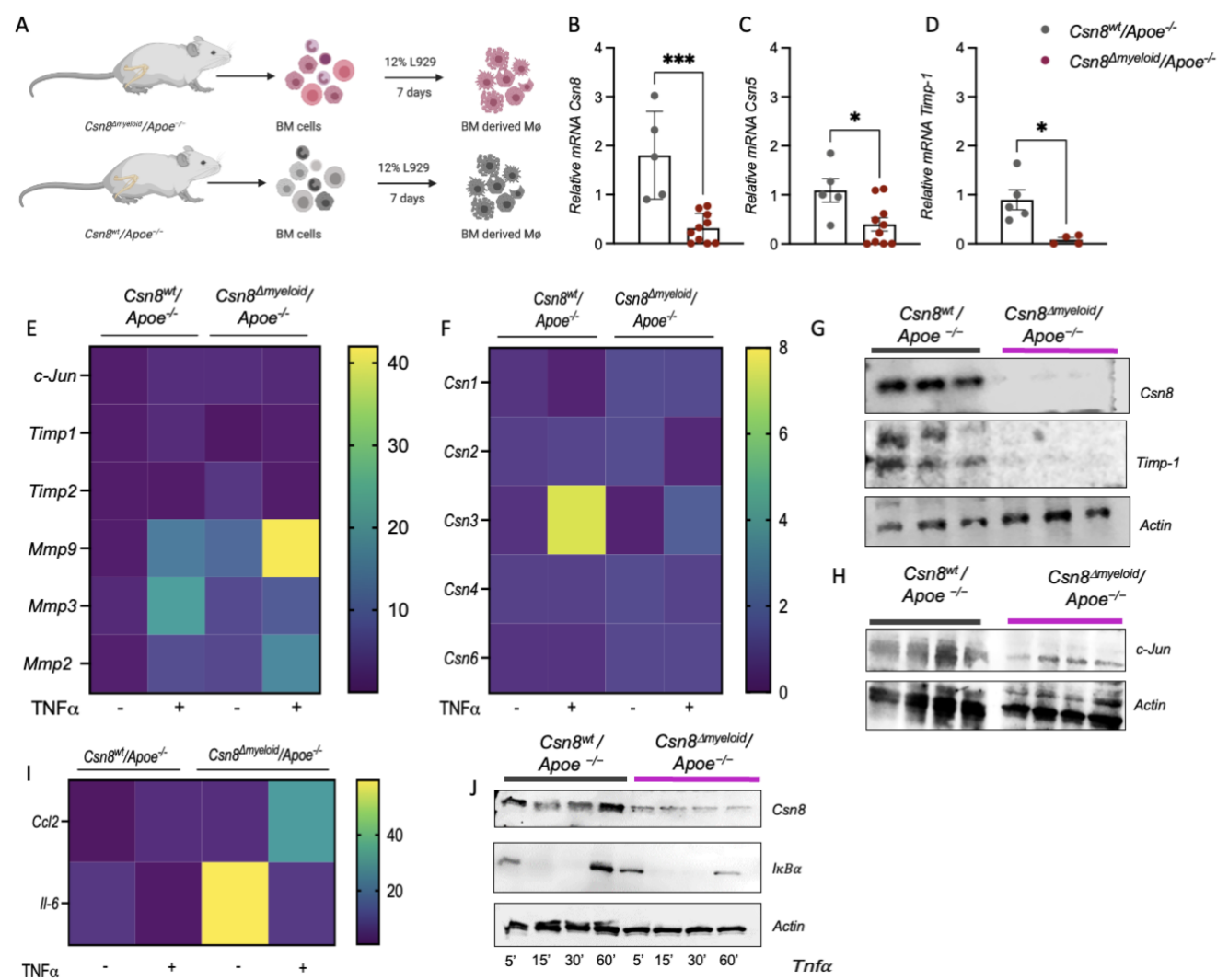


**Figure 37. Targeted deletion of the Csn8 gene in murine macrophages lowers TIMP1 expression via the AP-1 signalling axis.** Experimental outline. *Csn8<sup>Δamyloid</sup>Apoe<sup>-/-</sup>* mice or *Csn8<sup>wt</sup>Apoe<sup>-/-</sup>* were fed HFD for 12 weeks. That was followed by sacrificing the animals and bone marrow harvesting, which is further differentiated into macrophages. RNA from the LCM (L929 conditioned media) bone marrow-derived macrophages (BMDMs) was isolated. **B-D**, Relative gene expression of the *Csn8* (**B**), *Csn5* (**C**), and *Timp1* (**D**) of the bone marrow-derived macrophages were harvested from the *Csn8<sup>Δamyloid</sup>Apoe<sup>-/-</sup>* (n=10 mice) and *Csn8<sup>wt</sup>Apoe<sup>-/-</sup>* (n=5

mice). **E**, Relative mRNA gene expression histogram of *c-Jun*, *Timp1*, *Timp2*, *Mmp9*, *Mmp3*, and *Mmp2*, of BMDMs that are harvested from *Csn8<sup>Amyloid</sup>* (n=5-7) or *Csn8<sup>wt</sup>* controls (n=5) with or without, over-night pro-inflammatory TNF $\alpha$  (20 ng/ml) stimulation; **F**, Relative mRNA gene expression histogram of the expression of the COP9 subunits. BMDMs of *Csn8<sup>Amyloid</sup>Apoe<sup>-/-</sup>* (n=5-7) or their controls, *Csn8<sup>wt</sup>Apoe<sup>-/-</sup>* (n=5) with or without over-night pro-inflammatory TNF $\alpha$  (20 ng/ml) stimulation **G**, Representative immunoblots of *Csn8* and *Timp1* of *Csn8* knock-down (n=3) or their controls (n=3); **H**, Representative immunoblots of *c-Jun* in BMDMs of *Csn8<sup>Amyloid</sup>Apoe<sup>-/-</sup>* (n=3) and *Csn8<sup>wt</sup>Apoe<sup>-/-</sup>* (n=3) mice; **I** Relative mRNA gene expression histogram of *Ccl2* and *Il-6* expression in BMDMs that were *Csn8* knock-down (n=5-7) or their controls (n=5) with or without TNF $\alpha$  (20 ng/ml) stimulation; **J**, Representative immunoblots of *IkB $\alpha$*  in *Csn8<sup>Amyloid</sup>Apoe<sup>-/-</sup>* (n=3) and *Csn8<sup>wt</sup>Apoe<sup>-/-</sup>* (n=3). These data represent means  $\pm$  SD.

#### 4.12 TIMP-1 levels are changed in human atherosclerotic lesions depending on the plaque stability

Atherosclerosis is not clinically relevant unless it reaches adverse effects and life-threatening coronary thrombosis by exposing thrombogenic material (Libby et al., 2019). One of the responsible culprits that determine the atheropprogression is the MMP-associated ECM degradation (Bentzon et al., 2014). However, studies remain elusive so far.

To understand whether TIMP-1 levels change with plaque instability, we aimed to investigate the human carotid endarterectomy kindly profiled and provided by Dr Mägdefessel (TUM, Vascular Medicine).

Immunofluorescent staining of the male patient carotid endarterectomy lesions (**Fig. 38A**) has yielded unclear TIMP-1 expressions. While in the healthy human plaques, we could observe unformal distribution, stable and unstable plaques have yielded lower expression in the endothelial and sub-endothelial regions while showing strong TIMP-1 expression in the macrophage/foam cells regions and necrotic core area (**Fig. 38A**).

Moreover, TIMP-1 positive signal distribution was visualised upon DAB-based immunohistochemistry staining. While healthy human plaques are seemingly having low unformal TIMP-1 expression, stable and unstable are showing a loss of TIMP-1 expression in the subendothelial region and a more pronounced signal in the area flanking the necrotic core (**Fig. 38B**). By employing ImageJ plugins integrating deconvolution, histogram profiling, and scoring, IHC profiler, we managed to quantify the percentage of the TIMP-1 positive areas and score them into 4 groups: high positive, positive, low positive, and negative zones. The intensity of the signal for the high positive zones is ranged from 0 to 60, the positive zone was found to be ranging from 61 to 120; 121 to 180 for the low positive zone; and 181 to 235 for the negative zone, respectively (Ruifrok & Johnston, 2001; Varghese et al., 2014). *Timp1* positive area has been depleted in the positive ranked pixel range, as well as in the high positive pixel range of the signal intensities, while the low positive range was not showing significant differences among the unstable lesions compared to the stable lesions found in the human carotid endarterectomy (**Fig. 38C**). Altogether suggesting that higher pixel intensity signals found in the lesions were showing more pronounced expression differences than the basic constitutive TIMP1 signal.

To verify the finding, we extracted total mRNA from the human carotid endarterectomy and analysed gene expression of TIMP1 gene expression in the total vessel (**Fig. 38D**). Whereby, I could observe elevated gene expression in TIMP1 in the stable and unstable human lesions. Interestingly, TIMP1 gene expression in unstable compared to stable human lesions was lowered.

The TIMP1 gene expression found in the lesion was lower in the unstable human lesions compared to stable ones, while mRNA gene expression data hasn't yielded the same outline. The endothelial lining has been depleted of the TIMP-1 expression with the atherosclerosis progression and elevated vulnerability factors.

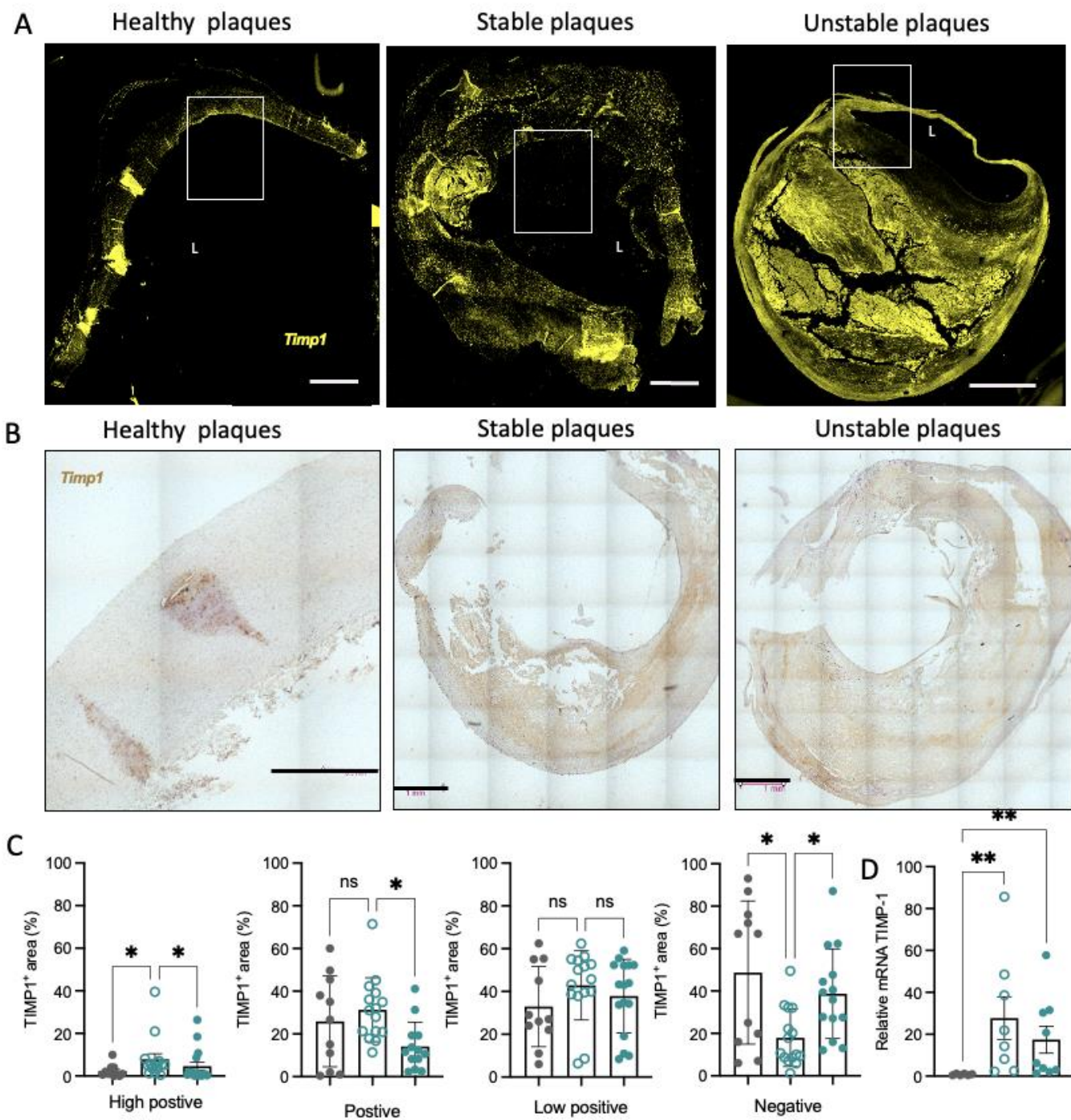


**Figure 38. TIMP-1 expression is changed in human carotid artery atherosclerotic lesions depending on the plaque stability.** **A** Representative immunofluorescence staining of TIMP-1 in human healthy vessels or healthy, stable, and unstable atherosclerotic plaques. Scale bar, 1mm **B**, Immunohistochemical staining (DAB) for TIMP-1. Scale bar 1mm. **C**, Quantification of DAB stained healthy (n=11), stable (n=15) and unstable (n=16) human plaques. **D**, Gene expression of *CSN5* and *TIMP-1* in healthy (n=7), stable (n=8), and unstable (n=9) human CAs sections (10 sections per data point). Each data point represents an individual patient sample. These data represent means  $\pm$  SD.

### 4.13 Human aortic endothelial cells Csn5 depletion determines Timp1 levels and matrix-metalloproteinase activity

Previous studies have outlined that CSN5 depletion in the human endothelial lining *in vitro* elevates the NF- $\kappa$ B signalling and well monocyte adhesion (Asare et al., 2013b).

To understand how the CSN5 depletion impacts endothelial lining and how to do that overall impacts factors of extracellular matrix remodelling (Fig. 39A), hCSN5 siPOOL was applied in Ecs, and it managed to deplete more than 50% of the CSN5 gene expression compared to their scrRNA control (Fig. 39B). Moreover, TIMP-1 gene expression followed up the lowering trend, as it was significantly lowered once the CSN5 gene expression was depleted in endothelial cells (Fig. 39C). Secreted levels of TIMP-1 were measured in the supernatants of the *hCSN5 siPOOL* treated HAoECs. I could report TIMP-1 depletion in the supernatants of *CSN5 siPOOL-treated* endothelial cells compared to the scrRNA-treated HAoECs (Fig. 39D).

As previously observed AP-1 axis is being destabilised by the CSN5 loss in MAECs. Yet again, the intracellular level of *c-JUN* gene expression was lowered upon the CSN5 depletion, triggering potential TIMP-1 downregulation. Interestingly, MMP2 gene expression hasn't been altered under the CSN5 loss, while MMP9 has significantly downregulated (Fig. 39, F-G). To clarify the potential role of the TIMP-1/ MMP activity disbalance, MMP gelatinase zymography, and MMP activity

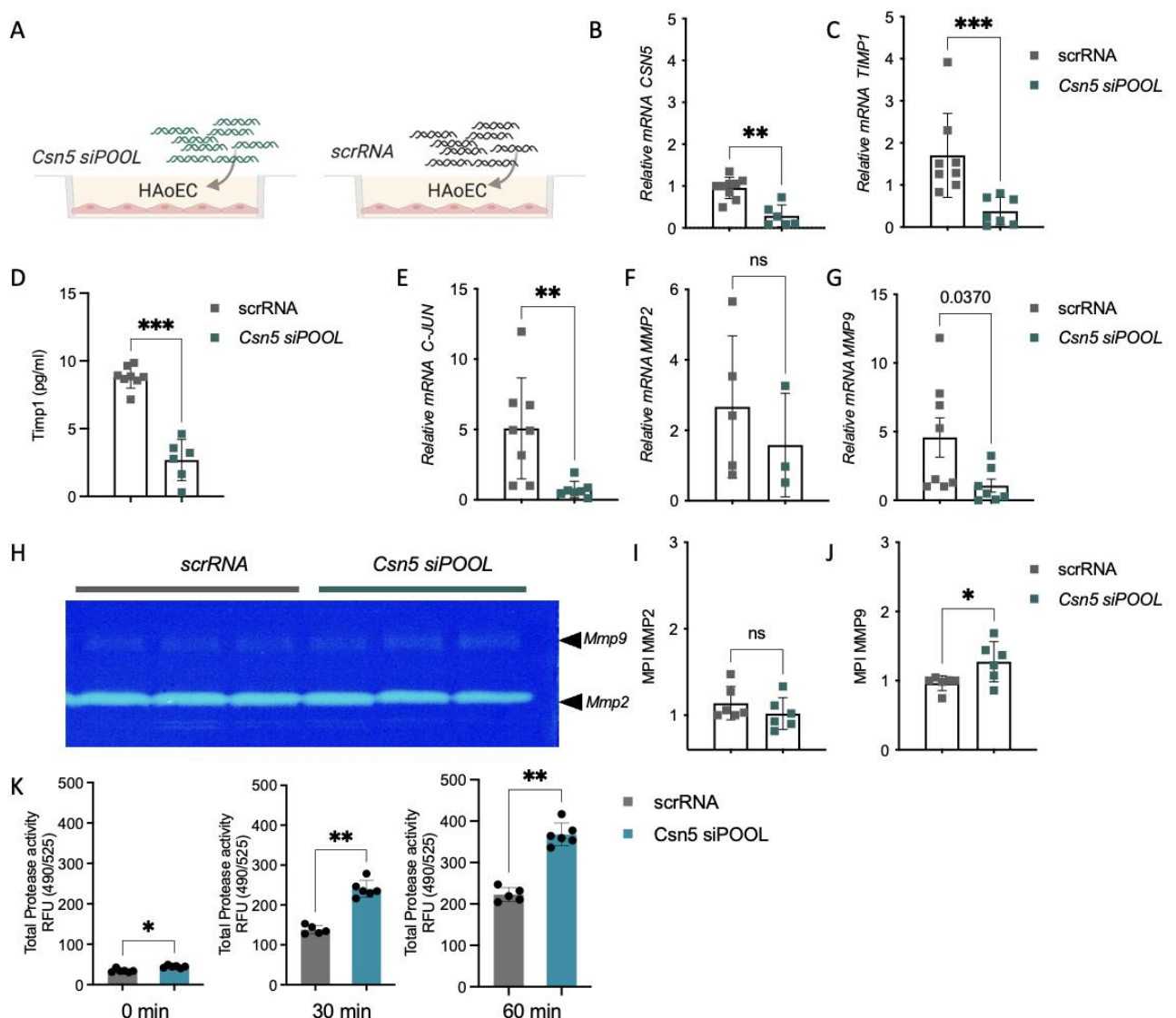


**Figure 39. CSN5 regulates matrix remodeling players in human aortic endothelial cells (HAoECs).** **A**, Experimental outline employing the human aortic endothelial cells (HAoECs) and depletion of *CSN5* by employing 10nM *siPOOL* technology (blue-green) was compared to their scrambled RNA (*scrRNA*) controls (gray) *in vitro*. **B-C**, Relative mRNA gene expression of *CSN5* (B) and *TIMP1* (D) in HAoECs *in vitro*. *Csn5 siPOOL* (n=8), *scrRNA* controls (n=8). **D**, Timp1 secreted levels in MAEC supernatants that were *Csn5* gene depleted (n=6) compared to the supernatants of the HAoEC that were *scrRNA* treated controls (n=8). **E-G**, Relative mRNA gene expression of *C-JUN* I, *MMP2* (F), and *MMP9* (G) in HAoECs *in vitro*. *Csn5 siPOOL* (n=3-7), *scrRNA* controls (n=5-8). **H**, Representative zymogram gel of *Csn5 siPOOL* treated MAECs supernatants compared to the RNA scrambled controls (*scrRNA*). **I-J**, Quantification of the mean pixel intensity of the MMP2 (I) and MMP9 (J) enzyme activity upon *Csn5 siPOOL* treatment (n=9-11) versus *scrRNA* control treatment (n=8). **K**, Quantification of the total MMP activity in MAEC supernatants of the controls *scrRNA* (n=4-5) and *Csn5 siPOOL* (n=6). These data represent means  $\pm$  SD.

The assay was performed in human endothelial cell culture supernatants (Fig. 39, H-K). Zymography has shown a surprising elevation of the MMP9 activity, while MMP2 hasn't changed (Fig. 39, H-J). Interestingly, once total MMP activity was analysed in the HAoECs supernatants, CSN5 depletion did elevate the total matrix-metalloproteinase activity from the first moment of exposure to the fluorescent-MMP substrate (Fig. 39K).

Overall, CSN5 loss in HAoECs, indeed by destabilising c-JUN levels, depletes tissue-inhibitor matrix metalloproteinase inhibitor levels and disturbs the TIMP-1/MMP balance. That might be the underlining mechanism behind the vulnerable plaque phenotype upon arterial-endothelial *Csn5* depletion *in vivo*. Moreover, total MMP activity is more pronounced in the TIMP-1 absence with CSN5 depletion, which the MMP9 gelatinase activity might lead.

#### 4.14 MLN4924 treatment of human aortic endothelial elevates Timp1 levels

The endothelial-specific CSN5/CSN8 depletion *in vitro* and *in vivo* lowers the TIMP-1 expression, possibly via the c-JUN axis in mice and humans. Conversely, NEDDylation activation inhibition (by employing MLN4924) and the CSN5 overexpression enable the TIMP-1 elevation in mice, which might have a therapeutical value.

If this is the case in the human aortic endothelial cells, it was investigated. Namely, HAoECs were exposed for 16h under the small molecule inhibitor, MLN4924 (500nM), or its vehicle control (Fig. 40A). Gene expression of the TIMP-1 was significantly elevated under the small molecule inhibitor influence, thus confirming the previously observed effects on the mouse aortic endothelial cells (Fig. 40B). Conversely, MLN4924 treatment didn't impact the gene expression of the *MMP9* or *MMP2* in HAoECs (Fig. 40, C-D). TIMP-1 secretory levels in the MLN4924 treated HAoEC supernatants under the TNF $\alpha$  pro-inflammatory stimulation didn't alter *in vitro* compared to the supernatants of the vehicle-treated HAoECs (Fig. 40E). However, without any stimulation besides the NEDDylation inhibitor or its vehicle control, MLN4924 treated HAoECs did enhance the TIMP-1 levels in their supernatants (Fig. 40F). That overall did impose a question upon whether MMP activity is altered under the MLN4924 treatment, and it was investigated on the gelatinase zymography assay (Fig. 40G). Thereby revealing that although MMP2 activity didn't change, MMP9 decreased upon the NEDDylation ablation treatment compared to its vehicle control (Fig. 40, H-I). Thus, overall confirming the previous observations that 'CSN5

hyperactivity mimics' depletes MMP9 gelatinase activity while elevating TIMP1 expression.

CSN5 loss did elevate the overall MMP activity. However, I couldn't observe significant changes in the total MMP activity under the influence of the MLN4924, suggesting that other MMPs might play a role besides the MMP9 gelatinase (Fig. 40J).

Intriguingly we could, for the first, provide an overview of where CSN5 levels and the COP9 signalosome might regulate the ratio of the MMP9/TIMP1 fine-tuned balance in endothelial cells. Since MMP9/TIMP1 ratio balance has been identified previously as one of the biomarkers of the poor outcome in atherosclerosis progression and revealing factors in the atherosclerotic plaque destabilisation (Kremastiotis et al., 2021; T. Li et al., 2020).

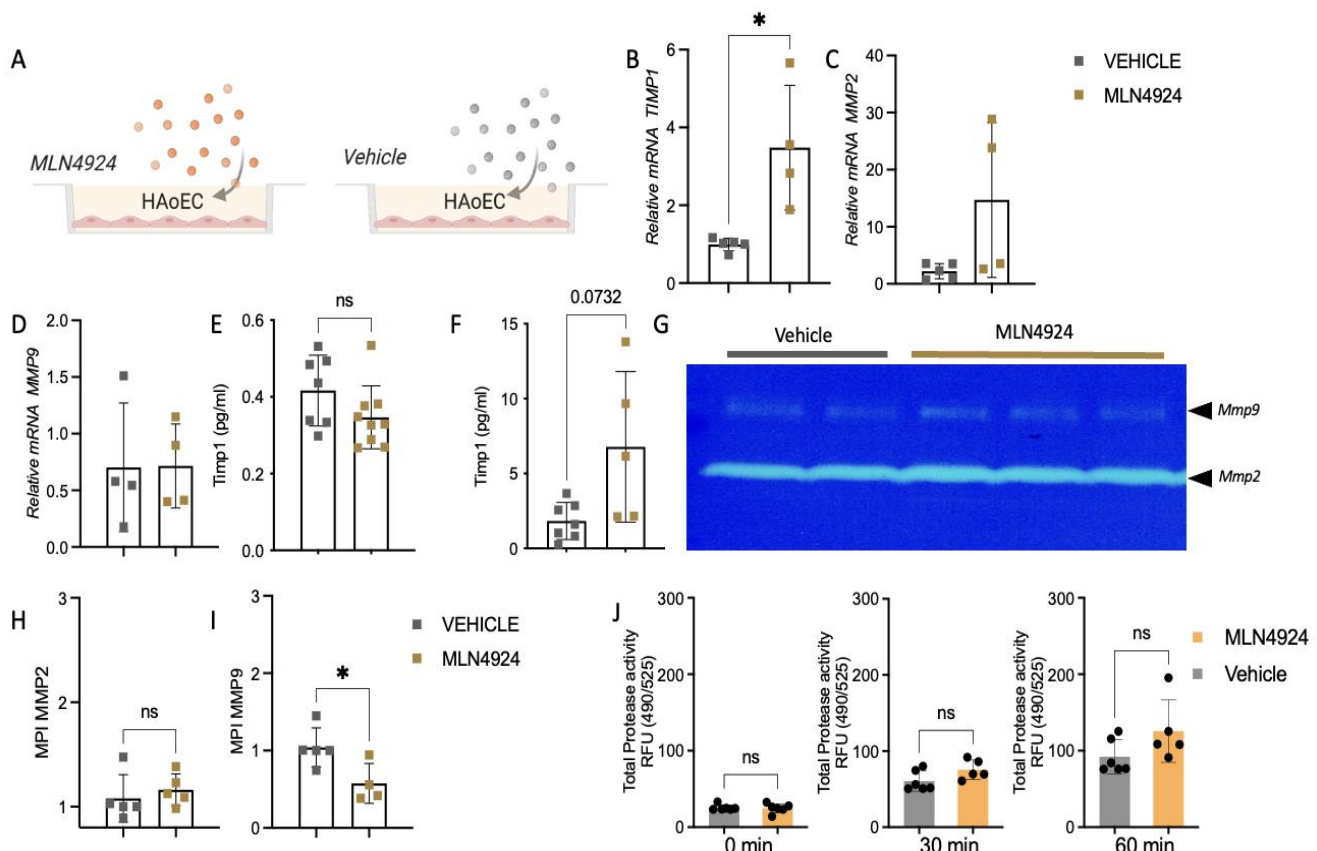


**Figure 40. Neddylation ablation by employing MLN4924 upregulates Timp1 levels and ablates pro-MMP9 activity in human aortic endothelial cells while it does not impact the overall MMP activity.** Experimental outline. Human aortic endothelial cells were treated overnight with either 500nM MLN4924 treatment or vehicle to deplete neddylation and mimic 'CSN5 overexpression' conditions. **B-D**, Gene expression of human TIMP1, MMP2, MMP9 in aortic endothelial cells upon MLN4924 (n=4) or vehicle (n=5) treated samples. **E-F**, Secreted Timp1 from HaoECs treated overnight with MLN4924 (n=5-9) or vehicle (n=7), levels under the TNF $\alpha$  (20 ng/ml) stimulation (E) or without (F). **G**, Representative zymogram gel of gelatinase activity of MLN4924 (n=4-5) treated HAoECs supernatants compared to the vehicle (n=5) treated supernatant controls. **H-I**, Quantification of the MMP2 and MMP9 gelatinase activity in HAoECs supernatants as a mean pixel intensity (MPI) developed on zymography. **J**, Quantified total matrix-metalloproteinase (MMP) activity measure on HAoECs supernatants after the MLN4924 treatment (n=3) or vehicle treatment (n=3). These data represent means  $\pm$  SD.



## 5. Discussion<sup>2</sup>

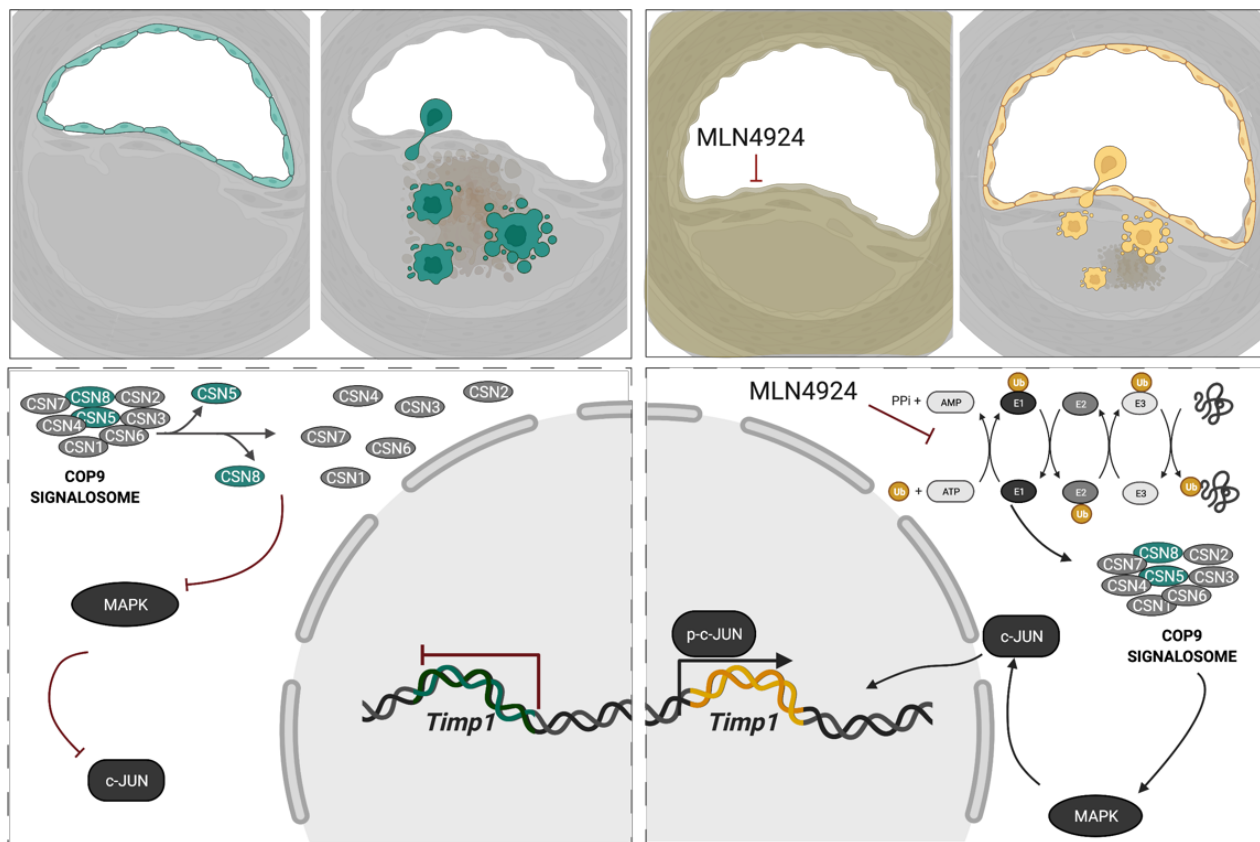


**Figure. 41 Graphical Abstract.** **Left side panel**, Schematic representation of the arterial-specific deletion of Csn5, and myeloid-specific Csn5/-8 depletion that all together induces the COP9 signalosome complex disassembly, that in turn via depleting MAPKs signaling, destabilize c-JUN (AP-1 signaling) and finally inhibits TIMP-1 gene expression. Overall, these conditions stimulate unfavorable TIMP1/MMP9 ratio, and atherosclerotic lesions are more prone to be vulnerable. **Right side panel**, Schematic representation of the intercellular environment upon ‘Csn5 overexpression mimics’ in total macrophages and endothelial cells (by employing the MLN4924 small molecule inhibitor) and a Csn5 overexpression (fibroblasts). In murine and humane endothelial cells as well as macrophages, MLN4924 by blocking the NEDDylation activation, without an impact on the overall COP9 signalosome complex, induces the MAPKs and elevates and stabilizes the c-JUN which in turn elevates the TIMP-1 gene expression. Overall, these conditions stimulate the TIMP1/MMP9 beneficial ratio, and atherosclerotic lesions are less prone to rupture (Created with Biorender).

<sup>2</sup> parts of the discussion have been published in a review of articles that I have contributed to as a first author: Milic, J., Tian, Y., & Bernhagen, J. (2019). Role of the COP9 Signalosome (CSN) in Cardiovascular Diseases. *Biomolecules*, 9(6), 217.

### 5.1 Arterial-specific Deletion of Csn5 enhances early atherosclerosis, while MLN4924 mimics atheroprotection by CSN5 in vivo after 4 weeks of a Western diet

The CSN is a conserved protein complex consisting of 8 subunits (CSN1 to -8) and regulates the degradation of critical cell cycle and inflammatory proteins by controlling another family of proteins CRLs. It removes the NEDD8 molecule, which is attached to CRLs by a posttranslational modification process called “Neddylation” Field (Chamovitz & Segal, 2001; Cope & (Chamovitz & Segal, 2001; Cope & Deshaies, 2003; Wei et al., 2008).

So far, published research investigating CSN as a regulator of inflammatory mechanisms involved in atherosclerosis development has focused on investigating its role in the NF- $\kappa$ B signalling axis (Asare et al., 2013a, 2017; Schweitzer et al., 2007). Moreover, prior studies on siRNA derived-*CSN5* depletion *in vitro* in human aortic endothelial cells trigger NF- $\kappa$ B signalling via destabilising Culling-RING ligases and that *CSN5* attenuation promotes monocyte adhesion on endothelium *in vitro* (Asare et al., 2013b, 2017). While truly relevant, NF- $\kappa$ B signalling is seemingly only partially involved in atherosclerosis progression upon *CSN5* loss of function. Therefore, we were curious about investigating the other signalling axis beyond the NF- $\kappa$ B that might contribute to the observed exacerbated phenotype. Interestingly, previous studies have also reported elevation of the *Csn5*, *Csn8*, and *Csn3* positive areas of the COP9 signalosome in human atherosclerotic lesions. Most of the positive *Csn5* signal in these human lesions could be ‘pin-pointed’ to the CD31+ endothelial layer of the human blood vessels (Asare et al., 2013). Thus, this puzzled us to question what kind of role the CSN holo-complex plays in atherosclerosis progression. Thereby, one of the major observations I made here has been that an arterial-/endothelial-specific *Csn5* knock-out (KO) in an atherogenic *Apoe*<sup>-/-</sup> background (*Csn5*<sup>Δarterial</sup> *Apoe*<sup>-/-</sup>) upon high-fat diet recapitulates the exacerbated atherosclerotic phenotype *in vivo* that was seen previously upon a myeloid-specific *Csn5* knock-out mice (Asare et al., 2017).

Arterial-/endothelial-specific *Csn5* knock-out *in vivo* was not evaluated in an *Apoe*<sup>-/-</sup> atherogenic background. We have shown that arterial endothelial-*Csn5* depletion exacerbates early formation. Our study shows that hyperlipidemic male mice show more pronounced atherosclerosis after 4 weeks of a Western diet. In contrast, this cannot be observed in the female *Apoe*<sup>-/-</sup> mice. The *Apoe*<sup>-/-</sup> female atherogenic mice upon *Csn5* arterial-endothelial depletion have only shown early lesion exacerbation in the abdominal aorta and the aortic arch, while aortic root and thoracic aorta hasn’t been altered compared to their *Csn5* constitutively- expressing controls. Moreover, as previous reports suggest, atherosclerotic lesions are more pronounced in females than in male *Apoe*<sup>-/-</sup> mice. Interestingly atherogenic female mice, after 12 weeks of HFD, upon CSN5 loss in myeloid cells, have presented strong lesion exacerbation in female mice only in the abdominal aorta, which is also observed in this thesis (Asare et al., 2017).

These gender-specific effects could be partially assigned to the action of estrogen. Namely, the athero-protective effects of estrogen have been previously confirmed in multiple animal models and humans. It is considered a beneficial factor in premenopausal women in the coronary disease prevention (Bruck et al., 1997; Grodstein et al., 1996; Kassi et al., 2015). Interestingly one of the interacting partners found to bind to CSN5 directly and thereby being targeted via proteasome degradation is estrogen receptor  $\alpha$  (ER $\alpha$ ) (Calligé et al., 2005). Furthermore, estrogen exerts its protective effects in humans and mice via its receptor ER $\alpha$  on the endothelium. In that manner, estrogen partakes cardiovascular protective actions by regulating endothelial

proliferation, migration, and apoptosis and by triggering anti-inflammatory effects via downregulating IKK activation of NF- $\kappa$ B signalling ((Kassi et al., 2015; Simoncini & Genazzani, 2000). Hence, gender-specific effects would possibly assign to the loss of CSN5 in the endothelium, consequently up-regulation of the ER $\alpha$  and thereby downregulation of the pro-atherogenic signalling and elevation of estrogen protective effects.

Male atheroprone- *Apoe*<sup>-/-</sup> mice have shown early lesion exacerbation upon arterial-endothelial *Csn5* depletion in the aortic root, aortic arch, and abdominal aorta. In contrast, the thoracic part of the aorta was not impacted. This study first investigates COP9 signalosome loss in atherosclerosis progression in early atherosclerosis lesion formation. Similarly to this study, yet another study, employing *CSN3* siRNA *in vivo* has been able to corroborate exacerbation of the aortic root lesions and aorta after the 10 weeks of Western-type of diet, thus confirming that COP9 signalosome loss of function indeed exacerbates atherosclerosis progression (Boro et al., 2021).

Not male nor female arterial-/endothelial *Csn5* attenuated mice have shown any changes in their weight progression, lipid metabolism, or blood cell count compared to the controls. The hence corroborates previous finding that lipid metabolism and blood cell count haven't been altered and are responsible culprits for pronounced atherosclerosis upon the COP9 signalosome loss of function (Asare et al., 2017).

Therapeutic value and potential inverting the effects of the CSN5 loss were probed by employing the small molecule inhibitor MLN4924 (Pevonedistat) *in vivo* which was previously tested in a clinical trial in the therapy of cancer patients (Sarantopoulos et al., 2016). Thus, by employing a neddylation activation inhibitor (MLN4924), we could 'mimic' the *Csn5* overexpression conditions in *Apoe*<sup>-/-</sup> atherogenic male and female mice.

MLN4924 has been previously described as a NEDDylation inhibitor that attenuates small atherosclerotic lesions partially acting through the atherogenesis development via NF- $\kappa$ B signalling axis inhibition but was unable to cope with the middle size and large atherosclerosis lesions (Asare et al., 2017; Soucy et al., 2009; Swords et al., 2015; Y. Wang et al., 2015). So, we tested for the first time whether this small molecule inhibitor could affect an early atherosclerosis progression. Indeed, early atherosclerotic lesion size found in the aorta and aortic root was reduced after the 4-week simultaneous western diet and MLN4924 application in 6 weeks male *Apoe*<sup>-/-</sup> mice. While on the other hand, no athero-protective MLN4924 effects were observed on an early lesion in hyperlipidaemic female mice.

Inhibition of the NEDDylation activation by employing the small molecule inhibitor, MLN4924, affects the factors of the matrix remodelling system by promoting the expression of the TIMP-1 *in vivo*. MLN4924 led to higher serum TIMP-1 levels in atherogenic male mice and its expression in their atherosclerotic lesions.

Hence, *in vivo*, studies demonstrate that MLN4924 acts preventively in an early stage of atherosclerosis by impairing the progression and elevating protease factors inhibiting matrix-remodelling machinery. While on the other hand, CSN5 loss in endothelial lining has promoted early atherosclerosis lesion exacerbation in the male aorta and aortic root.

## 5.2 Csn5 loss in arterial endothelial lining promotes advanced atherosclerosis and enhances atherosclerotic plaque vulnerability *in vivo* via eliciting matrix-remodelling players

Atheropprogression starts with ECD and activation at the focal sites of disturbed blood flow. That is followed by multiple inflammations, VSMC proliferation, and ECM degradation (Chistiakov et al., 2013; Cunningham & Gotlieb, 2005; Libby, 2012). While the atherogenic process can pass unnoticed, it can evolve into an irreversible advanced fibrous lesion and a necrotic core, which involves an immense remodelling of the vessel wall (Bentzon et al., 2014; Libby et al., 2019). This is accompanied by narrowing to the vessel lumen and stenosis. Eventually, it can promote plaque vulnerability and rupture/ erosion of plaques, leading to significant CVD events such as myocardial infarction or stroke (Bentzon et al., 2014; Libby et al., 2019). In many cases, atherosclerosis is therefore not life-threatening or clinically symptomatic unless there is an event of plaque rupture and thus exposure to highly thrombogenic necrotic core material (Bentzon et al., 2014; Loftus et al., 2000).

COP9 signalosome disassembly by the CSN5 loss in myeloid cells has previously been shown to elevate the plaque load in male mice, trigger elevated atherogenic inflammation, and up-regulate gene expression of MMP9 in macrophages (Asare et al., 2017). MMPs implication in enabling the arterial wall remodelling through eliciting the ECD has been prior shown (J. L. Johnson, 2017; Olejarcz et al., 2020). Moreover, the elevation of the MMP9 in its active form and macrophage population elevation is the marker of advanced lesions and might lead to traumatic events (Gough et al., 2006). Hence plaque load and advanced atherosclerotic lesion profile of the arterial-/endothelial *Csn5* depleted *Apoe*<sup>-/-</sup> mice after the 12 weeks of the Western diet *in vivo* were investigated.

Initially, I could observe that *Csn5*<sup>Δarterial</sup> *Apoe*<sup>-/-</sup> male mice have more pounced atherosclerosis in their aortas. This was in line with the previous studies whereby *Csn5* depletion in myeloid cells and *Csn3* depletion studies had caused higher plaque load in atherogenic male mice after the 12 weeks of Western diet (Asare et al., 2017; Boro et al., 2021). Interestingly, although blood count, lipid metabolism, and mouse weight didn't change, upon *Csn5* depletion in the endothelial lining, the elevation of the lesion macrophage content can be observed alongside the significant lowering of the plaque smooth muscle cell content in male atherogenic mice, which was deemed interesting as SMCs' high lesion content is athero-protective and plaque-stabilizing. In contrast, macrophages are athero-promoting and destabilising in advanced lesions (Bennett et al., 2016). Moreover, prior studies on *TIMP-1*<sup>-/-</sup> *Apoe*<sup>-/-</sup> mice *in vivo* did show a lowering of the plaque SMCs, macrophage, and lipid increase in atherosclerotic lesions of these mice (Silence et al., 2002). Thus, encountered phenotype did trigger the question of the underlying endothelial signalling mechanism upon the loss of *Csn5* *in vivo*. Although the mechanism and phenotype underlying COP9 signalosome depletion in endothelial cells, besides the NF- $\kappa$ B signalling exacerbation upon *Csn5* depletion *in vitro*, was not so far investigated, unbiased screening for over a hundred cytokines and chemokines enabled the possibility to further the understanding of endothelial phenotype *in vivo*. The vascular endothelium lining is crucial in vascular health, and it was previously shown to regulate all the processes from initiation, and vasotone regulation to thrombus formation, SMC proliferation, well cell adhesion, and finally, more recently in promoting the plaque vulnerability (Libby, 2012; Ross, 1999).

*Csn5*<sup>Δarterial</sup> *Apoe*<sup>-/-</sup> male mice had elevated inflammatory-endothelial-derived factors such as adhesion molecules, macrophage colony-stimulating factor (MCS-F), B cell attracting factors CXC13, T-cell chemoattractant CCL21, Angiotensin-2 and -L3, CD93 glycoproteins, complement factor C5a. Still, we could also observe endothelial apoptosis factors defining factors, such as CRP, IGFBP-3, and PCSK9. But the most interesting finding could be seen in changes observed in striking systemic depletion of

the serum-derived Timp-1 in *Csn5<sup>Δarterial</sup> Apoe<sup>-/-</sup>* mice and elevation in factors matrix-remodelling proteases.

TIMP-1 is a member of a family of broad-spectrum endogenous inhibitors that, essentially in a steady state, exerts negative effects on MMPs, by forming non-covalent complexes with them (Brew & Nagase, 2010; Clark et al., 2008). Hence, the MMP elevation regularly invokes it (J. L. Johnson, 2017). TIMP-1 was shown to prevent medial degradation associated with atherosclerosis through its ability to inhibition of the MMPs *in vivo* (Lemaître et al., 2003). Moreover, TIMP1's role in endothelial integrity has been described as beneficial, while its loss showed clinically significant outcomes (Kremastiotis et al., 2021; Tang et al., 2020). Inflammatory lesion environment and immune mechanisms induce MMP expression in endothelial cells, which is indispensable in angiogenesis, arterial-wall remodelling, vascular injury, and plaque vulnerability (Newby, 2005). Interestingly, MMP activity is detectable in endothelial-conditioned media, implying that ECs are more active in matrix remodelling than VSMC. They respond to the oscillatory stress by expressing MMPs (Inoue et al., 2001; Magid et al., 2003). Finally, the MMPs/TIMP-1 expression ratio was deemed important as a contributor determined the advanced atherosclerotic plaque progression and its vulnerability (Orbe et al., 2003).

Hence, collagen content, necrotic core size, and fibrous cap thickness have been evaluated as part of the *Csn5<sup>Δarterial</sup> Apoe<sup>-/-</sup>* atherosclerotic lesion profiling after the 12 weeks of the HFD.

Indeed, the necrotic core was significantly enhanced in size with the *Csn5* loss in the endothelial lining, possibly due to total macrophage content in their advanced lesions. This would be in line with the earlier studies' findings, whereas coronary arteries with ECD were found to have abundant necrotic core in their lesion and more lipid deposition (Choi et al., 2013; Matsuzawa & Lerman, 2014). Moreover, thinning of the fibrous cap could be seen. On the other hand, no significant impact on the overall collagen content can be reported, suggesting differential MMP activity might be at stake *in vivo*. These observations could align with previously described studies, whereas endothelial dysfunction plays an important role in a higher frequency of thin-caped fibroatheroma (Loftus et al., 2000). Plaque collagen content is 'fine-tuned' by its synthesis and degradation. SMCs and ECs are major collagen producers. Local factors TGF- $\beta$ , PDGF-BB, IL-1, endothelin-1, and angiotensin-II are consistent stimulators of collagen synthesis. In contrast, IFN- $\gamma$ , nitric oxide as well as fibroblast growth factor inhibit collagen production (Rekhter, 1999) as factors such as Ang-2 and PDGF-BB were found to be significantly systemically elevated in the *Csn5<sup>Δarterial</sup> Apoe<sup>-/-</sup>* mouse serum, that might partially explain no overall lesion collagen differences observed.

The mechanism promoting plaque vulnerability has been extensively investigated in past years (Holm Nielsen et al., 2020; Moreno et al., 2004; Newby, 2007; Virmani et al., 2002). One of the permissive requirements for this to occur is an extremely thin fibrous cap, and thus, ruptures (Bentzon et al., 2014). A fibrotic cap might be developed under the cell of the SMC that undergoes cell, hence are unable to produce excessive collagen, eventually causing thinning of the cap. Moreover, major contributors to the cap are the MMPs that excessively degrade the ECM fibres and grow necrotic core due to the lipid-loaded cell bursting in their inability to uptake and properly efflux cholesterol. Overall, those conditions burden the thin cap, promoting the lesion prone to rupture (Stefanadis et al., 2017).

Deciphering the clear mechanisms that lead to plaques prone to rupturing would be essential in combating the clinically significant outcomes of the CVDs (Bentzon et al., 2014; Loftus et al., 2000).

Interestingly, I could report here that the lesion vulnerability index was significantly higher in *Csn5<sup>Arterial</sup>Apoe<sup>-/-</sup>* compared to the *Apoe<sup>-/-</sup>* controls. *Csn5* loss in arterial-ECs elevates factors of plaque vulnerability and biomarkers such as MMPs. Thus, endothelial-*Csn5* in male atherogenic mice is athero-protective as it demotes lesion proneness to vulnerability. While females, *Csn5<sup>Arterial</sup>Apoe<sup>-/-</sup>* mice didn't have significantly elevated plaque load or cap thickness changes in their aortic root or aorta. Stipulating yet again the potential role of the *Csn5* loss being counteracted by the athero-protective estrogen effects (Calligé et al., 2005; Kassi et al., 2015).

A prior study reported that employing TIMP-1 stimulation *in vivo* could yield less atheroma load at the aortic root of *Apoe<sup>-/-</sup>* mice. At the same time, adding the TIMP1 enhances ECM fibre content and SMCs content *in vivo* (Rouis et al., 1999). Conversely, yet another demonstrates that *Timp-1* loss shows a promising tendency to lower the lesion load *in vivo* but doesn't protect atherogenic mice from developing them (Cuaz-Pérolin et al., 2006).

Hence the interest of this thesis was whether the therapeutical agent, MLN4924, can reduce plaque size in male *Apoe<sup>-/-</sup>* by mimicking *Csn5* overexpression. Moreover, does it possibly elevate levels of TIMP-1 *in vivo*?

Therefore, upon MLN4924 application, serum TIMP-1 levels and its lesion content are up-regulated *in vivo*, suggesting novel atheroprotective action of the small molecule inhibitor.

Finally, TIMP-1 elevation upon global MLN4924 application *in vivo* might have originated from inhibition of the neddylation and TIMP-mediated degradation. Namely, studies did identify that TIMP-1 is being recognised by FBXO22 adaptor of CRLs, that targets TIMP-1 and MMP-9 for a proteosome mediated degradation *in vitro* (J. Cheng et al., 2020; F. Guo et al., 2019).

The role of *Csn5* of the COP9 in endothelial cells *in vivo* hasn't been studied. Prior *in vitro* studies employing the *Csn5* siRNA mediated depletion have identified elicited NF-*κB* signalling in macrophages and ECs. Moreover, myeloid-*CSN5* loss induced MAPK-mediated *Abca1* expression in foam cell (Asare et al., 2013b; Azuma et al., 2009). Our *in vivo* study corroborates that *CSN5* in an early and advanced stage of atherosclerosis acts protectively via asserting its activity of the ECM factors.

### 5.3 Endothelial *Csn5* depletion downregulates the TIMP1 levels, while MLN4924 treatment up-regulates TIMP1 levels *in vitro*

*Csn5* and *Timp-1* are not direct protein interacting partners and have not been described previously to regulate each other (Grünwald et al., 2019). Evidence suggests that *CSN5* might regulate TIMP-1 gene expression, but the mechanism underneath remains deciphered.

*Csn5* siPOOL technology has enabled effective depletion of the *CSN5* in the mouse aortic endothelial cells, where indeed, gene expression of TIMP1 was lowering below 50%, compared to their scrambled mRNA control. The effects observed on gene expression levels are recapitulated on the TIMP-1 intracellular protein content and its secreted levels. Thus interestingly, these observations would reaffirm our *in vivo* observations found in mouse atherosclerotic lesions and TIMP-1 serum level depletion upon *Csn5* loss in an arterial-/endothelial manner.

*Timp-1* gene expression has been previously investigated *in vitro*. Its promoter was structurally homolog as it contains binding sites for AP-1 (c-Fos/c-Jun), Pea3, and SP-1 and LBP-1 TFs (Bahr et al., 1999). *Timp1* promoter AP-1 site binding site is found to be of high affinity for the cJun and JunD (Bahr et al., 1999; Smart et al., 2001). At the

same time, CSN5 has been described to bind c-Jun, in a complex-independent manner, whereby this interaction stands behind the control of several inflammatory pathways, as well as is being modulated by several inflammatory factors (Bianchi et al., 2000; Chamovitz & Segal, 2001; Claret et al., 1996; Kleemann et al., 2000). CSN interaction with the c-Jun results in c-Jun phosphorylation at its N-terminal serines -63 and 73, which overall induces stabilisation and elevation of its activity (Naumann et al., 1999). That suggests that this might be the missing link behind the TIMP-1 gene expression loss mechanism upon CSN5 depletion in ECs.

Next to the TIMP-1 being regulated by the AP-1 signalling, its expression is elicited by serum, growth factors, and cytokines (Gardner & Ghorpade, 2003; S.-Y. Guo et al., 2007). One of the positive regulators of the TIMP-1 gene expression is TGF $\beta$ , which is also an inducer of the AP-1 signalling under the disturbed blood flow in the ECs (Hall et al., 2003a; Uchida & Haas, 2014). Interestingly CSN5 promotes the increase of TGF- $\beta$  signalling by promoting the degradation of its inhibitor Smad7 (B.-C. Kim et al., 2004; Tian & Schiemann, 2009). Furthermore, positive regulators of TIMP-1 expression are Sp-1 and Smad2/3, which are also initiated upon the shear stress in ECs (Hall et al., 2003a; Uchida & Haas, 2014). Finally, CSN5 up-regulation was also shown to induce Smad2 phosphorylation and TGF- $\beta$ -signaling elevation (B.-C. Kim et al., 2004; Tian & Schiemann, 2009). Hence several candidate proteins are responsible for instigating TIMP-1 expression while being under the CSN5 regulation axis. Thus, signalling axes that might be responsible for CSN5-TIMP1 levels are Smad2 of TGF- $\beta$  and c-Jun of AP-1 signalling.

Once the c-Jun expression was evaluated, we could notice its trend-line down-regulation upon Csn5 and Timp-1 gene expression lowering.

Conversely, several studies on chronic inflammation have shown that upregulation of TIMP-1 is triggered via NF- $\kappa$ B, p50/p65 heterodimer activation, and TIMP-1/CD63 activation (Gong et al., 2015; Wilczynska et al., 2006). CSN is known to exert negative control over the NF- $\kappa$ B axis. On the one side, it prevents I $\kappa$ B $\alpha$  degradation by employing USP15 activity and consequently inhibits NF- $\kappa$ B (Schweitzer et al., 2007). Conversely, by regulating NF- $\kappa$ B through DEneddylation of SCF $\beta$ -TRCP1 directed proteasome degradation, CSN promotes NF- $\kappa$ B signalling (Cope & Deshaies, 2003; Schweitzer et al., 2007). Thereby consideration of, balancing all three signalling axes, AP-1, TGF $\beta$ , and NF- $\kappa$ B, must be carefully considered once evaluating the prospective outcome of this study. Moreover, MMP/TIMP - mediated proteolysis alterations have been considered, as it is the basis in pathological states such as adverse outcomes of atherosclerosis (Di Gregoli et al., 2016a). To further understand the signalling employed in ECs upon CSN5 depletion, other targets were considered, such as the matrix-remodeling players and another major inhibitor of matrix-metalloproteinases, Timp-2. Primarily, we could observe *Mmp9* gene expression elevation with the CSN5 loss in MAECs, while there was no response on the *Timp-2* or *Mmp2* gene expression levels compared to the screen control treatment.

To better understand this finding MMP promoters were considered. Namely, it is previously shown that several cytokines or growth factors can promote activation of the MMP promoters (Yan & Boyd, 2007). Compared to the rest of the MMPs, the MMP-9 promoter has specificity for an NF- $\kappa$ B-binding site that renders its expression (Mercurio & Manning, 1999; Yan & Boyd, 2007). As previously shown, siRNA Csn5 depletion elevates the NF- $\kappa$ B signalling (Asare et al., 2013b). Thus NF- $\kappa$ B elevation could at least partially stand behind the *MMP9* gene expression elevation.

*Mmp2* and its inhibitor *Timp2* strongly correlate gene expression under the inflammation (Nonino et al., 2021). Firstly, MMP2 lacks AP-1 responsive elements (De Clerck et al., 1994). Interestingly, TIMP-2 expression in atherosclerosis study on human

VSMCs, upon PDGF or TGF $\beta$  stimulation, is seemingly unaffected (Fabunmi et al., 1998). Moreover, TIMP-2 has been found to have several important cellular functions: it can indeed directly upregulate the transcriptional activity of NF- $\kappa$ B; it has a function to suppress the proliferation of endothelial cells; as well it negatively regulates atherosclerosis progression has been revealed (Di Gregoli et al., 2016b; Seo et al., 2003; J. Sun & Stetler-Stevenson, 2009). But hereby, we couldn't detect any alterations in its expression levels upon *Csn5* loss in mouse aortic endothelial cells, suggesting a stricter regulation mechanism and constitutive gene expression compared to the *Timp-1*.

Depletion of *Timp1* levels as a consequence of the *Csn5* loss in MAECs is hereby shown to have an impact on elevating the total MMP proteinase activity. It shows a particular enhancing activity of the MMP2 and MMP9 *in vitro*.

MMP2 induces ECD, and its plasma levels are elevated with atherosclerosis advancement. Also, high circulatory levels of MMP2 have been found in patients suffering from atherosclerotic plaque complications and less stable carotid artery atherosclerosis (Alvarez et al., 2004; J. Liu et al., 2003; Phatharajaree et al., 2007; Sluijter et al., 2006).

MMP9 is expressed in many atheroma-relevant cells, such as SMCs, ECs, and macrophages, and it has significantly higher activity in diseases arteries compared to the healthy tissues

(Galis et al., 1994; Galis & Khatri, 2002, 2002; Magid et al., 2003)

MMP-2 and -9 are next to their most well-described function in ECM remodelling, involved in the ECs and VSMCs proliferation (Newby, 2007).

Overall, the AP-1 axis, and its major player c-Jun, seemingly are destabilised upon *Csn5* depletion, and we have here found evidence of its direct causality in destabilising the *Timp1* gene expression. Moreover, loss of CSN5 favours conditions of TIMP-1 depletion, elevating MMP activity while not affecting the *Timp-2* expression and activity in mass *in vitro*. Thus, we suggest an athero-protective role of the COP9 signalosome as they deem an important missing link overlooked among the factors that combat the plaque vulnerability adversity.

To decipher if endothelial CSN5 acts as a part of the CSN holo complex or it's a complex-independent function of the CSN5, another complex subunit was investigated - CSN8. Previously, functions outside of the holo-complex, CSN subunits 2, 4, 7, and 8 to act independently have been reported (Abdullah et al., 2017; Fukumoto et al., 2005; Kato & Yoneda-Kato, 2009; Pacurar et al., 2017; Sharon et al., 2009). The *Csn8* subunit has been probed here as the least conserved cross-kingdom subunit and as a member of the PCI-containing subunits described alongside the CSN3 and CSN5 to be up-regulated with the atherosclerosis progression in the human endothelial lining (Asare et al., 2013). Moreover, its *Csn8* deficiency has been described to impair the CSN holo-complex formation and cullin deNEDDylation (H. Su, Li, Menon, et al., 2011). *Csn8*-/- mice developed cardiac hypertrophy, followed by the heart-failure and premature death. Thus, *Csn8* governs the cardiomyocyte survival (H. Su, Li, Menon, et al., 2011). Hence, the overall *Csn8* subunit is deemed important for cardiovascular health and was here investigated in ECs.

*Timp-1* mRNA levels declined with the *Csn8* gene-expression depletion in endothelial cells *in vitro*, suggesting the CSN holo-complex-dependent function in regulating its expression. Curiously, total MMP peptidase activity hasn't changed over the investigated time as previously observed, suggesting possible other mechanisms solely reserved for the CSN5 function might be involved in regulating the MMP activity regulation.

CSN5 functions are independent of the CSN complex and have been shown in HIF-1 $\alpha$  stabilisation independent of Cullin 2 deneddylation, also partially regarding its AP-1

stabilisation (Bemis et al., 2004). Thus possibly, hereby MMP activity might be partially affected via AP-1 directly inducing MMPs or via axis or HIF-1 $\alpha$  /VEGF cell signalling eliciting MMP9/MMP2 signalling as previously reported in hypoxic conditions (Benbow & Brinckerhoff, 1997; BERGMAN et al., 2003; Hashimoto et al., 2007; S. J. Kim et al., 2005; Misra et al., 2010).

*In vitro* evidence obtained from experiments performed on mouse aortic ECs (MAECs) suggest that the application of MLN4924, by mimicking CSN5 hyperactivity, lowers the inflammatory response *in vitro* and *in vivo* fields(Asare et al., 2013). The anti-atherogenic effect of small molecule inhibitor MLN4924 in ECs coincided with down-regulated NF- $\kappa$ B gene targets (Asare et al., 2013). Once the effects of MLN4924 were investigated in the model of mouse-bone marrow-derived macrophages, not all NF- $\kappa$ B gene targets were affected (Asare et al., 2017; Kanters et al., 2003). Thus, I questioned the signalling network behind the ECM-factors dysregulation under the endothelial-Csn5 loss and its overexpression.

Hereby, we have shown that by employing MLN4924, we could elevate the TIMP1 levels and its gene expression. as well as its secreted levels. While small-molecule inhibitors negatively impact the total MMP activity. Interestingly, while MMP2 activity was down-regulated, MMP9 was only trendline down-regulated.

Various factors enable enhancement of the expression of the MMPS, while their processing to their active form is enabled intracellularly by TIMPs. While AP-1, PEA3, and NF- $\kappa$ B transcriptional factors drive MPP9 gelatinase expression. MMP2 gene expression is more ‘constitutive’ and regulated by the Sp-1 TFs and AP-2 binding regulatory sites (Yan & Boyd, 2007).

A prior study shows that AP-1 and NF- $\kappa$ B TFs act together in MMP gene expression instigation (X. Wang & Khalil, 2018). Whereby NF- $\kappa$ B signalling decrease would inhibit MMPs upregulation and, hence, decrease matrix turnover *in vivo* (Chase et al., 2002). Conversely, another study suggests MMP-9 secretion in macrophages might be an NF- $\kappa$ B independent (X. Wang & Khalil, 2018). Thus, that might explain the absence of the MMP9 activity being unaltered upon the MLN4924 application.

Thus, MLN4924 has a strong anti-atherogenic effect in murine ECs by causing depletion of the total MMP activity and a significant decrease of the Mmp2 activity while elevating Timp-1 levels *in vitro*.

#### **5.4 Csn5 overexpression in mouse fibroblasts reveals the involvement of the MAPK and AP-1 signalling axis in controlling the levels of TIMP-1**

MLN4924 only partially mimics the CSN5 overexpression with having several off-target; thus, results obtained from its employment yield not a complete picture of the athero-protective effects of the COP9 signalosome. Hence, to fully understand the therapeutical value of MLN4924, the signalling mechanism under the CSN5 overexpression, and the athero-protective role of the CSN5, mouse fibroblasts (NIH/3T3) overexpressing CSN5 were used.

Namely, Csn5 overexpression has indeed triggered Timp-1 elevated gene expression. One of the possible culprits underneath the protein interaction was speculated to stand behind the AP-1 signalling axis.

c-Jun of AP-1 signalling is a prototypical prompt early gene. Upon stimulation of its expression, c-Jun is rapid and transient (Kayahara et al., 2005; Naumann et al., 1999). AP-1 signalling is regulated on two levels, either by extracellular stimuli (UV radiation, proinflammatory cytokines, growth factors) that can affect activity and protein levels as

well as its gene expression regulation or, on the other hand, by modulating its stability via a reduction in ubiquitination as well as post-translational modification (Angel et al., 1988; Fuchs et al., 1996; Karin et al., 1997; Musti et al., 1997; Treier et al., 1994). AP1-binding sites are essential for both Timp-1 and MMPs in response to the TGF- $\beta$  (Hall et al., 2003a). I have been curious about the AP-1 expression in the fibroblasts overexpressing CSN5 compared to their CSN5 constitutively expressing cells. I could observe that without TNF $\alpha$  stimulation, cell lines over-expressing the Csn5 have been shown to have positively up-regulated AP-1 signalling players c-Jun, JunB, as well as c-Fos. Upon TNF $\alpha$  stimulation, c-Jun and c-Fos were up-regulated, while the JunB gene didn't respond to the conditions of Csn5 overexpression. Prior findings demonstrated that AP1 factors necessary for the Timp-1 gene expression are c-Fos and c-Jun (Hall et al., 2003a). In these mouse fibroblasts, protein levels of Csn5/c-Jun/Timp-1 were, without stimulation, elevated upon CSN5 overexpression conditions.

To further evaluate if it is the role of the COP9 signalosome at stake, stabilising c-Jun and thus levels of tissue inhibitor of matrix-metalloproteinases, JNK signalling was blocked. That was considered as CSN5 acts in a dual-manner while regulating the c-Jun stability, JNK-dependent or CSN-dependent (JNK-independent) (Naumann et al., 1999). Thus, we excluded the JNK-mediated c-Jun activation, so we could report c-Jun/p-c-Jun being elevated upon CSN5 overexpression and the c-Fos. While JunB was only transiently affected upon TNF $\alpha$  stimulation.

MAPKs are known to exert a major role in c-Jun expression. Our results show that only by overexpressing CSN5 is there an effect on p-ERK1/2 being downregulated, while p-p38 was elevated and evaluated upon CSN5 overexpression, JNK signalling exclusion, and TNF $\alpha$  stimulation.

Prior studies show that MMP9 expression is being instigated upon ERK1/2 and p38 activation in human kidney (HK-2) cells, which was not so far verified in endothelial cells except here but might have similar mechanisms and regulation patterns (Nee et al., 2004). Similarly, in human hepatocarcinoma cells, activation of p38 MAPK signalling is responsible for the TIMP-1 overexpression and MMP-2 inhibition in these models (N. Wang et al., 2012). Thus, signalling that p-38/c-Jun mediated Timp-1 overexpression might stand behind the Csn5 athero-protective function.

Conversely, once mouse fibroblasts endogenously were experiencing loss of Csn5, Timp-1 levels could decrease. In contrast, curiously, overall c-Jun levels remained unchanged might imply that another AP-1 heterodimer plays a role in regulating Timp-1 gene expression.

In conclusion, we could observe in mouse fibroblasts that c-Jun and c-Fos of the AP-1 signalling complex stand in between Csn5, indirectly regulating the Timp-1 expression. Csn5 stabilises active c-Jun stabilises c-Jun by enabling its phosphorylation and impeding their degradation. That enables the environment to enable c-Jun elevated levels able to form homo- or heterodimers. Finally, with elevated active AP-1 levels, p-38 MAPK can exert their signalling and trigger AP-1 response.

## 5.5 The CSN holo-complex plays a role in regulating the levels of the TIMP1 via the AP-1 signalling axis and impacts atherosclerosis progression

In plants and mammals, the loss of any of the 8 subunits of the complex instigates the disassembly of the entire CSN holo-complex (X. Wang et al., 2002). Loss of Csn2, Csn3, Csn5, or Csn8 subunit of the COP9 signalosome is embryonically lethal (Lykke-Andersen et al., 2003; Menon et al., 2007; Sharon et al., 2009; Tomoda et al., 2004).

To investigate if the prior described phenotype of  $Csn5^{\Delta\text{arterial}} Apoe^{-/-}$  and  $Csn5^{\Delta\text{myeloid}} Apoe^{-/-}$  originated solely from *Csn5* loss, or the CSN holo-complex or other subunits such as *Csn8* do play a role as well.

Loss of the *CSN8* subunit in myeloid cells *in vivo* in an atherogenic *Apoe^{-/-}* mouse background has been performed here for the first time. *Csn8* expression in the cardiomyocytes enables protection against cardiac proteotoxicity, while its hylomorphism has caused adverse mouse cardiac problems and heart hypertrophy. Also, CSN8 might act on the transcriptional level (Abdullah et al., 2017; H. Su, Li, Ranek, et al., 2011). Firstly, our findings observe high levels of CSN8 in a lesion macrophage area of the *Apoe^{-/-}* mouse aortic roots after 10 weeks of HFD. Lesion size in the male aorta of  $Csn8^{\Delta\text{myeloid}} Apoe^{-/-}$  shows exacerbated atherosclerosis, with only the thoracic part unaffected. While interestingly, female aortas do show the same lesion content profile of aorta as males compared to the prior studies that showed no changes in aortic lesion size in female aortas upon myeloid *Csn5* loss, which didn't alter aortic lesions. On the other hand, aortic root lesions of the  $Csn8^{\Delta\text{myeloid}} Apoe^{-/-}$  did recapitulate the prior aggravated lesion size encountered in  $Csn5^{\Delta\text{arterial}} Apoe^{-/-}$  and  $Csn5^{\Delta\text{myeloid}} Apoe^{-/-}$ . While female  $Csn8^{\Delta\text{myeloid}} Apoe^{-/-}$  lesion size in aortic roots didn't show elevated lesion size compared to the  $Csn5^{\text{wt}} Apoe^{-/-}$ , control, as previously shown upon myeloid-specific *Csn5* loss (Asare et al., 2017).

Interestingly compared to the arterial-endothelial loss of *Csn5*,  $Csn8^{\Delta\text{myeloid}} Apoe^{-/-}$  male mice indeed experience loss of collagen content possibly because of *Timp-1* downregulation. As the necrotic core size is not overall affected in males upon CSN8 depletion and the cap thickness in male and female  $Csn8^{\Delta\text{myeloid}} Apoe^{-/-}$  mice after 12 weeks of HFD, elevation in vulnerability index in male mice haven't been observed. Interestingly myeloid-specific depletion of CSN8 has no effects on the SMC content, while it does exacerbate macrophage contents in the lesions. But *Csn8* myeloid deletion does have a lowering of the *Timp-1* levels in the male atherosclerotic plaque lesion and male circulatory *Timp-1* levels.

Interestingly total lymphocyte blood count has been shown initially to be declined upon myeloid *Csn8* loss. Still, the FACS analysis of the individual blood cell population revealed an elevation in T-cell count in the blood of mice upon myeloid-*Csn8* depletion, while B-cell count was unchanged.

In one prior study, CSN5 loss did affect the B-cell count (Sitte et al., 2012). Moreover, CSN5 loss was found to lower the proliferation of hematopoietic progenitors (Mori et al., 2008). Conversely, T-cell-derived *Csn8* deletion has been shown to negatively impact their survival and proliferation (Menon et al., 2007). But as the T- cells *Csn8* gene expression wasn't affected by the *LysMCre* expression, but rather by myeloid-derived *Csn8*, this phenotype remains to be elucidated.

To further the understanding, how does the CSN8 loss and, thus, CSN holo-complex disassembly affect the mouse BMDMs levels of CSN subunits. BMDMs from the  $Csn8^{\Delta\text{myeloid}} Apoe^{-/-}$  males were *in vitro* cultured and compared to their littermate controls  $Csn8^{\text{wt}} Apoe^{-/-}$ , after the 12 weeks of HFD while differentiated upon the L929 conditioned media.

What was firstly apparent is that myeloid loss of *Csn8* did affect the levels of *Csn5* gene expression decline. At the same time, CSN 1,4, and 6 were depleted on the gene expression with and without atherogenic stimulation. Interestingly, CSN3 was elevated upon the TNFa stimulation in  $Csn8^{\text{wt}} Apoe^{-/-}$ , BMDMs, which indeed affirms the recent report by Boro et al., regarding the role of the *Csn3* in atherogenic inflammation in macrophages (Boro et al., 2021). Moreover, CSN3 elevates the NF- $\kappa$ B nuclear localisation (Ba et al., 2017). Hence, I wanted to investigate if loss of PCI subunit *in vitro* influences the NF-KB signalling.

Upon CSN8 loss in BMDMs, NF- $\kappa$ B targeted genes were elevated. IL-6 expression was elevated without, while Ccl2 was elevated with the Tnfa stimulation, and accordingly, IkBa levels were less abundant with the myeloid- Csn8 loss. Firstly, the downregulation of the CSN holo-complex results in a persistent instigation of the NF- $\kappa$ B targeted genes (Schweitzer et al., 2007).

It is a consequence of loss in IkB- $\alpha$  levels, which have been previously reported to be depleted upon myeloid- Csn5 deletion in BMDMs in vitro (Asare et al., 2017). Hence in that way, NF- $\kappa$ B inhibitors, IkBs are being phosphorylated and subsequently ubiquitinated by CRLs to be finally degraded by the proteasome, as prior suggested by (K. Brown et al., 1995; Z. Chen et al., 1995; Rothwarf & Karin, 1999; Senftleben & Karin, 2002). Holo-complex participates in IkB $\alpha$  stability regulation by its CSN-associated deubiquitinase activity (Schweitzer et al., 2007).

Hence, by CSN holo-complex loss of function, removal of covalently attached ubiquitin-like Nedd8 modification is absolute. Thus, IkB $\alpha$  is targeted for proteasome degradation, shown here to elevate atherogenic inflammation and NF- $\kappa$ B regulated gene expression. Overall, that, in turn, does lead to the aggravation of the *Csn8*<sup>Δmyeloid</sup>*Apoe*<sup>-/-</sup> atherosclerosis and disturbs the homeostasis of ECM regulators, such as TIMP-1, but doesn't affect their vulnerability, suggesting a more profoundly function of the endothelial CSN holo-complex role in determining the adverse effects of atherosclerosis. In vivo study employing the endothelial-Csn8 loss would be deemed necessary in deciphering the role of the holo-complex in atherosclerotic plaque stability.

## 5.6 Human atherosclerosis and atherogenic inflammation in endothelial cells show that Timp1 levels determine plaque stability

The pathology of atherosclerosis development in humans is a multi-factorial complex disease, which leads to immunometabolism dysregulation and clinical outcomes, which can only be partially mimicked in animal models.

One of the major differences does reside in the core driver underlining atherosclerosis development, lipoprotein metabolisms, as mice are rich in HDL-mediated cholesterol particles, while humans are LDL cholesterol-enriched. This is partially compensated by employing genetic manipulation (*Apoe*<sup>-/-</sup> mice) and 'humanised diets', such as Western-type of diet, but indeed atherosclerotic lesion development between humans and mice in their entirety is different. Namely, humans are more prone to develop atherosclerotic lesions in their coronary artery and carotid arteries. At the same time, mice mainly generate lesions in the aortic root, aortic arch, and brachiocephalic aorta. Another major point of this study was that mice do not develop larger fibrous atheromas or unstable lesions (Breslow, 1996). Hence, herby I aimed to investigate if, indeed, observed phenotype upon endothelial/myeloid Csn5/Csn8 loss in atherogenic mice could be verified on human carotid endarterectomy (CEA), that was pre-profiled on their stability and gender sorted by the Munich Vascular Biobank (Department of Vascular Surgery, Technical University Munich, Germany). These CEAs were morphologically graded by the Atherosclerosis Council of the American Heart Association classification; their vulnerability was analysed under the previous report by Redgrave and his team (Redgrave et al., 2008; Stary et al., 1995). Whereby only male atherosclerotic plaques were used based on the study conducted here.

Factors of extracellular remodelling, TIMP-1s/MMPs function in atherosclerosis remains elusive, and plenty of studies have been conducted on deciphering and

understanding its predictability as a biomarker in human atherosclerosis. On the other hand, CSN5 is heavily elevated in advanced human stages of atherosclerosis, while its role instability hasn't been investigated so far (Asare et al., 2013).

Hereby in vivo expression of TIMP1 with plaque stability was analysed in CEAs lesions and its mRNA total expression in the lesion was evaluated. I could conclude that total TIMP-1 levels in atherosclerotic lesions varied depending on their stability and only upon splitting the zones of the lesions depending on the TIMP1 severity of expressions (TIMP1: negative, low positive, positive, and high positive) as previously described, could I detect the differences in its expression in lesions.

Mainly expression of TIMP-1 could be seen in the necrotic core area of advanced human atherosclerotic lesions. In contrast, the TIMP-1+ area was absent in the fibrous cap and sub- and endothelial lining areas. TIMP-1 expression was also present in the plaque shoulder regions, where macrophage-like cells expressed it abundance in the advanced lesions. The prior study does indeed observe MMP and TIMP-1 abundantly expressed in the macrophage-rich area in regions prone to rupture and in areas surrounding the lipid core (Orbe et al., 2003). Moreover, TIMP-1 levels in lesions were quantified by an automated separation of the positive regions for its expression. Reveals that only in high-positive and positive TIMP-1 regions of the unstable plaques found lower TIMP-1 expression than the stable plaques. In contrast, the stable plaques had higher or less significantly different TIMP1 content than the healthy plaques. Yet another prior study does indeed as well report on TIMP-1 concentration being more elevated in healthy tissue compared to the atherosclerotic plaques in human patients. Hence the observed phenotype falls into those lines (V Baroncini et al., 2011). Conversely, once the TIMP-1 mRNA expression was evaluated in these total CEAs lesions, mRNA expression of TIMP-1 was higher, while CSN5 gene expression was not significantly changing. Thus, I could conclude that overall TIMP-1 expression in vivo is seemingly lower in unstable compared to the stable plaques, while its gene expression doesn't confirm this.

To confirm if the endothelial-specific CSN5 loss does impact TIMP-1 via modulating the c-JUN axis, HAOECs were employed. Indeed, upon CSN5 gene expression depletion in HAOECs, TIMP-1 levels were significantly lowered together with the c-JUN levels, while on the other hand, TIMP-1 levels with the MLN4924 treatment were significantly elevated. Prior studies do show that exacerbated TIMP-1 levels reduce atheropprogression in mice. Hence possibly, MLN4924 could act in impeding atherosclerosis by elevating TIMP-1 levels (Rouis et al., 1999).

MMP2 and MMP9 gene expression was evaluated, and CSN5 loss does not impact MMP2 gene expression on HAOECs. On the other side, MMP9 expression in HAOECs was surprisingly downregulated. Conversely, CSN5 overexpression mimics by employing the neddylation inhibitor MLN4924 have revealed no effects on the MMP9 expression, while MMP2 was slightly elevated.

MMP9 activity was elevated upon CSN5 loss, while the MLN4924 silenced it in human aortic endothelial cells. There were no effects upon MMP2 activity changes with the Csn5 loss or Csn5 "overexpression mimics". Interestingly, while CSN5 depletion did cause total MMP activity eliciting shift, no changes in their activity were observed upon MLN4924 application. Thus, possibly implying that MLN4924 might impact other MMPs in HAOECs.

Markers of vulnerable lesions are set in the disbalance between the MMPs and TIMPs (Sapienza et al., 2005).

Prior studies on human atheropprogression demonstrate that MMP-9 might be a suitable marker for unstable lesions (Loftus et al., 2000; Peeters et al., 2011). Elevated circulatory MMP2 levels in human atheropprogression have been associated with the

adverse effects of the disease, but it has been reported to be more a trait of stable lesions and/or early lesions (Alvarez et al., 2004; Choudhary et al., 2006; Z. Li et al., 1996; Sluijter et al., 2006). Moreover, MMP-2 and -9 levels are considered to be a good indicator of therapy success and identifying patients that would gain from the therapy.

Activation of endothelial MMP-2 can induce endothelial dysfunction and its disintegration (Carmona-Rivera et al., 2015; Olejarz et al., 2020).

Finally, we could confirm that Timp1 expressed in human carotid endarterectomy lesions is lowered with the plaque being more unstable. In the endothelial cells- Csn5 depletion, Timp1 levels were also impaired, as well as the AP-1 signalling axis. That overall suggests that endothelial cells do indeed control the TIMP/MMP balance in human patients, and possibly its homeostasis is controlled by the COP9 signalosome.

## 6. Conclusion

Our findings hereby provide a first mechanistic overview of how depletion of one of the arterial-endothelial derived COP9 subunits, CSN5, through regulating factors of the extracellular matrix-remodelling system (ECM) exert a pivotal role in favouring the rupture-prone atherosclerotic plaques *in vivo*.

Mouse and human arterial-endothelial CSN5 depletion down-regulates the TIMP-1 levels, and favour pronounced MMP enzymatic activity via destabilised AP-1 signalling axis. On the other hand, our studies show that employing the selective pharmacological inhibitor of NEDDylation, MLN4924, thus mimicking the CSN5 overexpression, inhibits early murine atherosclerotic lesion progression *in vivo*. We could also observe athero-protective effects extending on human and mouse aortic endothelial cells upon MLN4924 application via downregulated total matrix-metalloproteinase enzymatic activity and elevated Timp1 levels *in vitro*. Our data confirms as well that Csn5 overexpression *in vitro* could equally trigger the Timp1 elevation via AP-1 signalling, hence ‘mirroring’ the MLN4924 conditioned Csn5 overexpression ‘mimics’ *in vitro*.

Furthermore, we could establish the importance of the role of COP9 in the negative regulation of atherosclerosis progression by removing yet another subunit of the holo-complex in myeloid cells, Csn8. We could observe the role of the COP9 complex in stabilising the AP-1 signalling axis and ECMs in macrophages and endothelial cells *in vitro*. Destabilised CSN holo-complex plays a role in atheroprogression and more pronounced atherosclerosis but not the vulnerability of the plaques.

Finally, we provide evidence that the Timp1 levels in lesions differ in advanced stages of human atherosclerosis, with Timp1 positive areas being more elevated in stable and, conversely, depleted in unstable plaques compared to the healthy plaques, which was not reflected in their mRNA levels. Therefore, overall showing that the COP9 signalosome acts as one of the ‘decisive points’ in regulating the clinical apparentness of atherosclerosis, the vulnerability of the plaques.

## References

Aarup, A., Pedersen, T. X., Junker, N., Christoffersen, C., Bartels, E. D., Madsen, M., Nielsen, C. H., & Nielsen, L. B. (2016). Hypoxia-Inducible Factor-1 $\alpha$  Expression in Macrophages Promotes Development of Atherosclerosis. *Arteriosclerosis, Thrombosis, and Vascular Biology*, 36(9), 1782–1790. <https://doi.org/10.1161/ATVBAHA.116.307830>

Abdullah, A., Eyster, K. M., Bjordahl, T., Xiao, P., Zeng, E., & Wang, X. (2017). Murine Myocardial Transcriptome Analysis Reveals a Critical Role of COPS8 in the Gene Expression of Cullin-RING Ligase Substrate Receptors and Redox and Vesicle Trafficking Pathways. *Frontiers in Physiology*, 8, 594. <https://doi.org/10.3389/fphys.2017.00594>

Ai, T.-J., Sun, J.-Y., Du, L.-J., Shi, C., Li, C., Sun, X.-N., Liu, Y., Li, L., Xia, Z., Jia, L., Liu, J., & Duan, S.-Z. (2018). Inhibition of neddylation by MLN4924 improves neointimal hyperplasia and promotes apoptosis of vascular smooth muscle cells through p53 and p62. *Cell Death & Differentiation*, 25(2), 319–329. <https://doi.org/10.1038/cdd.2017.160>

Aiello, R. J., Bourassa, P. A., Lindsey, S., Weng, W., Natoli, E., Rollins, B. J., & Milos, P. M. (1999). Monocyte chemoattractant protein-1 accelerates atherosclerosis in apolipoprotein E-deficient mice. *Arteriosclerosis, Thrombosis, and Vascular Biology*, 19(6), 1518–1525. <https://doi.org/10.1161/01.atv.19.6.1518>

Aird, W. C. (2007). Phenotypic heterogeneity of the endothelium: I. Structure, function, and mechanisms. *Circulation Research*, 100(2), 158–173. <https://doi.org/10.1161/01.RES.0000255691.76142.4a>

Alique, M., Luna, C., Carracedo, J., & Ramírez, R. (2015). LDL biochemical modifications: A link between atherosclerosis and aging. *Food & Nutrition Research*, 59, 10.3402/fnr.v59.29240. <https://doi.org/10.3402/fnr.v59.29240>

Allahverdian, S., Chehroudi, A. C., McManus, B. M., Abraham, T., & Francis, G. A. (2014). Contribution of Intimal Smooth Muscle Cells to Cholesterol Accumulation and Macrophage-Like Cells in Human Atherosclerosis. *Circulation*, 129(15), 1551–1559. <https://doi.org/10.1161/CIRCULATIONAHA.113.005015>

Alon, R., & Shulman, Z. (2011). Chemokine triggered integrin activation and actin remodeling events guiding lymphocyte migration across vascular barriers. *Experimental Cell Research*, 317(5), 632–641. <https://doi.org/10.1016/j.yexcr.2010.12.007>

Alvarez, B., Ruiz, C., Chacón, P., Alvarez-Sabin, J., & Matas, M. (2004). Serum values of metalloproteinase-2 and metalloproteinase-9 as related to unstable plaque and inflammatory cells in patients with greater than 70% carotid artery stenosis. *Journal of Vascular Surgery*, 40(3), 469–475. <https://doi.org/10.1016/j.jvs.2004.06.023>

Amin, M., Pushpakumar, S., Muradashvili, N., Kundu, S., Tyagi, S. C., & Sen, U. (2016). Regulation and involvement of matrix metalloproteinases in vascular diseases. *Frontiers in Bioscience (Landmark Edition)*, 21, 89–118. <https://doi.org/10.2741/4378>

Amini, N., Boyle, J. J., Moers, B., Warboys, C. M., Malik, T. H., Zakkar, M., Francis, S. E., Mason, J. C., Haskard, D. O., & Evans, P. C. (2014). Requirement of JNK1 for endothelial cell injury in atherosgenesis. *Atherosclerosis*, 235(2), 613–618. <https://doi.org/10.1016/j.atherosclerosis.2014.05.950>

Ancuta, P., Rao, R., Moses, A., Mehle, A., Shaw, S. K., Luscinskas, F. W., & Gabuzda, D. (2003). Fractalkine preferentially mediates arrest and migration of CD16 $+$  monocytes. *The Journal of Experimental Medicine*, 197(12), 1701–1707. <https://doi.org/10.1084/jem.20022156>

Andreeva, E. R., Pugach, I. M., & Orekhov, A. N. (1997). Subendothelial smooth muscle cells of human aorta express macrophage antigen in situ and in vitro. *Atherosclerosis*, 135(1), 19–27. [https://doi.org/10.1016/s0021-9150\(97\)00136-6](https://doi.org/10.1016/s0021-9150(97)00136-6)

Angel, P., Hattori, K., Smeal, T., & Karin, M. (1988). The jun proto-oncogene is positively autoregulated by its product, Jun/AP-1. *Cell*, 55(5), 875–885. [https://doi.org/10.1016/0092-8674\(88\)90143-2](https://doi.org/10.1016/0092-8674(88)90143-2)

Anstensrud, A. K., Woxholt, S., Sharma, K., Broch, K., Bendz, B., Aakhus, S., Ueland, T., Amundsen, B. H., Damås, J. K., Hopp, E., Kleveland, O., Stensæth, K. H., Opdahl, A., Kløw, N.-E., Seljeflot, I., Andersen, G. Ø., Wiseth, R., Aukrust, P., & Gullestad, L. (2019). Rationale for the ASSAIL-MI-trial: A randomised controlled trial designed to assess the effect of tocilizumab on myocardial salvage in patients with acute ST-elevation myocardial infarction (STEMI). *Open Heart*, 6(2), e001108. <https://doi.org/10.1136/openhrt-2019-001108>

Arbel, Y., Abuzeid, W., Rosenson, R. S., Weisman, A., & Farkouh, M. E. (2018). Old Drugs for New Indications in Cardiovascular Medicine. *Cardiovascular Drugs and Therapy*, 32(2), 223–232. <https://doi.org/10.1007/s10557-018-6785-y>

Armstrong, M. L., Heistad, D. D., Megan, M. B., Lopez, J. A., & Harrison, D. G. (1990). Reversibility of atherosclerosis. *Cardiovascular Clinics*, 20(3), 113–126.

Asare, Y., Ommer, M., Azombo, F. A., Alampour-Rajabi, S., Sternkopf, M., Sanati, M., Gijbels, M. J., Schmitz, C., Sinitski, D., Tilstam, P. V., Lue, H., Gessner, A., Lange, D., Schmid, J. A., Weber, C., Dichgans, M., Jankowski, J., Pardi, R., Winther, M. P. J. de, ... Bernhagen, J. (2017). Inhibition of atherogenesis by the COP9 signalosome subunit 5 in vivo. *Proceedings of the National Academy of Sciences*, 114(13), E2766–E2775.  
<https://doi.org/10.1073/pnas.1618411114>

Asare, Y., Shagdarsuren, E., Schmid, J. A., Tilstam, P. V., Grommes, J., El Bounkari, O., Schütz, A. K., Weber, C., de Winther, M. P. J., Noels, H., & Bernhagen, J. (2013a). Endothelial CSN5 impairs NF-κB activation and monocyte adhesion to endothelial cells and is highly expressed in human atherosclerotic lesions. *Thrombosis and Haemostasis*, 110(1), 141–152.  
<https://doi.org/10.1160/TH13-02-0155>

Asare, Y., Shagdarsuren, E., Schmid, J., Tilstam, P., Grommes, J., El Bounkari, O., Schütz, A., Weber, C., de Winther, M., Noels, H., & Bernhagen, J. (2013b). Endothelial CSN5 impairs NF-κB activation and monocyte adhesion to endothelial cells and is highly expressed in human atherosclerotic lesions. *Thrombosis and Haemostasis*, 110(07), 141–152.  
<https://doi.org/10.1160/TH13-02-0155>

Autieri, M. V., Yue, T. L., Ferstein, G. Z., & Ohlstein, E. (1995). Antisense oligonucleotides to the p65 subunit of NF-κB inhibit human vascular smooth muscle cell adherence and proliferation and prevent neointima formation in rat carotid arteries. *Biochemical and Biophysical Research Communications*, 213(3), 827–836. <https://doi.org/10.1006/bbrc.1995.2204>

Aw, N. H., Canetti, E., Suzuki, K., & Goh, J. (2018). Monocyte Subsets in Atherosclerosis and Modification with Exercise in Humans. *Antioxidants*, 7(12), 196.  
<https://doi.org/10.3390/antiox7120196>

Azuma, Y., Takada, M., Maeda, M., Kioka, N., & Ueda, K. (2009). The COP9 signalosome controls ubiquitinylation of ABCA1. *Biochemical and Biophysical Research Communications*, 382(1), 145–148. <https://doi.org/10.1016/j.bbrc.2009.02.161>

Ba, M. A., Surina, J., Singer, C. A., & Valencik, M. L. (2017). Knockdown of subunit 3 of the COP9 signalosome inhibits C2C12 myoblast differentiation via NF-KappaB signaling pathway. *BMC Pharmacology and Toxicology*, 18(1), 47. <https://doi.org/10.1186/s40360-017-0154-5>

Bäck, M., Yurdagul, A., Tabas, I., Öörni, K., & Kovanen, P. T. (2019). Inflammation and its resolution in atherosclerosis: Mediators and therapeutic opportunities. *Nature Reviews Cardiology*.  
<https://doi.org/10.1038/s41569-019-0169-2>

Bahr, M. J., Vincent, K. J., Arthur, M. J. P., Fowler, A. V., Smart, D. E., Wright, M. C., Clark, I. M., Benyon, R. C., Iredale, J. P., & Mann, D. A. (1999). Control of the tissue inhibitor of metalloproteinases-1 promoter in culture-activated rat hepatic stellate cells: Regulation by activator protein-1 DNA binding proteins. *Hepatology*, 29(3), 839–848.  
<https://doi.org/10.1002/hep.510290333>

Baker, A. H., Edwards, D. R., & Murphy, G. (2002). Metalloproteinase inhibitors: Biological actions and therapeutic opportunities. *Journal of Cell Science*, 115(Pt 19), 3719–3727.  
<https://doi.org/10.1242/jcs.00063>

Baldassare, J. J., Bi, Y., & Bellone, C. J. (1999). The role of p38 mitogen-activated protein kinase in IL-1 beta transcription. *Journal of Immunology (Baltimore, Md.: 1950)*, 162(9), 5367–5373.

Banda, N. K., Guthridge, C., Sheppard, D., Cairns, K. S., Muggli, M., Bech-Otschir, D., Dubiel, W., & Arend, W. P. (2005). Intracellular IL-1 receptor antagonist type 1 inhibits IL-1-induced cytokine production in keratinocytes through binding to the third component of the COP9 signalosome. *Journal of Immunology (Baltimore, Md.: 1950)*, 174(6), 3608–3616.  
<https://doi.org/10.4049/jimmunol.174.6.3608>

Barreiro, O., Yanez-Mo, M., Serrador, J. M., Montoya, M. C., Vicente-Manzanares, M., Tejedor, R., Furthmayr, H., & Sanchez-Madrid, F. (2002). Dynamic interaction of VCAM-1 and ICAM-1 with moesin and ezrin in a novel endothelial docking structure for adherent leukocytes. *The Journal of Cell Biology*, 157(7), 1233–1245. <https://doi.org/10.1083/jcb.200112126>

Bauer, E. A., Stricklin, G. P., Jeffrey, J. J., & Eisen, A. Z. (1975). Collagenase production by human skin fibroblasts. *Biochemical and Biophysical Research Communications*, 64(1), 232–240.  
[https://doi.org/10.1016/0006-291X\(75\)90243-0](https://doi.org/10.1016/0006-291X(75)90243-0)

Belge, K.-U., Dayyani, F., Horelt, A., Siedlar, M., Frankenberger, M., Frankenberger, B., Espenvik, T., & Ziegler-Heitbrock, L. (2002). The proinflammatory CD14+CD16+DR++ monocytes are a major source of TNF. *Journal of Immunology (Baltimore, Md.: 1950)*, 168(7), 3536–3542.  
<https://doi.org/10.4049/jimmunol.168.7.3536>

Belkhiri, A., Richards, C., Whaley, M., McQueen, S. A., & Orr, F. W. (1997). Increased expression of activated matrix metalloproteinase-2 by human endothelial cells after sublethal H<sub>2</sub>O<sub>2</sub> exposure. *Laboratory Investigation; a Journal of Technical Methods and Pathology*, 77(5), 533–539.

Bemis, L., Chan, D. A., Finkielstein, C. V., Qi, L., Sutphin, P. D., Chen, X., Stenmark, K., Giaccia, A. J., & Zundel, W. (2004). Distinct aerobic and hypoxic mechanisms of HIF- $\alpha$  regulation by CSN5. *Genes & Development*, 18(7), 739–744. <https://doi.org/10.1101/gad.1180104>

Benbow, U., & Brinckerhoff, C. E. (1997). The AP-1 site and MMP gene regulation: What is all the fuss about? *Matrix Biology: Journal of the International Society for Matrix Biology*, 15(8–9), 519–526. [https://doi.org/10.1016/s0945-053x\(97\)90026-3](https://doi.org/10.1016/s0945-053x(97)90026-3)

Bennett, M. R., Sinha, S., & Owens, G. K. (2016). Vascular smooth muscle cells in atherosclerosis. *Circulation Research*, 118(4), 692–702. <https://doi.org/10.1161/CIRCRESAHA.115.306361>

Bentzon, J. F., Otsuka, F., Virmani, R., & Falk, E. (2014). Mechanisms of plaque formation and rupture. *Circulation Research*, 114(12), 1852–1866. <https://doi.org/10.1161/CIRCRESAHA.114.302721>

Berg, K. E., Ljungcrantz, I., Andersson, L., Bryngelsson, C., Hedblad, B., Fredrikson, G. N., Nilsson, J., & Björkbacka, H. (2012). Elevated CD14++CD16- monocytes predict cardiovascular events. *Circulation. Cardiovascular Genetics*, 5(1), 122–131. <https://doi.org/10.1161/CIRCGENETICS.111.960385>

BERGMAN, M. R., CHENG, S., HONBO, N., PIACENTINI, L., KARLINER, J. S., & LOVETT, D. H. (2003). A functional activating protein 1 (AP-1) site regulates matrix metalloproteinase 2 (MMP-2) transcription by cardiac cells through interactions with JunB-Fra1 and JunB-FosB heterodimers. *Biochemical Journal*, 369(3), 485–496. <https://doi.org/10.1042/bj20020707>

Berndsen, C. E., & Wolberger, C. (2014). New insights into ubiquitin E3 ligase mechanism. *Nature Structural & Molecular Biology*, 21(4), 301–307. <https://doi.org/10.1038/nsmb.2780>

Best, S., Lam, V., Liu, T., Bruss, N., Kittai, A., Danilova, O. V., Murray, S., Berger, A., Pennock, N. D., Lind, E. F., & Danilov, A. V. (2021). Immunomodulatory effects of pevonedistat, a NEDD8-activating enzyme inhibitor, in chronic lymphocytic leukemia-derived T cells. *Leukemia*, 35(1), 156–168. <https://doi.org/10.1038/s41375-020-0794-0>

Bevilacqua, M. P., Pober, J. S., Wheeler, M. E., Cotran, R. S., & Gimbrone, M. A. (1985). Interleukin-1 activation of vascular endothelium. Effects on procoagulant activity and leukocyte adhesion. *The American Journal of Pathology*, 121(3), 394–403.

Bi, Y., Chen, J., Hu, F., Liu, J., Li, M., & Zhao, L. (2019). M2 Macrophages as a Potential Target for Antiatherosclerosis Treatment. *Neural Plasticity*, 2019, 6724903. <https://doi.org/10.1155/2019/6724903>

Bianchi, E., Denti, S., Catena, R., Rossetti, G., Polo, S., Gasparian, S., Putignano, S., Rogge, L., & Pardi, R. (2003). Characterization of human constitutive photomorphogenesis protein 1, a RING finger ubiquitin ligase that interacts with Jun transcription factors and modulates their transcriptional activity. *The Journal of Biological Chemistry*, 278(22), 19682–19690. <https://doi.org/10.1074/jbc.M212681200>

Bianchi, E., Denti, S., Granata, A., Bossi, G., Gegginat, J., Villa, A., Rogge, L., & Pardi, R. (2000). Integrin LFA-1 interacts with the transcriptional co-activator JAB1 to modulate AP-1 activity. *Nature*, 404(6778), 617–621. <https://doi.org/10.1038/35007098>

Birkedal-Hansen, H., Moore, W. G., Bodden, M. K., Windsor, L. J., Birkedal-Hansen, B., DeCarlo, A., & Engler, J. A. (1993). Matrix metalloproteinases: A review. *Critical Reviews in Oral Biology and Medicine: An Official Publication of the American Association of Oral Biologists*, 4(2), 197–250. <https://doi.org/10.1177/10454411930040020401>

Bobryshev, Y. V., Ivanova, E. A., Chistiakov, D. A., Nikiforov, N. G., & Orekhov, A. N. (2016). Macrophages and Their Role in Atherosclerosis: Pathophysiology and Transcriptome Analysis. *BioMed Research International*, 2016, 9582430. <https://doi.org/10.1155/2016/9582430>

Bobryshev, Y. V., & Lord, R. S. (1995). Ultrastructural recognition of cells with dendritic cell morphology in human aortic intima. Contacting interactions of Vascular Dendritic Cells in athero-resistant and athero-prone areas of the normal aorta. *Archives of Histology and Cytology*, 58(3), 307–322. <https://doi.org/10.1679/aohc.58.307>

Bohula, E. A., Giugliano, R. P., Cannon, C. P., Zhou, J., Murphy, S. A., White, J. A., Tershakovec, A. M., Blazing, M. A., & Braunwald, E. (2015). Achievement of Dual Low-Density Lipoprotein Cholesterol and High-Sensitivity C-Reactive Protein Targets More Frequent With the Addition of Ezetimibe to Simvastatin and Associated With Better Outcomes in IMPROVE-IT. *Circulation*, 132(13), 1224–1233. <https://doi.org/10.1161/CIRCULATIONAHA.115.018381>

Bond, M., Fabunmi, R. P., Baker, A. H., & Newby, A. C. (1998). Synergistic upregulation of metalloproteinase-9 by growth factors and inflammatory cytokines: An absolute requirement for transcription factor NF- $\kappa$ B. *FEBS Letters*, 435(1), 29–34. [https://doi.org/10.1016/s0014-5793\(98\)01034-5](https://doi.org/10.1016/s0014-5793(98)01034-5)

Bonizzi, G., & Karin, M. (2004). The two NF-kappaB activation pathways and their role in innate and adaptive immunity. *Trends in Immunology*, 25(6), 280–288. <https://doi.org/10.1016/j.it.2004.03.008>

Bonomini, F., Favero, G., & Rezzani, R. (2015). NF- $\kappa$ B — A Key Factor in Atherogenesis and Atheropprogression. In *Thrombosis, Atherosclerosis and Atherothrombosis—New Insights and Experimental Protocols*. IntechOpen. <https://doi.org/10.5772/61894>

Boro, M., Govatati, S., Kumar, R., Singh, N. K., Pichavaram, P., Taylor, J. G., Orr, A. W., & Rao, G. N. (2021). Thrombin-Par1 signaling axis disrupts COP9 signalosome subunit 3-mediated ABCA1 stabilization in inducing foam cell formation and atherogenesis. *Cell Death & Differentiation*, 28(2), 780–798. <https://doi.org/10.1038/s41418-020-00623-9>

Boucherat, O., Bourbon, J. R., Barlier-Mur, A.-M., Chailley-Heu, B., D'ortho, M.-P., & Delacourt, C. (2007). Differential Expression of Matrix Metalloproteinases and Inhibitors in Developing Rat Lung Mesenchymal and Epithelial Cells. *Pediatric Research*, 62(1), 20–25. <https://doi.org/10.1203/PDR.0b013e3180686cc5>

Bouday, G., Fitau, J., Coupel, S., Soulillou, J.-P., & Charreau, B. (2004). Exogenous Tissue Inhibitor of Metalloproteinase-1 Promotes Endothelial Cell Survival Through Activation of the Phosphatidylinositol 3-Kinase/Akt Pathway. *Annals of the New York Academy of Sciences*, 1030(1), 28–36. <https://doi.org/10.1196/annals.1329.004>

Bounkari, O. E., Zan, C., Wagner, J., Bugar, E., Bourilhon, P., Kontos, C., Zarwel, M., Sinitski, D., Milic, J., Jansen, Y., Kempf, W. E., Mägdefessel, L., Hoffmann, A., Brandhofer, M., Bucala, R., Megens, R. T. A., Weber, C., Kapurniotu, A., & Bernhagen, J. (2021). *MIF-2/D-DT is an atypical atherogenic chemokine that promotes advanced atherosclerosis and hepatic lipogenesis* (p. 2021.12.28.474328). <https://doi.org/10.1101/2021.12.28.474328>

Boyle, J. J., Weissberg, P. L., & Bennett, M. R. (2002). Human Macrophage-Induced Vascular Smooth Muscle Cell Apoptosis Requires NO Enhancement of Fas/Fas-L Interactions. *Arteriosclerosis, Thrombosis, and Vascular Biology*, 22(10), 1624–1630. <https://doi.org/10.1161/01.ATV.0000033517.48444.1A>

Brach, M. A., Henschler, R., Mertelsmann, R. H., & Herrmann, F. (1991). Regulation of M-CSF expression by M-CSF: Role of protein kinase C and transcription factor NF kappa B. *Pathobiology: Journal of Immunopathology, Molecular and Cellular Biology*, 59(4), 284–288. <https://doi.org/10.1159/000163664>

Breitenstein, A., Akhmedov, A., Camici, G. G., Lüscher, T. F., & Tanner, F. C. (2013). P27(Kip1) inhibits tissue factor expression. *Biochemical and Biophysical Research Communications*, 439(4), 559–563. <https://doi.org/10.1016/j.bbrc.2013.09.002>

Breslow, J. L. (1996). Mouse Models of Atherosclerosis. *Science*. <https://doi.org/10.1126/science.272.5262.685>

Breviario, F., d'Aniello, E. M., Golay, J., Peri, G., Bottazzi, B., Bairoch, A., Saccone, S., Marzella, R., Predazzi, V., & Rocchi, M. (1992). Interleukin-1-inducible genes in endothelial cells. Cloning of a new gene related to C-reactive protein and serum amyloid P component. *Journal of Biological Chemistry*, 267(31), 22190–22197. [https://doi.org/10.1016/S0021-9258\(18\)41653-5](https://doi.org/10.1016/S0021-9258(18)41653-5)

Brew, K., & Nagase, H. (2010). The tissue inhibitors of metalloproteinases (TIMPs): An ancient family with structural and functional diversity. *Biochimica Et Biophysica Acta*, 1803(1), 55–71. <https://doi.org/10.1016/j.bbamcr.2010.01.003>

Brown, B. A., Williams, H., & George, S. J. (2017). Evidence for the Involvement of Matrix-Degrading Metalloproteinases (MMPs) in Atherosclerosis. *Progress in Molecular Biology and Translational Science*, 147, 197–237. <https://doi.org/10.1016/bs.pmbts.2017.01.004>

Brown, K., Gerstberger, S., Carlson, L., Franzoso, G., & Siebenlist, U. (1995). Control of I kappa B-alpha proteolysis by site-specific, signal-induced phosphorylation. *Science (New York, N.Y.)*, 267(5203), 1485–1488. <https://doi.org/10.1126/science.7878466>

Bruck, B., Brehme, U., Gugel, N., Hanke, S., Finking, G., Lutz, C., Benda, N., Schmahl, F. W., Haasis, R., & Hanke, H. (1997). Gender-Specific Differences in the Effects of Testosterone and Estrogen on the Development of Atherosclerosis in Rabbits. *Arteriosclerosis, Thrombosis, and Vascular Biology*, 17(10), 2192–2199. <https://doi.org/10.1161/01.ATV.17.10.2192>

Burke, A. P., Farb, A., Malcom, G. T., Liang, Y. H., Smialek, J., & Virmani, R. (1997). Coronary risk factors and plaque morphology in men with coronary disease who died suddenly. *The New England Journal of Medicine*, 336(18), 1276–1282. <https://doi.org/10.1056/NEJM199705013361802>

Burke, A. P., Kolodgie, F. D., Farb, A., Weber, D. K., Malcom, G. T., Smialek, J., & Virmani, R. (2001). Healed plaque ruptures and sudden coronary death: Evidence that subclinical rupture has a role in plaque progression. *Circulation*, 103(7), 934–940. <https://doi.org/10.1161/01.cir.103.7.934>

Burleigh, M. E., Babaev, V. R., Oates, J. A., Harris, R. C., Gautam, S., Riendeau, D., Marnett, L. J., Morrow, J. D., Fazio, S., & Linton, M. F. (2002). Cyclooxygenase-2 Promotes Early

Atherosclerotic Lesion Formation in LDL Receptor–Deficient Mice. *Circulation*, 105(15), 1816–1823. <https://doi.org/10.1161/01.CIR.0000014927.74465.7F>

Busch, S., Schwier, E. U., Nahlik, K., Bayram, Ö., Helmstaedt, K., Draht, O. W., Krappmann, S., Valerius, O., Lipscomb, W. N., & Braus, G. H. (2007). An eight-subunit COP9 signalosome with an intact JAMM motif is required for fungal fruit body formation. *Proceedings of the National Academy of Sciences*, 104(19), 8089–8094. <https://doi.org/10.1073/pnas.0702108104>

Calligé, M., Kieffer, I., & Richard-Foy, H. (2005). CSN5/Jab1 Is Involved in Ligand-Dependent Degradation of Estrogen Receptor  $\alpha$  by the Proteasome. *Molecular and Cellular Biology*, 25(11), 4349–4358. <https://doi.org/10.1128/MCB.25.11.4349-4358.2005>

Carman, C. V., Jun, C.-D., Salas, A., & Springer, T. A. (2003). Endothelial cells proactively form microvilli-like membrane projections upon intercellular adhesion molecule 1 engagement of leukocyte LFA-1. *Journal of Immunology (Baltimore, Md.: 1950)*, 171(11), 6135–6144. <https://doi.org/10.4049/jimmunol.171.11.6135>

Carman, C. V., Sage, P. T., Sciuto, T. E., de la Fuente, M. A., Geha, R. S., Ochs, H. D., Dvorak, H. F., Dvorak, A. M., & Springer, T. A. (2007). Transcellular Diapedesis Is Initiated by Invasive Podosomes. *Immunity*, 26(6), 784–797. <https://doi.org/10.1016/j.immuni.2007.04.015>

Carman, C. V., & Springer, T. A. (2004). A transmigratory cup in leukocyte diapedesis both through individual vascular endothelial cells and between them. *The Journal of Cell Biology*, 167(2), 377–388. <https://doi.org/10.1083/jcb.200404129>

Carmona-Rivera, C., Zhao, W., Yalavarthi, S., & Kaplan, M. J. (2015). Neutrophil extracellular traps induce endothelial dysfunction in systemic lupus erythematosus through the activation of matrix metalloproteinase-2. *Annals of the Rheumatic Diseases*, 74(7), 1417–1424. <https://doi.org/10.1136/annrheumdis-2013-204837>

Cauwe, B., Van den Steen, P. E., & Opdenakker, G. (2007). The biochemical, biological, and pathological kaleidoscope of cell surface substrates processed by matrix metalloproteinases. *Critical Reviews in Biochemistry and Molecular Biology*, 42(3), 113–185. <https://doi.org/10.1080/10409230701340019>

Chakraborty, A., Diefenbacher, M. E., Mylona, A., Kassel, O., & Behrens, A. (2015). The E3 ubiquitin ligase Trim7 mediates c-Jun/AP-1 activation by Ras signalling. *Nature Communications*, 6, 6782. <https://doi.org/10.1038/ncomms7782>

Chamovitz, D. A., & Segal, D. (2001). JAB1/CSN5 and the COP9 signalosome. A complex situation. *EMBO Reports*, 2(2), 96–101. <https://doi.org/10.1093/embo-reports/kve028>

Chamovitz, D. A., Wei, N., Osterlund, M. T., von Arnim, A. G., Staub, J. M., Matsui, M., & Deng, X. W. (1996). The COP9 complex, a novel multisubunit nuclear regulator involved in light control of a plant developmental switch. *Cell*, 86(1), 115–121. [https://doi.org/10.1016/s0092-8674\(00\)80082-3](https://doi.org/10.1016/s0092-8674(00)80082-3)

Chang, F.-M., Reyna, S. M., Granados, J. C., Wei, S.-J., Innis-Whitehouse, W., Maffi, S. K., Rodriguez, E., Slaga, T. J., & Short, J. D. (2012). Inhibition of Neddylation Represses Lipopolysaccharide-induced Proinflammatory Cytokine Production in Macrophage Cells. *The Journal of Biological Chemistry*, 287(42), 35756–35767. <https://doi.org/10.1074/jbc.M112.397703>

Chang, S. C., & Ding, J. L. (2014). Ubiquitination by SAG regulates macrophage survival/death and immune response during infection. *Cell Death and Differentiation*, 21(9), 1388–1398. <https://doi.org/10.1038/cdd.2014.54>

Chappell, J., Harman, J. L., Narasimhan, V. M., Yu, H., Foote, K., Simons, B. D., Bennett, M. R., & Jørgensen, H. F. (2016). Extensive Proliferation of a Subset of Differentiated, yet Plastic, Medial Vascular Smooth Muscle Cells Contributes to Neointimal Formation in Mouse Injury and Atherosclerosis Models. *Circulation Research*, 119(12), 1313–1323. <https://doi.org/10.1161/CIRCRESAHA.116.309799>

Charo, I. F., & Ransohoff, R. M. (2006). The many roles of chemokines and chemokine receptors in inflammation. *The New England Journal of Medicine*, 354(6), 610–621. <https://doi.org/10.1056/NEJMra052723>

Chase, A. J., Bond, M., Crook, M. F., & Newby, A. C. (2002). Role of Nuclear Factor- $\kappa$ B Activation in Metalloproteinase-1, -3, and -9 Secretion by Human Macrophages In Vitro and Rabbit Foam Cells Produced In Vivo. *Arteriosclerosis, Thrombosis, and Vascular Biology*, 22(5), 765–771. <https://doi.org/10.1161/01.ATV.0000015078.09208.92>

Chatzizisis, Y. S., Coskun, A. U., Jonas, M., Edelman, E. R., Feldman, C. L., & Stone, P. H. (2007). Role of Endothelial Shear Stress in the Natural History of Coronary Atherosclerosis and Vascular Remodeling. *Journal of the American College of Cardiology*, 49(25), 2379–2393. <https://doi.org/10.1016/j.jacc.2007.02.059>

Chaudhury, H., Zakkar, M., Boyle, J., Cuhlmann, S., van der Heiden, K., Luong, L. A., Davis, J., Platt, A., Mason, J. C., Krams, R., Haskard, D. O., Clark, A. R., & Evans, P. C. (2010). C-Jun N-Terminal Kinase Primes Endothelial Cells at Atheroprone Sites for Apoptosis. *Arteriosclerosis, Thrombosis, and Vascular Biology*, 30(10), 2260–2267. <https://doi.org/10.1161/ATVBAHA.110.299000>

*Thrombosis, and Vascular Biology*, 30(3), 546–553.  
<https://doi.org/10.1161/ATVBAHA.109.201368>

Chen, B. D., Clark, C. R., & Chou, T. H. (1988). Granulocyte/macrophage colony-stimulating factor stimulates monocyte and tissue macrophage proliferation and enhances their responsiveness to macrophage colony-stimulating factor. *Blood*, 71(4), 997–1002.

Chen, F., Eriksson, P., Hansson, G. K., Herzfeld, I., Klein, M., Hansson, L.-O., & Valen, G. (2005). Expression of matrix metalloproteinase 9 and its regulators in the unstable coronary atherosclerotic plaque. *International Journal of Molecular Medicine*, 15(1), 57–65.

Chen, J., Su, Y., Pi, S., Hu, B., & Mao, L. (2021). The Dual Role of Low-Density Lipoprotein Receptor-Related Protein 1 in Atherosclerosis. *Frontiers in Cardiovascular Medicine*, 8, 522.  
<https://doi.org/10.3389/fcvm.2021.682389>

Chen, M.-S., Lin, C.-Y., Chiu, Y.-H., Chen, C.-P., Tsai, P.-J., & Wang, H.-S. (2018). IL-1  $\beta$  -Induced Matrix Metalloprotease-1 Promotes Mesenchymal Stem Cell Migration via PAR1 and G-Protein-Coupled Signaling Pathway. *Stem Cells International*, 2018, 1–11.  
<https://doi.org/10.1155/2018/3524759>

Chen, Y., & Currie, R. W. (2005). Heat shock treatment suppresses angiotensin II-induced SP-1 and AP-1 and stimulates Oct-1 DNA-binding activity in heart. *Inflammation Research: Official Journal of the European Histamine Research Society ... [et Al.]*, 54(8), 338–343.  
<https://doi.org/10.1007/s00011-005-1360-y>

Chen, Z., Hagler, J., Palombella, V. J., Melandri, F., Scherer, D., Ballard, D., & Maniatis, T. (1995). Signal-induced site-specific phosphorylation targets I kappa B alpha to the ubiquitin-proteasome pathway. *Genes & Development*, 9(13), 1586–1597. <https://doi.org/10.1101/gad.9.13.1586>

Cheng, J., Lin, M., Chu, M., Gong, L., Bi, Y., & Zhao, Y. (2020). Emerging role of FBXO22 in carcinogenesis. *Cell Death Discovery*, 6(1), 66. <https://doi.org/10.1038/s41420-020-00303-0>

Cheng, X. W., Song, H., Sasaki, T., Hu, L., Inoue, A., Bando, Y. K., Shi, G.-P., Kuzuya, M., Okumura, K., & Murohara, T. (2011). Angiotensin type 1 receptor blocker reduces intimal neovascularization and plaque growth in apolipoprotein E-deficient mice. *Hypertension (Dallas, Tex.: 1979)*, 57(5), 981–989. <https://doi.org/10.1161/HYPERTENSIONAHA.110.168385>

Chinenov, Y., & Kerppola, T. K. (2001). Close encounters of many kinds: Fos-Jun interactions that mediate transcription regulatory specificity. *Oncogene*, 20(19), 2438–2452.  
<https://doi.org/10.1038/sj.onc.1204385>

Chinetti-Gbaguidi, G., Baron, M., Bouhlel, M. A., Vanhoutte, J., Copin, C., Sebti, Y., Derudas, B., Mayi, T., Bories, G., Tailleux, A., Haulon, S., Zawadzki, C., Jude, B., & Staels, B. (2011). Human atherosclerotic plaque alternative macrophages display low cholesterol handling but high phagocytosis because of distinct activities of the PPAR $\gamma$  and LXR $\alpha$  pathways. *Circulation Research*, 108(8), 985–995. <https://doi.org/10.1161/CIRCRESAHA.110.233775>

Chistiakov, D. A., Bobryshev, Y. V., & Orekhov, A. N. (2016). Macrophage-mediated cholesterol handling in atherosclerosis. *Journal of Cellular and Molecular Medicine*, 20(1), 17–28.  
<https://doi.org/10.1111/jcmm.12689>

Chistiakov, D. A., Sobenin, I. A., & Orekhov, A. N. (2013). Vascular extracellular matrix in atherosclerosis. *Cardiology in Review*, 21(6), 270–288.  
<https://doi.org/10.1097/CRD.0b013e31828c5ced>

Chiu, R., Angel, P., & Karin, M. (1989). Jun-B differs in its biological properties from, and is a negative regulator of, c-Jun. *Cell*, 59(6), 979–986. [https://doi.org/10.1016/0092-8674\(89\)90754-x](https://doi.org/10.1016/0092-8674(89)90754-x)

Choi, B.-J., Prasad, A., Gulati, R., Best, P. J., Lennon, R. J., Barsness, G. W., Lerman, L. O., & Lerman, A. (2013). Coronary endothelial dysfunction in patients with early coronary artery disease is associated with the increase in intravascular lipid core plaque. *European Heart Journal*, 34(27), 2047–2054. <https://doi.org/10.1093/eurheartj/eht132>

Choi, H. H., Gully, C., Su, C.-H., Velazquez-Torres, G., Chou, P.-C., Tseng, C., Zhao, R., Phan, L., Shaiken, T., Chen, J., Yeung, S. C., & Lee, M.-H. (2011). COP9 signalosome subunit 6 stabilizes COP1, which functions as an E3 ubiquitin ligase for 14-3-3 $\sigma$ . *Oncogene*, 30(48), 4791–4801. <https://doi.org/10.1038/onc.2011.192>

Choudhary, S., Higgins, C. L., Chen, I. Y., Reardon, M., Lawrie, G., Vick, G. W., Karmonik, C., Via, D. P., & Morissett, J. D. (2006). Quantitation and Localization of Matrix Metalloproteinases and Their Inhibitors in Human Carotid Endarterectomy Tissues. *Arteriosclerosis, Thrombosis, and Vascular Biology*, 26(10), 2351–2358. <https://doi.org/10.1161/01.ATV.0000239461.87113.0b>

Ciechanover, A., & Schwartz, A. L. (1998). The ubiquitin-proteasome pathway: The complexity and myriad functions of proteins death. *Proceedings of the National Academy of Sciences*, 95(6), 2727–2730. <https://doi.org/10.1073/pnas.95.6.2727>

Claret, F.-X., Hibi, M., Dhut, S., Toda, T., & Karin, M. (1996). A new group of conserved coactivators that increase the specificity of AP-1 transcription factors. *Nature*, 383(6599), 453–457.  
<https://doi.org/10.1038/383453a0>

Clark, I. M., Swingler, T. E., Sampieri, C. L., & Edwards, D. R. (2008). The regulation of matrix metalloproteinases and their inhibitors. *The International Journal of Biochemistry & Cell Biology*, 40(6), 1362–1378. <https://doi.org/10.1016/j.biocel.2007.12.006>

Claudio, E., Brown, K., Park, S., Wang, H., & Siebenlist, U. (2002). BAFF-induced NEMO-independent processing of NF- $\kappa$ B2 in maturing B cells. *Nature Immunology*, 3(10), 958–965. <https://doi.org/10.1038/ni842>

Cochain, C., Vafadarnejad, E., Arampatzis, P., Pelisek, J., Winkels, H., Ley, K., Wolf, D., Saliba, A.-E., & Zernecke, A. (2018). Single-Cell RNA-Seq Reveals the Transcriptional Landscape and Heterogeneity of Aortic Macrophages in Murine Atherosclerosis. *Circulation Research*, 122(12), 1661–1674. <https://doi.org/10.1161/CIRCRESAHA.117.312509>

Cole, J. E., Park, I., Ahern, D. J., Kassiteridi, C., Danso Abeam, D., Goddard, M. E., Green, P., Maffia, P., & Monaco, C. (2018). Immune cell census in murine atherosclerosis: Cytometry by time of flight illuminates vascular myeloid cell diversity. *Cardiovascular Research*, 114(10), 1360–1371. <https://doi.org/10.1093/cvr/cvy109>

Collins, R. G., Velji, R., Guevara, N. V., Hicks, M. J., Chan, L., & Beaudet, A. L. (2000). P-Selectin or intercellular adhesion molecule (ICAM)-1 deficiency substantially protects against atherosclerosis in apolipoprotein E-deficient mice. *The Journal of Experimental Medicine*, 191(1), 189–194. <https://doi.org/10.1084/jem.191.1.189>

Cope, G. A., & Deshaies, R. J. (2003). COP9 signalosome: A multifunctional regulator of SCF and other cullin-based ubiquitin ligases. *Cell*, 114(6), 663–671. [https://doi.org/10.1016/s0092-8674\(03\)00722-0](https://doi.org/10.1016/s0092-8674(03)00722-0)

Cope, G. A., Suh, G. S. B., Aravind, L., Schwarz, S. E., Zipursky, S. L., Koonin, E. V., & Deshaies, R. J. (2002). Role of predicted metalloprotease motif of Jab1/Csn5 in cleavage of Nedd8 from Cul1. *Science (New York, N.Y.)*, 298(5593), 608–611. <https://doi.org/10.1126/science.1075901>

Crucet, M., Wüst, S. J. A., Spielmann, P., Lüscher, T. F., Wenger, R. H., & Matter, C. M. (2013). Hypoxia enhances lipid uptake in macrophages: Role of the scavenger receptors Lox1, SRA, and CD36. *Atherosclerosis*, 229(1), 110–117. <https://doi.org/10.1016/j.atherosclerosis.2013.04.034>

Cuaz-Pérolin, C., Jguirim, I., Larigauderie, G., Jlassi, A., Furman, C., Moreau, M., Chapman, M. J., Fruchart, J.-C., Slimane, M. N., Mezdour, H., & Rouis, M. (2006). Apolipoprotein E knockout mice over-expressing human tissue inhibitor of metalloproteinase 1 are protected against aneurysm formation but not against atherosclerotic plaque development. *Journal of Vascular Research*, 43(6), 493–501. <https://doi.org/10.1159/000095309>

Cullinan, S. B., Gordan, J. D., Jin, J., Harper, J. W., & Diehl, J. A. (2004). The Keap1-BTB Protein Is an Adaptor That Bridges Nrf2 to a Cul3-Based E3 Ligase: Oxidative Stress Sensing by a Cul3-Keap1 Ligase. *Molecular and Cellular Biology*, 24(19), 8477–8486. <https://doi.org/10.1128/MCB.24.19.8477-8486.2004>

Cunningham, K. S., & Gotlieb, A. I. (2005). The role of shear stress in the pathogenesis of atherosclerosis. *Laboratory Investigation*, 85(1), 9–23. <https://doi.org/10.1038/labinvest.3700215>

Cybulsky, M. I., Iiyama, K., Li, H., Zhu, S., Chen, M., Iiyama, M., Davis, V., Gutierrez-Ramos, J. C., Connelly, P. W., & Milstone, D. S. (2001). A major role for VCAM-1, but not ICAM-1, in early atherosclerosis. *The Journal of Clinical Investigation*, 107(10), 1255–1262. <https://doi.org/10.1172/JCI11871>

Dai, G., Kaazempur-Mofrad, M. R., Natarajan, S., Zhang, Y., Vaughn, S., Blackman, B. R., Kamm, R. D., García-Cardeña, G., & Gimbrone, M. A. (2004). Distinct endothelial phenotypes evoked by arterial waveforms derived from atherosclerosis-susceptible and -resistant regions of human vasculature. *Proceedings of the National Academy of Sciences of the United States of America*, 101(41), 14871–14876. <https://doi.org/10.1073/pnas.0406073101>

Damås, J. K., Smith, C., Øie, E., Fevang, B., Halvorsen, B., Waehre, T., Boullier, A., Breland, U., Yndestad, A., Ovchinnikova, O., Robertson, A.-K. L., Sandberg, W. J., Kjekshus, J., Taskén, K., Frøland, S. S., Gullestad, L., Hansson, G. K., Quehenberger, O., & Aukrust, P. (2007). Enhanced expression of the homeostatic chemokines CCL19 and CCL21 in clinical and experimental atherosclerosis: Possible pathogenic role in plaque destabilization. *Arteriosclerosis, Thrombosis, and Vascular Biology*, 27(3), 614–620. <https://doi.org/10.1161/01.ATV.0000255581.38523.7c>

De Clerck, Y. A., Darville, M. I., Eeckhout, Y., & Rousseau, G. G. (1994). Characterization of the promoter of the gene encoding human tissue inhibitor of metalloproteinases-2 (TIMP-2). *Gene*, 139(2), 185–191. [https://doi.org/10.1016/0378-1119\(94\)90753-6](https://doi.org/10.1016/0378-1119(94)90753-6)

de Winther, M. P. J., Kanders, E., Kraal, G., & Hofker, M. H. (2005). Nuclear factor kappaB signaling in atherogenesis. *Arteriosclerosis, Thrombosis, and Vascular Biology*, 25(5), 904–914. <https://doi.org/10.1161/01.ATV.0000160340.72641.87>

Dejana, E. (2004). Endothelial cell-cell junctions: Happy together. *Nature Reviews. Molecular Cell Biology*, 5(4), 261–270. <https://doi.org/10.1038/nrm1357>

Dejardin, E. (2006). The alternative NF- $\kappa$ B pathway from biochemistry to biology: Pitfalls and promises for future drug development. *Biochemical Pharmacology*, 72(9), 1161–1179. <https://doi.org/10.1016/j.bcp.2006.08.007>

Deng, Z., Pardi, R., Cheadle, W., Xiang, X., Zhang, S., Shah, S. V., Grizzle, W., Miller, D., Mountz, J., & Zhang, H.-G. (2011). Plant homologue constitutive photomorphogenesis 9 (COP9) signalosome subunit CSN5 regulates innate immune responses in macrophages. *Blood*, 117(18), 4796–4804. <https://doi.org/10.1182/blood-2010-10-314526>

Deshaires, R. J., & Joazeiro, C. A. P. (2009). RING domain E3 ubiquitin ligases. *Annual Review of Biochemistry*, 78, 399–434. <https://doi.org/10.1146/annurev.biochem.78.101807.093809>

Di Gregoli, K., George, S. J., Jackson, C. L., Newby, A. C., & Johnson, J. L. (2016a). Differential effects of tissue inhibitor of metalloproteinase (TIMP)-1 and TIMP-2 on atherosclerosis and monocyte/macrophage invasion. *Cardiovascular Research*, 109(2), 318–330. <https://doi.org/10.1093/cvr/cvv268>

Di Gregoli, K., George, S. J., Jackson, C. L., Newby, A. C., & Johnson, J. L. (2016b). Differential effects of tissue inhibitor of metalloproteinase (TIMP)-1 and TIMP-2 on atherosclerosis and monocyte/macrophage invasion. *Cardiovascular Research*, 109(2), 318–330. <https://doi.org/10.1093/cvr/cvv268>

Dinarello, C. A. (2009). Immunological and Inflammatory Functions of the Interleukin-1 Family. *Annual Review of Immunology*, 27(1), 519–550. <https://doi.org/10.1146/annurev.immunol.021908.132612>

Dong, Z. M., Chapman, S. M., Brown, A. A., Frenette, P. S., Hynes, R. O., & Wagner, D. D. (1998). The combined role of P- and E-selectins in atherosclerosis. *Journal of Clinical Investigation*, 102(1), 145–152.

Dubiel, W., Chaithongyot, S., Dubiel, D., & Naumann, M. (2020). The COP9 Signalosome: A Multi-DUB Complex. *Biomolecules*, 10(7), 1082. <https://doi.org/10.3390/biom10071082>

Duda, D. M., Borg, L. A., Scott, D. C., Hunt, H. W., Hammel, M., & Schulman, B. A. (2008). Structural insights into NEDD8 activation of cullin-RING ligases: Conformational control of conjugation. *Cell*, 134(6), 995–1006. <https://doi.org/10.1016/j.cell.2008.07.022>

Eble, J. A., & Niland, S. (2009). The extracellular matrix of blood vessels. *Current Pharmaceutical Design*, 15(12), 1385–1400. <https://doi.org/10.2174/1381612097846757>

Echalier, A., Pan, Y., Birol, M., Tavernier, N., Pintard, L., Hoh, F., Ebel, C., Galophe, N., Claret, F. X., & Dumas, C. (2013). Insights into the regulation of the human COP9 signalosome catalytic subunit, CSN5/Jab1. *Proceedings of the National Academy of Sciences of the United States of America*, 110(4), 1273–1278. <https://doi.org/10.1073/pnas.1209345110>

Eferl, R., & Wagner, E. F. (2003). AP-1: A double-edged sword in tumorigenesis. *Nature Reviews Cancer*, 3(11), 859–868. <https://doi.org/10.1038/nrc1209>

Ehrentraut, S. F., Kominsky, D. J., Glover, L. E., Campbell, E. L., Kelly, C. J., Bowers, B. E., Bayless, A. J., & Colgan, S. P. (2013). Central Role for Endothelial Human Deneddylase-1/SENP8 in Fine-Tuning the Vascular Inflammatory Response. *The Journal of Immunology*, 190(1), 392–400. <https://doi.org/10.4049/jimmunol.1202041>

Emanuele, M. J., & Enrico, T. P. (2019). Ubiquitin Signaling in Regulation of the Start of the Cell Cycle. In *Ubiquitin Proteasome System—Current Insights into Mechanism Cellular Regulation and Disease*. IntechOpen. <https://doi.org/10.5772/intechopen.82874>

Enchev, R. I., Schulman, B. A., & Peter, M. (2015). Protein Neddylation: Beyond Cullin-RING Ligases. *Nature Reviews Molecular Cell Biology*, 16(1), 30–44. <https://doi.org/10.1038/nrm3919>

Fabunmi, R. P., Sukhova, G. K., Sugiyama, S., & Libby, P. (1998). Expression of Tissue Inhibitor of Metalloproteinases-3 in Human Atheroma and Regulation in Lesion-Associated Cells. *Circulation Research*, 83(3), 270–278. <https://doi.org/10.1161/01.RES.83.3.270>

Fadok, V. A., Bratton, D. L., Konowal, A., Freed, P. W., Westcott, J. Y., & Henson, P. M. (1998). Macrophages that have ingested apoptotic cells in vitro inhibit proinflammatory cytokine production through autocrine/paracrine mechanisms involving TGF- $\beta$ , PGE2, and PAF. *The Journal of Clinical Investigation*, 101(4), 890–898. <https://doi.org/10.1172/JCI1112>

Falk, E. (2006). Pathogenesis of atherosclerosis. *Journal of the American College of Cardiology*, 47(8 Suppl), C7–C12. <https://doi.org/10.1016/j.jacc.2005.09.068>

Feng, B., Yao, P. M., Li, Y., Devlin, C. M., Zhang, D., Harding, H. P., Sweeney, M., Rong, J. X., Kuriakose, G., Fisher, E. A., Marks, A. R., Ron, D., & Tabas, I. (2003). The endoplasmic reticulum is the site of cholesterol-induced cytotoxicity in macrophages. *Nature Cell Biology*, 5(9), 781–792. <https://doi.org/10.1038/ncb1035>

Fernandez, D. M., Rahman, A. H., Fernandez, N. F., Chudnovskiy, A., Amir, E.-A. D., Amadori, L., Khan, N. S., Wong, C. K., Shamailova, R., Hill, C. A., Wang, Z., Remark, R., Li, J. R., Pina, C., Faries, C., Awad, A. J., Moss, N., Bjorkgren, J. L. M., Kim-Schulze, S., ... Giannarelli, C.

(2019). Single-cell immune landscape of human atherosclerotic plaques. *Nature Medicine*, 25(10), 1576–1588. <https://doi.org/10.1038/s41591-019-0590-4>

Fernandez-Catalan, C., Bode, W., Huber, R., Turk, D., Calvete, J. J., Lichte, A., Tschesche, H., & Maskos, K. (1998). Crystal structure of the complex formed by the membrane type 1-matrix metalloproteinase with the tissue inhibitor of metalloproteinases-2, the soluble progelatinase A receptor. *The EMBO Journal*, 17(17), 5238–5248. <https://doi.org/10.1093/emboj/17.17.5238>

Filippi, M.-D. (2016). Mechanism of Diapedesis: Importance of the Transcellular Route. *Advances in Immunology*, 129, 25–53. <https://doi.org/10.1016/bs.ai.2015.09.001>

Fledderus, J., Vanchin, B., Rots, M. G., & Krenning, G. (2021). The Endothelium as a Target for Anti-Atherogenic Therapy: A Focus on the Epigenetic Enzymes EZH2 and SIRT1. *Journal of Personalized Medicine*, 11(2), 103. <https://doi.org/10.3390/jpm11020103>

Flynn, M. C., Pernes, G., Lee, M. K. S., Nagareddy, P. R., & Murphy, A. J. (2019). Monocytes, Macrophages, and Metabolic Disease in Atherosclerosis. *Frontiers in Pharmacology*, 10, 666. <https://doi.org/10.3389/fphar.2019.00666>

Fong, A., & Sun, S.-C. (2002). Genetic evidence for the essential role of beta-transducin repeat-containing protein in the inducible processing of NF- $\kappa$ B2/p100. *The Journal of Biological Chemistry*, 277(25), 22111–22114. <https://doi.org/10.1074/jbc.C200151200>

Fonseca, M. I., Carpenter, P. M., Park, M., Palmarini, G., Nelson, E. L., & Tenner, A. J. (2001). C1qR(P), a myeloid cell receptor in blood, is predominantly expressed on endothelial cells in human tissue. *Journal of Leukocyte Biology*, 70(5), 793–800.

Forbes, B., McCarthy, P., & Norton, R. (2012). Insulin-Like Growth Factor Binding Proteins: A Structural Perspective. *Frontiers in Endocrinology*, 3, 38. <https://doi.org/10.3389/fendo.2012.00038>

Fuchs, S. Y., Dolan, L., Davis, R. J., & Ronai, Z. (1996). Phosphorylation-dependent targeting of c-Jun ubiquitination by Jun N-kinase. *Oncogene*, 13(7), 1531–1535.

Fukumoto, A., Tomoda, K., Kubota, M., Kato, J., & Yoneda-Kato, N. (2005). Small Jab1-containing subcomplex is regulated in an anchorage- and cell cycle-dependent manner, which is abrogated by ras transformation. *FEBS Letters*, 579(5), 1047–1054. <https://doi.org/10.1016/j.febslet.2004.12.076>

Galis, Z. S., Johnson, C., Godin, D., Magid, R., Shipley, J. M., Senior, R. M., & Ivan, E. (2002). Targeted Disruption of the Matrix Metalloproteinase-9 Gene Impairs Smooth Muscle Cell Migration and Geometrical Arterial Remodeling. *Circulation Research*, 91(9), 852–859. <https://doi.org/10.1161/01.RES.0000041036.86977.14>

Galis, Z. S., & Khatri, J. J. (2002). Matrix Metalloproteinases in Vascular Remodeling and Atherogenesis: The Good, the Bad, and the Ugly. *Circulation Research*, 90(3), 251–262. <https://doi.org/10.1161/01.res.90.3.251>

Galis, Z. S., Sukhova, G. K., Lark, M. W., & Libby, P. (1994). Increased expression of matrix metalloproteinases and matrix degrading activity in vulnerable regions of human atherosclerotic plaques. *The Journal of Clinical Investigation*, 94(6), 2493–2503. <https://doi.org/10.1172/JCI117619>

Galkina, E., & Ley, K. (2009a). Immune and Inflammatory Mechanisms of Atherosclerosis. *Annual Review of Immunology*, 27, 165–197. <https://doi.org/10.1146/annurev.immunol.021908.132620>

Galkina, E., & Ley, K. (2009b). Immune and Inflammatory Mechanisms of Atherosclerosis. *Annual Review of Immunology*, 27(1), 165–197. <https://doi.org/10.1146/annurev.immunol.021908.132620>

Gardner, J., & Ghorpade, A. (2003). Tissue Inhibitor of Metalloproteinase (TIMP)-1: The TIMPed Balance of Matrix Metalloproteinases in the Central Nervous System. *Journal of Neuroscience Research*, 74(6), 10.1002/jnr.10835. <https://doi.org/10.1002/jnr.10835>

Gareus, R., Kotsaki, E., Xanthoulea, S., van der Made, I., Gijbels, M. J. J., Kardakaris, R., Polykratis, A., Kollias, G., de Winther, M. P. J., & Pasparakis, M. (2008). Endothelial cell-specific NF- $\kappa$ B inhibition protects mice from atherosclerosis. *Cell Metabolism*, 8(5), 372–383. <https://doi.org/10.1016/j.cmet.2008.08.016>

Geissmann, F., Jung, S., & Littman, D. R. (2003). Blood monocytes consist of two principal subsets with distinct migratory properties. *Immunity*, 19(1), 71–82. [https://doi.org/10.1016/s1074-7613\(03\)00174-2](https://doi.org/10.1016/s1074-7613(03)00174-2)

George, J., Shoenfeld, Y., Gilburd, B., Afek, A., Shaish, A., & Harats, D. (2000). Requisite Role for Interleukin-4 in the Acceleration of Fatty Streaks Induced by Heat Shock Protein 65 or *Mycobacterium tuberculosis*. *Circulation Research*, 86(12), 1203–1210. <https://doi.org/10.1161/01.RES.86.12.1203>

Ghanem, A., Schweitzer, K., & Naumann, M. (2019). Catalytic domain of deubiquitinylase USP48 directs interaction with Rel homology domain of nuclear factor kappaB transcription factor

RelA. *Molecular Biology Reports*, 46(1), 1369–1375. <https://doi.org/10.1007/s11033-019-04587-z>

Gimbrone, M. A., & García-Cardeña, G. (2016). Endothelial Cell Dysfunction and the Pathobiology of Atherosclerosis. *Circulation Research*, 118(4), 620–636. <https://doi.org/10.1161/CIRCRESAHA.115.306301>

Godbersen, J. C., Humphries, L. A., Danilova, O. V., Kebbekus, P. E., Brown, J. R., Eastman, A., & Danilov, A. V. (2014). The Nedd8-activating enzyme inhibitor MLN4924 thwarts microenvironment-driven NF- $\kappa$ B activation and induces apoptosis in chronic lymphocytic leukemia B cells. *Clinical Cancer Research: An Official Journal of the American Association for Cancer Research*, 20(6), 1576–1589. <https://doi.org/10.1158/1078-0432.CCR-13-0987>

Goldenberg, S. J., Cascio, T. C., Shumway, S. D., Garbutt, K. C., Liu, J., Xiong, Y., & Zheng, N. (2004). Structure of the Cnd1-Cul1-Roc1 Complex Reveals Regulatory Mechanisms for the Assembly of the Multisubunit Cullin-Dependent Ubiquitin Ligases. *Cell*, 119(4), 517–528. <https://doi.org/10.1016/j.cell.2004.10.019>

Gonçalves, I., Stollenwerk, M. M., Lindholm, M. W., Dias, N., Pedro, L. M., Fernandes, J. F. E., Moses, J., Fredrikson, G. N., Nilsson, J., & Ares, M. P. S. (2011). Activator protein-1 in carotid plaques is related to cerebrovascular symptoms and cholesterin ester content. *Cardiovascular Pathology: The Official Journal of the Society for Cardiovascular Pathology*, 20(1), 36–43. <https://doi.org/10.1016/j.carpath.2009.09.003>

Gong, Y., Chippada-Venkata, U. D., Galsky, M. D., Huang, J., & Oh, W. K. (2015). Elevated circulating tissue inhibitor of metalloproteinase 1 (TIMP-1) levels are associated with neuroendocrine differentiation in castration resistant prostate cancer: TIMP-1 and NED in CRPC. *The Prostate*, 75(6), 616–627. <https://doi.org/10.1002/pros.22945>

Gordon, S., & Martinez, F. O. (2010). Alternative activation of macrophages: Mechanism and functions. *Immunity*, 32(5), 593–604. <https://doi.org/10.1016/j.immuni.2010.05.007>

Gorp, H. V., Saavedra, P. H. V., Vasconcelos, N. M. de, Opdenbosch, N. V., Walle, L. V., Matusiak, M., Prencipe, G., Insalaco, A., Hauwermeiren, F. V., Demon, D., Bogaert, D. J., Dullaers, M., Baere, E. D., Hochepied, T., Dehoorne, J., Vermaelen, K. Y., Haerlynck, F., Benedetti, F. D., & Lamkanfi, M. (2016). Familial Mediterranean fever mutations lift the obligatory requirement for microtubules in Pyrin inflammasome activation. *Proceedings of the National Academy of Sciences*, 113(50), 14384–14389. <https://doi.org/10.1073/pnas.1613156113>

Gough, P. J., Gomez, I. G., Wille, P. T., & Raines, E. W. (2006). Macrophage expression of active MMP-9 induces acute plaque disruption in apoE-deficient mice. *The Journal of Clinical Investigation*, 116(1), 59–69. <https://doi.org/10.1172/JCI25074>

Granata, R., Trovato, L., Lupia, E., Sala, G., Settanni, F., Camussi, G., Ghidoni, R., & Ghigo, E. (2007). Insulin-like growth factor binding protein-3 induces angiogenesis through IGF-I- and SphK1-dependent mechanisms. *Journal of Thrombosis and Haemostasis*, 5(4), 835–845. <https://doi.org/10.1111/j.1538-7836.2007.02431.x>

Grebe, A., Hoss, F., & Latz, E. (2018). NLRP3 Inflammasome and the IL-1 Pathway in Atherosclerosis. *Circulation Research*, 122(12), 1722–1740. <https://doi.org/10.1161/CIRCRESAHA.118.311362>

Greenberg, M. E., Sun, M., Zhang, R., Febbraio, M., Silverstein, R., & Hazen, S. L. (2006). Oxidized phosphatidylserine–CD36 interactions play an essential role in macrophage-dependent phagocytosis of apoptotic cells. *Journal of Experimental Medicine*, 203(12), 2613–2625. <https://doi.org/10.1084/jem.20060370>

Grodstein, F., Stampfer, M. J., Manson, J. E., Colditz, G. A., Willett, W. C., Rosner, B., Speizer, F. E., & Hennekens, C. H. (1996). Postmenopausal Estrogen and Progestin Use and the Risk of Cardiovascular Disease. *New England Journal of Medicine*, 335(7), 453–461. <https://doi.org/10.1056/NEJM199608153350701>

Grünwald, B., Schoeps, B., & Krüger, A. (2019). Recognizing the Molecular Multifunctionality and Interactome of TIMP-1. *Trends in Cell Biology*, 29(1), 6–19. <https://doi.org/10.1016/j.tcb.2018.08.006>

Gu, L., Okada, Y., Clinton, S. K., Gerard, C., Sukhova, G. K., Libby, P., & Rollins, B. J. (1998). Absence of monocyte chemoattractant protein-1 reduces atherosclerosis in low density lipoprotein receptor-deficient mice. *Molecular Cell*, 2(2), 275–281. [https://doi.org/10.1016/s1097-2765\(00\)80139-2](https://doi.org/10.1016/s1097-2765(00)80139-2)

Guo, F., Liu, J., Han, X., Zhang, X., Lin, T., Wang, Y., Bai, J., & Han, J. (2019). FBXO22 Suppresses Metastasis in Human Renal Cell Carcinoma via Inhibiting MMP-9-Mediated Migration and Invasion and VEGF-Mediated Angiogenesis. *International Journal of Biological Sciences*, 15(3), 647–656. <https://doi.org/10.7150/ijbs.31293>

Guo, R., Yang, L., Wang, H., Liu, B., & Wang, L. (2008). Angiotensin II induces matrix metalloproteinase-9 expression via a nuclear factor- $\kappa$ B-dependent pathway in vascular

smooth muscle cells. *Regulatory Peptides*, 147(1–3), 37–44. <https://doi.org/10.1016/j.regpep.2007.12.005>

Guo, S.-Y., Shen, X., Yang, J., Yuan, J., Yang, R.-L., Mao, K., Zhao, D.-H., & Li, C.-J. (2007). TIMP-1 mediates the inhibitory effect of interleukin-6 on the proliferation of a hepatocarcinoma cell line in a STAT3-dependent manner. *Brazilian Journal of Medical and Biological Research*, 40, 621–631. <https://doi.org/10.1590/S0100-879X2006005000084>

Gutman, A., & Waslylyk, B. (1990). The collagenase gene promoter contains a TPA and oncogene-responsive unit encompassing the PEA3 and AP-1 binding sites. *The EMBO Journal*, 9(7), 2241–2246.

Hajra, L., Evans, A. I., Chen, M., Hyduk, S. J., Collins, T., & Cybulsky, M. I. (2000). The NF- $\kappa$ B signal transduction pathway in aortic endothelial cells is primed for activation in regions predisposed to atherosclerotic lesion formation. *Proceedings of the National Academy of Sciences of the United States of America*, 97(16), 9052–9057. <https://doi.org/10.1073/pnas.97.16.9052>

Hall, M.-C., Young, D. A., Waters, J. G., Rowan, A. D., Chantry, A., Edwards, D. R., & Clark, I. M. (2003a). The Comparative Role of Activator Protein 1 and Smad Factors in the Regulation of Timp-1 and MMP-1 Gene Expression by Transforming Growth Factor- $\beta$ 1. *Journal of Biological Chemistry*, 278(12), 10304–10313. <https://doi.org/10.1074/jbc.M212334200>

Hall, M.-C., Young, D. A., Waters, J. G., Rowan, A. D., Chantry, A., Edwards, D. R., & Clark, I. M. (2003b). The comparative role of activator protein 1 and Smad factors in the regulation of Timp-1 and MMP-1 gene expression by transforming growth factor-beta 1. *The Journal of Biological Chemistry*, 278(12), 10304–10313. <https://doi.org/10.1074/jbc.M212334200>

Hammill, J. T., Bhasin, D., Scott, D. C., Min, J., Chen, Y., Lu, Y., Yang, L., Kim, H. S., Connelly, M. C., Hammill, C., Holbrook, G., Jeffries, C., Singh, B., Schulman, B. A., & Guy, R. K. (2018). Discovery of an Orally Bioavailable Inhibitor of Defective in Cullin Neddylation 1 (DCN1)-Mediated Cullin Neddylation. *Journal of Medicinal Chemistry*, 61(7), 2694–2706. <https://doi.org/10.1021/acs.jmedchem.7b01282>

Hannemann, N., Jordan, J., Paul, S., Reid, S., Baenkler, H.-W., Sonnewald, S., Bäuerle, T., Vera, J., Schett, G., & Bozec, A. (2017). The AP-1 Transcription Factor c-Jun Promotes Arthritis by Regulating Cyclooxygenase-2 and Arginase-1 Expression in Macrophages. *The Journal of Immunology*, 198(9), 3605–3614. <https://doi.org/10.4049/jimmunol.1601330>

Hansson, G. K. (2005). Inflammation, atherosclerosis, and coronary artery disease. *The New England Journal of Medicine*, 352(16), 1685–1695. <https://doi.org/10.1056/NEJMra043430>

Hansson, G. K., Chao, S., Schwartz, S. M., & Reidy, M. A. (1985). Aortic endothelial cell death and replication in normal and lipopolysaccharide-treated rats. *The American Journal of Pathology*, 111(1), 123–127.

Hansson, G. K., & Hermansson, A. (2011). The immune system in atherosclerosis. *Nature Immunology*, 12(3), 204–212. <https://doi.org/10.1038/ni.2001>

Hansson, G. K., & Libby, P. (2006). The immune response in atherosclerosis: A double-edged sword. *Nature Reviews. Immunology*, 6(7), 508–519. <https://doi.org/10.1038/nri1882>

Hansson, G. K., Libby, P., Schönbeck, U., & Yan, Z.-Q. (2002). Innate and adaptive immunity in the pathogenesis of atherosclerosis. *Circulation Research*, 91(4), 281–291. <https://doi.org/10.1161/01.res.0000029784.15893.10>

Hashimoto, K., Kataoka, N., Nakamura, E., Tsujioka, K., & Kajiya, F. (2007). Oxidized LDL specifically promotes the initiation of monocyte invasion during transendothelial migration with upregulated PECAM-1 and downregulated VE-cadherin on endothelial junctions. *Atherosclerosis*, 194(2), e9–17. <https://doi.org/10.1016/j.atherosclerosis.2006.11.029>

He, H., Xu, J., Warren, C. M., Duan, D., Li, X., Wu, L., & Iruela-Arispe, M. L. (2012). Endothelial cells provide an instructive niche for the differentiation and functional polarization of M2-like macrophages. *Blood*, 120(15), 3152–3162. <https://doi.org/10.1182/blood-2012-04-422758>

Hemdahl, A.-L., Gabrielsen, A., Zhu, C., Eriksson, P., Hedin, U., Kastrup, J., Thorén, P., & Hansson, G. K. (2006). Expression of neutrophil gelatinase-associated lipocalin in atherosclerosis and myocardial infarction. *Arteriosclerosis, Thrombosis, and Vascular Biology*, 26(1), 136–142. <https://doi.org/10.1161/01.ATV.0000193567.88685.f4>

Herrmann, J., Edwards, W. D., Holmes, D. R., Shogren, K. L., Lerman, L. O., Ciechanover, A., & Lerman, A. (2002). Increased ubiquitin immunoreactivity in unstable atherosclerotic plaques associated with acute coronary syndromes. *Journal of the American College of Cardiology*, 40(11), 1919–1927. [https://doi.org/10.1016/s0735-1097\(02\)02564-0](https://doi.org/10.1016/s0735-1097(02)02564-0)

Ho, F. M., Liu, S. H., Liau, C. S., Huang, P. J., & Lin-Shiau, S. Y. (2000). High glucose-induced apoptosis in human endothelial cells is mediated by sequential activations of c-Jun NH(2)-terminal kinase and caspase-3. *Circulation*, 101(22), 2618–2624. <https://doi.org/10.1161/01.cir.101.22.2618>

Hofmann, K., & Bucher, P. (1998). The PCI domain: A common theme in three multiprotein complexes. *Trends in Biochemical Sciences*, 23(6), 204–205. [https://doi.org/10.1016/s0968-0004\(98\)01217-1](https://doi.org/10.1016/s0968-0004(98)01217-1)

Hojo, Y., Ikeda, U., Takahashi, M., Sakata, Y., Takizawa, T., Okada, K., Saito, T., & Shimada, K. (2000). Matrix metalloproteinase-1 expression by interaction between monocytes and vascular endothelial cells. *Journal of Molecular and Cellular Cardiology*, 32(8), 1459–1468. <https://doi.org/10.1006/jmcc.2000.1179>

Holm Nielsen, S., Jonasson, L., Kalogeropoulos, K., Karsdal, M. A., Reese-Petersen, A. L., auf dem Keller, U., Genovese, F., Nilsson, J., & Goncalves, I. (2020). Exploring the role of extracellular matrix proteins to develop biomarkers of plaque vulnerability and outcome. *Journal of Internal Medicine*, 287(5), 493–513. <https://doi.org/10.1111/joim.13034>

Hommes, D. W., Peppelenbosch, M. P., & van Deventer, S. J. H. (2003). Mitogen activated protein (MAP) kinase signal transduction pathways and novel anti-inflammatory targets. *Gut*, 52(1), 144–151. <https://doi.org/10.1136/gut.52.1.144>

Hori, T., Osaka, F., Chiba, T., Miyamoto, C., Okabayashi, K., Shimbara, N., Kato, S., & Tanaka, K. (1999). Covalent modification of all members of human cullin family proteins by NEDD8. *Oncogene*, 18(48), 6829–6834. <https://doi.org/10.1038/sj.onc.1203093>

Hoshi, O., & Ushiki, T. (2004). Neutrophil extravasation in rat mesenteric venules induced by the chemotactic peptide N-formyl-methionyl-luecylphenylalanine (fMLP), with special attention to a barrier function of the vascular basal lamina for neutrophil migration. *Archives of Histology and Cytology*, 67(1), 107–114. <https://doi.org/10.1679/aohc.67.107>

Hoshi, S., Goto, M., Koyama, N., Nomoto, K., & Tanaka, H. (2000). Regulation of vascular smooth muscle cell proliferation by nuclear factor-kappaB and its inhibitor, I-kappaB. *The Journal of Biological Chemistry*, 275(2), 883–889. <https://doi.org/10.1074/jbc.275.2.883>

Howe, K. L., & Fish, J. E. (2019). Transforming endothelial cells in atherosclerosis. *Nature Metabolism*, 1(9), 856–857. <https://doi.org/10.1038/s42255-019-0100-5>

Hsieh, V., Kim, M.-J., Gelissen, I. C., Brown, A. J., Sandoval, C., Hallab, J. C., Kockx, M., Traini, M., Jessup, W., & Kritharides, L. (2014). Cellular Cholesterol Regulates Ubiquitination and Degradation of the Cholesterol Export Proteins ABCA1 and ABCG1 \*. *Journal of Biological Chemistry*, 289(11), 7524–7536. <https://doi.org/10.1074/jbc.M113.515890>

Hu, X., & Beeton, C. (2010). Detection of Functional Matrix Metalloproteinases by Zymography. *JoVE (Journal of Visualized Experiments)*, 45, e2445. <https://doi.org/10.3791/2445>

Huang, W., Febbraio, M., & Silverstein, R. L. (2011). CD9 Tetraspanin Interacts with CD36 on the Surface of Macrophages: A Possible Regulatory Influence on Uptake of Oxidized Low Density Lipoprotein. *PLOS ONE*, 6(12), e29092. <https://doi.org/10.1371/journal.pone.0029092>

Huff, M. W., & Pickering, J. G. (2015). Can a Vascular Smooth Muscle–Derived Foam-Cell Really Change its Spots? *Arteriosclerosis, Thrombosis, and Vascular Biology*, 35(3), 492–495. <https://doi.org/10.1161/ATVBAHA.115.305225>

Ikonomidis, I., Lekakis, J. P., Nikolaou, M., Paraskevaidis, I., Andreadou, I., Kaplanoglou, T., Katsimbri, P., Skarantavos, G., Soucacos, P. N., & Kremastinos, D. T. (2008). Inhibition of interleukin-1 by anakinra improves vascular and left ventricular function in patients with rheumatoid arthritis. *Circulation*, 117(20), 2662–2669. <https://doi.org/10.1161/CIRCULATIONAHA.107.731877>

Inoue, N., Takeshita, S., Gao, D., Ishida, T., Kawashima, S., Akita, H., Tawa, R., Sakurai, H., & Yokoyama, M. (2001). Lysophosphatidylcholine increases the secretion of matrix metalloproteinase 2 through the activation of NADH/NADPH oxidase in cultured aortic endothelial cells. *Atherosclerosis*, 155(1), 45–52. [https://doi.org/10.1016/s0021-9150\(00\)00530-x](https://doi.org/10.1016/s0021-9150(00)00530-x)

Isoda, K., & Ohsuzu, F. (2006). The Effect of Interleukin-1 Receptor Antagonist on Arteries and Cholesterol Metabolism. *Journal of Atherosclerosis and Thrombosis*, 13(1), 21–30. <https://doi.org/10.5551/jat.13.21>

Ivandic, B., Castellani, L. W., Wang, X. P., Qiao, J. H., Mehrabian, M., Navab, M., Fogelman, A. M., Grass, D. S., Swanson, M. E., de Beer, M. C., de Beer, F., & Lusis, A. J. (1999). Role of group II secretory phospholipase A2 in atherosclerosis: 1. Increased atherogenesis and altered lipoproteins in transgenic mice expressing group IIa phospholipase A2. *Arteriosclerosis, Thrombosis, and Vascular Biology*, 19(5), 1284–1290. <https://doi.org/10.1161/01.atv.19.5.1284>

Iyer, S., Wei, S., Brew, K., & Acharya, K. R. (2007). Crystal structure of the catalytic domain of matrix metalloproteinase-1 in complex with the inhibitory domain of tissue inhibitor of metalloproteinase-1. *The Journal of Biological Chemistry*, 282(1), 364–371. <https://doi.org/10.1074/jbc.M607625200>

Jiang, Y., Li, L., Li, Y., Liu, G., Hoffman, R. M., & Jia, L. (2021). Neddylation Regulates Macrophages and Implications for Cancer Therapy. *Frontiers in Cell and Developmental Biology*, 9, 1367. <https://doi.org/10.3389/fcell.2021.681186>

Jin, J., Jing, Z., Ye, Z., Guo, L., Hua, L., Wang, Q., Wang, J., Cheng, Q., Zhang, J., Xu, Y., & Wei, L. (2018). MLN4924 suppresses lipopolysaccharide-induced proinflammatory cytokine production in neutrophils in a dose-dependent manner. *Oncology Letters*, 15(5), 8039–8045. <https://doi.org/10.3892/ol.2018.8333>

Jobin, P. G., Butler, G. S., & Overall, C. M. (2017). New intracellular activities of matrix metalloproteinases shine in the moonlight. *Biochimica Et Biophysica Acta. Molecular Cell Research*, 1864(11 Pt A), 2043–2055. <https://doi.org/10.1016/j.bbamcr.2017.05.013>

Johnson, J. L. (2017). Metalloproteinases in atherosclerosis. *European Journal of Pharmacology*, 816, 93–106. <https://doi.org/10.1016/j.ejphar.2017.09.007>

Johnson, J. L., & Newby, A. C. (2009). Macrophage heterogeneity in atherosclerotic plaques. *Current Opinion in Lipidology*, 20(5), 370–378. <https://doi.org/10.1097/MOL.0b013e3283309848>

Johnson, R. C., Chapman, S. M., Dong, Z. M., Ordovas, J. M., Mayadas, T. N., Herz, J., Hynes, R. O., Schaefer, E. J., & Wagner, D. D. (1997). Absence of P-selectin delays fatty streak formation in mice. *The Journal of Clinical Investigation*, 99(5), 1037–1043. <https://doi.org/10.1172/JCI119231>

Jung, T. W., Park, H. S., Choi, G. H., Kim, D., Jeong, J. H., & Lee, T. (2018). Chitinase-3-like protein 1 ameliorates atherosclerotic responses via PPAR $\delta$ -mediated suppression of inflammation and ER stress. *Journal of Cellular Biochemistry*, 119(8), 6795–6805. <https://doi.org/10.1002/jcb.26873>

Junqueira, L. C., Bignolas, G., & Brentani, R. R. (1979). Picosirius staining plus polarization microscopy, a specific method for collagen detection in tissue sections. *The Histochemical Journal*, 11(4), 447–455. <https://doi.org/10.1007/BF01002772>

Kallunki, T., Su, B., Tsigelny, I., Sluss, H. K., Dérijard, B., Moore, G., Davis, R., & Karin, M. (1994). JNK2 contains a specificity-determining region responsible for efficient c-Jun binding and phosphorylation. *Genes & Development*, 8(24), 2996–3007. <https://doi.org/10.1101/gad.8.24.2996>

Kamei, M., & Carman, C. V. (2010). New observations on the trafficking and diapedesis of monocytes. *Current Opinion in Hematology*, 17(1), 43–52. <https://doi.org/10.1097/MOH.0b013e328333949>

Kaminska, B. (2005). MAPK signalling pathways as molecular targets for anti-inflammatory therapy—From molecular mechanisms to therapeutic benefits. *Biochimica Et Biophysica Acta*, 1754(1–2), 253–262. <https://doi.org/10.1016/j.bbapap.2005.08.017>

Kandala, S., Kim, I., & Su, H. (2014). Neddylation and deneddylation in cardiac biology. *American Journal of Cardiovascular Disease*, 4(4), 140–158.

Kanters, E., Pasparakis, M., Gijbels, M. J. J., Vergouwe, M. N., Partouns-Hendriks, I., Fijneman, R. J. A., Clausen, B. E., Förster, I., Kockx, M. M., Rajewsky, K., Kraal, G., Hofker, M. H., & de Winther, M. P. J. (2003). Inhibition of NF- $\kappa$ B activation in macrophages increases atherosclerosis in LDL receptor-deficient mice. *The Journal of Clinical Investigation*, 112(8), 1176–1185. <https://doi.org/10.1172/JCI18580>

Karin, M., & Ben-Neriah, Y. (2000). Phosphorylation Meets Ubiquitination: The Control of NF- $\kappa$ B Activity. *Annual Review of Immunology*, 18(1), 621–663. <https://doi.org/10.1146/annurev.immunol.18.1.621>

Karin, M., & Delhase, M. (2000). The I kappa B kinase (IKK) and NF- $\kappa$ B B: Key elements of proinflammatory signalling. *Seminars in Immunology*, 12(1), 85–98. <https://doi.org/10.1006/smim.2000.0210>

Karin, M., Liu, Z., & Zandi, E. (1997). AP-1 function and regulation. *Current Opinion in Cell Biology*, 9(2), 240–246. [https://doi.org/10.1016/S0955-0674\(97\)80068-3](https://doi.org/10.1016/S0955-0674(97)80068-3)

Kassi, E., Spilioti, E., Nasiri-Ansari, N., Adamopoulos, C., Moutsatsou, P., Papapanagiotou, A., Siasos, G., Tousoulis, D., & Papavassiliou, A. G. (2015). Vascular Inflammation and Atherosclerosis: The Role of Estrogen Receptors. *Current Medicinal Chemistry*, 22(22), 2651–2665. <https://doi.org/10.2174/092986732266150608093607>

Kato, J., & Yoneda-Kato, N. (2009). Mammalian COP9 signalosome. *Genes to Cells*, 14(11), 1209–1225. <https://doi.org/10.1111/j.1365-2443.2009.01349.x>

Kaur, J., Adya, R., Tan, B. K., Chen, J., & Randeva, H. S. (2010). Identification of chemerin receptor (ChemR23) in human endothelial cells: Chemerin-induced endothelial angiogenesis. *Biochemical and Biophysical Research Communications*, 391(4), 1762–1768. <https://doi.org/10.1016/j.bbrc.2009.12.150>

Kayahara, M., Wang, X., & Tournier, C. (2005). Selective Regulation of c-jun Gene Expression by Mitogen-Activated Protein Kinases via the 12-O-Tetradecanoylphorbol-13-Acetate- Responsive Element and Myocyte Enhancer Factor 2 Binding Sites. *Molecular and Cellular Biology*, 25(9), 3784–3792. <https://doi.org/10.1128/MCB.25.9.3784-3792.2005>

Keidar, S., Heinrich, R., Kaplan, M., Hayek, T., & Aviram, M. (2001). Angiotensin II administration to atherosclerotic mice increases macrophage uptake of oxidized LDL: A possible role for

interleukin-6. *Arteriosclerosis, Thrombosis, and Vascular Biology*, 21(9), 1464–1469. <https://doi.org/10.1161/hq0901.095547>

Kelley, J. L., Ozment, T. R., Li, C., Schweitzer, J. B., & Williams, D. L. (2014). Scavenger Receptor-A (CD204): A Two-Edged Sword in Health and Disease. *Critical Reviews&trade; in Immunology*, 34(3). <https://doi.org/10.1615/CritRevImmunol.2014010267>

Kelly-Arnold, A., Maldonado, N., Laudier, D., Aikawa, E., Cardoso, L., & Weinbaum, S. (2013). Revised microcalcification hypothesis for fibrous cap rupture in human coronary arteries. *Proceedings of the National Academy of Sciences of the United States of America*, 110(26), 10741–10746. <https://doi.org/10.1073/pnas.1308814110>

Khan, R., Spagnoli, V., Tardif, J.-C., & L'Allier, P. L. (2015). Novel anti-inflammatory therapies for the treatment of atherosclerosis. *Atherosclerosis*, 240(2), 497–509. <https://doi.org/10.1016/j.atherosclerosis.2015.04.783>

Kim, B.-C., Lee, H.-J., Park, S. H., Lee, S. R., Karpova, T. S., McNally, J. G., Felici, A., Lee, D. K., & Kim, S.-J. (2004). Jab1/CSN5, a Component of the COP9 Signalosome, Regulates Transforming Growth Factor  $\beta$  Signaling by Binding to Smad7 and Promoting Its Degradation. *Molecular and Cellular Biology*, 24(6), 2251–2262. <https://doi.org/10.1128/MCB.24.6.2251-2262.2004>

Kim, D. N., Schmee, J., Lee, K. T., & Thomas, W. A. (1987). Atherosclerotic lesions in the coronary arteries of hyperlipidemic swine Part 1. Cell increases, divisions, losses and cells of origin in first 90 days on diet. *Atherosclerosis*, 64(2), 231–242. [https://doi.org/10.1016/0021-9150\(87\)90251-6](https://doi.org/10.1016/0021-9150(87)90251-6)

Kim, K., Shim, D., Lee, J. S., Zaitsev, K., Williams, J. W., Kim, K.-W., Jang, M.-Y., Seok Jang, H., Yun, T. J., Lee, S. H., Yoon, W. K., Prat, A., Seidah, N. G., Choi, J., Lee, S.-P., Yoon, S.-H., Nam, J. W., Seong, J. K., Oh, G. T., ... Choi, J.-H. (2018). Transcriptome Analysis Reveals Nonfoamy Rather Than Foamy Plaque Macrophages Are Proinflammatory in Atherosclerotic Murine Models. *Circulation Research*, 123(10), 1127–1142. <https://doi.org/10.1161/CIRCRESAHA.118.312804>

Kim, S. J., Rabbani, Z. N., Dewhirst, M. W., Vujskovic, Z., Vollmer, R. T., Schreiber, E.-G., Oosterwijk, E., & Kelley, M. J. (2005). Expression of HIF-1 $\alpha$ , CA IX, VEGF, and MMP-9 in surgically resected non-small cell lung cancer. *Lung Cancer*, 49(3), 325–335. <https://doi.org/10.1016/j.lungcan.2005.03.036>

Kiss, R. S., Elliott, M. R., Ma, Z., Marcel, Y. L., & Ravichandran, K. S. (2006). Apoptotic Cells Induce a Phosphatidylserine-Dependent Homeostatic Response from Phagocytes. *Current Biology*, 16(22), 2252–2258. <https://doi.org/10.1016/j.cub.2006.09.043>

Kisseleva, T., Song, L., Vorontchikhina, M., Feirt, N., Kitajewski, J., & Schindler, C. (2006). NF- $\kappa$ B regulation of endothelial cell function during LPS-induced toxemia and cancer. *The Journal of Clinical Investigation*, 116(11), 2955–2963. <https://doi.org/10.1172/JCI27392>

Kitagawa, K., Matsumoto, M., Sasaki, T., Hashimoto, H., Kuwabara, K., Ohtsuki, T., & Hori, M. (2002). Involvement of ICAM-1 in the progression of atherosclerosis in APOE-knockout mice. *Atherosclerosis*, 160(2), 305–310. [https://doi.org/10.1016/s0021-9150\(01\)00587-1](https://doi.org/10.1016/s0021-9150(01)00587-1)

Kleemann, R., Hauser, A., Geiger, G., Mischke, R., Burger-Kentischer, A., Flieger, O., Johannes, F.-J., Roger, T., Calandra, T., Kapurniotu, A., Grell, M., Finkelmeier, D., Brunner, H., & Bernhagen, J. (2000). Intracellular action of the cytokine MIF to modulate AP-1 activity and the cell cycle through Jab1. *Nature*, 408(6809), 211–216. <https://doi.org/10.1038/35041591>

Kleemann, R., Zadelaar, S., & Kooistra, T. (2008). Cytokines and atherosclerosis: A comprehensive review of studies in mice. *Cardiovascular Research*, 79(3), 360–376. <https://doi.org/10.1093/cvr/cvn120>

Kloc, M., Uosef, A., Kubiak, J. Z., & Ghobrial, R. M. (2021). Role of Macrophages and RhoA Pathway in Atherosclerosis. *International Journal of Molecular Sciences*, 22(1), 216. <https://doi.org/10.3390/ijms22010216>

Koenig, W., & Khuseyinova, N. (2007). Biomarkers of atherosclerotic plaque instability and rupture. *Arteriosclerosis, Thrombosis, and Vascular Biology*, 27(1), 15–26. <https://doi.org/10.1161/01.ATV.0000251503.35795.4f>

Kojima, Y., Weissman, I. L., & Leeper, N. J. (2017). The Role of Efferocytosis in Atherosclerosis. *Circulation*, 135(5), 476–489. <https://doi.org/10.1161/CIRCULATIONAHA.116.025684>

Koltsova, E. K., Garcia, Z., Chodaczek, G., Landau, M., McArdle, S., Scott, S. R., von Vietinghoff, S., Galkina, E., Miller, Y. I., Acton, S. T., & Ley, K. (2012). Dynamic T cell-APC interactions sustain chronic inflammation in atherosclerosis. *The Journal of Clinical Investigation*, 122(9), 3114–3126. <https://doi.org/10.1172/JCI61758>

Koo, A., Dewey, C. F., & García-Cardeña, G. (2013). Hemodynamic shear stress characteristic of atherosclerosis-resistant regions promotes glycocalyx formation in cultured endothelial cells. *American Journal of Physiology. Cell Physiology*, 304(2), C137-146. <https://doi.org/10.1152/ajpcell.00187.2012>

Kovačević, I., Sakaue, T., Majoleé, J., Pronk, M. C., Maekawa, M., Geerts, D., Fernandez-Borja, M., Higashiyama, S., & Hordijk, P. L. (2018). The Cullin-3-Rbx1-KCTD10 complex controls endothelial barrier function via K63 ubiquitination of RhoB. *The Journal of Cell Biology*, 217(3), 1015–1032. <https://doi.org/10.1083/jcb.201606055>

Kremastiotis, G., Handa, I., Jackson, C., George, S., & Johnson, J. (2021). Disparate effects of MMP and TIMP modulation on coronary atherosclerosis and associated myocardial fibrosis. *Scientific Reports*, 11(1), 23081. <https://doi.org/10.1038/s41598-021-02508-4>

Kruth, H. S., Jones, N. L., Huang, W., Zhao, B., Ishii, I., Chang, J., Combs, C. A., Malide, D., & Zhang, W.-Y. (2005). Macropinocytosis is the endocytic pathway that mediates macrophage foam cell formation with native low density lipoprotein. *The Journal of Biological Chemistry*, 280(3), 2352–2360. <https://doi.org/10.1074/jbc.M407167200>

Kumar, P., Hosaka, S., & Koch, A. E. (2001). Soluble E-selectin induces monocyte chemotaxis through Src family tyrosine kinases. *The Journal of Biological Chemistry*, 276(24), 21039–21045. <https://doi.org/10.1074/jbc.M009099200>

Kurz, T., Özlu, N., Rudolf, F., O'Rourke, S. M., Luke, B., Hofmann, K., Hyman, A. A., Bowerman, B., & Peter, M. (2005). The conserved protein DCN-1/Dcn1p is required for cullin neddylation in *C. elegans* and *S. cerevisiae*. *Nature*, 435(7046), 1257–1261. <https://doi.org/10.1038/nature03662>

Kyriakis, J. M., & Avruch, J. (2001). Mammalian mitogen-activated protein kinase signal transduction pathways activated by stress and inflammation. *Physiological Reviews*, 81(2), 807–869. <https://doi.org/10.1152/physrev.2001.81.2.807>

Lahoute, C., Herbin, O., Mallat, Z., & Tedgui, A. (2011). Adaptive immunity in atherosclerosis: Mechanisms and future therapeutic targets. *Nature Reviews Cardiology*, 8(6), 348–358. <https://doi.org/10.1038/nrcardio.2011.62>

Lawrence, T. (2009). The nuclear factor NF- $\kappa$ B pathway in inflammation. *Cold Spring Harbor Perspectives in Biology*, 1(6), a001651. <https://doi.org/10.1101/cshperspect.a001651>

Lee, G. W., Lee, T. H., & Vilcek, J. T. (1993). TSG-14, a tumor necrosis factor- and IL-1-inducible protein, is a novel member of the pentraxin family of acute phase proteins. *Journal of Immunology*, 150(5), 1804–1812.

Lee, J. C., Kassis, S., Kumar, S., Badger, A., & Adams, J. L. (1999). p38 mitogen-activated protein kinase inhibitors—Mechanisms and therapeutic potentials. *Pharmacology & Therapeutics*, 82(2–3), 389–397. [https://doi.org/10.1016/s0163-7258\(99\)00008-x](https://doi.org/10.1016/s0163-7258(99)00008-x)

Lee, J. Y., Chung, J., Kim, K. H., An, S. H., Kim, M., Park, J., & Kwon, K. (2018). Fluid shear stress regulates the expression of Lectin-like oxidized low density lipoprotein receptor-1 via KLF2-AP-1 pathway depending on its intensity and pattern in endothelial cells. *Atherosclerosis*, 270, 76–88. <https://doi.org/10.1016/j.atherosclerosis.2018.01.038>

Lei, D., Li, F., Su, H., Tian, Z., Ye, B., Wei, N., & Wang, X. (2011). COP9 signalosome subunit 8 is required for postnatal hepatocyte survival and effective proliferation. *Cell Death & Differentiation*, 18(2), 259–270. <https://doi.org/10.1038/cdd.2010.98>

Lemaître, V., Soloway, P. D., & D'Armiento, J. (2003). Increased medial degradation with pseudo-aneurysm formation in apolipoprotein E-knockout mice deficient in tissue inhibitor of metalloproteinases-1. *Circulation*, 107(2), 333–338. <https://doi.org/10.1161/01.cir.0000044915.37074.5c>

Leucker, T. M., Amat-Codina, N., Chelko, S., & Gerstenblith, G. (2021). *Proprotein Convertase Subtilisin/kexin Type 9 Links Inflammation to Vascular Endothelial Cell Dysfunction* (p. 2021.01.15.426820). <https://doi.org/10.1101/2021.01.15.426820>

Li, J., Liang, X., Wang, Y., Xu, Z., & Li, G. (2017). Investigation of highly expressed PCSK9 in atherosclerotic plaques and ox-LDL-induced endothelial cell apoptosis. *Molecular Medicine Reports*, 16(2), 1817–1825. <https://doi.org/10.3892/mmr.2017.6803>

Li, J., Zou, J., Littlejohn, R., Liu, J., & Su, H. (2020). Neddylation, an Emerging Mechanism Regulating Cardiac Development and Function. *Frontiers in Physiology*, 11, 1624. <https://doi.org/10.3389/fphys.2020.612927>

Li, L., & Deng, X. W. (2003). The COP9 signalosome: An alternative lid for the 26S proteasome? *Trends in Cell Biology*, 13(10), 507–509. <https://doi.org/10.1016/j.tcb.2003.08.002>

Li, M., Qian, M., Kyler, K., & Xu, J. (2018). Endothelial–Vascular Smooth Muscle Cells Interactions in Atherosclerosis. *Frontiers in Cardiovascular Medicine*, 5, 151. <https://doi.org/10.3389/fcvm.2018.00151>

Li, T., Li, X., Feng, Y., Dong, G., Wang, Y., & Yang, J. (2020). The Role of Matrix Metalloproteinase-9 in Atherosclerotic Plaque Instability. *Mediators of Inflammation*, 2020, e3872367. <https://doi.org/10.1155/2020/3872367>

Li, X., Zhang, Q., Nasser, M., Xu, L., Zhang, X., Zhu, P., He, Q., & Zhao, M. (2020). Oxygen homeostasis and cardiovascular disease: A role for HIF? *Biomedicine & Pharmacotherapy*, 128, 110338. <https://doi.org/10.1016/j.biopha.2020.110338>

Li, Y. Y., Feng, Y. Q., Kadokami, T., McTiernan, C. F., Draviam, R., Watkins, S. C., & Feldman, A. M. (2000). Myocardial extracellular matrix remodeling in transgenic mice overexpressing tumor necrosis factor  $\alpha$  can be modulated by anti-tumor necrosis factor  $\alpha$  therapy. *Proceedings of the National Academy of Sciences*, 97(23), 12746–12751. <https://doi.org/10.1073/pnas.97.23.12746>

Li, Z., Li, L., Zielke, H. R., Cheng, L., Xiao, R., Crow, M. T., Stetler-Stevenson, W. G., Froehlich, J., & Lakatta, E. G. (1996). Increased expression of 72-kd type IV collagenase (MMP-2) in human aortic atherosclerotic lesions. *The American Journal of Pathology*, 148(1), 121–128.

Liang, C., Zhang, M., & Sun, S.-C. (2006). Beta-TrCP binding and processing of NF- $\kappa$ B2/p100 involve its phosphorylation at serines 866 and 870. *Cellular Signalling*, 18(8), 1309–1317. <https://doi.org/10.1016/j.cellsig.2005.10.011>

Liao, G., Zhang, M., Harhaj, E. W., & Sun, S.-C. (2004). Regulation of the NF- $\kappa$ B-inducing kinase by tumor necrosis factor receptor-associated factor 3-induced degradation. *The Journal of Biological Chemistry*, 279(25), 26243–26250. <https://doi.org/10.1074/jbc.M403286200>

Libby, P. (2002a). Inflammation in atherosclerosis. *Nature*, 420(6917), 868–874. <https://doi.org/10.1038/nature01323>

Libby, P. (2002b). Inflammation in atherosclerosis. *Nature*, 420(6917), 868–874. <https://doi.org/10.1038/nature01323>

Libby, P. (2012). Inflammation in Atherosclerosis. *Arteriosclerosis, Thrombosis, and Vascular Biology*, 32(9), 2045–2051. <https://doi.org/10.1161/ATVBAHA.108.179705>

Libby, P., Aikawa, M., & Schönbeck, U. (2000). Cholesterol and atherosclerosis. *Biochimica Et Biophysica Acta*, 1529(1–3), 299–309. [https://doi.org/10.1016/s1388-1981\(00\)00161-x](https://doi.org/10.1016/s1388-1981(00)00161-x)

Libby, P., Buring, J. E., Badimon, L., Hansson, G. K., Deanfield, J., Bittencourt, M. S., Tokgözoglu, L., & Lewis, E. F. (2019). Atherosclerosis. *Nature Reviews Disease Primers*, 5(1), 56. <https://doi.org/10.1038/s41572-019-0106-z>

Libby, P., & Everett, B. M. (2019). Novel Antiatherosclerotic Therapies. *Arteriosclerosis, Thrombosis, and Vascular Biology*, 39(4), 538–545. <https://doi.org/10.1161/ATVBAHA.118.310958>

Libby, P., & Pasterkamp, G. (2015). Requiem for the “vulnerable plaque.” *European Heart Journal*, 36(43), 2984–2987. <https://doi.org/10.1093/eurheartj/ehv349>

Lillis, A. P., Muratoglu, S. C., Au, D. T., Migliorini, M., Lee, M.-J., Fried, S. K., Mikhailenko, I., & Strickland, D. K. (2016). Correction: LDL Receptor-Related Protein-1 (LRP1) Regulates Cholesterol Accumulation in Macrophages. *PLOS ONE*, 11(1), e0147457. <https://doi.org/10.1371/journal.pone.0147457>

Lin, J.-D., Nishi, H., Poles, J., Niu, X., Mccauley, C., Rahman, K., Brown, E. J., Yeung, S. T., Vozhilla, N., Weinstock, A., Ramsey, S. A., Fisher, E. A., & Loke, P. (2019). Single-cell analysis of fate-mapped macrophages reveals heterogeneity, including stem-like properties, during atherosclerosis progression and regression. *JCI Insight*, 4(4), 124574. <https://doi.org/10.1172/jci.insight.124574>

Lin, S., Saxena, N. K., Ding, X., Stein, L. L., & Anania, F. A. (2006). Leptin Increases Tissue Inhibitor of Metalloproteinase 1 (TIMP-1) Gene Expression by a Specificity Protein 1/Signal Transducer and Activator of Transcription 3 Mechanism. *Molecular Endocrinology (Baltimore, Md.)*, 20(12), 3376–3388. <https://doi.org/10.1210/me.2006-0177>

Lindeman, J. H. N., Abdul-Hussien, H., van Bockel, J. H., Wolterbeek, R., & Kleemann, R. (2009). Clinical trial of doxycycline for matrix metalloproteinase-9 inhibition in patients with an abdominal aneurysm: Doxycycline selectively depletes aortic wall neutrophils and cytotoxic T cells. *Circulation*, 119(16), 2209–2216. <https://doi.org/10.1161/CIRCULATIONAHA.108.806505>

Lingaraju, G. M., Bunker, R. D., Cavadini, S., Hess, D., Hassiepen, U., Renatus, M., Fischer, E. S., & Thomä, N. H. (2014). Crystal structure of the human COP9 signalosome. *Nature*, 512(7513), 161–165. <https://doi.org/10.1038/nature13566>

Liu, C., Guo, L.-Q., Menon, S., Jin, D., Pick, E., Wang, X., Deng, X. W., & Wei, N. (2013). COP9 Signalosome Subunit Csn8 Is Involved in Maintaining Proper Duration of the G1 Phase. *The Journal of Biological Chemistry*, 288(28), 20443–20452. <https://doi.org/10.1074/jbc.M113.468959>

Liu, G., Ye, X., Miller, E. J., & Liu, S. F. (2014). NF- $\kappa$ B-to-AP-1 Switch: A Mechanism Regulating Transition From Endothelial Barrier Injury to Repair in Endotoxemic Mice. *Scientific Reports*, 4(1), 5543. <https://doi.org/10.1038/srep05543>

Liu, H., Xiong, W., Luo, Y., Chen, H., He, Y., Cao, Y., & Dong, S. (2019). Adipokine Chemerin Stimulates Progression of Atherosclerosis in ApoE $^{-/-}$  Mice. *BioMed Research International*, 2019, e7157865. <https://doi.org/10.1155/2019/7157865>

Liu, J., Furukawa, M., Matsumoto, T., & Xiong, Y. (2002). NEDD8 modification of CUL1 dissociates p120(CAND1), an inhibitor of CUL1-SKP1 binding and SCF ligases. *Molecular Cell*, 10(6), 1511–1518. [https://doi.org/10.1016/s1097-2765\(02\)00783-9](https://doi.org/10.1016/s1097-2765(02)00783-9)

Liu, J., Xiong, W., Baca-Regen, L., Nagase, H., & Baxter, B. T. (2003). Mechanism of inhibition of matrix metalloproteinase-2 expression by doxycycline in human aortic smooth muscle cells. *Journal of Vascular Surgery*, 38(6), 1376–1383. [https://doi.org/10.1016/S0741-5214\(03\)01022-X](https://doi.org/10.1016/S0741-5214(03)01022-X)

Liu, T., Zhang, L., Joo, D., & Sun, S.-C. (2017a). NF-κB signaling in inflammation. *Signal Transduction and Targeted Therapy*, 2(1), 1–9. <https://doi.org/10.1038/sigtrans.2017.23>

Liu, T., Zhang, L., Joo, D., & Sun, S.-C. (2017b). NF-κB signaling in inflammation. *Signal Transduction and Targeted Therapy*, 2(1), 1–9. <https://doi.org/10.1038/sigtrans.2017.23>

Liu, Y., Shepherd, E. G., & Nelin, L. D. (2007). MAPK phosphatases—Regulating the immune response. *Nature Reviews Immunology*, 7(3), 202–212. <https://doi.org/10.1038/nri2035>

Lobato-Gil, S., Heidelberger, J. B., Maghames, C., Bailly, A., Brunello, L., Rodriguez, M. S., Beli, P., & Xirodimas, D. P. (2021). Proteome-wide identification of NEDD8 modification sites reveals distinct proteomes for canonical and atypical NEDDylation. *Cell Reports*, 34(3), 108635. <https://doi.org/10.1016/j.celrep.2020.108635>

Loftus, I. M., Naylor, A. R., Goodall, S., Crowther, M., Jones, L., Bell, P. R. F., & Thompson, M. M. (2000). Increased Matrix Metalloproteinase-9 Activity in Unstable Carotid Plaques. *Stroke*, 31(1), 40–47. <https://doi.org/10.1161/01.STR.31.1.40>

Logan, S. K., Garabedian, M. J., Campbell, C. E., & Werb, Z. (1996). Synergistic Transcriptional Activation of the Tissue Inhibitor of Metalloproteinases-1 Promoter via Functional Interaction of AP-1 and Ets-1 Transcription Factors. *Journal of Biological Chemistry*, 271(2), 774–782. <https://doi.org/10.1074/jbc.271.2.774>

Lok, Z. S. Y., & Lyle, A. N. (2019). Osteopontin in Vascular Disease. *Arteriosclerosis, Thrombosis, and Vascular Biology*, 39(4), 613–622. <https://doi.org/10.1161/ATVBAHA.118.311577>

Loor, G., & Schumacker, P. T. (2008). Role of hypoxia-inducible factor in cell survival during myocardial ischemia–reperfusion. *Cell Death & Differentiation*, 15(4), 686–690. <https://doi.org/10.1038/cdd.2008.13>

Lorenzatti, A. J. (2021). Anti-inflammatory Treatment and Cardiovascular Outcomes: Results of Clinical Trials. *European Cardiology Review*, 16, e15. <https://doi.org/10.15420/ecr.2020.51>

Lozito, T. P., & Tuan, R. S. (2012). Endothelial cell microparticles act as centers of matrix metalloproteinase-2 (MMP-2) activation and vascular matrix remodeling. *Journal of Cellular Physiology*, 227(2), 534–549. <https://doi.org/10.1002/jcp.22744>

Lu, Y., & Yang, X. (2020). The pivotal roles of neddylation pathway in immunoregulation. *Immunity, Inflammation and Disease*, 8(4), 782–792. <https://doi.org/10.1002/iid3.335>

Ludwig, A., Fechner, M., Wilck, N., Meiners, S., Grimbo, N., Baumann, G., Stangl, V., & Stangl, K. (2009). Potent anti-inflammatory effects of low-dose proteasome inhibition in the vascular system. *Journal of Molecular Medicine (Berlin, Germany)*, 87(8), 793–802. <https://doi.org/10.1007/s00109-009-0469-9>

Lusis, A. J. (2000). Atherosclerosis. *Nature*, 407(6801), 233–241. <https://doi.org/10.1038/35025203>

Luttun, A., Lutgens, E., Manderveld, A., Maris, K., Collen, D., Carmeliet, P., & Moons, L. (2004). Loss of Matrix Metalloproteinase-9 or Matrix Metalloproteinase-12 Protects Apolipoprotein E–Deficient Mice Against Atherosclerotic Media Destruction but Differentially Affects Plaque Growth. *Circulation*, 109(11), 1408–1414. <https://doi.org/10.1161/01.CIR.0000121728.14930.DE>

Lydeard, J. R., Schulman, B. A., & Harper, J. W. (2013). Building and remodelling Cullin–RING E3 ubiquitin ligases. *EMBO Reports*, 14(12), 1050–1061. <https://doi.org/10.1038/embor.2013.173>

Lykke-Andersen, K., Schaefer, L., Menon, S., Deng, X.-W., Miller, J. B., & Wei, N. (2003). Disruption of the COP9 Signalosome Csn2 Subunit in Mice Causes Deficient Cell Proliferation, Accumulation of p53 and Cyclin E, and Early Embryonic Death. *Molecular and Cellular Biology*. <https://doi.org/10.1128/MCB.23.19.6790-6797.2003>

Ma, J., & Chen, X. (2021). Anti-inflammatory Therapy for Coronary Atherosclerotic Heart Disease: Unanswered Questions Behind Existing Successes. *Frontiers in Cardiovascular Medicine*, 7, 415. <https://doi.org/10.3389/fcvm.2020.631398>

MacColl, E., & Khalil, R. A. (2015). Matrix Metalloproteinases as Regulators of Vein Structure and Function: Implications in Chronic Venous Disease. *The Journal of Pharmacology and Experimental Therapeutics*, 355(3), 410–428. <https://doi.org/10.1124/jpet.115.227330>

MacMicking, J., Xie, Q. W., & Nathan, C. (1997). Nitric oxide and macrophage function. *Annual Review of Immunology*, 15, 323–350. <https://doi.org/10.1146/annurev.immunol.15.1.323>

Madan, M., Bishayi, B., Hoge, M., Messas, E., & Amar, S. (2007). Doxycycline affects diet- and bacteria-associated atherosclerosis in an ApoE heterozygote murine model: Cytokine profiling implications. *Atherosclerosis*, 190(1), 62–72. <https://doi.org/10.1016/j.atherosclerosis.2006.02.026>

Magid, R., Murphy, T. J., & Galis, Z. S. (2003). Expression of matrix metalloproteinase-9 in endothelial cells is differentially regulated by shear stress. Role of c-Myc. *The Journal of Biological Chemistry*, 278(35), 32994–32999. <https://doi.org/10.1074/jbc.M304799200>

Majolée, J., Pronk, M. C. A., Jim, K. K., van Bezu, J. S. M., van der Sar, A. M., Hordijk, P. L., & Kovačević, I. (2019). CSN5 inhibition triggers inflammatory signaling and Rho/ROCK-dependent loss of endothelial integrity. *Scientific Reports*, 9(1), 8131. <https://doi.org/10.1038/s41598-019-44595-4>

Manning, M. W., Cassis, L. A., & Daugherty, A. (2003). Differential effects of doxycycline, a broad-spectrum matrix metalloproteinase inhibitor, on angiotensin II-induced atherosclerosis and abdominal aortic aneurysms. *Arteriosclerosis, Thrombosis, and Vascular Biology*, 23(3), 483–488. <https://doi.org/10.1161/01.ATV.0000058404.92759.32>

Manthey, C. L., Wang, S. W., Kinney, S. D., & Yao, Z. (1998). SB202190, a selective inhibitor of p38 mitogen-activated protein kinase, is a powerful regulator of LPS-induced mRNAs in monocytes. *Journal of Leukocyte Biology*, 64(3), 409–417. <https://doi.org/10.1002/jlb.64.3.409>

Marfella, R., D'Amico, M., Esposito, K., Baldi, A., Filippo, C. D., Siniscalchi, M., Sasso, F. C., Portoghesi, M., Cirillo, F., Cacciapuoti, F., Carbonara, O., Crescenzi, B., Baldi, F., Ceriello, A., Nicoletti, G. F., D'Andrea, F., Verza, M., Coppola, L., Rossi, F., & Giugliano, D. (2006). The Ubiquitin-Proteasome System and Inflammatory Activity in Diabetic Atherosclerotic Plaques: Effects of Rosiglitazone Treatment. *Diabetes*, 55(3), 622–632. <https://doi.org/10.2337/diabetes.55.03.06.db05-0832>

Marin, T., Gongol, B., Chen, Z., Woo, B., Subramaniam, S., Chien, S., & Shyy, J. Y.-J. (2013). Mechanosensitive microRNAs-role in endothelial responses to shear stress and redox state. *Free Radical Biology & Medicine*, 64, 61–68. <https://doi.org/10.1016/j.freeradbiomed.2013.05.034>

Martin, R. M., Gunnell, D., Whitley, E., Nicolaides, A., Griffin, M., Georgiou, N., Davey Smith, G., Ebrahim, S., & Holly, J. M. P. (2008). Associations of Insulin-Like Growth Factor (IGF)-I, IGF-II, IGF Binding Protein (IGFBP)-2 and IGFBP-3 with Ultrasound Measures of Atherosclerosis and Plaque Stability in an Older Adult Population. *The Journal of Clinical Endocrinology & Metabolism*, 93(4), 1331–1338. <https://doi.org/10.1210/jc.2007-2295>

Martinez, F. O., Gordon, S., Locati, M., & Mantovani, A. (2006). Transcriptional profiling of the human monocyte-to-macrophage differentiation and polarization: New molecules and patterns of gene expression. *Journal of Immunology (Baltimore, Md.: 1950)*, 177(10), 7303–7311. <https://doi.org/10.4049/jimmunol.177.10.7303>

Martinez, F. O., Sica, A., Mantovani, A., & Locati, M. (2008). Macrophage activation and polarization. *Frontiers in Bioscience: A Journal and Virtual Library*, 13, 453–461. <https://doi.org/10.2741/2692>

Martínez, G. J., Celermajer, D. S., & Patel, S. (2018). The NLRP3 inflammasome and the emerging role of colchicine to inhibit atherosclerosis-associated inflammation. *Atherosclerosis*, 269, 262–271. <https://doi.org/10.1016/j.atherosclerosis.2017.12.027>

Martinon, F., Pétrilli, V., Mayor, A., Tardivel, A., & Tschopp, J. (2006). Gout-associated uric acid crystals activate the NALP3 inflammasome. *Nature*, 440(7081), 237–241. <https://doi.org/10.1038/nature04516>

Masaki, T., & Sawamura, T. (2006). Endothelin and endothelial dysfunction. *Proceedings of the Japan Academy. Series B, Physical and Biological Sciences*, 82(1), 17–24.

Matsuzawa, Y., & Lerman, A. (2014). Endothelial Dysfunction and Coronary Artery Disease: Assessment, Prognosis and Treatment. *Coronary Artery Disease*, 25(8), 713–724. <https://doi.org/10.1097/MCA.0000000000000178>

Maxfield, F. R., & Tabas, I. (2005). Role of cholesterol and lipid organization in disease. *Nature*, 438(7068), 612–621. <https://doi.org/10.1038/nature04399>

McGILL, H. C., Geer, J. C., & Holman, R. L. (1957). Sites of vascular vulnerability in dogs demonstrated by Evans blue. *A.M.A. Archives of Pathology*, 64(3), 303–311.

McPherson, A. J., Snell, L. M., Mak, T. W., & Watts, T. H. (2012). Opposing roles for TRAF1 in the alternative versus classical NF-κB pathway in T cells. *The Journal of Biological Chemistry*, 287(27), 23010–23019. <https://doi.org/10.1074/jbc.M112.350538>

Medzhitov, R., & Janeway, C. (2000). Innate immunity. *The New England Journal of Medicine*, 343(5), 338–344. <https://doi.org/10.1056/NEJM200008033430506>

Meijer, C. A., Le Haen, P. A. A., van Dijk, R. A., Hira, M., Hamming, J. F., van Bockel, J. H., & Lindeman, J. H. (2012). Activator protein-1 (AP-1) signalling in human atherosclerosis: Results of a systematic evaluation and intervention study. *Clinical Science (London, England)*, 122(9), 421–428. <https://doi.org/10.1042/cs20110234>

Menon, S., Chi, H., Zhang, H., Deng, X. W., Flavell, R. A., & Wei, N. (2007). COP9 signalosome subunit 8 is essential for peripheral T cell homeostasis and antigen receptor-induced entry into

the cell cycle from quiescence. *Nature Immunology*, 8(11), 1236–1245. <https://doi.org/10.1038/ni1514>

Mercadante, A. A., & Raja, A. (2021). Anatomy, Arteries. In *StatPearls*. StatPearls Publishing. <http://www.ncbi.nlm.nih.gov/books/NBK547743/>

Mercurio, F., & Manning, A. M. (1999). NF-kappaB as a primary regulator of the stress response. *Oncogene*, 18(45), 6163–6171. <https://doi.org/10.1038/sj.onc.1203174>

Mestas, J., & Ley, K. (2008). Monocyte-endothelial cell interactions in the development of atherosclerosis. *Trends in Cardiovascular Medicine*, 18(6), 228–232. <https://doi.org/10.1016/j.tcm.2008.11.004>

Metzler, B., Hu, Y., Dietrich, H., & Xu, Q. (2000). Increased expression and activation of stress-activated protein kinases/c-Jun NH(2)-terminal protein kinases in atherosclerotic lesions coincide with p53. *The American Journal of Pathology*, 156(6), 1875–1886. [https://doi.org/10.1016/S0002-9440\(10\)65061-4](https://doi.org/10.1016/S0002-9440(10)65061-4)

Michlewski, S., Dransfield, I., Megson, I. L., & Rossi, A. G. (2009). Macrophage phagocytosis of apoptotic neutrophils is critically regulated by the opposing actions of pro-inflammatory and anti-inflammatory agents: Key role for TNF- $\alpha$ . *The FASEB Journal*, 23(3), 844–854. <https://doi.org/10.1096/fj.08-121228>

Migliorini, D., Bogaerts, S., Defever, D., Vyas, R., Denecker, G., Radaelli, E., Zwolinska, A., Depaepe, V., Hochepied, T., Skarnes, W. C., & Marine, J.-C. (2011). Cop1 constitutively regulates c-Jun protein stability and functions as a tumor suppressor in mice. *The Journal of Clinical Investigation*, 121(4), 1329–1343. <https://doi.org/10.1172/JCI45784>

Milic, J., Tian, Y., & Bernhagen, J. (2019). Role of the COP9 Signalosome (CSN) in Cardiovascular Diseases. *Biomolecules*, 9(6), 217. <https://doi.org/10.3390/biom9060217>

Mills, C. D., Kincaid, K., Alt, J. M., Heilman, M. J., & Hill, A. M. (2000). M-1/M-2 macrophages and the Th1/Th2 paradigm. *Journal of Immunology (Baltimore, Md.: 1950)*, 164(12), 6166–6173. <https://doi.org/10.4049/jimmunol.164.12.6166>

Milutinović, A., Šuput, D., & Zorc-Plesković, R. (2020). Pathogenesis of atherosclerosis in the tunica intima, media, and adventitia of coronary arteries: An updated review. *Bosnian Journal of Basic Medical Sciences*, 20(1), 21–30. <https://doi.org/10.17305/bjbjms.2019.4320>

Misawa, T., Takahama, M., Kozaki, T., Lee, H., Zou, J., Saitoh, T., & Akira, S. (2013). Microtubule-driven spatial arrangement of mitochondria promotes activation of the NLRP3 inflammasome. *Nature Immunology*, 14(5), 454–460. <https://doi.org/10.1038/ni.2550>

Misra, S., Shergill, U., Yang, B., Janardhanan, R., & Misra, K. D. (2010). Increased expression of HIF-1 $\alpha$ , VEGF-A and its receptors, MMP-2, TIMP-1, and ADAMTS-1 at the venous stenosis of arteriovenous fistula in a mouse model with renal insufficiency. *Journal of Vascular and Interventional Radiology*, 21(8), 1255–1261. <https://doi.org/10.1016/j.jvir.2010.02.043>

Mitra, R., O’Neil, G. L., Harding, I. C., Cheng, M. J., Mensah, S. A., & Ebong, E. E. (2017). Glycocalyx in Atherosclerosis-Relevant Endothelium Function and as a Therapeutic Target. *Current Atherosclerosis Reports*, 19(12), 63. <https://doi.org/10.1007/s11883-017-0691-9>

Mohindra, R., Agrawal, D. K., & Thankam, F. G. (2021). Altered Vascular Extracellular Matrix in the Pathogenesis of Atherosclerosis. *Journal of Cardiovascular Translational Research*, 14(4), 647–660. <https://doi.org/10.1007/s12265-020-10091-8>

Moreno, P. R., Purushothaman, K. R., Fuster, V., Echeverri, D., Truszczynska, H., Sharma, S. K., Badimon, J. J., & O’Connor, W. N. (2004). Plaque neovascularization is increased in ruptured atherosclerotic lesions of human aorta: Implications for plaque vulnerability. *Circulation*, 110(14), 2032–2038. <https://doi.org/10.1161/01.CIR.0000143233.87854.23>

Moreno, P. R., Purushothaman, K.-R., Sirol, M., Levy, A. P., & Fuster, V. (2006). Neovascularization in Human Atherosclerosis. *Circulation*, 113(18), 2245–2252. <https://doi.org/10.1161/CIRCULATIONAHA.105.578955>

Mori, M., Yoneda-Kato, N., Yoshida, A., & Kato, J. (2008). Stable Form of JAB1 Enhances Proliferation and Maintenance of Hematopoietic Progenitors \*. *Journal of Biological Chemistry*, 283(43), 29011–29021. <https://doi.org/10.1074/jbc.M804539200>

Mosser, D. M., & Edwards, J. P. (2008). Exploring the full spectrum of macrophage activation. *Nature Reviews Immunology*, 8(12), 958–969. <https://doi.org/10.1038/nri2448>

Mosser, D. M., & Handman, E. (1992). Treatment of murine macrophages with interferon-gamma inhibits their ability to bind leishmania promastigotes. *Journal of Leukocyte Biology*, 52(4), 369–376. <https://doi.org/10.1002/jlb.52.4.369>

Mozaffarian, D., Benjamin, E. J., Go, A. S., Arnett, D. K., Blaha, M. J., Cushman, M., de Ferranti, S., Després, J.-P., Fullerton, H. J., Howard, V. J., Huffman, M. D., Judd, S. E., Kissela, B. M., Lackland, D. T., Lichtman, J. H., Lisabeth, L. D., Liu, S., Mackey, R. H., Matchar, D. B., ... Turner, M. B. (2015). Heart Disease and Stroke Statistics—2015 Update. *Circulation*, 131(4), e29–e322. <https://doi.org/10.1161/CIR.0000000000000152>

Mullick, A. E., Soldau, K., Kiosses, W. B., Bell, T. A., Tobias, P. S., & Curtiss, L. K. (2008). Increased endothelial expression of Toll-like receptor 2 at sites of disturbed blood flow exacerbates early atherogenic events. *The Journal of Experimental Medicine*, 205(2), 373–383. <https://doi.org/10.1084/jem.20071096>

Murdoch, C., Muthana, M., Coffelt, S. B., & Lewis, C. E. (2008). The role of myeloid cells in the promotion of tumour angiogenesis. *Nature Reviews. Cancer*, 8(8), 618–631. <https://doi.org/10.1038/nrc2444>

Murphy, G., & Nagase, H. (2008). Progress in matrix metalloproteinase research. *Molecular Aspects of Medicine*, 29(5), 290–308. <https://doi.org/10.1016/j.mam.2008.05.002>

Muslin, A. J. (2008). MAPK signalling in cardiovascular health and disease: Molecular mechanisms and therapeutic targets. *Clinical Science (London, England: 1979)*, 115(7), 203–218. <https://doi.org/10.1042/CS20070430>

Mussbacher, M., Salzmann, M., Brostjan, C., Hoesel, B., Schoergenhofer, C., Datler, H., Hohensinner, P., Basílio, J., Petzelbauer, P., Assinger, A., & Schmid, J. A. (2019). Cell Type-Specific Roles of NF-κB Linking Inflammation and Thrombosis. *Frontiers in Immunology*, 10, 85. <https://doi.org/10.3389/fimmu.2019.00085>

Musti, A. M., Treier, M., & Bohmann, D. (1997). Reduced ubiquitin-dependent degradation of c-Jun after phosphorylation by MAP kinases. *Science (New York, N.Y.)*, 275(5298), 400–402. <https://doi.org/10.1126/science.275.5298.400>

Nagase, H., Visse, R., & Murphy, G. (2006). Structure and function of matrix metalloproteinases and TIMPs. *Cardiovascular Research*, 69(3), 562–573. <https://doi.org/10.1016/j.cardiores.2005.12.002>

Nagelin, M. H., Srinivasan, S., Nadler, J. L., & Hedrick, C. C. (2009). Murine 12/15-Lipoxygenase Regulates ATP-binding Cassette Transporter G1 Protein Degradation through p38- and JNK2-dependent Pathways. *The Journal of Biological Chemistry*, 284(45), 31303–31314. <https://doi.org/10.1074/jbc.M109.028910>

Nakashima, Y., Fujii, H., Sumiyoshi, S., Wight, T. N., & Sueishi, K. (2007). Early human atherosclerosis: Accumulation of lipid and proteoglycans in intimal thickenings followed by macrophage infiltration. *Arteriosclerosis, Thrombosis, and Vascular Biology*, 27(5), 1159–1165. <https://doi.org/10.1161/ATVBAHA.106.134080>

Nakashima, Y., Wight, T. N., & Sueishi, K. (2008). Early atherosclerosis in humans: Role of diffuse intimal thickening and extracellular matrix proteoglycans. *Cardiovascular Research*, 79(1), 14–23. <https://doi.org/10.1093/cvr/cvn099>

Nakaya, M., Tanaka, M., Okabe, Y., Hanayama, R., & Nagata, S. (2006). Opposite Effects of Rho Family GTPases on Engulfment of Apoptotic Cells by Macrophages \*. *Journal of Biological Chemistry*, 281(13), 8836–8842. <https://doi.org/10.1074/jbc.M510972200>

Narula, J., Garg, P., Achenbach, S., Motoyama, S., Virmani, R., & Strauss, H. W. (2008). Arithmetic of vulnerable plaques for noninvasive imaging. *Nature Clinical Practice Cardiovascular Medicine*, 5(2), S2–S10. <https://doi.org/10.1038/ncpcardio1247>

Naumann, M., Bech-Otschir, D., Huang, X., Ferrell, K., & Dubiel, W. (1999). COP9 Signalosome-directed c-Jun Activation/Stabilization Is Independent of JNK \*. *Journal of Biological Chemistry*, 274(50), 35297–35300. <https://doi.org/10.1074/jbc.274.50.35297>

Navab, M., Fogelman, A. M., Berliner, J. A., Territo, M. C., Demer, L. L., Frank, J. S., Watson, A. D., Edwards, P. A., & Lusis, A. J. (1995). Pathogenesis of atherosclerosis. *The American Journal of Cardiology*, 76(9), 18C–23C. [https://doi.org/10.1016/s0002-9149\(99\)80466-4](https://doi.org/10.1016/s0002-9149(99)80466-4)

Nee, L. E., McMorrow, T., Campbell, E., Slattery, C., & Ryan, M. P. (2004). TNF-α and IL-1β-mediated regulation of MMP-9 and TIMP-1 in renal proximal tubular cells. *Kidney International*, 66(4), 1376–1386. <https://doi.org/10.1111/j.1523-1755.2004.00900.x>

Newby, A. C. (2005). Dual Role of Matrix Metalloproteinases (Matrixins) in Intimal Thickening and Atherosclerotic Plaque Rupture. *Physiological Reviews*, 85(1), 1–31. <https://doi.org/10.1152/physrev.00048.2003>

Newby, A. C. (2007). Metalloproteinases and Vulnerable Atherosclerotic Plaques. *Trends in Cardiovascular Medicine*, 17(8), 253–258. <https://doi.org/10.1016/j.tcm.2007.09.001>

Newby, A. C. (2016). Metalloproteinase production from macrophages – a perfect storm leading to atherosclerotic plaque rupture and myocardial infarction. *Experimental Physiology*, 101(11), 1327–1337. <https://doi.org/10.1113/EP085567>

Nguyen, H. C., Wang, W., & Xiong, Y. (2017). Cullin-RING E3 Ubiquitin Ligases: Bridges to Destruction. *Sub-Cellular Biochemistry*, 83, 323–347. [https://doi.org/10.1007/978-3-319-46503-6\\_12](https://doi.org/10.1007/978-3-319-46503-6_12)

Niccoli, G., Montone, R. A., Sabato, V., & Crea, F. (2018). Role of Allergic Inflammatory Cells in Coronary Artery Disease. *Circulation*, 138(16), 1736–1748. <https://doi.org/10.1161/CIRCULATIONAHA.118.035400>

Nidorf, S. M., Eikelboom, J. W., Budgeon, C. A., & Thompson, P. L. (2013). Low-Dose Colchicine for Secondary Prevention of Cardiovascular Disease. *Journal of the American College of Cardiology*, 61(4), 404–410. <https://doi.org/10.1016/j.jacc.2012.10.027>

Nishimoto, A., Lu, L., Hayashi, M., Nishiya, T., Horinouchi, T., & Miwa, S. (2010). Jab1 regulates levels of endothelin type A and B receptors by promoting ubiquitination and degradation. *Biochemical and Biophysical Research Communications*, 391(4), 1616–1622. <https://doi.org/10.1016/j.bbrc.2009.12.087>

Nissen, S. E., Tuzcu, E. M., Schoenhagen, P., Crowe, T., Sasiela, W. J., Tsai, J., Orazem, J., Magorien, R. D., O'Shaughnessy, C., & Ganz, P. (2005). Statin Therapy, LDL Cholesterol, C-Reactive Protein, and Coronary Artery Disease. *New England Journal of Medicine*, 352(1), 29–38. <https://doi.org/10.1056/NEJMoa042000>

Nomura, Y., Nakano, M., Woo Sung, H., Han, M., & Pandey, D. (2021). Inhibition of HDAC6 Activity Protects Against Endothelial Dysfunction and Atherogenesis in vivo: A Role for HDAC6 Neddylation. *Frontiers in Physiology*, 12, 838. <https://doi.org/10.3389/fphys.2021.675724>

Nonino, C. B., Noronha, N. Y., de Araújo Ferreira-Julio, M., Moriguchi Watanabe, L., Cassia, K. F., Ferreira Nicoletti, C., Rossi Welendorf, C., Salgado Junior, W., Rossi Silva Souza, D., & Augusta de Souza Pinhel, M. (2021). Differential Expression of MMP2 and TIMP2 in Peripheral Blood Mononuclear Cells After Roux-en-Y Gastric Bypass. *Frontiers in Nutrition*, 8, 773. <https://doi.org/10.3389/fnut.2021.628759>

Norata, G. D., Garlanda, C., & Catapano, A. L. (2010). The Long Pentraxin PTX3: A Modulator of the Immunoinflammatory Response in Atherosclerosis and Cardiovascular Diseases. *Trends in Cardiovascular Medicine*, 20(2), 35–40. <https://doi.org/10.1016/j.tcm.2010.03.005>

Novack, V., MacFadyen, J., Malhotra, A., Almog, Y., Glynn, R. J., & Ridker, P. M. (2012). The effect of rosuvastatin on incident pneumonia: Results from the JUPITER trial. *CMAJ*, 184(7), E367–E372. <https://doi.org/10.1503/cmaj.111017>

Oeckinghaus, A., & Ghosh, S. (2009). The NF-κB Family of Transcription Factors and Its Regulation. *Cold Spring Harbor Perspectives in Biology*, 1(4), a000034. <https://doi.org/10.1101/csdperspect.a000034>

Ogura, M., Ayaori, M., Terao, Y., Hisada, T., Iizuka, M., Takiguchi, S., Uto-Kondo, H., Yakushiji, E., Nakaya, K., Sasaki, M., Komatsu, T., Ozasa, H., Ohsuzu, F., & Ikewaki, K. (2011). Proteasomal inhibition promotes ATP-binding cassette transporter A1 (ABCA1) and ABCG1 expression and cholesterol efflux from macrophages in vitro and in vivo. *Arteriosclerosis, Thrombosis, and Vascular Biology*, 31(9), 1980–1987. <https://doi.org/10.1161/ATVBAHA.111.228478>

Okamoto, H. (2007). Osteopontin and cardiovascular system. *Molecular and Cellular Biochemistry*, 300(1), 1–7. <https://doi.org/10.1007/s11010-006-9368-3>

Olejarcz, W., Łacheta, D., & Kubiak-Tomaszewska, G. (2020). Matrix Metalloproteinases as Biomarkers of Atherosclerotic Plaque Instability. *International Journal of Molecular Sciences*, 21(11), 3946. <https://doi.org/10.3390/ijms21113946>

Orbe, J., Fernandez, L., Rodríguez, J. A., Rábago, G., Belzunce, M., Monasterio, A., Roncal, C., & Páramo, J. A. (2003). Different expression of MMPs/TIMP-1 in human atherosclerotic lesions. Relation to plaque features and vascular bed. *Atherosclerosis*, 170(2), 269–276. [https://doi.org/10.1016/s0021-9150\(03\)00251-x](https://doi.org/10.1016/s0021-9150(03)00251-x)

Osto, E., Matter, C. M., Kouroedov, A., Malinski, T., Bachschmid, M., Camici, G. G., Kilic, U., Stallmach, T., Boren, J., Iliceto, S., Lüscher, T. F., & Cosentino, F. (2008). C-Jun N-terminal kinase 2 deficiency protects against hypercholesterolemia-induced endothelial dysfunction and oxidative stress. *Circulation*, 118(20), 2073–2080. <https://doi.org/10.1161/CIRCULATIONAHA.108.765032>

Otsuka, F., Kramer, M. C. A., Woudstra, P., Yahagi, K., Ladich, E., Finn, A. V., de Winter, R. J., Kolodgie, F. D., Wight, T. N., Davis, H. R., Joner, M., & Virmani, R. (2015). Natural progression of atherosclerosis from pathologic intimal thickening to late fibroatheroma in human coronary arteries: A pathology study. *Atherosclerosis*, 241(2), 772–782. <https://doi.org/10.1016/j.atherosclerosis.2015.05.011>

Otsuka, F., Sakakura, K., Yahagi, K., Joner, M., & Virmani, R. (2014). Has our understanding of calcification in human coronary atherosclerosis progressed? *Arteriosclerosis, Thrombosis, and Vascular Biology*, 34(4), 724–736. <https://doi.org/10.1161/ATVBAHA.113.302642>

Otsuka, F., Yasuda, S., Noguchi, T., & Ishibashi-Ueda, H. (2016). Pathology of coronary atherosclerosis and thrombosis. *Cardiovascular Diagnosis and Therapy*, 6(4), 396–408. <https://doi.org/10.21037/cdt.2016.06.01>

Ouyang, W., & Frucht, D. M. (2021). Erk1/2 Inactivation-Induced c-Jun Degradation Is Regulated by Protein Phosphatases, UBE2d3, and the C-Terminus of c-Jun. *International Journal of Molecular Sciences*, 22(8), 3889. <https://doi.org/10.3390/ijms22083889>

Owsiany, K. M., Alencar, G. F., & Owens, G. K. (2019). Revealing the Origins of Foam Cells in Atherosclerotic Lesions. *Arteriosclerosis, Thrombosis, and Vascular Biology*, 39(5), 836–838. <https://doi.org/10.1161/ATVBAHA.119.312557>

Pacurar, D. I., Pacurar, M. L., Lakehal, A., Pacurar, A. M., Ranjan, A., & Bellini, C. (2017). The Arabidopsis Cop9 signalosome subunit 4 (CSN4) is involved in adventitious root formation. *Scientific Reports*, 7(1), 628. <https://doi.org/10.1038/s41598-017-00744-1>

Pandey, D., Hori, D., Kim, J. H., Bergman, Y., Berkowitz, D. E., & Romer, L. H. (2015). NEDDylation promotes endothelial dysfunction: A role for HDAC2. *Journal of Molecular and Cellular Cardiology*, 81, 18–22. <https://doi.org/10.1016/j.jmcc.2015.01.019>

Paone, S., Baxter, A. A., Hulett, M. D., & Poon, I. K. H. (2019). Endothelial cell apoptosis and the role of endothelial cell-derived extracellular vesicles in the progression of atherosclerosis. *Cellular and Molecular Life Sciences*, 76(6), 1093–1106. <https://doi.org/10.1007/s00018-018-2983-9>

Pariano, M., Pieroni, S., De Luca, A., Iannitti, R. G., Borghi, M., Puccetti, M., Giovagnoli, S., Renga, G., D’Onofrio, F., Bellet, M. M., Stincardini, C., Della-Fazia, M. A., Servillo, G., van de Veerdonk, F. L., Costantini, C., & Romani, L. (2021). Anakinra Activates Superoxide Dismutase 2 to Mitigate Inflammasome Activity. *International Journal of Molecular Sciences*, 22(12), 6531. <https://doi.org/10.3390/ijms22126531>

Park, H.-S., Ju, U.-I., Park, J.-W., Song, J. Y., Shin, D. H., Lee, K.-H., Jeong, L. S., Yu, J., Lee, H. W., Cho, J. Y., Kim, S. Y., Kim, S. W., Kim, J. B., Park, K. S., & Chun, Y.-S. (2016). PPAR $\gamma$  neddylation essential for adipogenesis is a potential target for treating obesity. *Cell Death and Differentiation*, 23(8), 1296–1311. <https://doi.org/10.1038/cdd.2016.6>

Park, J.-G., Ryu, S. Y., Jung, I.-H., Lee, Y.-H., Kang, K. J., Lee, M.-R., Lee, M.-N., Sonn, S. K., Lee, J. H., Lee, H., Oh, G. T., Moon, K., & Shim, H. (2013). Evaluation of VCAM-1 antibodies as therapeutic agent for atherosclerosis in apolipoprotein E-deficient mice. *Atherosclerosis*, 226(2), 356–363. <https://doi.org/10.1016/j.atherosclerosis.2012.11.029>

Park, K.-H., & Park, W. J. (2015). Endothelial Dysfunction: Clinical Implications in Cardiovascular Disease and Therapeutic Approaches. *Journal of Korean Medical Science*, 30(9), 1213–1225. <https://doi.org/10.3346/jkms.2015.30.9.1213>

Park, Y. M. (2014). CD36, a scavenger receptor implicated in atherosclerosis. *Experimental & Molecular Medicine*, 46, e99. <https://doi.org/10.1038/emm.2014.38>

Passlick, B., Flieger, D., & Ziegler-Heitbrock, H. W. (1989). Identification and characterization of a novel monocyte subpopulation in human peripheral blood. *Blood*, 74(7), 2527–2534.

Pawlowska, M., Gajda, M., Pyka-Fosciak, G., Toton-Zuranska, J., Niepsuj, A., Kus, K., Bujak-Gizycka, B., Suski, M., Olszanecki, R., Jawien, J., & Korbut, R. (2011). The effect of doxycycline on atherogenesis in apoE-knockout mice. *Journal of Physiology and Pharmacology: An Official Journal of the Polish Physiological Society*, 62(2), 247–250.

Pearson, G., Robinson, F., Gibson, T. B., Xu, B.-E., Karandikar, M., Berman, K., & Cobb, M. H. (2001). *Mitogen-Activated Protein (MAP) Kinase Pathways: Regulation and Physiological Functions*. 22(2), 31.

Peeters, W., Hellings, W. E., de Kleijn, D. P. V., de Vries, J. P. P. M., Moll, F. L., Vink, A., & Pasterkamp, G. (2009). Carotid atherosclerotic plaques stabilize after stroke: Insights into the natural process of atherosclerotic plaque stabilization. *Arteriosclerosis, Thrombosis, and Vascular Biology*, 29(1), 128–133. <https://doi.org/10.1161/ATVBAHA.108.173658>

Peeters, W., Moll, F. L., Vink, A., van der Spek, P. J., de Kleijn, D. P. V., de Vries, J.-P. P. M., Verheijen, J. H., Newby, A. C., & Pasterkamp, G. (2011). Collagenase matrix metalloproteinase-8 expressed in atherosclerotic carotid plaques is associated with systemic cardiovascular outcome. *European Heart Journal*, 32(18), 2314–2325. <https://doi.org/10.1093/eurheartj/ehq517>

Peng, Z., Serino, G., & Deng, X.-W. (2001). Molecular Characterization of Subunit 6 of the COP9 Signalosome and Its Role in Multifaceted Developmental Processes in Arabidopsis. *The Plant Cell*, 13(11), 2393–2407. <https://doi.org/10.1105/tpc.010248>

Petroski, M. D., & Deshaies, R. J. (2005). Function and regulation of cullin-RING ubiquitin ligases. *Nature Reviews. Molecular Cell Biology*, 6(1), 9–20. <https://doi.org/10.1038/nrm1547>

Petzold, T., Orr, A. W., Hahn, C., Jhaveri, K. A., Parsons, J. T., & Schwartz, M. A. (2009). Focal adhesion kinase modulates activation of NF- $\kappa$ B by flow in endothelial cells. *American Journal of Physiology-Cell Physiology*, 297(4), C814–C822. <https://doi.org/10.1152/ajpcell.00226.2009>

Phatharajaree, W., Phrommintikul, A., & Chattipakorn, N. (2007). Matrix metalloproteinases and myocardial infarction. *The Canadian Journal of Cardiology*, 23(9), 727–733.

Phillipson, M., Heit, B., Colarusso, P., Liu, L., Ballantyne, C. M., & Kubes, P. (2006). Intraluminal crawling of neutrophils to emigration sites: A molecularly distinct process from adhesion in the recruitment cascade. *The Journal of Experimental Medicine*, 203(12), 2569–2575. <https://doi.org/10.1084/jem.20060925>

Phillipson, M., Heit, B., Parsons, S. A., Petri, B., Mullaly, S. C., Colarusso, P., Gower, R. M., Neely, G., Simon, S. I., & Kubes, P. (2009). Vav1 is Essential for Mechanotactic Crawling and Migration of Neutrophils out of the Inflamed Microvasculature. *Journal of Immunology (Baltimore, Md. : 1950)*, 182(11), 6870–6878. <https://doi.org/10.4049/jimmunol.0803414>

Piepoli, M. F., Hoes, A. W., Agewall, S., Albus, C., Brotons, C., Catapano, A. L., Cooney, M.-T., Corrà, U., Cosyns, B., Deaton, C., Graham, I., Hall, M. S., Hobbs, F. D. R., Løchen, M.-L., Löllgen, H., Marques-Vidal, P., Perk, J., Prescott, E., Redon, J., ... ESC Scientific Document Group. (2016). 2016 European Guidelines on cardiovascular disease prevention in clinical practice: The Sixth Joint Task Force of the European Society of Cardiology and Other Societies on Cardiovascular Disease Prevention in Clinical Practice (constituted by representatives of 10 societies and by invited experts) Developed with the special contribution of the European Association for Cardiovascular Prevention & Rehabilitation (EACPR). *European Heart Journal*, 37(29), 2315–2381. <https://doi.org/10.1093/eurheartj/ehw106>

Pierce, N. W., Lee, J. E., Liu, X., Sweredoski, M. J., Graham, R. L. J., Larimore, E. A., Rome, M., Zheng, N., Clurman, B. E., Hess, S., Shan, S., & Deshaies, R. J. (2013). Cand1 promotes assembly of new SCF complexes through dynamic exchange of F box proteins. *Cell*, 153(1), 206–215. <https://doi.org/10.1016/j.cell.2013.02.024>

Piqueras, L., & Sanz, M.-J. (2020). Angiotensin II and leukocyte trafficking: New insights for an old vascular mediator. Role of redox-signaling pathways. *Free Radical Biology & Medicine*, 157, 38–54. <https://doi.org/10.1016/j.freeradbiomed.2020.02.002>

Pober, J. S., & Sessa, W. C. (2007). Evolving functions of endothelial cells in inflammation. *Nature Reviews Immunology*, 7(10), 803–815. <https://doi.org/10.1038/nri2171>

Ponnuchamy, B., & Khalil, R. A. (2008). Role of ADAMs in Endothelial Cell Permeability. Cadherin Shedding and Leukocyte Rolling. *Circulation Research*, 102(10), 1139–1142. <https://doi.org/10.1161/CIRCRESAHA.108.177394>

Potere, N., Del Buono, M. G., Mauro, A. G., Abbate, A., & Toldo, S. (2019). Low Density Lipoprotein Receptor-Related Protein-1 in Cardiac Inflammation and Infarct Healing. *Frontiers in Cardiovascular Medicine*, 6, 51. <https://doi.org/10.3389/fcvm.2019.00051>

Powell, S. R. (2006). The ubiquitin-proteasome system in cardiac physiology and pathology. *American Journal of Physiology. Heart and Circulatory Physiology*, 291(1), H1–H19. <https://doi.org/10.1152/ajpheart.00062.2006>

Powell, S. R., Herrmann, J., Lerman, A., Patterson, C., & Wang, X. (2012). The ubiquitin-proteasome system and cardiovascular disease. *Progress in Molecular Biology and Translational Science*, 109, 295–346. <https://doi.org/10.1016/B978-0-12-397863-9.00009-2>

Prashar, Y., Ritu, Bais, S., & Gill, N. S. (2017). Emerging role of various signaling pathways in the pathogenesis and therapeutics of atherosclerosis. *Reviews in Vascular Medicine*, 10–11, 1–12. <https://doi.org/10.1016/j.rvm.2017.05.001>

Prioreschi, P. (1967). Coronary thrombosis and myocardial infarction. *Canadian Medical Association Journal*, 97(22), 1339–1344.

Pruessmeyer, J., Hess, F. M., Alert, H., Groth, E., Pasqualon, T., Schwarz, N., Nyamoya, S., Kollert, J., van der Vorst, E., Donners, M., Martin, C., Uhlig, S., Saftig, P., Dreymueller, D., & Ludwig, A. (2014). Leukocytes require ADAM10 but not ADAM17 for their migration and inflammatory recruitment into the alveolar space. *Blood*, 123(26), 4077–4088. <https://doi.org/10.1182/blood-2013-09-511543>

Puchtler, H., Waldrop, F. S., & Valentine, L. S. (1973). Polarization Microscopic Studies of Connective Tissue Stained with Picro-Sirius Red FBA. *Beiträge Zur Pathologie*, 150(2), 174–187. [https://doi.org/10.1016/S0005-8165\(73\)80016-2](https://doi.org/10.1016/S0005-8165(73)80016-2)

Pueyo, M. E., Gonzalez, W., Nicoletti, A., Savoie, F., Arnal, J.-F., & Michel, J.-B. (2000). Angiotensin II Stimulates Endothelial Vascular Cell Adhesion Molecule-1 via Nuclear Factor- $\kappa$ B Activation Induced by Intracellular Oxidative Stress. *Arteriosclerosis, Thrombosis, and Vascular Biology*, 20(3), 645–651. <https://doi.org/10.1161/01.ATV.20.3.645>

Qi, Y.-X., Jiang, J., Jiang, X.-H., Wang, X.-D., Ji, S.-Y., Han, Y., Long, D.-K., Shen, B.-R., Yan, Z.-Q., Chien, S., & Jiang, Z.-L. (2011). PDGF-BB and TGF- $\beta$ 1 on cross-talk between endothelial and smooth muscle cells in vascular remodeling induced by low shear stress. *Proceedings of the National Academy of Sciences of the United States of America*, 108(5), 1908–1913. <https://doi.org/10.1073/pnas.1019219108>

Rabut, G., & Peter, M. (2008). Function and regulation of protein neddylation. “Protein modifications: Beyond the usual suspects” review series. *EMBO Reports*, 9(10), 969–976. <https://doi.org/10.1038/embor.2008.183>

Raffetto, J. D., & Khalil, R. A. (2008). Matrix metalloproteinases and their inhibitors in vascular remodeling and vascular disease. *Biochemical Pharmacology*, 75(2), 346–359. <https://doi.org/10.1016/j.bcp.2007.07.004>

Rahaman, S. O., Lennon, D. J., Febbraio, M., Podrez, E. A., Hazen, S. L., & Silverstein, R. L. (2006). A CD36-dependent signaling cascade is necessary for macrophage foam cell formation. *Cell Metabolism*, 4(3), 211–221. <https://doi.org/10.1016/j.cmet.2006.06.007>

Rahman, A., Anwar, K. N., True, A. L., & Malik, A. B. (1999). Thrombin-Induced p65 Homodimer Binding to Downstream NF-κB Site of the Promoter Mediates Endothelial ICAM-1 Expression and Neutrophil Adhesion. *The Journal of Immunology*, 162(9), 5466–5476.

Rai, V. (2019). *Role of Transcription Factors in Regulating Development and Progression of Atherosclerosis*. 2(1), 5.

Raingeaud, J., Whitmarsh, A. J., Barrett, T., Dérijard, B., & Davis, R. J. (1996). MKK3- and MKK6-regulated gene expression is mediated by the p38 mitogen-activated protein kinase signal transduction pathway. *Molecular and Cellular Biology*, 16(3), 1247–1255.

Rajavashisth, T. B., Liao, J. K., Galis, Z. S., Tripathi, S., Laufs, U., Tripathi, J., Chai, N.-N., Xu, X.-P., Jovinge, S., Shah, P. K., & Libby, P. (1999). Inflammatory Cytokines and Oxidized Low Density Lipoproteins Increase Endothelial Cell Expression of Membrane Type 1-Matrix Metalloproteinase. *Journal of Biological Chemistry*, 274(17), 11924–11929. <https://doi.org/10.1074/jbc.274.17.11924>

Recinos, A., LeJeune, W. S., Sun, H., Lee, C. Y., Tieu, B. C., Lu, M., Hou, T., Boldogh, I., Tilton, R. G., & Brasier, A. R. (2007). Angiotensin II induces IL-6 expression and the Jak-STAT3 pathway in aortic adventitia of LDL receptor-deficient mice. *Atherosclerosis*, 194(1), 125–133. <https://doi.org/10.1016/j.atherosclerosis.2006.10.013>

Redgrave, J. N., Gallagher, P., Lovett, J. K., & Rothwell, P. M. (2008). Critical Cap Thickness and Rupture in Symptomatic Carotid Plaques. *Stroke*, 39(6), 1722–1729. <https://doi.org/10.1161/STROKEAHA.107.507988>

Rekhter, M. D. (1999). Collagen synthesis in atherosclerosis: Too much and not enough. *Cardiovascular Research*, 41(2), 376–384. [https://doi.org/10.1016/S0008-6363\(98\)00321-6](https://doi.org/10.1016/S0008-6363(98)00321-6)

Reustle, A., & Torzewski, M. (2018). Role of p38 MAPK in Atherosclerosis and Aortic Valve Sclerosis. *International Journal of Molecular Sciences*, 19(12), 3761. <https://doi.org/10.3390/ijms19123761>

Ricci, R., Sumara, G., Sumara, I., Rozenberg, I., Kurrer, M., Akhmedov, A., Hersberger, M., Eriksson, U., Eberli, F. R., Becher, B., Borén, J., Chen, M., Cybulsky, M. I., Moore, K. J., Freeman, M. W., Wagner, E. F., Matter, C. M., & Lüscher, T. F. (2004). Requirement of JNK2 for scavenger receptor A-mediated foam cell formation in atherogenesis. *Science (New York, N.Y.)*, 306(5701), 1558–1561. <https://doi.org/10.1126/science.1101909>

Rich, S., & McLaughlin, V. V. (2003). Endothelin Receptor Blockers in Cardiovascular Disease. *Circulation*, 108(18), 2184–2190. <https://doi.org/10.1161/01.CIR.0000094397.19932.78>

Ridker, P. M. (2013). Closing the Loop on Inflammation and Atherothrombosis: Why Perform the Cirt and Cantos Trials? *Transactions of the American Clinical and Climatological Association*, 124, 174–190.

Ridker, P. M. (2019). Anticytokine Agents. *Circulation Research*, 124(3), 437–450. <https://doi.org/10.1161/CIRCRESAHA.118.313129>

Ridker, P. M., Cannon, C. P., Morrow, D., Rifai, N., Rose, L. M., McCabe, C. H., Pfeffer, M. A., & Braunwald, E. (2005). C-Reactive Protein Levels and Outcomes after Statin Therapy. *New England Journal of Medicine*, 352(1), 20–28. <https://doi.org/10.1056/NEJMoa042378>

Ridker, P. M., Everett, B. M., Pradhan, A., MacFadyen, J. G., Solomon, D. H., Zaharris, E., Mam, V., Hasan, A., Rosenberg, Y., Iturriaga, E., Gupta, M., Tsigouli, M., Verma, S., Clearfield, M., Libby, P., Goldhaber, S. Z., Seagle, R., Ofori, C., Saklayen, M., ... Glynn, R. J. (2019). Low-Dose Methotrexate for the Prevention of Atherosclerotic Events. *New England Journal of Medicine*, 380(8), 752–762. <https://doi.org/10.1056/NEJMoa1809798>

Ridker, P. M., Everett, B. M., Thuren, T., MacFadyen, J. G., Chang, W. H., Ballantyne, C., Fonseca, F., Nicolau, J., Koenig, W., Anker, S. D., Kastelein, J. J. P., Cornel, J. H., Pais, P., Pella, D., Genest, J., Cifkova, R., Lorenzatti, A., Forster, T., Kobalava, Z., ... Glynn, R. J. (2017). Antiinflammatory Therapy with Canakinumab for Atherosclerotic Disease. *New England Journal of Medicine*, 377(12), 1119–1131. <https://doi.org/10.1056/NEJMoa1707914>

Ridker, P. M., Howard, C. P., Walter, V., Everett, B., Libby, P., Hensen, J., & Thuren, T. (2012). Effects of Interleukin-1 $\beta$  Inhibition With Canakinumab on Hemoglobin A1c, Lipids, C-Reactive Protein, Interleukin-6, and Fibrinogen. *Circulation*, 126(23), 2739–2748. <https://doi.org/10.1161/CIRCULATIONAHA.112.122556>

Ries, C. (2014). Cytokine functions of TIMP-1. *Cellular and Molecular Life Sciences: CMLS*, 71(4), 659–672. <https://doi.org/10.1007/s00018-013-1457-3>

Robbins, C. S., Hilgendorf, I., Weber, G. F., Theurl, I., Iwamoto, Y., Figueiredo, J.-L., Gorbatov, R., Sukhova, G. K., Gerhardt, L. M. S., Smyth, D., Zavitz, C. C. J., Shikatani, E. A., Parsons, M., van Rooijen, N., Lin, H. Y., Husain, M., Libby, P., Nahrendorf, M., Weissleder, R., & Swirski,

F. K. (2013). Local proliferation dominates lesional macrophage accumulation in atherosclerosis. *Nature Medicine*, 19(9), 1166–1172. <https://doi.org/10.1038/nm.3258>

Rong, J. X., Shapiro, M., Trogan, E., & Fisher, E. A. (2003). Transdifferentiation of mouse aortic smooth muscle cells to a macrophage-like state after cholesterol loading. *Proceedings of the National Academy of Sciences of the United States of America*, 100(23), 13531–13536. <https://doi.org/10.1073/pnas.1735526100>

Ross, R. (1999). Atherosclerosis—An inflammatory disease. *The New England Journal of Medicine*, 340(2), 115–126. <https://doi.org/10.1056/NEJM199901143400207>

Rothwarf, D. M., & Karin, M. (1999). The NF- $\kappa$ B activation pathway: A paradigm in information transfer from membrane to nucleus. *Science's STKE: Signal Transduction Knowledge Environment*, 1999(5), RE1. <https://doi.org/10.1126/stke.1999.5.re1>

Rouis, M., Adamy, C., Duverger, N., Lesnik, P., Horellou, P., Moreau, M., Emmanuel, F., Caillaud, J. M., Laplaud, P. M., Dachet, C., & Chapman, M. J. (1999). Adenovirus-mediated overexpression of tissue inhibitor of metalloproteinase-1 reduces atherosclerotic lesions in apolipoprotein E-deficient mice. *Circulation*, 100(5), 533–540. <https://doi.org/10.1161/01.cir.100.5.533>

Roy, B., Bhattacharjee, A., Xu, B., Ford, D., Maizel, A. L., & Cathcart, M. K. (2002). IL-13 signal transduction in human monocytes: Phosphorylation of receptor components, association with Jak3, and phosphorylation/activation of Stats. *Journal of Leukocyte Biology*, 72(3), 580–589.

Ruifrok, A. C., & Johnston, D. A. (2001). Quantification of histochemical staining by color deconvolution. *Analytical and Quantitative Cytology and Histology*, 23(4), 291–299.

Saccani, S., Pantano, S., & Natoli, G. (2002). P38-Dependent marking of inflammatory genes for increased NF- $\kappa$ B recruitment. *Nature Immunology*, 3(1), 69–75. <https://doi.org/10.1038/ni748>

Saitoh, T., Nakayama, M., Nakano, H., Yagita, H., Yamamoto, N., & Yamaoka, S. (2003). TWEAK induces NF- $\kappa$ B2 p100 processing and long lasting NF- $\kappa$ B activation. *The Journal of Biological Chemistry*, 278(38), 36005–36012. <https://doi.org/10.1074/jbc.M304266200>

Saklatvala, J., Dean, J., & Clark, A. (2003). Control of the expression of inflammatory response genes. *Biochemical Society Symposium*, 70, 95–106. <https://doi.org/10.1042/bss0700095>

Salvador, B., Arranz, A., Francisco, S., Córdoba, L., Punzón, C., Llamas, M. Á., & Fresno, M. (2016). Modulation of endothelial function by Toll like receptors. *Pharmacological Research*, 108, 46–56. <https://doi.org/10.1016/j.phrs.2016.03.038>

Sanchez-Barcelo, E. J., Mediavilla, M. D., Vriend, J., & Reiter, R. J. (2016). Constitutive photomorphogenesis protein 1 (COP1) and COP9 signalosome, evolutionarily conserved photomorphogenic proteins as possible targets of melatonin. *Journal of Pineal Research*, 61(1), 41–51. <https://doi.org/10.1111/jpi.12340>

Sansilvestri-Morel, P., Fioretti, F., Rupin, A., Senni, K., Fabiani, J.-N., Godeau, G., & Verbeuren, T. J. (2006). Comparison of extracellular matrix in skin and saphenous veins of patients with varicose veins: Does the skin reflect venous matrix changes? *Clinical Science*, 112(4), 229–239. <https://doi.org/10.1042/CS20060170>

Sapienza, P., di Marzo, L., Borrelli, V., Sterpetti, A. V., Mingoli, A., Cresti, S., & Cavallaro, A. (2005). Metalloproteinases and their inhibitors are markers of plaque instability. *Surgery*, 137(3), 355–363. <https://doi.org/10.1016/j.surg.2004.10.011>

Sarantopoulos, J., Shapiro, G. I., Cohen, R. B., Clark, J. W., Kauh, J. S., Weiss, G. J., Cleary, J. M., Mahalingam, D., Pickard, M. D., Faessel, H. M., Berger, A. J., Burke, K., Mulligan, G., Dezube, B. J., & Harvey, R. D. (2016). Phase I Study of the Investigational NEDD8-Activating Enzyme Inhibitor Pevonedistat (TAK-924/MLN4924) in Patients with Advanced Solid Tumors. *Clinical Cancer Research: An Official Journal of the American Association for Cancer Research*, 22(4), 847–857. <https://doi.org/10.1158/1078-0432.CCR-15-1338>

Sarikas, A., Hartmann, T., & Pan, Z.-Q. (2011). The cullin protein family. *Genome Biology*, 12(4), 220. <https://doi.org/10.1186/gb-2011-12-4-220>

Schenkel, A. R., Mamdouh, Z., & Muller, W. A. (2004). Locomotion of monocytes on endothelium is a critical step during extravasation. *Nature Immunology*, 5(4), 393–400. <https://doi.org/10.1038/ni1051>

Schieffer, B., Selle, T., Hilfiker, A., Hilfiker-Kleiner, D., Grote, K., Tietge, U. J. F., Trautwein, C., Luchtefeld, M., Schmittkamp, C., Heeneman, S., Daemen, M. J. A. P., & Drexler, H. (2004). Impact of Interleukin-6 on Plaque Development and Morphology in Experimental Atherosclerosis. *Circulation*, 110(22), 3493–3500. <https://doi.org/10.1161/01.CIR.0000148135.08582.97>

Schimmel, L., Heemskerk, N., & van Buul, J. D. (2016). Leukocyte transendothelial migration: A local affair. *Small GTPases*, 8(1), 1–15. <https://doi.org/10.1080/21541248.2016.1197872>

Schindelin, J., Arganda-Carreras, I., Frise, E., Kaynig, V., Longair, M., Pietzsch, T., Preibisch, S., Rueden, C., Saalfeld, S., Schmid, B., Tinevez, J.-Y., White, D. J., Hartenstein, V., Eliceiri, K.,

Tomancak, P., & Cardona, A. (2012). Fiji: An open-source platform for biological-image analysis. *Nature Methods*, 9(7), 676–682. <https://doi.org/10.1038/nmeth.2019>

Schiopu, A., Bengtsson, E., Gonçalves, I., Nilsson, J., Fredrikson, G. N., & Björkbacka, H. (2016). Associations Between Macrophage Colony-Stimulating Factor and Monocyte Chemoattractant Protein 1 in Plasma and First-Time Coronary Events: A Nested Case–Control Study. *Journal of the American Heart Association: Cardiovascular and Cerebrovascular Disease*, 5(9), e002851. <https://doi.org/10.1161/JAHA.115.002851>

Schlierf, A., Altmann, E., Quancard, J., Jefferson, A. B., Assenberg, R., Renatus, M., Jones, M., Hassiepen, U., Schaefer, M., Kiffe, M., Weiss, A., Wiesmann, C., Sedrani, R., Eder, J., & Martoglio, B. (2016). Targeted inhibition of the COP9 signalosome for treatment of cancer. *Nature Communications*, 7(1), 13166. <https://doi.org/10.1038/ncomms13166>

Schnoor, M., Alcaide, P., Voisin, M.-B., & van Buul, J. D. (2015). Crossing the Vascular Wall: Common and Unique Mechanisms Exploited by Different Leukocyte Subsets during Extravasation. *Mediators of Inflammation*, 2015, 946509. <https://doi.org/10.1155/2015/946509>

Schoenhagen, P., Ziada, K. M., Vince, D. G., Nissen, S. E., & Tuzcu, E. M. (2001). Arterial remodeling and coronary artery disease: The concept of “dilated” versus “obstructive” coronary atherosclerosis. *Journal of the American College of Cardiology*, 38(2), 297–306. [https://doi.org/10.1016/S0735-1097\(01\)01374-2](https://doi.org/10.1016/S0735-1097(01)01374-2)

Schönthal, A., Herrlich, P., Rahmsdorf, H. J., & Ponta, H. (1988). Requirement for fos gene expression in the transcriptional activation of collagenase by other oncogenes and phorbol esters. *Cell*, 54(3), 325–334. [https://doi.org/10.1016/0092-8674\(88\)90195-x](https://doi.org/10.1016/0092-8674(88)90195-x)

Schwarz, A., Bonaterra, G. A., Schwarzbach, H., & Kinscherf, R. (2017). Oxidized LDL-induced JAB1 influences NF-κB independent inflammatory signaling in human macrophages during foam cell formation. *Journal of Biomedical Science*, 24, 12. <https://doi.org/10.1186/s12929-017-0320-5>

Schweitzer, K., Bozko, P. M., Dubiel, W., & Naumann, M. (2007). CSN controls NF-κappaB by deubiquitylation of IkappaBalp. *The EMBO Journal*, 26(6), 1532–1541. <https://doi.org/10.1038/sj.emboj.7601600>

Scott, D. C., Hammill, J. T., Min, J., Rhee, D. Y., Connelly, M., Sviderskiy, V. O., Bhasin, D., Chen, Y., Ong, S.-S., Chai, S. C., Goktug, A. N., Huang, G., Monda, J. K., Low, J., Kim, H. S., Paulo, J. A., Cannon, J. R., Shelat, A. A., Chen, T., ... Guy, R. K. (2017). Blocking an N-terminal acetylation-dependent protein interaction inhibits an E3 ligase. *Nature Chemical Biology*, 13(8), 850–857. <https://doi.org/10.1038/nchembio.2386>

Scott-Burden, T., & Vanhoutte, P. M. (1994). Regulation of smooth muscle cell growth by endothelium-derived factors. *Texas Heart Institute Journal*, 21(1), 91–97.

Seeger, M., Gordon, C., & Dubiel, W. (2001). Protein stability: The COP9 signalosome gets in on the act. *Current Biology: CB*, 11(16), R643–646. [https://doi.org/10.1016/s0960-9822\(01\)00382-7](https://doi.org/10.1016/s0960-9822(01)00382-7)

Seeger, M., Kraft, R., Ferrell, K., Bech-Otschir, D., Dumdey, R., Schade, R., Gordon, C., Naumann, M., & Dubiel, W. (1998). A novel protein complex involved in signal transduction possessing similarities to 26S proteasome subunits. *FASEB Journal: Official Publication of the Federation of American Societies for Experimental Biology*, 12(6), 469–478.

Segovia, J. A., Tsai, S.-Y., Chang, T.-H., Shil, N. K., Weintraub, S. T., Short, J. D., & Bose, S. (2015). Nedd8 regulates inflammasome-dependent caspase-1 activation. *Molecular and Cellular Biology*, 35(3), 582–597. <https://doi.org/10.1128/MCB.00775-14>

Seizer, P., & May, A. E. (2013). Platelets and matrix metalloproteinases. *Thrombosis and Haemostasis*, 110(5), 903–909. <https://doi.org/10.1160/TH13-02-0113>

Selzman, C. H., Shames, B. D., McIntyre, R. C., Banerjee, A., & Harken, A. H. (1999). The NFκappaB inhibitory peptide, IkappaBalp, prevents human vascular smooth muscle proliferation. *The Annals of Thoracic Surgery*, 67(5), 1227–1231; discussion 1231–1232. [https://doi.org/10.1016/s0003-4975\(99\)00252-0](https://doi.org/10.1016/s0003-4975(99)00252-0)

Sen, R., & Baltimore, D. (1986). Multiple nuclear factors interact with the immunoglobulin enhancer sequences. *Cell*, 46(5), 705–716. [https://doi.org/10.1016/0092-8674\(86\)90346-6](https://doi.org/10.1016/0092-8674(86)90346-6)

Senftleben, U., & Karin, M. (2002). The IKK/NF-κappaB pathway. *Critical Care Medicine*, 30(1 Supp), S18–S26.

Seo, D.-W., Li, H., Guedez, L., Wingfield, P. T., Diaz, T., Salloum, R., Wei, B., & Stetler-Stevenson, W. G. (2003). TIMP-2 mediated inhibition of angiogenesis: An MMP-independent mechanism. *Cell*, 114(2), 171–180. [https://doi.org/10.1016/s0092-8674\(03\)00551-8](https://doi.org/10.1016/s0092-8674(03)00551-8)

Serino, G., & Deng, X.-W. (2003). The COP9 Signalosome: Regulating Plant Development Through the Control of Proteolysis. *Annual Review of Plant Biology*, 54(1), 165–182. <https://doi.org/10.1146/annurev.arplant.54.031902.134847>

Serra, R., Gallelli, L., Butrico, L., Buffone, G., Caliò, F. G., De Caridi, G., Massara, M., Barbetta, A., Amato, B., Labonia, M., Mimmi, S., Iaccino, E., & de Franciscis, S. (2017). From varices to

venous ulceration: The story of chronic venous disease described by metalloproteinases. *International Wound Journal*, 14(1), 233–240. <https://doi.org/10.1111/iwj.12594>

Sha, X., Meng, S., Li, X., Xi, H., Maddaloni, M., Pascual, D. W., Shan, H., Jiang, X., Wang, H., & Yang, X. (2015). Interleukin-35 Inhibits Endothelial Cell Activation by Suppressing MAPK-AP-1 Pathway. *The Journal of Biological Chemistry*, 290(31), 19307–19318. <https://doi.org/10.1074/jbc.M115.663286>

Shah, P. K., Falk, E., Badimon, J. J., Fernandez-Ortiz, A., Mailhac, A., Villareal-Levy, G., Fallon, J. T., Regnstrom, J., & Fuster, V. (1995). Human monocyte-derived macrophages induce collagen breakdown in fibrous caps of atherosclerotic plaques. Potential role of matrix-degrading metalloproteinases and implications for plaque rupture. *Circulation*, 92(6), 1565–1569.

Shankman, L. S., Gomez, D., Cherepanova, O. A., Salmon, M., Alencar, G. F., Haskins, R. M., Swiatlowska, P., Newman, A. A. C., Greene, E. S., Straub, A. C., Isakson, B., Randolph, G. J., & Owens, G. K. (2015). KLF4-dependent phenotypic modulation of smooth muscle cells has a key role in atherosclerotic plaque pathogenesis. *Nature Medicine*, 21(6), 628–637. <https://doi.org/10.1038/nm.3866>

Sharon, M., Mao, H., Boeri Erba, E., Stephens, E., Zheng, N., & Robinson, C. V. (2009). Symmetrical modularity of the COP9 signalosome complex suggests its multifunctionality. *Structure (London, England: 1993)*, 17(1), 31–40. <https://doi.org/10.1016/j.str.2008.10.012>

Shaulian, E., & Karin, M. (2002). AP-1 as a regulator of cell life and death. *Nature Cell Biology*, 4(5), E131–136. <https://doi.org/10.1038/ncb0502-e131>

Shiomi, M., Ito, T., Hirouchi, Y., & Enomoto, M. (2001). Fibromuscular cap composition is important for the stability of established atherosclerotic plaques in mature WHHL rabbits treated with statins. *Atherosclerosis*, 157(1), 75–84. [https://doi.org/10.1016/s0021-9150\(00\)00708-5](https://doi.org/10.1016/s0021-9150(00)00708-5)

Silence, J., Collen, D., & Lijnen, H. R. (2002). Reduced Atherosclerotic Plaque but Enhanced Aneurysm Formation in Mice With Inactivation of the Tissue Inhibitor of Metalloproteinase-1 (TIMP-1) Gene. *Circulation Research*, 90(8), 897–903. <https://doi.org/10.1161/01.RES.0000016501.56641.83>

Silva, G. M., França-Falcão, M. S., Calzerra, N. T. M., Luz, M. S., Gadelha, D. D. A., Balarini, C. M., & Queiroz, T. M. (2020). Role of Renin-Angiotensin System Components in Atherosclerosis: Focus on Ang-II, ACE2, and Ang-1–7. *Frontiers in Physiology*, 11, 1067. <https://doi.org/10.3389/fphys.2020.01067>

Silverman, N., & Maniatis, T. (2001). NF-κB signaling pathways in mammalian and insect innate immunity. *Genes & Development*, 15(18), 2321–2342. <https://doi.org/10.1101/gad.909001>

Simes, R. J., Marschner, I. C., Hunt, D., Colquhoun, D., Sullivan, D., Stewart, R. A. H., Hague, W., Keech, A., Thompson, P., White, H., Shaw, J., Tonkin, A., & LIPID Study Investigators. (2002). Relationship between lipid levels and clinical outcomes in the Long-term Intervention with Pravastatin in Ischemic Disease (LIPID) Trial: To what extent is the reduction in coronary events with pravastatin explained by on-study lipid levels? *Circulation*, 105(10), 1162–1169. <https://doi.org/10.1161/hc1002.105136>

Simoncini, T., & Genazzani, A. R. (2000). Direct vascular effects of estrogens and selective estrogen receptor modulators. *Current Opinion in Obstetrics & Gynecology*, 12(3), 181–187. <https://doi.org/10.1097/00001703-200006000-00004>

Sirum-Connolly, K., & Brinckerhoff, C. E. (1991). Interleukin-1 or phorbol induction of the stromelysin promoter requires an element that cooperates with AP-1. *Nucleic Acids Research*, 19(2), 335–341. <https://doi.org/10.1093/nar/19.2.335>

Sitte, S., Gläsner, J., Jellusova, J., Weisel, F., Panattoni, M., Pardi, R., & Gessner, A. (2012). JAB1 Is Essential for B Cell Development and Germinal Center Formation and Inversely Regulates Fas Ligand and Bcl6 Expression. *The Journal of Immunology*, 188(6), 2677–2686. <https://doi.org/10.4049/jimmunol.1101455>

Skålén, K., Gustafsson, M., Rydberg, E. K., Hultén, L. M., Wiklund, O., Innerarity, T. L., & Borén, J. (2002). Subendothelial retention of atherogenic lipoproteins in early atherosclerosis. *Nature*, 417(6890), 750–754. <https://doi.org/10.1038/nature00804>

Skrzeczyńska-Moncznik, J., Bzowska, M., Loseke, S., Grage-Griebenow, E., Zembala, M., & Pryjma, J. (2008). Peripheral blood CD14high CD16+ monocytes are main producers of IL-10. *Scandinavian Journal of Immunology*, 67(2), 152–159. <https://doi.org/10.1111/j.1365-3083.2007.02051.x>

Slobodnick, A., Shah, B., Krasnokutsky, S., & Pillinger, M. H. (2018). Update on colchicine, 2017. *Rheumatology (Oxford, England)*, 57(suppl\_1), i4–i11. <https://doi.org/10.1093/rheumatology/kex453>

Sluijter, J. P. G., Pulskens, W. P. C., Schoneveld, A. H., Velema, E., Strijder, C. F., Moll, F., de Vries, J. P., Verheijen, J., Hanemaaijer, R., de Kleijn, D. P. V., & Pasterkamp, G. (2006). Matrix Metalloproteinase 2 Is Associated With Stable and Matrix Metalloproteinases 8 and 9 With

Vulnerable Carotid Atherosclerotic Lesions. *Stroke*, 37(1), 235–239. <https://doi.org/10.1161/01.STR.0000196986.50059.e0>

Sluiter, T. J., van Buul, J. D., Huveneers, S., Quax, P. H. A., & de Vries, M. R. (2021). Endothelial Barrier Function and Leukocyte Transmigration in Atherosclerosis. *Biomedicines*, 9(4), 328. <https://doi.org/10.3390/biomedicines9040328>

Smart, D. E., Vincent, K. J., Arthur, M. J. P., Eickelberg, O., Castellazzi, M., Mann, J., & Mann, D. A. (2001). JunD Regulates Transcription of the Tissue Inhibitor of Metalloproteinases-1 and Interleukin-6 Genes in Activated Hepatic Stellate Cells \*. *Journal of Biological Chemistry*, 276(26), 24414–24421. <https://doi.org/10.1074/jbc.M101840200>

Smith, E. B. (1965). THE INFLUENCE OF AGE AND ATHEROSCLEROSIS ON THE CHEMISTRY OF AORTIC INTIMA.2. COLLAGEN AND MUCOPOLYSACCHARIDES. *Journal of Atherosclerosis Research*, 5(2), 241–248. [https://doi.org/10.1016/s0368-1319\(65\)80065-5](https://doi.org/10.1016/s0368-1319(65)80065-5)

Smith, J. D., Trogan, E., Ginsberg, M., Grigaux, C., Tian, J., & Miyata, M. (1995). Decreased atherosclerosis in mice deficient in both macrophage colony-stimulating factor (op) and apolipoprotein E. *Proceedings of the National Academy of Sciences of the United States of America*, 92(18), 8264–8268. <https://doi.org/10.1073/pnas.92.18.8264>

Soehnlein, O., & Libby, P. (2021). Targeting inflammation in atherosclerosis—From experimental insights to the clinic. *Nature Reviews Drug Discovery*, 20(8), 589–610. <https://doi.org/10.1038/s41573-021-00198-1>

Soucy, T. A., Dick, L. R., Smith, P. G., Milhollen, M. A., & Brownell, J. E. (2010). The NEDD8 Conjugation Pathway and Its Relevance in Cancer Biology and Therapy. *Genes & Cancer*, 1(7), 708–716. <https://doi.org/10.1177/1947601910382898>

Soucy, T. A., Smith, P. G., Milhollen, M. A., Berger, A. J., Gavin, J. M., Adhikari, S., Brownell, J. E., Burke, K. E., Cardin, D. P., Critchley, S., Cullis, C. A., Doucette, A., Garnsey, J. J., Gaulin, J. L., Gershman, R. E., Lublinsky, A. R., McDonald, A., Mizutani, H., Narayanan, U., ... Langston, S. P. (2009). An inhibitor of NEDD8-activating enzyme as a new approach to treat cancer. *Nature*, 458(7239), 732–736. <https://doi.org/10.1038/nature07884>

Sozen, E., Karademir, B., Yazgan, B., Bozaykut, P., & Ozer, N. K. (2014). Potential role of proteasome on c-jun related signaling in hypercholesterolemia induced atherosclerosis. *Redox Biology*, 2, 732–738. <https://doi.org/10.1016/j.redox.2014.02.007>

Spann, N. J., Garmire, L. X., McDonald, J. G., Myers, D. S., Milne, S. B., Shibata, N., Reichart, D., Fox, J. N., Shaked, I., Heudobler, D., Raetz, C. R. H., Wang, E. W., Kelly, S. L., Sullards, M. C., Murphy, R. C., Merrill, A. H., Brown, H. A., Dennis, E. A., Li, A. C., ... Glass, C. K. (2012). Regulated accumulation of desmosterol integrates macrophage lipid metabolism and inflammatory responses. *Cell*, 151(1), 138–152. <https://doi.org/10.1016/j.cell.2012.06.054>

Spinale, F. G., & Villarreal, F. (2014). Targeting matrix metalloproteinases in heart disease: Lessons from endogenous inhibitors. *Biochemical Pharmacology*, 90(1), 7–15. <https://doi.org/10.1016/j.bcp.2014.04.011>

Sprague, A. H., & Khalil, R. A. (2009). Inflammatory cytokines in vascular dysfunction and vascular disease. *Biochemical Pharmacology*, 78(6), 539–552. <https://doi.org/10.1016/j.bcp.2009.04.029>

Srivastava, M., Saqib, U., Naim, A., Roy, A., Liu, D., Bhatnagar, D., Ravinder, R., & Baig, M. S. (2017). The TLR4–NOS1–AP1 signaling axis regulates macrophage polarization. *Inflammation Research*, 66(4), 323–334. <https://doi.org/10.1007/s0011-016-1017-z>

Stary, H. C., Chandler, A. B., Dinsmore, R. E., Fuster, V., Glagov, S., Insull, W., Rosenfeld, M. E., Schwartz, C. J., Wagner, W. D., & Wissler, R. W. (1995). A Definition of Advanced Types of Atherosclerotic Lesions and a Histological Classification of Atherosclerosis. *Circulation*, 92(5), 1355–1374. <https://doi.org/10.1161/01.CIR.92.5.1355>

Stary, H. C., Chandler, A. B., Glagov, S., Guyton, J. R., Insull, W., Rosenfeld, M. E., Schaffer, S. A., Schwartz, C. J., Wagner, W. D., & Wissler, R. W. (1994). A definition of initial, fatty streak, and intermediate lesions of atherosclerosis. A report from the Committee on Vascular Lesions of the Council on Arteriosclerosis, American Heart Association. *Circulation*, 89(5), 2462–2478. <https://doi.org/10.1161/01.CIR.89.5.2462>

Stefanadis, C., Antoniou, C.-K., Tsiaichris, D., & Pietri, P. (2017). Coronary Atherosclerotic Vulnerable Plaque: Current Perspectives. *Journal of the American Heart Association*, 6(3), e005543. <https://doi.org/10.1161/JAHA.117.005543>

Steinl, D. C., & Kaufmann, B. A. (2015). Ultrasound Imaging for Risk Assessment in Atherosclerosis. *International Journal of Molecular Sciences*, 16(5), 9749–9769. <https://doi.org/10.3390/ijms16059749>

Stoll, G., Kleinschmitz, C., & Nieswandt, B. (2008). Molecular mechanisms of thrombus formation in ischemic stroke: Novel insights and targets for treatment. *Blood*, 112(9), 3555–3562. <https://doi.org/10.1182/blood-2008-04-144758>

Su, H., Li, F., Ranek, M. J., Wei, N., & Wang, X. (2011). COP9 Signalosome Regulates Autophagosome Maturation. *Circulation*, 124(19), 2117–2128. <https://doi.org/10.1161/CIRCULATIONAHA.111.048934>

Su, H., Li, J., Menon, S., Liu, J., Kumarapeli, A. R., Wei, N., & Wang, X. (2011). Perturbation of Cullin Deneddylase via Conditional Csn8 Ablation Impairs the Ubiquitin–Proteasome System and Causes Cardiomyocyte Necrosis and Dilated Cardiomyopathy in Mice. *Circulation Research*, 108(1), 40–50. <https://doi.org/10.1161/CIRCRESAHA.110.230607>

Su, X., Cheng, Y., & Chang, D. (2021). Lipid-lowering therapy: Guidelines to precision medicine. *Clinica Chimica Acta*, 514, 66–73. <https://doi.org/10.1016/j.cca.2020.12.019>

Sugama, Y., Tiruppathi, C., offakidevi, K., Andersen, T. T., Fenton, J. W., & Malik, A. B. (1992). Thrombin-induced expression of endothelial P-selectin and intercellular adhesion molecule-1: A mechanism for stabilizing neutrophil adhesion. *The Journal of Cell Biology*, 119(4), 935–944. <https://doi.org/10.1083/jcb.119.4.935>

Sukovich, D. A., Kauser, K., Shirley, F. D., DelVecchio, V., Halks-Miller, M., & Rubanyi, G. M. (1998). Expression of interleukin-6 in atherosclerotic lesions of male ApoE-knockout mice: Inhibition by 17beta-estradiol. *Arteriosclerosis, Thrombosis, and Vascular Biology*, 18(9), 1498–1505. <https://doi.org/10.1161/01.atv.18.9.1498>

Sumagin, R., Prizant, H., Lomakina, E., Waugh, R. E., & Sarelius, I. H. (2010). LFA-1 and Mac-1 define characteristically different intraluminal crawling and emigration patterns for monocytes and neutrophils *in situ*. *Journal of Immunology (Baltimore, Md.: 1950)*, 185(11), 7057–7066. <https://doi.org/10.4049/jimmunol.1001638>

Sun, J., & Stetler-Stevenson, W. G. (2009). Overexpression of tissue inhibitors of metalloproteinase 2 up-regulates NF-kappaB activity in melanoma cells. *Journal of Molecular Signaling*, 4, 4. <https://doi.org/10.1186/1750-2187-4-4>

Sun, S. C., Ganchi, P. A., Béraud, C., Ballard, D. W., & Greene, W. C. (1994). Autoregulation of the NF-kappa B transactivator RelA (p65) by multiple cytoplasmic inhibitors containing ankyrin motifs. *Proceedings of the National Academy of Sciences of the United States of America*, 91(4), 1346–1350. <https://doi.org/10.1073/pnas.91.4.1346>

Sun, S.-C. (2012). The noncanonical NF-κB pathway. *Immunological Reviews*, 246(1), 125–140. <https://doi.org/10.1111/j.1600-065X.2011.01088.x>

Sun, S.-C. (2017). The non-canonical NF-κB pathway in immunity and inflammation. *Nature Reviews Immunology*, 17(9), 545–558. <https://doi.org/10.1038/nri.2017.52>

Suzuki, M., Minami, A., Nakanishi, A., Kobayashi, K., Matsuda, S., Ogura, Y., & Kitagishi, Y. (2014). Atherosclerosis and tumor suppressor molecules (Review). *International Journal of Molecular Medicine*, 34(4), 934–940. <https://doi.org/10.3892/ijmm.2014.1866>

Swords, R. T., Erba, H. P., DeAngelo, D. J., Bixby, D. L., Altman, J. K., Maris, M., Hua, Z., Blakemore, S. J., Faessel, H., Sedarati, F., Dezube, B. J., Giles, F. J., & Medeiros, B. C. (2015). Pevonedistat (MLN4924), a First-in-Class NEDD8-activating enzyme inhibitor, in patients with acute myeloid leukaemia and myelodysplastic syndromes: A phase 1 study. *British Journal of Haematology*, 169(4), 534–543. <https://doi.org/10.1111/bjh.13323>

Szasz, T., & Clinton Webb, R. (2012). Perivascular adipose tissue: More than just structural support. *Clinical Science (London, England : 1979)*, 122(1), 1–12. <https://doi.org/10.1042/CS20110151>

Szmitko, P. E., Wang, C.-H., Weisel, R. D., de Almeida, J. R., Anderson, T. J., & Verma, S. (2003). New Markers of Inflammation and Endothelial Cell Activation. *Circulation*, 108(16), 1917–1923. <https://doi.org/10.1161/01.CIR.0000089190.95415.9F>

Tabas, I., García-Cardeña, G., & Owens, G. K. (2015). Recent insights into the cellular biology of atherosclerosis. *Journal of Cell Biology*, 209(1), 13–22. <https://doi.org/10.1083/jcb.201412052>

Tabas, I., Williams, K. J., & Borén, J. (2007). Subendothelial lipoprotein retention as the initiating process in atherosclerosis: Update and therapeutic implications. *Circulation*, 116(16), 1832–1844. <https://doi.org/10.1161/CIRCULATIONAHA.106.676890>

Tabata, Y., Yoshino, D., Funamoto, K., Koens, R., Kamm, R. D., & Funamoto, K. (2019). Migration of vascular endothelial cells in monolayers under hypoxic exposure. *Integrative Biology: Quantitative Biosciences from Nano to Macro*, 11(1), 26–35. <https://doi.org/10.1093/intbio/zyz002>

Tacke, F., Alvarez, D., Kaplan, T. J., Jakubzick, C., Spanbroek, R., Llodra, J., Garin, A., Liu, J., Mack, M., van Rooijen, N., Lira, S. A., Habenicht, A. J., & Randolph, G. J. (2007). Monocyte subsets differentially employ CCR2, CCR5, and CX3CR1 to accumulate within atherosclerotic plaques. *The Journal of Clinical Investigation*, 117(1), 185–194. <https://doi.org/10.1172/JCI28549>

Tamaru, M., Tomura, K., Sakamoto, S., Tezuka, K., Tamatani, T., & Narumi, S. (1998). Interleukin-1β Induces Tissue- and Cell Type-Specific Expression of Adhesion Molecules In Vivo. *Arteriosclerosis, Thrombosis, and Vascular Biology*, 18(8), 1292–1303. <https://doi.org/10.1161/01.ATV.18.8.1292>

Tang, J., Kang, Y., Huang, L., Wu, L., & Peng, Y. (2020). TIMP1 preserves the blood–brain barrier through interacting with CD63/integrin  $\beta$ 1 complex and regulating downstream FAK/RhoA signaling. *Acta Pharmaceutica Sinica. B*, 10(6), 987–1003. <https://doi.org/10.1016/j.apsb.2020.02.015>

Tellides, G., & Pober, J. S. (2015). Inflammatory and immune responses in the arterial media. *Circulation Research*, 116(2), 312–322. <https://doi.org/10.1161/CIRCRESAHA.116.301312>

Thevenard, J., Verzeaux, L., Devy, J., Etique, N., Jeanne, A., Schneider, C., Hachet, C., Ferracci, G., David, M., Martiny, L., Charpentier, E., Khrestchatsky, M., Rivera, S., Dedieu, S., & Emonard, H. (2014). Low-Density Lipoprotein Receptor-Related Protein-1 Mediates Endocytic Clearance of Tissue Inhibitor of Metalloproteinases-1 and Promotes Its Cytokine-Like Activities. *PLOS ONE*, 9(7), e103839. <https://doi.org/10.1371/journal.pone.0103839>

Thorp, E., & Tabas, I. (2009). Mechanisms and consequences of efferocytosis in advanced atherosclerosis. *Journal of Leukocyte Biology*, 86(5), 1089–1095. <https://doi.org/10.1189/jlb.0209115>

Tian, M., & Schiemann, W. P. (2009). The TGF- $\beta$  paradox in human cancer: An update. *Future Oncology (London, England)*, 5(2), 259–271. <https://doi.org/10.2217/14796694.5.2.259>

Toldo, S., & Abbate, A. (2018). The NLRP3 inflammasome in acute myocardial infarction. *Nature Reviews Cardiology*, 15(4), 203–214. <https://doi.org/10.1038/nrcardio.2017.161>

Tomoda, K., Yoneda-Kato, N., Fukumoto, A., Yamanaka, S., & Kato, J.-Y. (2004). Multiple functions of Jab1 are required for early embryonic development and growth potential in mice. *The Journal of Biological Chemistry*, 279(41), 43013–43018. <https://doi.org/10.1074/jbc.M406559200>

Tong, D. C., Quinn, S., Nasis, A., Hiew, C., Roberts-Thomson, P., Adams, H., Sriamareswaran, R., Htun, N. M., Wilson, W., Stub, D., van Gaal, W., Howes, L., Collins, N., Yong, A., Bhindi, R., Whitbourn, R., Lee, A., Hengel, C., Asrress, K., ... Layland, J. (2020). Colchicine in Patients With Acute Coronary Syndrome. *Circulation*, 142(20), 1890–1900. <https://doi.org/10.1161/CIRCULATIONAHA.120.050771>

Tong, L., Smyth, D., Kerr, C., Catterall, J., & Richards, C. D. (2004). Mitogen-activated protein kinases Erk1/2 and p38 are required for maximal regulation of TIMP-1 by oncostatin M in murine fibroblasts. *Cellular Signalling*, 16(10), 1123–1132. <https://doi.org/10.1016/j.cellsig.2004.03.003>

Tousoulis, D. (2017). *Coronary Artery Disease: From Biology to Clinical Practice*. Academic Press.

Treier, M., Staszewski, L. M., & Bohmann, D. (1994). Ubiquitin-dependent c-Jun degradation in vivo is mediated by the delta domain. *Cell*, 78(5), 787–798. [https://doi.org/10.1016/s0092-8674\(94\)90502-9](https://doi.org/10.1016/s0092-8674(94)90502-9)

Tricot, O., Mallat, Z., Heymes, C., Belmin, J., Lesèche, G., & Tedgui, A. (2000). Relation between endothelial cell apoptosis and blood flow direction in human atherosclerotic plaques. *Circulation*, 101(21), 2450–2453. <https://doi.org/10.1161/01.cir.101.21.2450>

Tsuge, T., Matsui, M., & Wei, N. (2001). The subunit 1 of the COP9 signalosome suppresses gene expression through its N-terminal domain and incorporates into the complex through the PCI domain. *Journal of Molecular Biology*, 305(1), 1–9. <https://doi.org/10.1006/jmbi.2000.4288>

Tucker, E., O'Donnell, K., Fuchsberger, M., Hilton, A. A., Metcalf, D., Greig, K., Sims, N. A., Quinn, J. M., Alexander, W. S., Hilton, D. J., Kile, B. T., Tarlinton, D. M., & Starr, R. (2007). A novel mutation in the Nfkb2 gene generates an NF- $\kappa$ B2 “super repressor.” *Journal of Immunology (Baltimore, Md.: 1950)*, 179(11), 7514–7522. <https://doi.org/10.4049/jimmunol.179.11.7514>

Turnbull, I. R., Gilfillan, S., Cella, M., Aoshi, T., Miller, M., Piccio, L., Hernandez, M., & Colonna, M. (2006). Cutting edge: TREM-2 attenuates macrophage activation. *Journal of Immunology (Baltimore, Md.: 1950)*, 177(6), 3520–3524. <https://doi.org/10.4049/jimmunol.177.6.3520>

Uchida, C., & Haas, T. L. (2014). Endothelial cell TIMP-1 is upregulated by shear stress via Sp-1 and the TGF $\beta$ 1 signaling pathways. *Biochemistry and Cell Biology*, 92(1), 77–83. <https://doi.org/10.1139/bcb-2013-0086>

Uhle, S., Medalia, O., Waldron, R., Dumdey, R., Henklein, P., Bech-Otschir, D., Huang, X., Berse, M., Sperling, J., Schade, R., & Dubiel, W. (2003). Protein kinase CK2 and protein kinase D are associated with the COP9 signalosome. *The EMBO Journal*, 22(6), 1302–1312. <https://doi.org/10.1093/emboj/cdg127>

V Baroncini, L. A., Nakao, L. S., Ramos, S. G., Filho, A. P., Murta, L. O., Ingberman, M., Tefé-Silva, C., & Précoma, D. B. (2011). Assessment of MMP-9, TIMP-1, and COX-2 in normal tissue and in advanced symptomatic and asymptomatic carotid plaques. *Thrombosis Journal*, 9(1), 6. <https://doi.org/10.1186/1477-9560-9-6>

Vallabhlapurapu, S., Matsuzawa, A., Zhang, W., Tseng, P.-H., Keats, J. J., Wang, H., Vignali, D. A. A., Bergsagel, P. L., & Karin, M. (2008). Nonredundant and complementary functions of TRAF2

and TRAF3 in a ubiquitination cascade that activates NIK-dependent alternative NF- $\kappa$ B signaling. *Nature Immunology*, 9(12), 1364–1370. <https://doi.org/10.1038/ni.1678>

van Buul, J. D., Allingham, M. J., Samson, T., Meller, J., Boulter, E., García-Mata, R., & Burridge, K. (2007). RhoG regulates endothelial apical cup assembly downstream from ICAM1 engagement and is involved in leukocyte trans-endothelial migration. *The Journal of Cell Biology*, 178(7), 1279–1293. <https://doi.org/10.1083/jcb.200612053>

van den Berg, B. M., Spaan, J. A. E., & Vink, H. (2009). Impaired glycocalyx barrier properties contribute to enhanced intimal low-density lipoprotein accumulation at the carotid artery bifurcation in mice. *Pflugers Archiv: European Journal of Physiology*, 457(6), 1199–1206. <https://doi.org/10.1007/s00424-008-0590-6>

Van Herck, J. L., De Meyer, G. R. Y., Martinet, W., Bult, H., Vrints, C. J., & Herman, A. G. (2010). Proteasome inhibitor bortezomib promotes a rupture-prone plaque phenotype in ApoE-deficient mice. *Basic Research in Cardiology*, 105(1), 39–50. <https://doi.org/10.1007/s00395-009-0054-y>

Van Varik, B., Rennenberg, R., Reutelingsperger, C., Kroon, A., de Leeuw, P., & Schurgers, L. J. (2012). Mechanisms of arterial remodeling: Lessons from genetic diseases. *Frontiers in Genetics*, 0. <https://doi.org/10.3389/fgene.2012.00290>

van Wijk, S. J. L., & Timmers, H. T. M. (2010). The family of ubiquitin-conjugating enzymes (E2s): Deciding between life and death of proteins. *FASEB Journal: Official Publication of the Federation of American Societies for Experimental Biology*, 24(4), 981–993. <https://doi.org/10.1096/fj.09-136259>

Varghese, F., Bukhari, A. B., Malhotra, R., & De, A. (2014). IHC Profiler: An Open Source Plugin for the Quantitative Evaluation and Automated Scoring of Immunohistochemistry Images of Human Tissue Samples. *PLOS ONE*, 9(5), e96801. <https://doi.org/10.1371/journal.pone.0096801>

Veith, C., Schermuly, R. T., Brandes, R. P., & Weissmann, N. (2016). Molecular mechanisms of hypoxia-inducible factor-induced pulmonary arterial smooth muscle cell alterations in pulmonary hypertension. *The Journal of Physiology*, 594(5), 1167–1177. <https://doi.org/10.1113/JP270689>

Vengrenyuk, Y., Carlier, S., Xanthos, S., Cardoso, L., Ganatos, P., Virmani, R., Einav, S., Gilchrist, L., & Weinbaum, S. (2006). A hypothesis for vulnerable plaque rupture due to stress-induced debonding around cellular microcalcifications in thin fibrous caps. *Proceedings of the National Academy of Sciences of the United States of America*, 103(40), 14678–14683. <https://doi.org/10.1073/pnas.0606310103>

Vengrenyuk, Y., Nishi, H., Long, X., Ouimet, M., Savji, N., Martinez, F. O., Cassella, C. P., Moore, K. J., Ramsey, S. A., Miano, J. M., & Fisher, E. A. (2015). Cholesterol loading reprograms the microRNA-143/145-myocardin axis to convert aortic smooth muscle cells to a dysfunctional macrophage-like phenotype. *Arteriosclerosis, Thrombosis, and Vascular Biology*, 35(3), 535–546. <https://doi.org/10.1161/ATVBAHA.114.304029>

Vermeulen, L., De Wilde, G., Van Damme, P., Vanden Berghe, W., & Haegeman, G. (2003). Transcriptional activation of the NF- $\kappa$ B p65 subunit by mitogen- and stress-activated protein kinase-1 (MSK1). *The EMBO Journal*, 22(6), 1313–1324. <https://doi.org/10.1093/emboj/cdg139>

Vestweber, D. (2015). How leukocytes cross the vascular endothelium. *Nature Reviews Immunology*, 15(11), 692–704. <https://doi.org/10.1038/nri3908>

Virmani, R., Burke, A. P., Kolodgie, F. D., & Farb, A. (2002). Vulnerable plaque: The pathology of unstable coronary lesions. *Journal of Interventional Cardiology*, 15(6), 439–446. <https://doi.org/10.1111/j.1540-8183.2002.tb01087.x>

Virmani, R., Kolodgie, F. D., Burke, A. P., Farb, A., & Schwartz, S. M. (2000). Lessons From Sudden Coronary Death. *Arteriosclerosis, Thrombosis, and Vascular Biology*, 20(5), 1262–1275. <https://doi.org/10.1161/01.ATV.20.5.1262>

Visse, R., & Nagase, H. (2003). Matrix metalloproteinases and tissue inhibitors of metalloproteinases: Structure, function, and biochemistry. *Circulation Research*, 92(8), 827–839. <https://doi.org/10.1161/01.RES.0000070112.80711.3D>

Vogl, A. M., Brockmann, M. M., Giusti, S. A., Maccarrone, G., Vercelli, C. A., Bauder, C. A., Richter, J. S., Roselli, F., Hafner, A.-S., Dedic, N., Wotjak, C. T., Vogt-Weisenhorn, D. M., Choquet, D., Turck, C. W., Stein, V., Deussing, J. M., & Refojo, D. (2015). Neddylation inhibition impairs spine development, destabilizes synapses and deteriorates cognition. *Nature Neuroscience*, 18(2), 239–251. <https://doi.org/10.1038/nn.3912>

Wagner, A. H., Köhler, T., Rückschloss, U., Just, I., & Hecker, M. (2000). Improvement of nitric oxide-dependent vasodilatation by HMG-CoA reductase inhibitors through attenuation of endothelial superoxide anion formation. *Arteriosclerosis, Thrombosis, and Vascular Biology*, 20(1), 61–69. <https://doi.org/10.1161/01.atv.20.1.61>

Waller, B. F., Orr, C. M., Slack, J. D., Pinkerton, C. A., Van Tassel, J., & Peters, T. (1992). Anatomy, histology, and pathology of coronary arteries: A review relevant to new interventional and

imaging techniques--Part I. *Clinical Cardiology*, 15(6), 451–457. <https://doi.org/10.1002/clc.4960150613>

Wang, A., Al-Kuhlani, M., Johnston, S. C., Ojcius, D. M., Chou, J., & Dean, D. (2013). Transcription factor complex AP-1 mediates inflammation initiated by Chlamydia pneumoniae infection. *Cellular Microbiology*, 15(5), 779–794. <https://doi.org/10.1111/cmi.12071>

Wang, D., Wang, Z., Zhang, L., & Wang, Y. (2017). Roles of Cells from the Arterial Vessel Wall in Atherosclerosis. *Mediators of Inflammation*, 2017, 1–9. <https://doi.org/10.1155/2017/8135934>

Wang, J., An, F. S., Zhang, W., Gong, L., Wei, S. J., Qin, W. D., Wang, X. P., Zhao, Y. X., Zhang, Y., Zhang, C., & Zhang, M.-X. (2011). Inhibition of c-Jun N-terminal kinase attenuates low shear stress-induced atherogenesis in apolipoprotein E-deficient mice. *Molecular Medicine (Cambridge, Mass.)*, 17(9–10), 990–999. <https://doi.org/10.2119/molmed.2011.00073>

Wang, J., Hu, Q., Chen, H., Zhou, Z., Li, W., Wang, Y., Li, S., & He, Q. (2010). Role of Individual Subunits of the Neurospora crassa CSN Complex in Regulation of Deneddylation and Stability of Cullin Proteins. *PLOS Genetics*, 6(12), e1001232. <https://doi.org/10.1371/journal.pgen.1001232>

Wang, N., Zhu, M., Tsao, S.-W., Man, K., Zhang, Z., & Feng, Y. (2012). Up-Regulation of TIMP-1 by Genipin Inhibits MMP-2 Activities and Suppresses the Metastatic Potential of Human Hepatocellular Carcinoma. *PLOS ONE*, 7(9), e46318. <https://doi.org/10.1371/journal.pone.0046318>

Wang, S., Voisin, M.-B., Larbi, K. Y., Dangerfield, J., Scheiermann, C., Tran, M., Maxwell, P. H., Sorokin, L., & Nourshargh, S. (2006). Venular basement membranes contain specific matrix protein low expression regions that act as exit points for emigrating neutrophils. *The Journal of Experimental Medicine*, 203(6), 1519–1532. <https://doi.org/10.1084/jem.20051210>

Wang, X., Kang, D., Feng, S., Serino, G., Schwechheimer, C., & Wei, N. (2002). CSN1 N-terminal-dependent activity is required for Arabidopsis development but not for Rub1/Nedd8 deconjugation of cullins: A structure-function study of CSN1 subunit of COP9 signalosome. *Molecular Biology of the Cell*, 13(2), 646–655. <https://doi.org/10.1091/mbc.01-08-0427>

Wang, X., & Khalil, R. A. (2018). Matrix Metalloproteinases, Vascular Remodeling, and Vascular Disease. *Advances in Pharmacology (San Diego, Calif.)*, 81, 241–330. <https://doi.org/10.1016/bs.apha.2017.08.002>

Wang, Y., Dubland, J. A., Allahverdian, S., Asonye, E., Sahin, B., Jaw, J. E., Sin, D. D., Seidman, M. A., Leeper, N. J., & Francis, G. A. (2019). Smooth Muscle Cells Contribute the Majority of Foam Cells in ApoE (Apolipoprotein E)-Deficient Mouse Atherosclerosis. *Arteriosclerosis, Thrombosis, and Vascular Biology*, 39(5), 876–887. <https://doi.org/10.1161/ATVBAHA.119.312434>

Wang, Y., Luo, Z., Pan, Y., Wang, W., Zhou, X., Jeong, L. S., Chu, Y., Liu, J., & Jia, L. (2015). Targeting protein neddylation with an NEDD8-activating enzyme inhibitor MLN4924 induced apoptosis or senescence in human lymphoma cells. *Cancer Biology & Therapy*, 16(3), 420–429. <https://doi.org/10.1080/15384047.2014.1003003>

Wang, Z., Kong, L., Kang, J., Vaughn, D. M., Bush, G. D., Walding, A. L., Grigorian, A. A., Robinson, J. S., & Nakayama, D. K. (2011). Interleukin-1 $\beta$  induces migration of rat arterial smooth muscle cells through a mechanism involving increased matrix metalloproteinase-2 activity. *The Journal of Surgical Research*, 169(2), 328–336. <https://doi.org/10.1016/j.jss.2009.12.010>

Watson, I. R., Irwin, M. S., & Ohh, M. (2011). NEDD8 pathways in cancer, Sine Quibus Non. *Cancer Cell*, 19(2), 168–176. <https://doi.org/10.1016/j.ccr.2011.01.002>

Weber, C., & Noels, H. (2011). Atherosclerosis: Current pathogenesis and therapeutic options. *Nature Medicine*, 17(11), 1410–1422. <https://doi.org/10.1038/nm.2538>

Wee, S., Hetfeld, B., Dubiel, W., & Wolf, D. A. (2002). Conservation of the COP9/signalosome in budding yeast. *BMC Genetics*, 3, 15. <https://doi.org/10.1186/1471-2156-3-15>

Wei, N., & Deng, X. W. (1998). Characterization and purification of the mammalian COP9 complex, a conserved nuclear regulator initially identified as a repressor of photomorphogenesis in higher plants. *Photochemistry and Photobiology*, 68(2), 237–241. [https://doi.org/10.1562/0031-8655\(1998\)068<0237:capotm>2.3.co;2](https://doi.org/10.1562/0031-8655(1998)068<0237:capotm>2.3.co;2)

Wei, N., & Deng, X. W. (2003). The COP9 signalosome. *Annual Review of Cell and Developmental Biology*, 19, 261–286. <https://doi.org/10.1146/annurev.cellbio.19.111301.112449>

Wei, N., Serino, G., & Deng, X.-W. (2008). The COP9 signalosome: More than a protease. *Trends in Biochemical Sciences*, 33, 592–600. <https://doi.org/10.1016/j.tibs.2008.09.004>

Wei, N., Tsuge, T., Serino, G., Dohmae, N., Takio, K., Matsui, M., & Deng, X. W. (1998). The COP9 complex is conserved between plants and mammals and is related to the 26S proteasome regulatory complex. *Current Biology: CB*, 8(16), 919–922. [https://doi.org/10.1016/s0960-9822\(07\)00372-7](https://doi.org/10.1016/s0960-9822(07)00372-7)

Weih, F., & Caamaño, J. (2003). Regulation of secondary lymphoid organ development by the nuclear factor-kappaB signal transduction pathway. *Immunological Reviews*, 195, 91–105. <https://doi.org/10.1034/j.1600-065x.2003.00064.x>

Weitz-Schmidt, G., Welzenbach, K., Brinkmann, V., Kamata, T., Kallen, J., Bruns, C., Cottens, S., Takada, Y., & Hommel, U. (2001). Statins selectively inhibit leukocyte function antigen-1 by binding to a novel regulatory integrin site. *Nature Medicine*, 7(6), 687–692. <https://doi.org/10.1038/89058>

Wilck, N., Fechner, M., Dan, C., Stangl, V., Stangl, K., & Ludwig, A. (2017). The Effect of Low-Dose Proteasome Inhibition on Pre-Existing Atherosclerosis in LDL Receptor-Deficient Mice. *International Journal of Molecular Sciences*, 18(4), 781. <https://doi.org/10.3390/ijms18040781>

Wilck, N., Fechner, M., Dreger, H., Hewing, B., Arias, A., Meiners, S., Baumann, G., Stangl, V., Stangl, K., & Ludwig, A. (2012). Attenuation of Early Atherogenesis in Low-Density Lipoprotein Receptor-Deficient Mice by Proteasome Inhibition. *Arteriosclerosis, Thrombosis, and Vascular Biology*, 32(6), 1418–1426. <https://doi.org/10.1161/ATVBAHA.112.249342>

Wilczynska, K. M., Gopalan, S. M., Bugno, M., Kasza, A., Konik, B. S., Bryan, L., Wright, S., Griswold-Prenner, I., & Kordula, T. (2006a). A Novel Mechanism of Tissue Inhibitor of Metalloproteinases-1 Activation by Interleukin-1 in Primary Human Astrocytes. *Journal of Biological Chemistry*, 281(46), 34955–34964. <https://doi.org/10.1074/jbc.M604616200>

Wilczynska, K. M., Gopalan, S. M., Bugno, M., Kasza, A., Konik, B. S., Bryan, L., Wright, S., Griswold-Prenner, I., & Kordula, T. (2006b). A Novel Mechanism of Tissue Inhibitor of Metalloproteinases-1 Activation by Interleukin-1 in Primary Human Astrocytes. *Journal of Biological Chemistry*, 281(46), 34955–34964. <https://doi.org/10.1074/jbc.M604616200>

Willemse, L., & de Winther, M. P. (2020). Macrophage subsets in atherosclerosis as defined by single-cell technologies. *The Journal of Pathology*, 250(5), 705–714. <https://doi.org/10.1002/path.5392>

Willenbrock, F., & Murphy, G. (1994). Structure-function relationships in the tissue inhibitors of metalloproteinases. *American Journal of Respiratory and Critical Care Medicine*, 150(6 Pt 2), S165–170. [https://doi.org/10.1164/ajrccm/150.6\\_Pt\\_2.S165](https://doi.org/10.1164/ajrccm/150.6_Pt_2.S165)

Williams, H. J., Fisher, E. A., & Greaves, D. R. (2012). Macrophage differentiation and function in atherosclerosis: Opportunities for therapeutic intervention? *Journal of Innate Immunity*, 4(5–6), 498–508. <https://doi.org/10.1159/000336618>

Williams, K. J., & Tabas, I. (1995). The response-to-retention hypothesis of early atherogenesis. *Arteriosclerosis, Thrombosis, and Vascular Biology*, 15(5), 551–561. <https://doi.org/10.1161/01.atv.15.5.551>

Williamson, R. A., Marston, F. A., Angal, S., Koklitis, P., Panico, M., Morris, H. R., Carne, A. F., Smith, B. J., Harris, T. J., & Freedman, R. B. (1990). Disulphide bond assignment in human tissue inhibitor of metalloproteinases (TIMP). *Biochemical Journal*, 268(2), 267–274.

Wissler, R. W., & Vesselinovitch, D. (1968). Comparative Pathogenetic Patterns in Atherosclerosis. In R. Paoletti & D. Kritchevsky (Eds.), *Advances in Lipid Research* (Vol. 6, pp. 181–206). Elsevier. <https://doi.org/10.1016/B978-1-4831-9942-9.50011-5>

Wolf, D. A., Zhou, C., & Wee, S. (2003). The COP9 signalosome: An assembly and maintenance platform for cullin ubiquitin ligases? *Nature Cell Biology*, 5(12), 1029–1033. <https://doi.org/10.1038/ncb1203-1029>

Wong, E. T., & Tergaonkar, V. (2009). Roles of NF-κB in health and disease: Mechanisms and therapeutic potential. *Clinical Science*, 116(6), 451–465. <https://doi.org/10.1042/CS20080502>

Wong, K. L., Tai, J. J.-Y., Wong, W.-C., Han, H., Sem, X., Yeap, W.-H., Kourilsky, P., & Wong, S.-C. (2011). Gene expression profiling reveals the defining features of the classical, intermediate, and nonclassical human monocyte subsets. *Blood*, 118(5), e16-31. <https://doi.org/10.1182/blood-2010-12-326355>

Wong, K. L., Yeap, W. H., Tai, J. J. Y., Ong, S. M., Dang, T. M., & Wong, S. C. (2012). The three human monocyte subsets: Implications for health and disease. *Immunologic Research*, 53(1–3), 41–57. <https://doi.org/10.1007/s12026-012-8297-3>

Woollard, K. J., & Geissmann, F. (2010). Monocytes in atherosclerosis: Subsets and functions. *Nature Reviews Cardiology*, 7(2), 77–86. <https://doi.org/10.1038/nrcardio.2009.228>

Wu, C., Ivars, F., Anderson, P., Hallmann, R., Vestweber, D., Nilsson, P., Robenek, H., Tryggvason, K., Song, J., Korpos, E., Loser, K., Beissert, S., Georges-Labouesse, E., & Sorokin, L. M. (2009). Endothelial basement membrane laminin alpha5 selectively inhibits T lymphocyte extravasation into the brain. *Nature Medicine*, 15(5), 519–527. <https://doi.org/10.1038/nm.1957>

Wu, C.-M., Zheng, L., Wang, Q., & Hu, Y.-W. (2021). The emerging role of cell senescence in atherosclerosis. *Clinical Chemistry and Laboratory Medicine (CCLM)*, 59(1), 27–38. <https://doi.org/10.1515/cclm-2020-0601>

Xia, Y., Wang, J., Xu, S., Johnson, G. L., Hunter, T., & Lu, Z. (2007). MEKK1 Mediates the Ubiquitination and Degradation of c-Jun in Response to Osmotic Stress. *Molecular and Cellular Biology*. <https://doi.org/10.1128/MCB.01355-06>

Xiao, G., Harhaj, E. W., & Sun, S. C. (2001). NF- $\kappa$ B-inducing kinase regulates the processing of NF- $\kappa$ B2 p100. *Molecular Cell*, 7(2), 401–409. [https://doi.org/10.1016/s1097-2765\(01\)00187-3](https://doi.org/10.1016/s1097-2765(01)00187-3)

Xirodimas, D. P. (2008). Novel substrates and functions for the ubiquitin-like molecule NEDD8. *Biochemical Society Transactions*, 36(Pt 5), 802–806. <https://doi.org/10.1042/BST0360802>

Xu, J., & Shi, G.-P. (2014). Vascular wall extracellular matrix proteins and vascular diseases. *Biochimica et Biophysica Acta (BBA) - Molecular Basis of Disease*, 1842(11), 2106–2119. <https://doi.org/10.1016/j.bbadi.2014.07.008>

Xue, J., Thippegowda, P. B., Hu, G., Bachmaier, K., Christman, J. W., Malik, A. B., & Tiruppathi, C. (2009). NF- $\kappa$ B regulates thrombin-induced ICAM-1 gene expression in cooperation with NFAT by binding to the intronic NF- $\kappa$ B site in the ICAM-1 gene. *Physiological Genomics*, 38(1), 42–53. <https://doi.org/10.1152/physiolgenomics.00012.2009>

Yan, C., & Boyd, D. D. (2007). Regulation of matrix metalloproteinase gene expression. *Journal of Cellular Physiology*, 211(1), 19–26. <https://doi.org/10.1002/jcp.20948>

Yang, D. D., Kuan, C. Y., Whitmarsh, A. J., Rincón, M., Zheng, T. S., Davis, R. J., Rakic, P., & Flavell, R. A. (1997). Absence of excitotoxicity-induced apoptosis in the hippocampus of mice lacking the Jnk3 gene. *Nature*, 389(6653), 865–870. <https://doi.org/10.1038/39899>

Yang, Q., Bell, J. J., & Bhandoola, A. (2010). T-Cell Lineage Determination. *Immunological Reviews*, 238(1), 12–22. <https://doi.org/10.1111/j.1600-065X.2010.00956.x>

Yang, S. H., Galanis, A., & Sharrocks, A. D. (1999). Targeting of p38 mitogen-activated protein kinases to MEF2 transcription factors. *Molecular and Cellular Biology*, 19(6), 4028–4038. <https://doi.org/10.1128/MCB.19.6.4028>

Ye, N., Ding, Y., Wild, C., Shen, Q., & Zhou, J. (2014). Small Molecule Inhibitors Targeting Activator Protein 1 (AP-1). *Journal of Medicinal Chemistry*, 57(16), 6930–6948. <https://doi.org/10.1021/jm5004733>

Yoshimura, K., Aoki, H., Ikeda, Y., Fujii, K., Akiyama, N., Furutani, A., Hoshii, Y., Tanaka, N., Ricci, R., Ishihara, T., Esato, K., Hamano, K., & Matsuzaki, M. (2005). Regression of abdominal aortic aneurysm by inhibition of c-Jun N-terminal kinase. *Nature Medicine*, 11(12), 1330–1338. <https://doi.org/10.1038/nm1335>

Youn, J.-C., Yu, H. T., Jeon, J.-W., Lee, H. S., Jang, Y., Park, Y. W., Park, Y.-B., Shin, E.-C., & Ha, J.-W. (2014). Soluble CD93 Levels in Patients with Acute Myocardial Infarction and Its Implication on Clinical Outcome. *PLOS ONE*, 9(5), e96538. <https://doi.org/10.1371/journal.pone.0096538>

Young, D., Das, N., Anowai, A., & Dufour, A. (2019). Matrix Metalloproteases as Influencers of the Cells' Social Media. *International Journal of Molecular Sciences*, 20(16), 3847. <https://doi.org/10.3390/ijms20163847>

Yu, J., Zhou, X., Nakaya, M., Jin, W., Cheng, X., & Sun, S.-C. (2014). T cell-intrinsic function of the noncanonical NF- $\kappa$ B pathway in the regulation of GM-CSF expression and experimental autoimmune encephalomyelitis pathogenesis. *Journal of Immunology (Baltimore, Md.: 1950)*, 193(1), 422–430. <https://doi.org/10.4049/jimmunol.1303237>

Yu, P.-J., Ferrari, G., Pirelli, L., Gulkarov, I., Galloway, A. C., Mignatti, P., & Pintucci, G. (2007). Vascular injury and modulation of MAPKs: A targeted approach to therapy of restenosis. *Cellular Signalling*, 19(7), 1359–1371. <https://doi.org/10.1016/j.cellsig.2007.03.002>

Yu, Q., Jiang, Y., & Sun, Y. (2020). Anticancer drug discovery by targeting cullin neddylation. *Acta Pharmaceutica Sinica B*, 10(5), 746–765. <https://doi.org/10.1016/j.apsb.2019.09.005>

Zakkar, M., Chaudhury, H., Sandvik, G., Enesa, K., Luong, L. A., Cuhlmann, S., Mason, J. C., Krams, R., Clark, A. R., Haskard, D. O., & Evans, P. C. (2008). Increased endothelial mitogen-activated protein kinase phosphatase-1 expression suppresses proinflammatory activation at sites that are resistant to atherosclerosis. *Circulation Research*, 103(7), 726–732. <https://doi.org/10.1161/CIRCRESAHA.108.183913>

Zarbock, A., Ley, K., McEver, R. P., & Hidalgo, A. (2011). Leukocyte ligands for endothelial selectins: Specialized glycoconjugates that mediate rolling and signaling under flow. *Blood*, 118(26), 6743–6751. <https://doi.org/10.1182/blood-2011-07-343566>

Zarnegar, B. J., Wang, Y., Mahoney, D. J., Dempsey, P. W., Cheung, H. H., He, J., Shiba, T., Yang, X., Yeh, W.-C., Mak, T. W., Korneluk, R. G., & Cheng, G. (2008). Noncanonical NF- $\kappa$ B activation requires coordinated assembly of a regulatory complex of the adaptors cIAP1, cIAP2, TRAF2 and TRAF3 and the kinase NIK. *Nature Immunology*, 9(12), 1371–1378. <https://doi.org/10.1038/ni.1676>

Zeng, L., Zampetaki, A., Margariti, A., Pepe, A. E., Alam, S., Martin, D., Xiao, Q., Wang, W., Jin, Z.-G., Cockerill, G., Mori, K., Li, Y.-S. J., Hu, Y., Chien, S., & Xu, Q. (2009). Sustained activation of XBP1 splicing leads to endothelial apoptosis and atherosclerosis development in response to disturbed flow. *Proceedings of the National Academy of Sciences of the United States of America*, 106(20), 8326–8331. <https://doi.org/10.1073/pnas.0903197106>

Zhang, H., & Sun, S.-C. (2015). NF-κB in inflammation and renal diseases. *Cell & Bioscience*, 5, 63. <https://doi.org/10.1186/s13578-015-0056-4>

Zhang, J., Zhao, R., Bryant, C. L. N., Wu, K., Liu, Z., Ding, Y., Zhao, Y., Xue, B., Pan, Z.-Q., Li, C., Huang, L., & Fang, L. (2020). IKK-mediated Regulation of the COP9 Signalosome via Phosphorylation of CSN5. *Journal of Proteome Research*, 19(3), 1119–1130. <https://doi.org/10.1021/acs.jproteome.9b00626>

Zhang, L.-Z., & Lei, S. (2016). Changes of junctions of endothelial cells in coronary sclerosis: A review. *Chronic Diseases and Translational Medicine*, 2(1), 22–26. <https://doi.org/10.1016/j.cdtm.2016.05.001>

Zhang, X., Zhang, Y.-L., Qiu, G., Pian, L., Guo, L., Cao, H., Liu, J., Zhao, Y., Li, X., Xu, Z., Huang, X., Huang, J., Dong, J., Shen, B., Wang, H.-X., Ying, X., Zhang, W. J., Cao, X., & Zhang, J. (2020). Hepatic neddylation targets and stabilizes electron transfer flavoproteins to facilitate fatty acid β-oxidation. *Proceedings of the National Academy of Sciences*, 117(5), 2473–2483. <https://doi.org/10.1073/pnas.1910765117>

Zhang, X.-C., Chen, J., Su, C.-H., Yang, H.-Y., & Lee, M.-H. (2008). Roles for CSN5 in control of p53/MDM2 activities. *Journal of Cellular Biochemistry*, 103(4), 1219–1230. <https://doi.org/10.1002/jcb.21504>

Zhao, L., & Funk, C. D. (2004). Lipoxygenase pathways in atherogenesis. *Trends in Cardiovascular Medicine*, 14(5), 191–195. <https://doi.org/10.1016/j.tcm.2004.04.003>

Zhao, M., Liu, Y., Wang, X., New, L., Han, J., & Brunk, U. T. (2002). Activation of the p38 MAP kinase pathway is required for foam cell formation from macrophages exposed to oxidized LDL. *APMIS: Acta Pathologica, Microbiologica, et Immunologica Scandinavica*, 110(6), 458–468. <https://doi.org/10.1034/j.1600-0463.2002.100604.x>

Zheng, J., Yang, X., Harrell, J. M., Ryzhikov, S., Shim, E. H., Lykke-Andersen, K., Wei, N., Sun, H., Kobayashi, R., & Zhang, H. (2002). CAND1 binds to unnedylated CUL1 and regulates the formation of SCF ubiquitin E3 ligase complex. *Molecular Cell*, 10(6), 1519–1526. [https://doi.org/10.1016/s1097-2765\(02\)00784-0](https://doi.org/10.1016/s1097-2765(02)00784-0)

Zhou, G., Hamik, A., Nayak, L., Tian, H., Shi, H., Lu, Y., Sharma, N., Liao, X., Hale, A., Boerboom, L., Feaver, R. E., Gao, H., Desai, A., Schmaier, A., Gerson, S. L., Wang, Y., Atkins, G. B., Blackman, B. R., Simon, D. I., & Jain, M. K. (2012). Endothelial Kruppel-like factor 4 protects against atherothrombosis in mice. *The Journal of Clinical Investigation*, 122(12), 4727–4731. <https://doi.org/10.1172/JCI66056>

Zhou, J., Li, Y.-S., & Chien, S. (2014). Shear stress-initiated signaling and its regulation of endothelial function. *Arteriosclerosis, Thrombosis, and Vascular Biology*, 34(10), 2191–2198. <https://doi.org/10.1161/ATVBAHA.114.303422>

Zhou, L., Jiang, Y., Liu, X., Li, L., Yang, X., Dong, C., Liu, X., Lin, Y., Li, Y., Yu, J., He, R., Huang, S., Liu, G., Zhang, Y., Jeong, L. S., Hoffman, R. M., & Jia, L. (2019). Promotion of tumor-associated macrophages infiltration by elevated neddylation pathway via NF-κB-CCL2 signaling in lung cancer. *Oncogene*, 38(29), 5792–5804. <https://doi.org/10.1038/s41388-019-0840-4>

Zhou, L., Jiang, Y., Luo, Q., Li, L., & Jia, L. (2019). Neddylated: A novel modulator of the tumor microenvironment. *Molecular Cancer*, 18(1), 77. <https://doi.org/10.1186/s12943-019-0979-1>

Zhou, X., Yin, Z., Guo, X., Hajjar, D., & Han, J. (2010). Inhibition of ERK1/2 and Activation of Liver X Receptor Synergistically Induce Macrophage ABCA1 Expression and Cholesterol Efflux. *The Journal of Biological Chemistry*, 285, 6316–6326. <https://doi.org/10.1074/jbc.M109.073601>

Zhu, Y., Lin, J. H.-C., Liao, H.-L., Friedli, O., Verna, L., Marten, N. W., Straus, D. S., & Stemerman, M. B. (1998). LDL Induces Transcription Factor Activator Protein-1 in Human Endothelial Cells. *Arteriosclerosis, Thrombosis, and Vascular Biology*, 18(3), 473–480. <https://doi.org/10.1161/01.ATV.18.3.473>

Zhu, Y.-C., Jiang, X.-Z., Bai, Q.-K., Deng, S.-H., Zhang, Y., Zhang, Z.-P., & Jiang, Q. (2019). Evaluating the Efficacy of Atorvastatin on Patients with Carotid Plaque by an Innovative Ultrasonography. *Journal of Stroke and Cerebrovascular Diseases*, 28(3), 830–837. <https://doi.org/10.1016/j.jstrokecerebrovasdis.2018.11.027>

Zhu, Z., Sun, L., Hao, R., Jiang, H., Qian, F., & Ye, R. D. (2017). Nedd8 modification of Cullin-5 regulates lipopolysaccharide-induced acute lung injury. *American Journal of Physiology. Lung Cellular and Molecular Physiology*, 313(1), L104–L114. <https://doi.org/10.1152/ajplung.00410.2016>

Ziegler-Heitbrock, H. W., Ströbel, M., Kieper, D., Fingerle, G., Schlunck, T., Petersmann, I., Ellwart, J., Blumenstein, M., & Haas, J. G. (1992). Differential expression of cytokines in human blood monocyte subpopulations. *Blood*, 79(2), 503–511.

Ziegler-Heitbrock, L., Ancuta, P., Crowe, S., Dalod, M., Grau, V., Hart, D. N., Leenen, P. J. M., Liu, Y.-J., MacPherson, G., Randolph, G. J., Scherberich, J., Schmitz, J., Shortman, K., Sozzani, S., Strobl, H., Zembala, M., Austyn, J. M., & Lutz, M. B. (2010). Nomenclature of monocytes and dendritic cells in blood. *Blood*, 116(16), e74-80. <https://doi.org/10.1182/blood-2010-02-258558>

Ziegler-Heitbrock, L., & Hofer, T. P. J. (2013). Toward a refined definition of monocyte subsets. *Frontiers in Immunology*, 4, 23. <https://doi.org/10.3389/fimmu.2013.00023>

Zitka, O., Kukacka, J., Krizkova, S., Huska, D., Adam, V., Masarik, M., Prusa, R., & Kizek, R. (2010). Matrix metalloproteinases. *Current Medicinal Chemistry*, 17(31), 3751–3768. <https://doi.org/10.2174/092986710793213724>

Zuckerbraun, B. S., McCloskey, C. A., Mahidhara, R. S., Kim, P. K. M., Taylor, B. S., & Tzeng, E. (2003). Overexpression of mutated IkappaBalphα inhibits vascular smooth muscle cell proliferation and intimal hyperplasia formation. *Journal of Vascular Surgery*, 38(4), 812–819. [https://doi.org/10.1016/s0741-5214\(03\)00427-0](https://doi.org/10.1016/s0741-5214(03)00427-0)

## Acknowledgements

This long-awaited moment has finally arrived, and I am filled with immense excitement as I write to acknowledge the outstanding individuals who helped make this dream a reality.

My time at Prof. Bernhagen's Vascular Biology Laboratory has been the most enriching life experience, and I will always cherish the personal and professional growth it fostered. Many people have contributed directly and indirectly through support, advice, or inspiration; I am genuinely grateful.

I want to express my gratitude to the following persons:

Prof. Dr Bernhagen, thank you for your unwavering trust and support throughout my studies, providing me with opportunities that exceeded my expectations. Your scientific enthusiasm, methodical mind, and guidance on professionalism and science discussions have been instrumental in shaping my career. I am also profoundly grateful for your openness to exploring unconventional ideas and making this work possible. Thank you for always being available and helping me grow as a scientist.

Dr. Yaw Asare, your foundational work on the project and continuous support have been invaluable. I could not have asked for a better supervisor and role model.

Dr. Dzmitry Sinitski, thank you for being both a guide and a true friend. Your availability and genuine scientific enthusiasm sustained me through challenging times. Your teachings on my work's practical and theoretical aspects were invaluable to completing this thesis.

Dr. Omar El Bounkari, your great personality and passion for science constantly inspired me to work hard. Thank you for all your help and engaging discussions.

Priscila, thank you for enduring the immense workload and assisting with genotyping, which made this project possible.

Chung Fang, Yuan, Dario, Ruben, and Eva, your exceptional support made this thesis possible, and I am truly grateful. It was an honour and a pleasure to work with the entire COP9 team.

To all the AG Bernhagen and AG Gokce lab members, thank you for the warm atmosphere you provided throughout this thesis, especially during the pandemic. Your presence and motivation kept me going.

My thesis advisory board, Prof. Dr. Soehneline and Dr Schulman thank you for mentoring my work and providing invaluable input. I enjoyed our rich and constructive discussions.

To the IRTG1123 students, colleagues, friends, and team, I am honoured to be one of you. You have all been an inspiration and a guiding force in this work, and I appreciate the discussions, collaborations, and advice I received from you.

To the Animal Facility team, thank you for managing the extensive mouse project and supporting it.

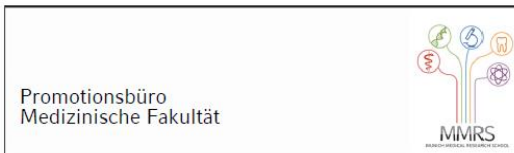
I want to thank the Studienstiftung des Deutschen Volkes and Deutsche Forschungsgemeinschaft for their financial support and incredible programs that fostered my professional development.

To the ISD team Stefan, Carmelo, Josh, Daniel and Paul, thank you for your scientific input, inspiration, friendship, and support in science and life. You made work more enjoyable.

My loving family and friends, thank you for your unwavering support and the emotional journey you have shared with me. They say, 'It takes a village,' and it indeed did, as none of this would have been possible without you all. Mum and Dad, thank you for your love, support, patience, and understanding throughout my studies. I am forever grateful to my sister Jovana and Quentin, for their unwavering encouragement. I also want to thank my extended family for their support throughout my studies abroad.

Bernie, Steffie, Severin, Peter, the Soapbox Science Munich team, Ana, Svetlana, and Marijana, thank you for believing in me and nurturing my scientific enthusiasm and curiosity. Your unwavering friendship is invaluable, and I feel fortunate to have friends like you.

## Affidavit



### Affidavit

Milic, Jelena

Surname, first name

I hereby declare, that the submitted thesis entitled:

***Role of the COP9 Signalosome in Atherogenic Inflammation***

is my work. I have only used the sources indicated and have not made unauthorized use of services of a third party. Where the work of others has been quoted or reproduced, the source is always given.

I further declare that the submitted thesis or parts thereof have not been presented as part of an examination degree to any other university.

Munich, 08/02/2022

place, date

Jelena Milic  
Signature doctoral candidate

## Confirmation of congruency



**Confirmation of congruency between printed and electronic version of  
the doctoral thesis**

Milic, Jelena

-----  
Surname, first name

I hereby declare that the submitted thesis entitled:

***Role of the COP9 Signalosome in Atherogenic Inflammation***

.....

is congruent with the printed version both in content and format.

Munich, 08/02/2022  
place, date

Jelena Milic  
Signature doctoral candidate

## List of publications:

- **Milic, J.**, Tian, Y., & Bernhagen, J. (2019). Role of the COP9 signalosome (CSN) in cardiovascular diseases. *Biomolecules*, 9(6), 217;
- Bounkari, O. E., Zan, C., Wagner, J., Bugar, E., Bourilhon, P., Kontos, C., Zarwel, M., Sinitski, D., **Milic, J.**, Jansen, Y., Kempf, W. E., Mägdefessel, L., Hoffmann, A., Brandhofer, M., Bucala, R., Megens, R. T. A., Weber, C., Kapurniotu, A., & Bernhagen, J. (2021). MIF-2/D-DT is an atypical atherogenic chemokine that promotes advanced atherosclerosis and hepatic lipogenesis (p. 2021.12.28.474328). <https://doi.org/10.1101/2021.12.28.474328>;
- Tian, Y., **Milic, J.**, Sebastián-Monasor, L., Chakraborty, R., Wang, S., Yuan, Y., Asare, Y., Behrends, C., Tahirovic, S. & Bernhagen J. The COP9 signalosome reduces neuroinflammation and attenuates ischemic neuronal stress in organotypic brain slice culture model. (Submitted 2023: CMLS-D-23-01061);
- Sharifi, M.A., Wierer, M., Dang, T.A., **Milic, J.**, Moggio, A., Sachs, N., Scheidt, M., Hinterdobler, J., Müller P., Werner J., Stiller B., Aherrahrou Z., Erdmann J., Zaliani, A., Graettinger, M., Reinshagen, J., Gul, S., Gribbon, P., Maegdefessel, L., Bernhagen, J., Sager, H.B., Mann, M., Schunkert, H., & Kessler, T (2023). The novel coronary artery disease risk factor ADAMTS-7 modulates atherosclerotic plaque formation by degradation of TIMP-1. (Submitted 2023: CIRCRES/2023/322737D);
- **Milic, J.**, Tian, Y., Mägdefessel, L., Yuan, Y., Asare, & Bernhagen, J. Role of the COP9 signalosome in the ECM remodelling (in preparation 2023);